

**UNIVERSITY OF EDINBURGH**

College of Science and Engineering

School of Chemistry

**Cell Penetrating Peptoid Carriers:  
Microwave Assisted Synthesis and Bioactive  
Molecules Delivery**

by

**Mario Antonio Fara**

Thesis for the degree of Doctor of Philosophy

---

May 2008

# UNIVERSITY OF EDINBURGH

College of Science and Engineering

School of Chemistry

## ABSTRACT

### Doctor of Philosophy

Cell Penetrating Peptoid Carriers:

Microwave Assisted Synthesis and Bioactive Molecules Delivery.

*by Mario Antonio Fara*

Effective methods for the selective passage of therapeutic molecules or probes through biological barriers are essential for the study of *cellular functions*. Cell penetrating cationic peptoids, based on a lysine like unit, were efficiently synthesised using a combination of solid phase synthesis strategies and microwave heating.

A linear 7mer peptoid was thus prepared by direct solid phase synthesis and conjugated to both a peptide hormone ( $\alpha$ - Melanocyte Stimulating Hormone, a 13mer peptide) and to peptide nucleic acids (9mer, 12mer and 15mer prepared using Dde/Mmt protected monomers) targeting tyrosinase mRNA. These conjugates were able to efficiently penetrate different cell lines (average uptake > 90%), and even more, to penetrate human skin, with the heptapeptoid carrier being able to deliver a 12mer PNA deep inside the dermis stratus.

Antisense DNA oligomers (19mer, targeting tyrosinase mRNA) conjugated to the heptapeptoid carrier by a disulfide linkage was able to down-regulate tyrosinase expression, showing the potential of the carrier in delivering DNA into cells.

Delivery of macromolecules such as protein and plasmid DNA were attempted. Heptapeptoids functionalised with a tetradentate  $\text{Ni}^{2+}$  ligand were tested for the delivery of hexahistidine ( $\text{His}_6$ ) tagged GFP protein into cells, while 3 generations of a novel peptoid dendrimer were prepared and tested for the cellular delivery of DNA.



## DECLARATION

I, Mario Antonio Fara, declare that the thesis entitled “*Cell Penetrating Peptoid Carriers: Microwave Assisted Synthesis and Bioactive Molecules Delivery*” and the work presented in it are my own.


I confirm that:

- The research described in this thesis was carried out under the supervision of Prof. Mark Bradley at the University of Southampton (Oct. 2003 – Jan. 2005) and the University of Edinburgh (Feb. 2005 – March 2007).
- Where I have consulted the published work of others, this is always clearly attributed;
- Where I have quoted from the work of others, the source is always given. With the exception of such quotations, this thesis is entirely my own work;
- I have acknowledged all main sources of help;
- Where the thesis is based on work done by myself jointly with others, I have made clear exactly what was done by others and what I have contributed myself;
- Parts of this work have been published as:

- Fara, M. A.; Diaz-Mochon, J. J.; Bradley, M. *Tetrahedron Lett.* **2006**, 47, 1011-1014.

- Diaz-Mochon, J. J.; Fara, M. A.; Sanchez-Martin, R. M.; Bradley, M. *Tetrahedron Lett.* **2008**, 49, 923-926.

- Unciti-Broceta, A.; Diezmann, F.; Ou-Yang, C. Y.; Fara, M. A.; Bradley, M. *Bioorg. Med. Chem.* **2008**, in press.

Signed: 

Date: 24/01/2009

## ACKNOWLEDGMENTS

I would like to thank my supervisor, Prof. Mark Bradley, for allowing me to do my PhD in his group, for his guidance and support during my PhD. I also thank Dr. Stifun Mittoo for his advice during the start of this work.

Thanks to all the members (past and present) of the Bradley group for making these years such a great time. Thanks to Mathilde, my “English” teacher, for all the help in the lab and not only, but mostly for having fun of me because of my awful English, I still laugh thinking about it. Thanks to Gianluca and Alessandra for sharing the good and bad moments of this experience. Thanks to Juanjo and Rosario for being the great persons they are, I can only consider myself very lucky for having worked with them. Thanks to Antonio, Christophe, Giuseppe, Loredana, Luciano, Maria, Salvo and Song for the challenging competitions (pool, squash, football), the diners, the drinks and all the things I cannot remember right now. It has been great fun with you guys.

Finally, I would like to thank some very special people who are my parents, my brothers and my sisters. Without their advice, encouragement, and enormous patience (I’m not an easy person) nothing of that would have been possible.



## TABLE OF CONTENT

<b>ABSTRACT .....</b>	<b>i</b>
<b>DECLARATION.....</b>	<b>ii</b>
<b>ACKNOWLEDGMENTS .....</b>	<b>iii</b>
<b>ABBREVIATIONS.....</b>	<b>vii</b>
<b>Chapter I. Introduction.....</b>	<b>1</b>
<b>I.1. Cellular membranes and uptake.....</b>	<b>2</b>
I.1.1. Transport across the cell membrane. ....	3
I.1.2. Transport of macromolecules across the cell membrane.....	4
<b>I.2. Loading molecules into the cytoplasm.....</b>	<b>8</b>
I.2.1. Physical methods. ....	8
I.2.2. Molecular carriers.....	10
<b>I.3. Cell penetrating peptides (CPPs).....</b>	<b>15</b>
I.3.1. Mechanisms for cellular uptake.....	17
I.3.2. Factors influencing cellular uptake.....	19
I.3.3. Cationic CPPs.....	21
I.3.4. Targeted and enhanced delivery.....	23
I.3.5. Delivery of proteins.....	24
I.3.6. Delivery of siRNA and other oligonucleotides.....	25
I.3.7. Commercially available CPPs.....	26
<b>Chapter II. Peptoid synthesis.....</b>	<b>27</b>
<b>II.1. Peptidomimetics.....</b>	<b>27</b>
II.1.1. $\beta$ -Peptides.....	28
II.1.2. Sulfonamide peptides.....	29
II.1.3. Oligourea peptidomimetics.....	30
<b>II.2. Peptoids.....</b>	<b>32</b>
II.2.1. Monomer based peptoid synthesis.....	33
II.2.2. Sub-monomer based peptoid synthesis.....	37
II.2.3. Monomer approach vs sub-monomer approach.....	41
<b>II.3. Cell penetrating peptoid transporter.....</b>	<b>43</b>
II.3.1. Peptoid monomer synthesis.....	43



II.3.2. Solid phase peptoid synthesis.....	45
II.3.3. MW assisted solid phase peptide synthesis.....	46
II.3.4. Microwave assisted peptoid synthesis.....	53
<b>Chapter III. Peptoid conjugation to cargoes and delivery.....</b>	<b>57</b>
<b>III.1. <math>\alpha</math>-Melanocyte stimulating hormone (<math>\alpha</math>-MSH).....</b>	<b>57</b>
III.1.1. $\alpha$ -MSH and peptoid conjugation: synthesis and labelling.....	58
III.1.2. Cell and skin delivery. ....	66
<b>III.2. Peptide nucleic acid (PNA).....</b>	<b>72</b>
III.2.1. PNA: Monomer synthesis.....	73
III.2.2. Oligomers synthesis.....	79
III.2.3. PNA delivery into cell and skin.....	84
<b>III.3. Antisense DNA delivery.....</b>	<b>86</b>
III.3.1. Conjugation to the heptapeptoid carrier.....	86
III.3.2 DNA-Peptoid conjugates: antisense activity.....	89
<b>Chapter IV. Macromolecules delivery.....</b>	<b>90</b>
<b>IV.1. Peptoid dendrimers for DNA delivery.....</b>	<b>90</b>
IV.1.1. Monomer synthesis.....	92
IV.1.2. Microwave assisted peptoid dendrimer synthesis: G1-G2-G3.....	93
IV.1.3. DNA delivery: peptoid dendrimers vs. PAMAM G2.....	95
<b>IV.2. Protein delivery.....</b>	<b>98</b>
IV.2.1. Synthesis of $Ni^{2+}$ -ligand functionalised peptoids.....	100
IV.2.2. Delivery of GFP protein.....	106
<b>IV.3. Peptoid carriers Summary: peptide, protein and plasmid delivery.....</b>	<b>109</b>
<b>Chapter V. Experimental.....</b>	<b>110</b>
<b>V.1. General information.....</b>	<b>110</b>
<b>V.2. Experimental: Chapters II and III.....</b>	<b>112</b>
V.2.1. Peptoid monomer synthesis.....	112
V.2.2. Detection of primary and secondary amines on solid supports.....	118
V.2.3. General protocols for peptide and PNA synthesis, labelling and cleavage. .....	119
V.2.4. $\alpha$ -MSH Peptides and Peptide-Peptoid conjugates.....	122
V.2.5. Dde-Mmt protected PNA monomers.....	127



V.2.6. PNAs and PNA-peptoid conjugates. ....	147
V.2.7. DNA oligo-peptoid conjugates. ....	152
<b>V.3. Experimental to chapter IV.....</b>	<b>155</b>
V.3.1. Peptoid dendrimer: synthesis and gene delivery.....	155
V.3.2. Ni <sup>2+</sup> complex mediated delivery of His <sub>6</sub> -GFP.....	160
<b>References.....</b>	<b>168</b>

## ABBREVIATIONS

A	Adenine
Ac	Acetyl
Ahx	Aminohexanoic acid
Aib	$\alpha$ -Aminoisobutyric acid
AMP	Adenosine monophosphate
ATP	Adenosine triphosphate
Boc	<i>t</i> -Butylcarbonyl
br	Broad
C	Cytosine
CAP	Catabolite activator protein
Cbz	Benzyloxycarbonyl
CPP	Cell Penetrating Peptide
d	Doublet (NMR assignment)
DCM	Dichloromethane
Dde	1-(4,4-Dimethyl-2,6-dioxocyclohex-1-ylidene)ethyl
DIC	<i>N,N</i> -Diisopropylcarbodiimide
DIPEA	Diisopropylethylamine
DME	Dimethoxyethane
DMF	Dimethylformamide
DNA	Deoxyribonucleic acid
DVB	Divinylbenzene
DTT	Dithiothreitol
EDTA	Ethylenedinitrilotetraacetic acid
ES	Electrospray (mass spectrometry)
ELSD	Evaporative light-scattering detector
FACS	Fluorescence activated cell sorting
FAM	Fluorescein amide
Fmoc	9-fluorenylmethoxycarbonyl
FRET	Fluorescence resonance energy transfer
G	Guanine
GFP	Green fluorescent protein



HA2	Hemadsorption virus type 2
HATU	O-(7-Azabenzotriazol-1-yl)-N,N,N',N'-tetramethyluronium hexafluorophosphate
HBTU	O-benzotriazolyl-N,N,N',N'-tetramethyluronium hexafluorophosphate
HIV	Human immunodeficiency virus
HOBt	1-Hydroxybenzotriazole
HPLC	High pressure liquid chromatography
HSV	Herpes simplex virus
IDA	Iminodiacetic acid
m	Multiplet (NMR assignement)
MALDI	Matrix-Assisted Laser Desorption Ionization
m/z	Mass/charge ratio (mass spectrometry)
Mmt	Monomethoxytrityl
MTS	Membrane translocation sequence
MTT	3-(4,5-dimethylthiazol-2-yl)-2,5-diphenyl-2H-tetrazolium bromide
NEM	N-Ethyl morpholine
NMR	Nuclear magnetic resonance
NLS	Nuclear localization sequence
NTA	Nitrilotriacetic acid
ON	Oligo nucleotide
OSu	Succinimide ester
PAMAM	Polyamidoamine
Pbf	2,2,4,6,7-pentamethyldihydrobenzofuran-5-sulfonyl
PEBBLE	Probe encapsulated by biologically localized embedding
PEG	Polyethylene glycol
PEGA	PEG-polyacrylamide
Pmc	2,2,5,7,8-pentamethylchroman-6-sulfonyl
PNA	Peptide nucleic acid
PyBOP	Benzotriazole-1-yloxytrispyrrolidinophosphonium



	hexafluorophosphate
PyBrOP	Bromotripyrrolidinophosphonium
	hexafluorophosphate
RNA	Ribonucleic acid
RNAi	RNA interference
RT	Retention time
siRNA	Short interfering RNA
s	Singlet (NMR assignement)
T	Tymine
t	Triplet (NMR assignement)
TAT	Transactivator protein
TBTU	O-Benzotriazole-1-yl-1,1,3,3
	tetramethyluroniumtetrafluoroborate
TFA	Trifluoroacetic acid
THF	Tetrahydrofurane
TIS	Triisopropylsilane
TLC	Thin layer chromatography
TOF	Time of flight
UV	Ultraviolet
VP	Virion protein

#### **Amino Acids**

A, Ala	Alanine
C, Cys	Cysteine
D, Asp	Aspartic acid
E, Glu	Glutamic acid
F, Phe	Phenylalanine
G, Gly	Glycine
H, His	Histidine
I, Ile	Isoleucine
K, Lys	Lysine
L, Leu	Leucine
M, Met	Methionine



N, Asn	Asparagine
P, Pro	Proline
Q, Gln	Glutamine
R, Arg	Arginine
S, Ser	Serine
T, Thr	Threonine
V, Val	Valine
W, Trp,	Tryptophan
Y, Tyr	Tyrosine

## **Chapter I. Introduction.**

Biological membranes are natural barriers, which isolate the content of cells from the extracellular medium, and compartmentalise the cellular environment. Through the membranes are distributed various proteins responsible for the controlled efflux-influx of solutes from cells and cellular organelles, regulating intracellular concentrations of ions and small molecules according to cellular demand, but otherwise being impermeable to most molecules. This “traffic control” activity of the cell membranes is a major problem in studying cells, because without sufficient cellular uptake any new promising probe for cellular functions cannot be applied. Clearly the development of effective methods for the selective passage of therapeutics or probes through biological barriers is a key step for the study of cellular functions and advancement of new drug therapies. This “technology” would offer the possibility of improving the bioavailability of existing drugs, enabling the delivery of new cargoes (e.g., RNAi, siRNA, DNA, proteins, imaging agents, and sensors), and allowing access to difficult sites such as through the blood–brain barrier, skin (topical administration of drugs avoiding the use of needles) and the eye. The possibility of having cell (tissue) selective entry, controlled drug release (and activation), could also minimize problems connected with drug toxicity.

This chapter will discuss the structure of the cellular membrane together with its role in cellular uptake, followed by a description of different methods used to deliver molecules into cells with focus on cell penetrating peptides (CPPs), the basis of this thesis.



## I.1. Cellular membranes and uptake.

Cells possess a physical boundary called the cellular membrane which delimits the intracellular space, isolating it from the extracellular environment. It is composed of a thin film (7.5-10 nm) of lipids, the majority of which are phospholipids which are amphipatic (or amphiphilic) molecules consisting of a hydrophilic polar head, a negatively charged phosphate group, and two hydrophobic fatty acid tails (Figure 1.1). The phospholipids are held together by non covalent interactions and arranged in a continuous double layer called the lipid bilayer.

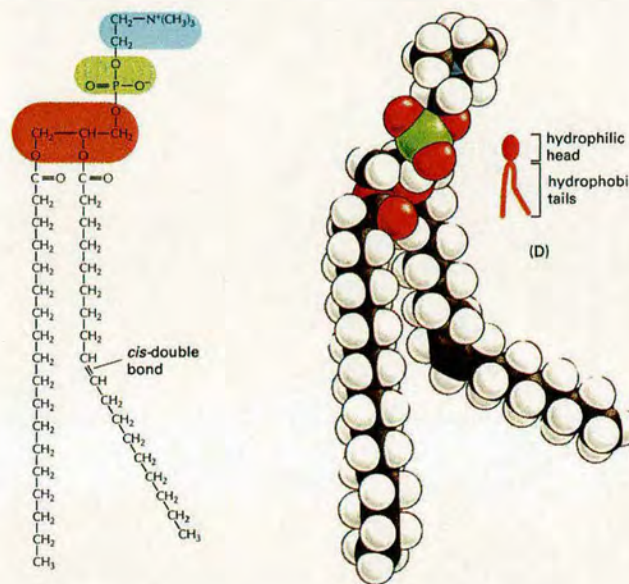


**Figure 1.1.** Schematic representation of a phospholipid.

From *Molecular Biology of the Cell*, forth edition, by Bruce Alberts et al. Copyright 2004 by Garland Publishing, Inc. Permission requested.

Because of their amphiphilicity, lipids naturally rearrange in such a way that the polar heads face the aqueous environment and the fatty acid chains are buried in the middle of the hydrophobic interior of the membrane which leads to the spontaneous formation of lamellar structures (Figure 1.2). In the case of cells, they organise with other lipids also constituting the physical barrier such as cholesterol, sphingolipids and glycolipids to form the closed vesicular bilayer structures. Studded throughout, or associated with the lipid bilayer, there are various membrane proteins which perform



numerous functions such as cell-cell attachment, communication with other cells or the transport of various substances into and out of the cell.

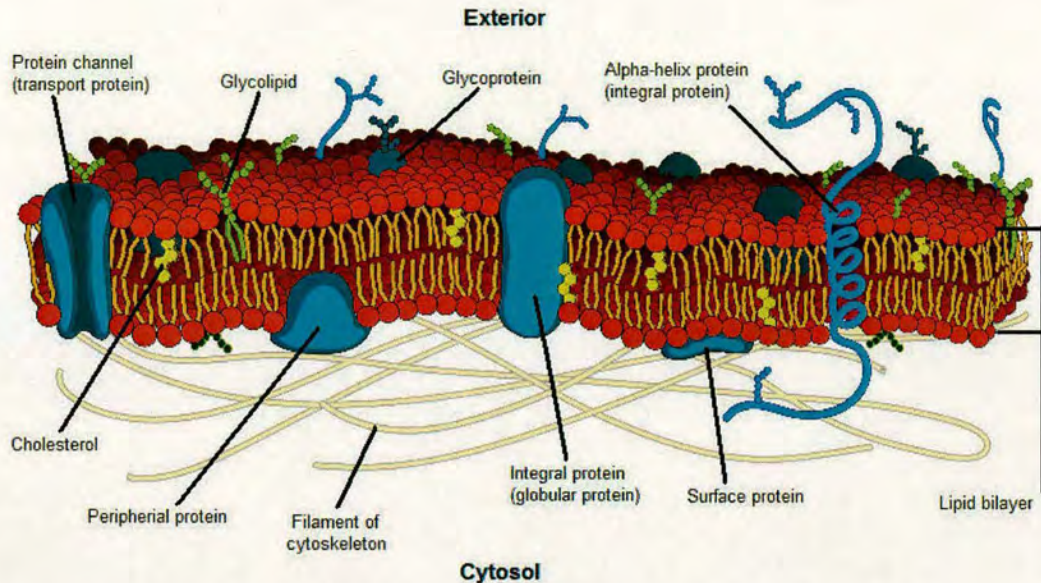


**Figure 1.2.** Schematic representation of a cell membrane (commons.wikimedia.org, reprinted with permission).

### ***1.1.1. Transport across the cell membrane.***

The lipid bilayer described above is semi-permeable, which means that it is impermeable to most molecules with only a few diffusing freely through according to their concentration gradient. This is the case for small non polar molecules (such as  $O_2$ ,  $CO_2$ ) and small uncharged polar molecules (such as urea, glycerol) which can diffuse slowly through the cell membrane. However small ions (such as  $Na^+$ ,  $K^+$ ,  $Ca^{2+}$ ,  $Cl^-$ ) cannot cross the membrane freely and are often transported *via* ion-channels across the membrane (Figure 1.3). Ion-channels are transmembrane proteins which response to changes in voltage or ligand binding, leading to conformational changes in the protein which results in the movement of the ions through the channel.



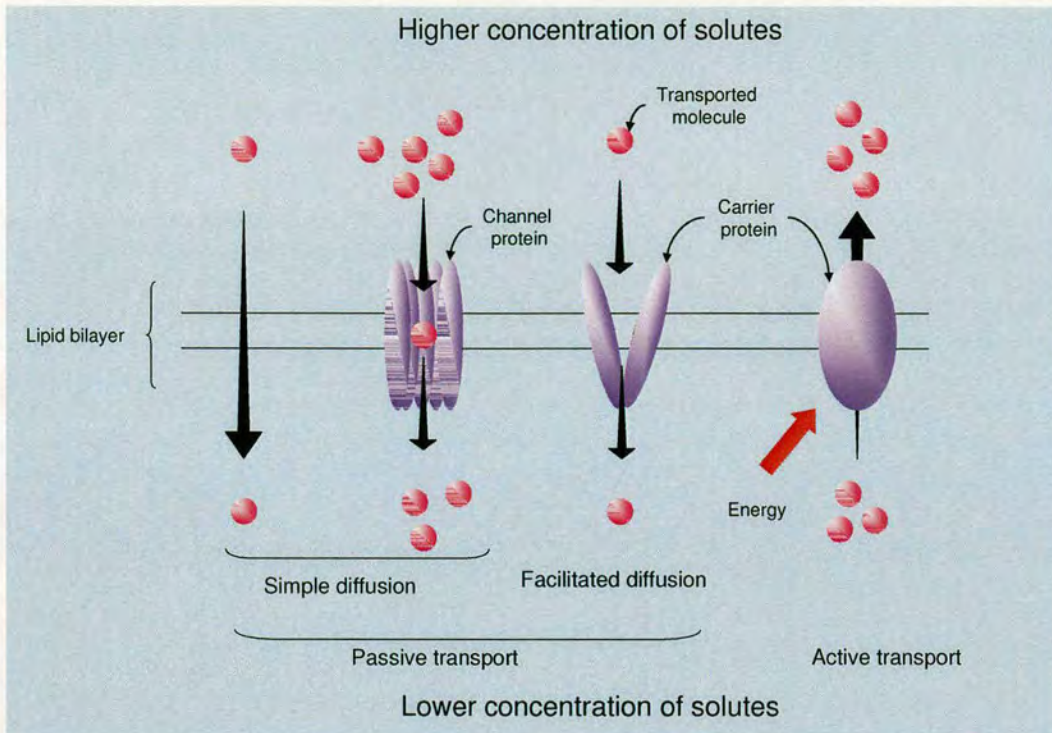


**Figure 1.3.** Different types of transport across the cell membrane requiring various proteins.

Transport of larger polar molecules (such as amino acids and sugars) across the membrane requires the involvement of membrane proteins called transporters (permeases, translocases or carrier proteins) and this family is divided into two categories: i) those that facilitate diffusion allowing transport down a concentration gradient, and ii) those involved in active transport, which transport substrates uphill against the concentration gradient requiring the consumption of ATP.

### ***1.1.2. Transport of macromolecules across the cell membrane.***

As explained above, the simplest way by which a molecule enters the cell is by diffusion, but it has been established<sup>1</sup> that only small, soluble, preferentially uncharged and of low molecular weight molecules can enter the cell in such a way. The large size and charge of macromolecules usually prevents them from entering the cell through diffusion<sup>2</sup> and their conventional mode of entry into cells is *via* an event called endocytosis.

Endocytosis is the process by which cells take up macromolecules, particulates, and sometimes other cells where the material to be ingested is progressively enclosed by



a small portion of cellular membrane which invaginates and eventually pinches off to form endosomes, or endocytic vesicles which contain the material of interest. The main types of mechanisms are distinguished by the size of endocytic particles formed: **phagocytosis** (cell eating), **pinocytosis** (cell drinking) and **receptor mediated endocytosis** that are mediated by clathrin proteins, and **caveolae dependent** endocytosis.

#### *1.2.1. Phagocytosis.*

Phagocytosis is an actin protein dependent process that involves the ingestion of large particles and microorganisms, or dead cells (generally > 500 nm) *via* particles called phagosomes. Phagocytosis is carried out only by specialised cells such as macrophages, neutrophils and dendritic cells. Once internalised the endosomes fuse with lysosomes inside the cells and ingested particles are degraded by numerous enzymes found in the lysosomes with degradation aided by an acidic pH, and peroxides.

#### *1.2.2. Pinocytosis.*

Micropinocytosis involves the continuous ingestion of fluids and solute *via* small pinocytic vesicles (usually about 100 nm in diameter) and can be carried out by most eukaryotic cells at quite a high rate depending on the cell type. It requires several steps, firstly, clathrin assembly at the inner surface of the cell membrane together with a complex called adaptin which results in the formation of a bud called a clathrin-coated pit. Clathrin proteins assemble to form the clathrin coat at the inner surface of the cell membrane which has a very distinctive net-like aspect on SEM images (Figure 1.4). After the formation of the clathrin-coated pit, the bud invaginates more and more and soluble cytoplasmic proteins such as dynamin assemble a ring around the neck of each bud and help to bend the membrane by distorting the bilayer structure locally, changing the lipid composition, or both. The later brings the two lipid bilayers together which eventually fuse and the vesicle pinches off from the membrane into the intracellular space where the clathrin coat is lost within seconds before it fuses with early endosomes (Figure 1.5). Macropinocytosis process is actin dependent, and occurs under more restrictive



conditions in a limited number of cells, such as dendritic cells, and generates vesicles with a diameter  $> 1\mu\text{m}$ .

### *1.2.3. Receptor mediated endocytosis.*

Receptor mediated endocytosis (Figure 1.5) is an internalisation process similar to pinocytosis with the difference that ligands have to be associated with transmembrane receptors, so called cargo receptors, to activate invagination of the cell membrane. It provides an efficient pathway for taking up specific macromolecules from the extracellular fluid and also acts as a concentrating mechanism as several receptor-ligand complexes are internalised together. As an example, iron is transferred to the cytosol by such a mechanism: in the blood, iron is bound by a protein called transferrin and on the external surface of the cell there are transmembrane receptors to transferrin which bind the protein when exposed to it. The iron-transferrin-receptor complex is then internalised by the mechanism described above and finally iron is released inside the cytosol by diffusion through the vesicle membrane.

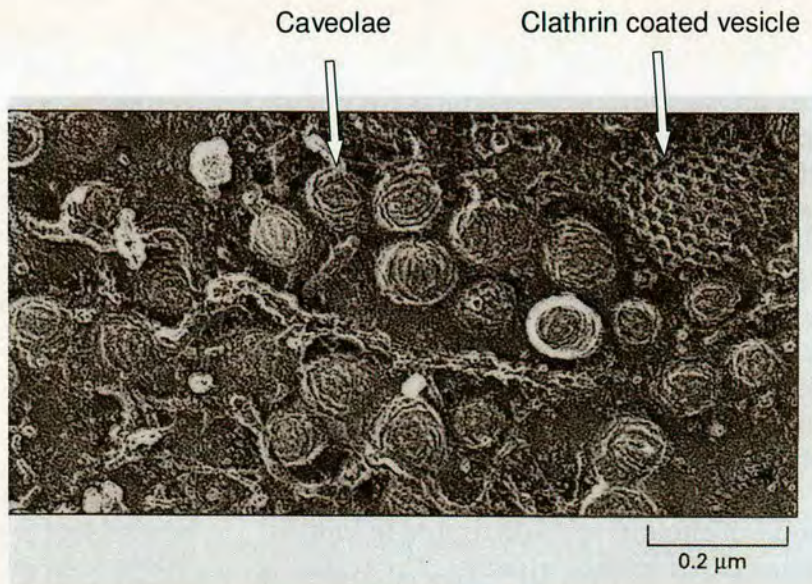


**Figure 1.4.** Picture of the inner surface of the plasma membrane after rapid freeze-drying.

Reprinted from Journal of Cell Biology, 84, J.Heuser, 560-583, Copyright 1980, with permission from The Rockefeller University Press.



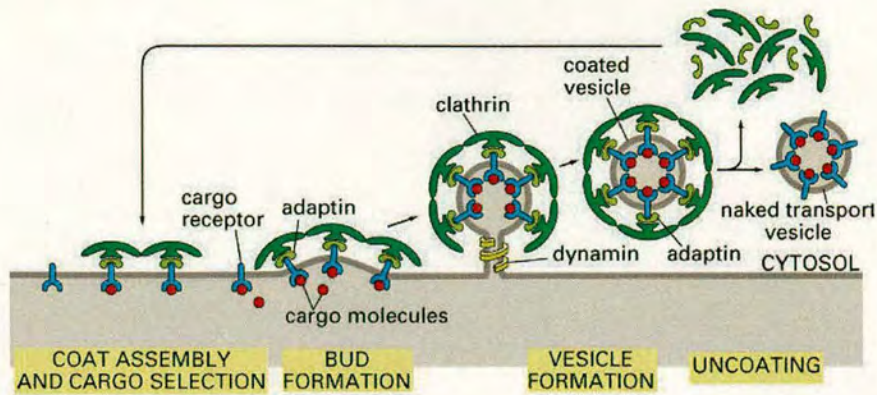


**Figure 1.5.** Different steps in the receptor mediated endocytosis process. From *Molecular Biology of the Cell*, forth edition, by Bruce Alberts et al. Copyright 2004 by Garland Publishing, Inc. Reprinted with permission

#### 1.2.4. Caveolae dependent endocytosis.

Caveolae are present in the plasma membrane of most cell types and look like deeply invaginated flasks as shown in Figure 1.6.

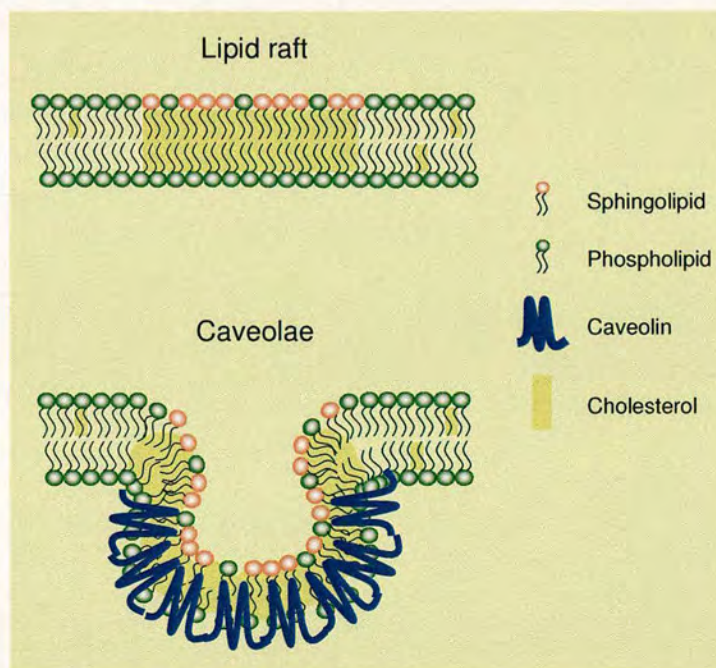


**Figure 1.6.** Schematic representation of lipid rafts and caveolae.

Caveolae are subdomains of lipid rafts, which are patches in the plasma membrane that exhibit a high level of cholesterol, sphingolipids and



glycosylphosphatidylinositol-anchored membrane proteins. Caveolae contain specific proteins called caveolins whose presence results in the invagination of the cell membrane and subsequently in the internalisation of the vesicle (Figure 1.6). Once formed the vesicles can fuse with early endosomes, but their overall function is believed to be more complex than only intracellular transport. The main difference with clathrin coated pits is that the caveolae's invagination is believed to be dependent on the lipid composition of the caveolar membrane and not only the result of the assembly of the caveolin protein coat as observed in clathrin mediated endocytosis.

**Uptaken macromolecules** (by endocytosis) are trapped by a biological membrane in endosomes, and not free to diffuse in the cytosol. As described above the endosomes reach and fuse with the lysosomes, where the compounds are exposed to the action of several enzymes and degraded. The delivery of macromolecules into cells without being degraded is one of the greatest obstacles in cellular targeting, meaning that methods need to be found to address macromolecule delivery into the intracellular space.

## **1.2. Loading molecules into the cytoplasm.**

Several physical and molecular techniques have been developed over the years to enable drug or probe uptake into cells and tissues.

### ***1.2.1. Physical methods.***

#### ***2.1.1. Microinjection.***

Microinjection uses a micro-needle with an outer tip diameter in the range of 200-250 nm, to literally inject the drug or molecule of interest into the cytosol. Relatively high volumes of the molecule can be reached (in the range of femtoliter to attoliter), and there is virtually no size limit of the material that can be injected as the microinjection of organelles, as well as nuclei, has been reported.<sup>3</sup> It is a rather universal method as most cells can be injected, however, the extent of the cellular damage is unpredictable and can be quite high<sup>4,5</sup> as cells have to be able to tolerate the introduction of a large



glass microinjection pipette (Figure 1.7). Furthermore, the tips are very fragile and extremely difficult to see under a light microscope making the positioning and injection difficult, which together with its low-speed highly limits the throughput.

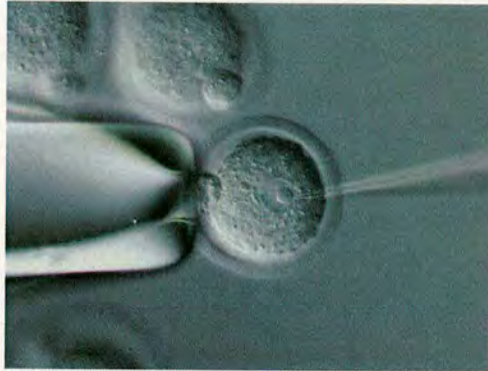


**Figure 1.7.** Microinjection in a cell embryo. Courtesy of Anne Bower and Manfred Baetscher, Oregon Health and Science University, Portland.

#### *2.1.2. Gene gun delivery.*

The gene gun delivery belongs to a method called biolistics (also known as the bioballistic) method. It uses bursts of helium to fire nanoparticles such as gold or tungsten colloids coated with RNA or DNA into cells. This technique has been used extensively to transfect cells with DNA, however, it has been used recently to introduce polymeric particles into cells<sup>6</sup> but the applications are limited due to shallow penetration of particles and the associated cell damage. However this technique has been successfully used to deliver various genes inside cells.<sup>7,8</sup>

#### *2.1.3. Electroporation.*

Also called electro-permeabilisation or electroinjection, electroporation is a well-proven tool for the introduction into living cells of various membrane-impermeable molecules, such as drugs, hormones, proteins, plasmids, and so on. It is based on the temporary increase of membrane permeability due to reversible electric breakdown of the plasma membrane upon the application of an external high-intensity electrical field of very short duration. Brief high-voltage electric pulses result in the formation of small (nanometer-sized) pores in the cell membrane which are reversible as the membrane heals itself as soon as the electrical field is removed. Cells placed in a



buffered solution of the purified protein of interest are exposed to a pulsed electrical field, with the protein entering the cell *via* these small pores or during the process of membrane reorganisation as the pores close and the cell returns to its normal state. The efficiency of delivery is dependent upon the strength of the applied electrical field, the length of the pulses, the temperature and the composition of the buffered medium, however, the poor loading efficiency of the method has limited its use to the delivery of genetic material such as RNA and DNA.<sup>4,5</sup>

### ***1.2.2. Molecular carriers.***

#### ***2.2.1. Liposomes.***

Liposomes are colloidal, vesicular structures of 20 nm to 10  $\mu\text{m}$  diameter based on phospholipid bilayers that can be unilamellar (meaning only one bilayer surrounds an aqueous core) (Figure 1.8) or multilamellar (several bilayers oriented concentrically around an aqueous core) which depends on the processing protocol and choice of bilayer components.<sup>9</sup>

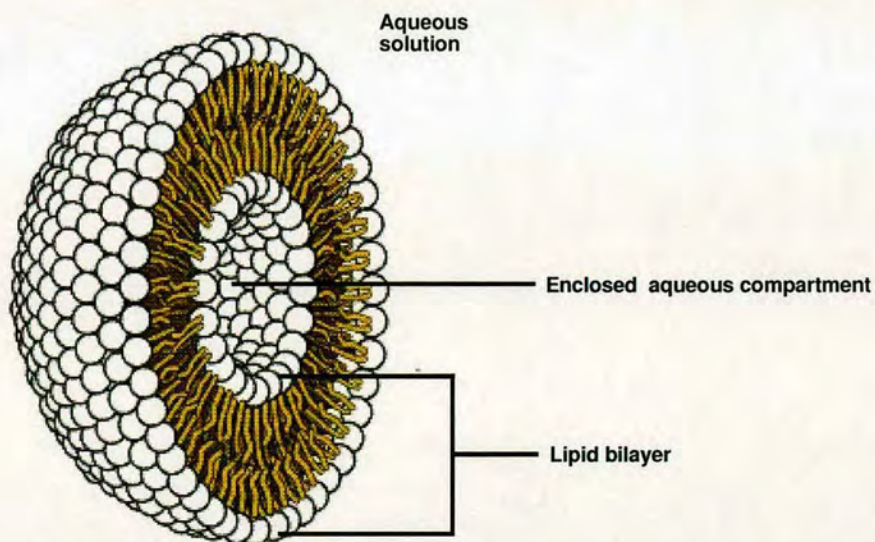


**Figure 1.8.** Schematic representation of a liposome section (commons.wikimedia.org, reprinted with permission).

The liposome drug-carrier concept was proposed and demonstrated in the early 70s<sup>10,11</sup> when it was proven that soluble molecules could be entrapped within the core



of the liposomes which can later be endocytosed by cells. Uptake of liposomes by cells can be highly efficient (depending on the particular cell line), however the poor release of material from the endosomal vesicles (endosomal escape), especially for high molecular weight species, is a serious limitation. Endosomal escape can be enhanced by modifications of the liposomes, such as pH sensitive monomers,<sup>12,13</sup> the addition of a lipid helpers (DOPE)<sup>14</sup> or complexation of the liposome with membrane disruptive substances.<sup>15</sup> Liposome based delivery is an extensively applied method which has been used to deliver many low molecular weight drugs, peptides, enzymes,<sup>16</sup> oligonucleotides (as a potential tool to unlock of “gene therapies”)<sup>17,18</sup> to cells but also ionic sensor-filled microparticles (PEBBLES).<sup>6</sup>

### *2.2.2. Dendrimers.*

Dendrimers and hyperbranched polymers are a relatively new class of materials with unique molecular architectures and dimensions in comparison to traditional linear polymers. Highly branched functionalised dendrimers have the potential to act as efficient drug carrier systems<sup>19</sup> (Figure 1.9). Drug molecules can be associated to the dendrimers in two different ways: one is the encapsulation of soluble drugs within the dendritic core which acts as a reservoir for drug molecules<sup>20</sup> and the other one is the coupling of drug molecules to the free surface functional groups.<sup>21,22</sup> Research to date has mainly been focused on the delivery of DNA where its use has enhanced the transfection of DNA into cells<sup>23,24</sup> but they have also been used to deliver drugs to cancer cells.<sup>25</sup>



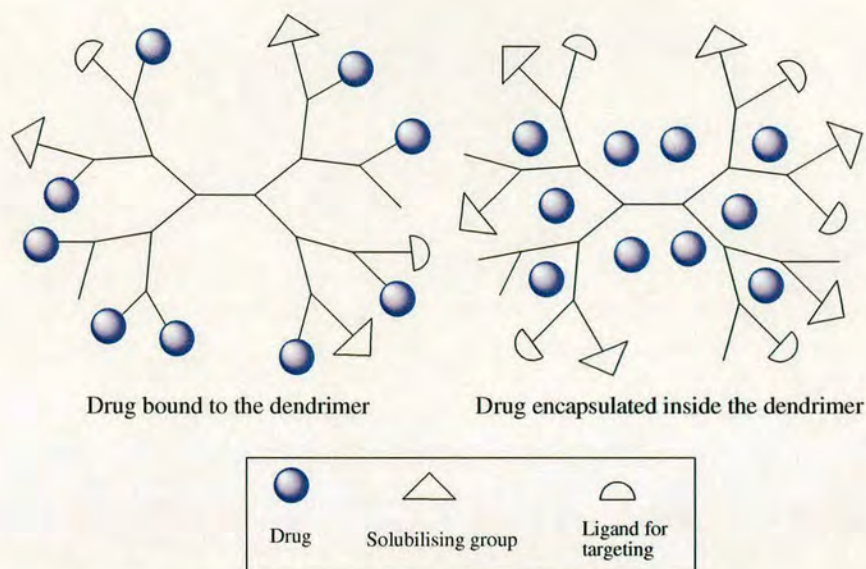


**Figure 1.9.** Example of a hyperbranched dendrimer drug delivery device.

As outlined before an efficient delivery protocol requires more than just high levels of cellular uptake, the ability of promoting effective endosomal release of the cargo is equally important. Certain materials, known as **proton-sponge polymers**,<sup>26,27,28</sup> are believed to mediate their own endosomal escape through a unique mechanism. Polyamidoamine (PAMAM) dendrimers belong to this class of compounds (Figure 1.10). These proton-sponge polymers, which contain a large number of secondary and tertiary amines, exhibit  $pK_a$  values between the physiological (pH 7.4) and lysosomal (pH 4.5) pH's. Endosomes are acidified by the action of an ATPase enzyme that actively transports protons from the cytosol into the vesicle. These polymers, therefore, undergo large changes in protonation during endocytic trafficking. It has been proposed that proton-sponge polymers prevent acidification of endocytic vesicles (buffer action), causing the ATPase to transport more protons to reach the desired pH. The accumulation of protons in the vesicle has to be balanced by an influx of counter ions. The increased ion concentration causes osmotic swelling and rupture of the endosome membrane, allowing dispersion of the dendrimer complexes into the cytosol (Figure 1.10).<sup>29</sup>



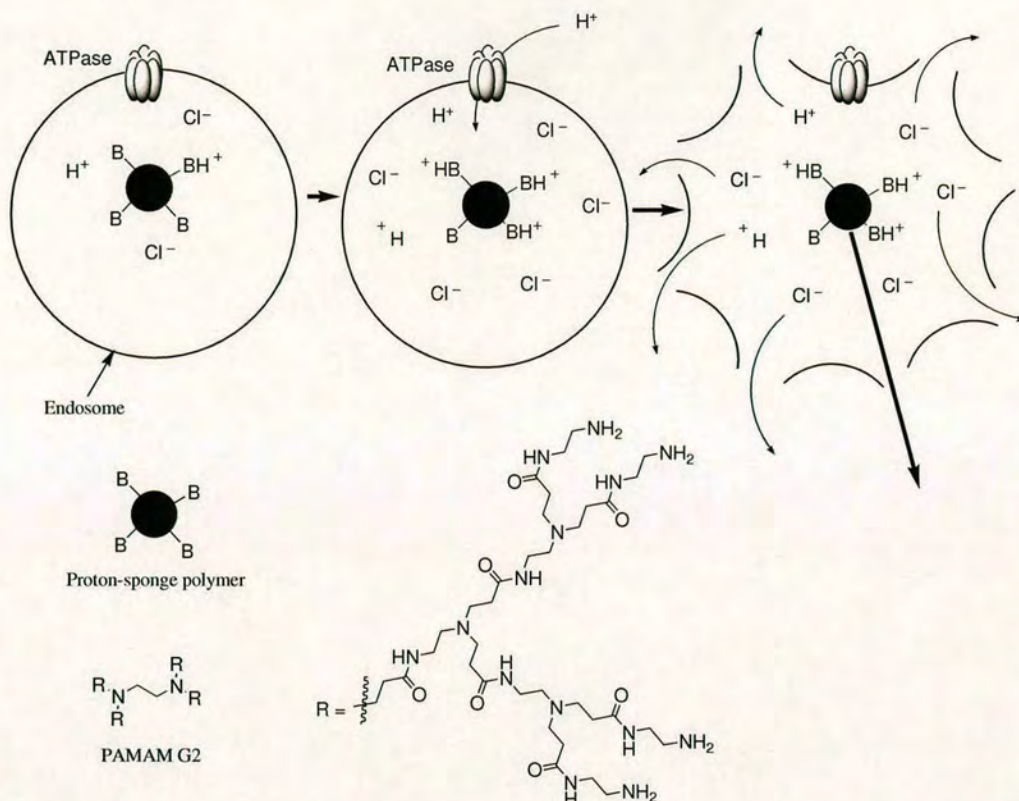


**Figure 1.10.** Schematic of the proton-sponge mechanism and structure of PAMAM (ethylenediamine core) G2. Protonation of the proton-sponge polymer causes increased influx of protons (and counter-ions) into endocytic vesicles. Increasing osmotic pressure causes the vesicle to swell and rupture.

### 2.2.3. Biodegradable microspheres.

Over the past few decades, there has been considerable interest in developing biodegradable microspheres as effective drug delivery devices. The drug is dissolved, entrapped, encapsulated or attached to a biodegradable matrix and depending upon the method of preparation, nanospheres (also called microspheres, nanoparticles) or nanocapsules ranging from 10 to 1000 nm diameter can be obtained. Nanocapsules are vesicular systems in which the drug is confined in a cavity surrounded by a unique polymer membrane, while nanospheres are made of a matrix in which the drug is physically and uniformly dispersed (Figure 1.11).



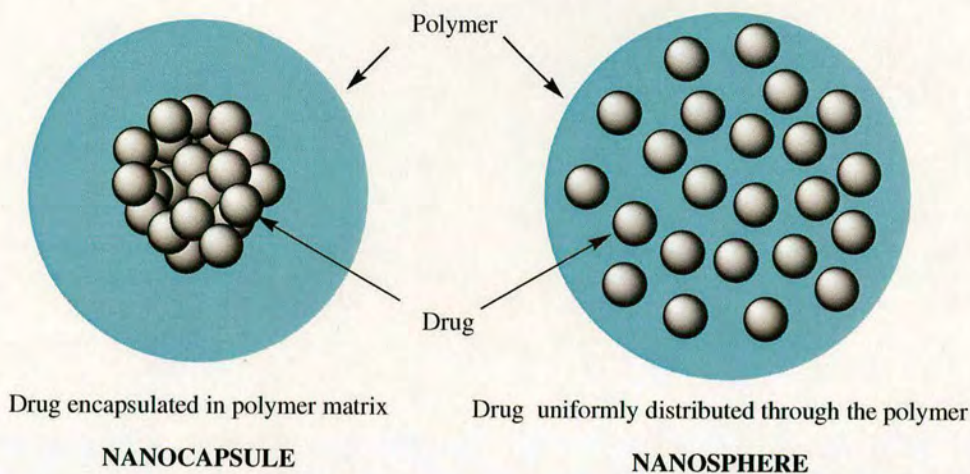


**Figure 1.11.** Schematic representation of the two different types of biodegradable microspheres.

Drugs are then released following different routes: drug release *via* diffusion through the microspheres and drug release *via* microsphere degradation and this mode of delivery has been successfully used to transport oligonucleotides,<sup>30</sup> proteins,<sup>31</sup> peptides and various drugs.<sup>32,33</sup> Early research into biodegradable systems focused on naturally occurring polymers such as collagen, cellulose, albumin, gelatin, etc, and has progressively moved into synthetic polymers such as poly(lactic acid), poly(glycolic acid), polyanhydrides, polyesters, polyacrylic acids and polyurethanes. The most widely used and studied types of biodegradable polymers for the synthesis of nanospheres are polyesters, including poly(lactic acid), poly(glycolic acid), and their copolymers.<sup>34</sup> Macrophages and dendritic cells are often their target,<sup>35</sup> but they have also been addressed to tissues, or solid tumours.



### I.3. Cell penetrating peptides (CPPs).

Delivery of bioactive compounds mediated by peptides is one of the most promising technologies in the field of delivery agents. Compared to others agents (or techniques), peptides offer high delivery yield and low toxicity. Peptides able to penetrate into cells are referred to as cell-penetrating peptides (CPPs), trojan peptides or membrane translocating peptides (MTS). For simplicity the Cell Penetrating Peptides will be employed here to indicate all these classes of peptides. CPPs have been reported to be able to deliver a wide range of bioactive molecules such as proteins,<sup>36,37</sup> peptides,<sup>38</sup> oligonucleotides,<sup>39,40</sup> and even nano-particles<sup>41</sup> into different cells types and to different cellular compartments, both *in vivo* and *in vitro*.

Name	Sequence <sup>a</sup>	Origin
Penetratin <sup>42</sup>	RQIKIWFAQNRRMKWKK	D. melanogaster transcription factor
HIV TAT <sup>43</sup> peptide (48–60)	GRKKRRQRRPPQ	Viral transcriptional regulator
HSV-1 VP22 <sup>44</sup> peptide	DAATATRGRSAASRPTERPR APARSASRPRRVD	Viral Capsid protein
MAP <sup>45</sup> (Model amphiphilic peptide)	KLALKLALKALKAALKLA-amide	Synthetic
Transportan <sup>46</sup>	GWTLSAGYLLGKINLKALAALAKKIL-amide	Chimeric galanin-mastoparan
R <sub>8</sub> <sup>47,48</sup>	RRRRRRRR	Synthetic
MPG <sup>49</sup>	GALFLGWLGAAGSTMGAPKKRKVC-amide	Chimeric HIV-1 gp41-SV40 large T antigen



SynB <sup>50,51</sup>	RGGRLSYSRRRFSTSTGR, RRLSYSRRRF	Antimicrobial peptide protegrin 1 (PG- 1)
Pep-1 <sup>52</sup> (Chariot)	KETWWETWWTEWSQPKKKRKV	Synthetic

**Table 1.1** A selection of commonly used CPPs. <sup>a</sup> All peptides are C-terminal free acids unless stated otherwise.

CPP's may vary in size, amino acid sequence and charge, but they all have the ability to rapidly translocate across the plasma membrane and enable delivery into the cytoplasm or nucleus.<sup>53</sup> The idea of using peptides as delivery vectors originated from the observation of the so-called membrane shuttling proteins such as the *Drosophila* homeobox protein Antennapedia, the HIV-1 transcriptional factor TAT, and the capsid protein VP22 from HSV-1. The field started when Green<sup>54</sup> and colleagues (1988) showed how rapidly the viral protein TAT was able to translocate across the cellular membrane into the cytoplasm. After this example, other proteins were shown to have the same properties, such as the *Drosophila* homeobox protein. Derossi<sup>42</sup> and colleagues (1994) demonstrated that a short 16 amino acid peptide from the third loop of the Antennapedia protein, was responsible for the translocation of the whole protein. Since these first examples many peptides have been reported to have cell-penetrating properties. These CPPs can be natural peptide sequences derived from virus proteins (TAT<sup>43</sup> and VP22<sup>44</sup>) and transcription factors (penetratin<sup>42</sup>), or chimeric peptides (transportan<sup>46</sup> and MGP<sup>49</sup>) or synthetic peptides (polyarginines<sup>47,48</sup> and Pep-1<sup>52</sup>) (table 1.1). Although there have been a number of studies regarding cellular uptake of CPP's, the mechanisms are still not well defined, and so there is not yet a clear classification of CPPs based on the internalisation pathways. The mechanism of CPP uptake remains ambiguous, with reports diverging even when using the same peptide and different cells. What appears evident is that different peptides may utilize different uptake pathways.<sup>55</sup>



### ***1.3.1. Mechanisms for cellular uptake.***

Initial studies on CPP uptake mechanisms suggested that peptide internalization was not inhibited by reduction of cellular ATP, low temperature (4 °C), or inhibitors of endocytosis. Neither was internalization affected by peptide modifications such as retro-, enantio-, or retroenantio-analogues.<sup>56</sup> These studies suggested that CPP translocation consisted of direct transfer through the lipid bilayer of the cellular membrane. Derossi proposed a mechanism which involved the formation of inverted micelles,<sup>56</sup> with the cationic residues interacting with the negatively charged plasma membrane, consequent invagination of tryptophans into the membrane induced the formation of inverted micelles which can open on the inside or outside of the cell (A, Figure 1.12). This model seems to explain some aspects of CPP translocation and appears to hold for some peptides. A carpet model<sup>57</sup> (C, Figure 1.12), in which aggregates of peptides coat the cell surface and disrupt its structure, has also been proposed. While pore formation in the membrane is also possible (B, Figure 1.12), this mechanism can be ruled out by testing for membrane leakage of lactate dehydrogenase or propidium iodide staining.<sup>58</sup> Wender has proposed another non-endocytotic mechanism of uptake called adaptive translocation<sup>59</sup> (Figure 1.13), which involves the recruitment of negatively-charged cell surface constituents by the positively-charged guanidine rich CPP as the latter contacts a cell surface, transiently forming an ion pair complex with attenuated polarity that is able to adaptively diffuse into the membrane and subsequently into the cell. The driving force for the passage of this ion pair complex across the cell membrane is proposed to be the membrane potential.



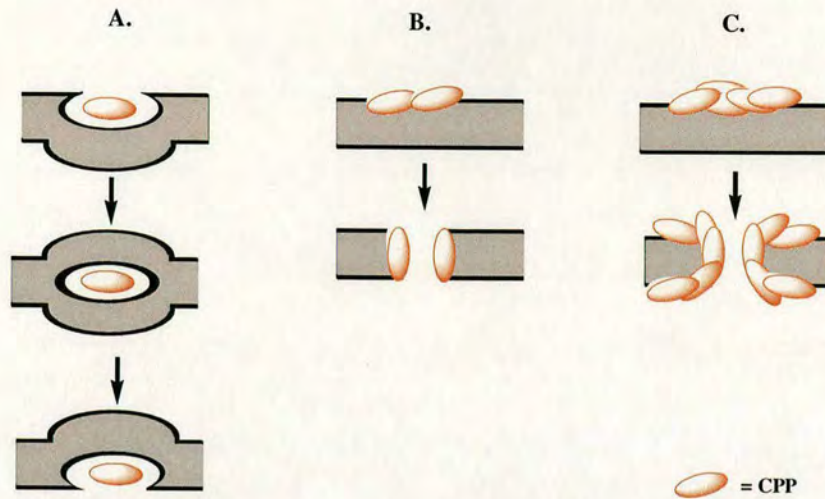


**Figure 1.12.** Uptake mechanism of CPP involving: (A) Inverted micelle formation, association of the peptide with the plasma membrane disturbs the lipid bilayer so that the inverted micelle is formed. (B) Pore formation, a limited number of peptides first assembles on the plasma membrane and then inserts into the lipid bilayer; further peptides are then recruited and a pore is formed. (C) Carpet model, peptides accumulate on the plasma membrane to the point where the integrity of the plasma membrane is breached and pores are formed. The lipid head groups are always oriented towards the peptide.

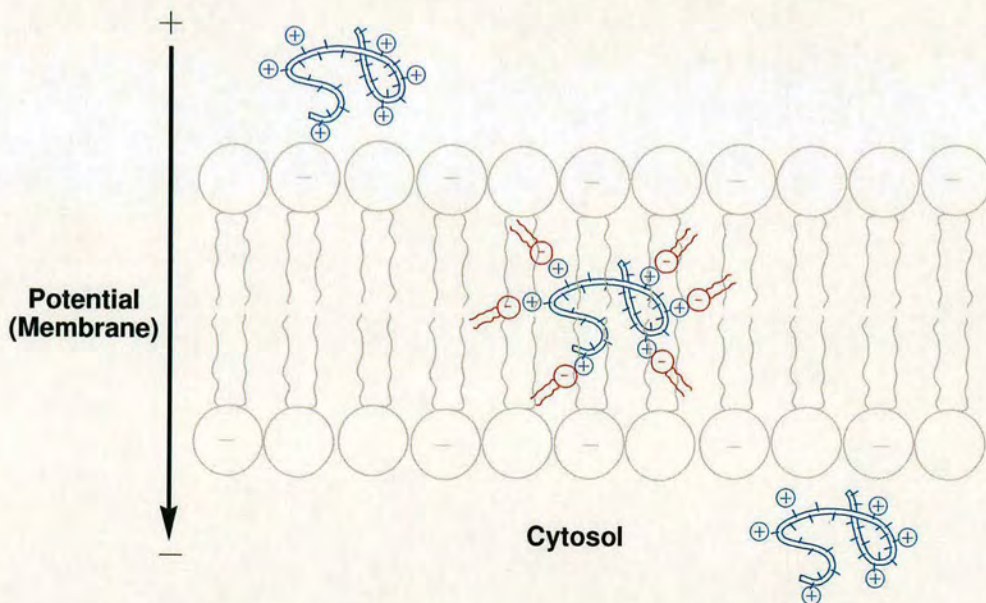


**Figure 1.13.** CPP uptake by adaptive translocation.

More recent studies, have shown that CPP translocation is mostly an energy-dependent process<sup>60</sup> and the proposed mechanism models involve extracellular heparane sulfate<sup>61</sup> and different types of endocytosis (Figure 1.14) such as



macropinocytosis, clathrin-dependent endocytosis, clathrin-independent endocytosis, caveole-dependent endocytosis and caveole-independent endocytosis.<sup>62,63</sup>

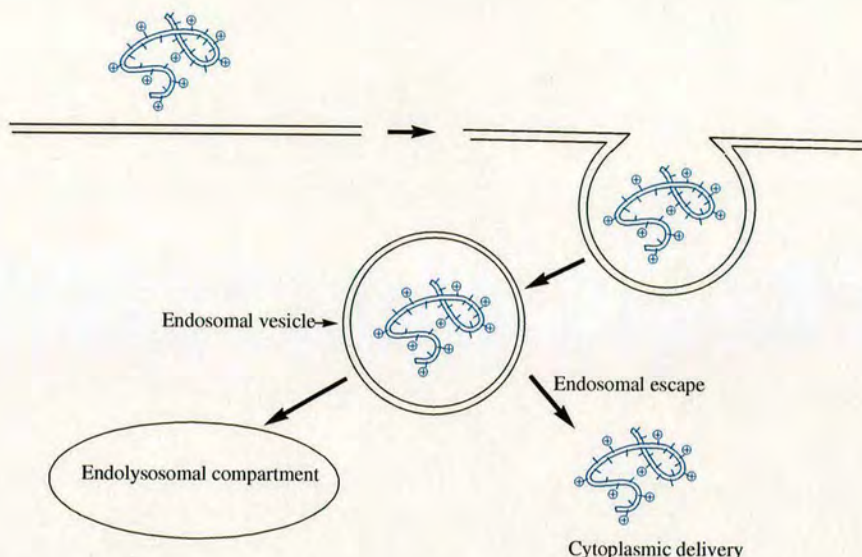


**Figure1.14.** Schematic representation of endocytic uptake of CPPs involving clathrin-dependent endocytosis, caveolin-dependent endocytosis, macropinocytosis, and clathrin (or caveolin) independent endocytosis. Endosomal escape is a crucial step for cytoplasmic delivery.

All these different models, derived by experimental observations, suggest that CPP translocation could be mediated by multiple different pathways simultaneously, or that different peptides use different uptake mechanisms depending on their biophysical properties and their cargo (Figure 1.15).<sup>64</sup>

### ***1.3.2. Factors influencing cellular uptake.***

The main interpretations of CPP indicate the endosomal pathway as the major route of uptake, although several reports show an uptake independent of endocytosis.<sup>55,65</sup> There are several factors that can influence the uptake mechanism such as size of the cargo, characteristic of the cargo (charge, interaction with the transporter to form complexes), temperature, as well as cell type.<sup>66</sup>

The *size of the cargo* attached to the transporter is one of the factors that affect the uptake mechanism. It has been shown that complexes or fusions of Tat with large 20 nm quantum dots or proteins (> 50 amino acids) enter cells primarily through an



endocytotic, vesicle-associated pathway, whereas a small peptide (< 50 amino acids) cargo can enter cells through a non-endocytotic pathway.<sup>67</sup> Conjugation of *negatively-charged amino acid* sequences to CPPs has been shown to dramatically reduce uptake with the CPP observed only inside endosomal vesicles, indicating the presence of an exclusive and limited endocytosis dependent uptake.<sup>68</sup>

A *temperature dependence* on the mechanism of uptake has also been demonstrated. While some studies have shown inhibition of uptake at 4 °C, others have proposed a temperature-independent mechanism for some CPPs translocation. A combination of two pathways has also been reported in the uptake study of Alexa488-R<sub>8</sub> (both L and D stereoisomers) into KG1a cells. At temperatures between 4 and 12 °C, fluorescence is observed in both the cytoplasm and the nucleus. At 12–30 °C, however, additional labeling is observed in endocytotic vesicles. Finally, when the cells are warmed to 37 °C fluorescence is observed solely in endosomal vesicles.<sup>69</sup>

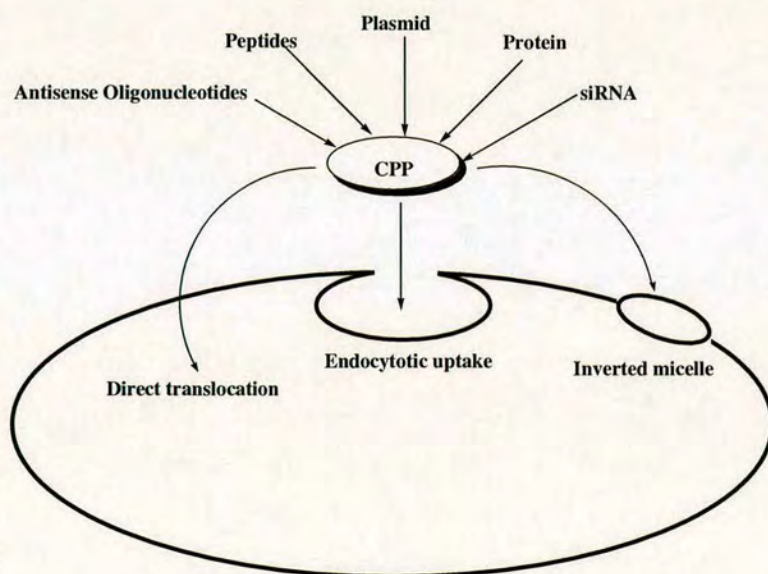


**Figure 1.15.** General representation of proposed uptake mechanisms for CPPs and examples of cargoes of interest.



### *1.3.3. Cationic CPPs.*

Regarding cationic CPPs, the kind of basic residues composing the peptide (such as lysine or arginine), has an important influence on uptake. Arginine rich CPPs have been shown to have a higher uptake than lysine and ornithine relatives.<sup>47</sup> The generally agreed first step of the translocation mechanism involving CPPs is the association of the transporter with the membrane (Figure 1.16). The positively-charged guanidinium head group features a specialized, rigid planar array of hydrogen bond donors that allows for highly effective bidentate hydrogen bonding (Figure 1.16) formation with negatively-charged carboxylates, phosphates, and sulfates which are components of many cell membrane constituents such as phospholipids, fatty acids, proteins, and heparan sulfate proteoglycans (HSPGs). Relative to the single hydrogen bond that would be possible with the ammonium group in lysine, the bidentate hydrogen bond network formed from guanidinium groups is stronger and thus has been proposed to provide structural rationalization for the differing abilities of oligolysines and oligoarginines to associate with and cross cellular membranes.<sup>47</sup> Obviously, the degree of protonation of the systems under assay conditions is another factor that could be of consequence, as oligomers of the more basic guanidinium group would be more protonated (have more cationic sites) relative to lysine analogs. To evaluate the influence of this bidentate hydrogen bond Wender<sup>59</sup> and colleagues studied the uptake properties of fluorescein labelled oligomers of arginine containing monomethyl- and dimethylguanidinium head groups (Figure 1.17). The monomethylated oligomer **1.2**, which was able to keep the charge but with a reduced ability to form a bidentate hydrogen bond, was 80% less effective than the unalkylated oligomer **1.1** (Figure 1.17). Dimethylated oligomer **1.3** (Figure 1.17), which was not able to form bidentate hydrogen bond, was 95% less effective than the unalkylated oligomer. These results indicated that although charge is necessary it might not be sufficient, and that hydrogen bond formation plays an important role in the uptake process.



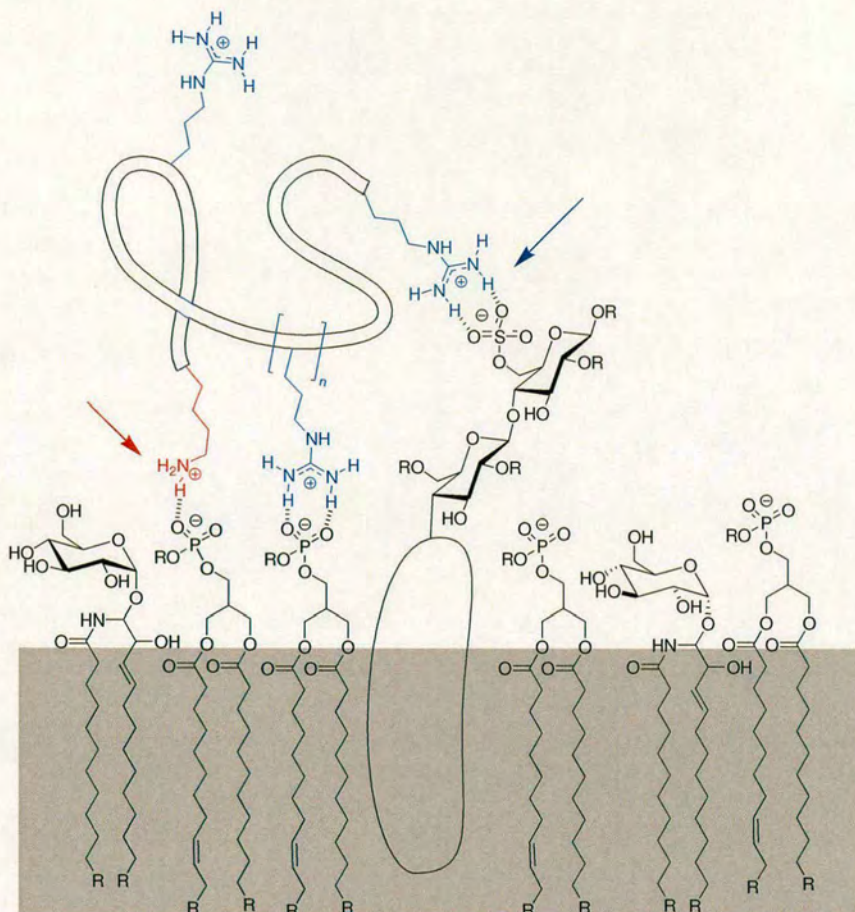
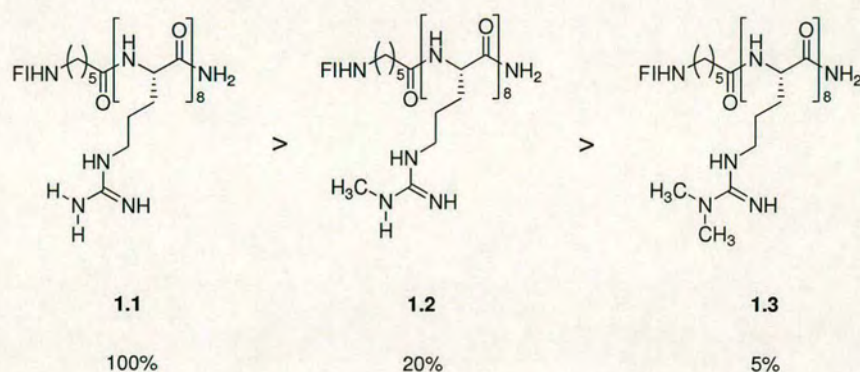


**Figure 1.16.** Proposed coordination of CPP to cell surface through hydrogen bonding: guanidinium ions form bidentate hydrogen bonding while ammonium ions only single hydrogen bonds. Counter ions not specified.



Relative Cell Penetration Efficiency

**Figure 1.17.** Cell penetration efficiency of oligomers of arginine containing monomethyl- and dimethylguanidinium head groups, compared to the efficiency of the corresponding unmodified oligoarginine (100% reference).



#### ***1.3.4. Targeted and enhanced delivery.***

CPPs are able to penetrate a very broad range of cell lines both *in vivo* and *in vitro*. This indiscriminate cellular uptake unfortunately restricts greatly the use of CPP as a pharmaceutical tool. However recent reports in targeted delivery have shown promising results.<sup>70,71</sup> Cell features such as extracellular receptors or proteases have been used to direct CPP uptake. CPP modification with the addition of cell specific ligands such as small molecules, vitamins, carbohydrates, other peptides or proteins (growth factors or antibodies) may improve targeted delivery. The intramolecular masking of a CPP by a negatively charged stretch of amino acids and proteolytic liberation of the active CPP at cancer cells that release a metalloproteinase is one elegant example of a combination of strategies.<sup>70</sup>

While most uptake studies have focused on cell entry, the ability of CPPs to enter tissue is of critical importance, and is required for the advancement of this class of molecular transporters toward therapeutic applications. Research into the tissue distribution of cell-penetrating peptides has yielded promising results with examples of CPPs penetration in kidney, liver, bone and muscle tissues.<sup>72-74</sup> An octaarginine transporter linked to Cyclosporin A has been advanced to phase II clinical trials for dermatological applications<sup>75</sup> and a Tat 9-mer linked to a biologically active peptide cargo has been advanced clinically for the treatment of ischemia.<sup>76</sup>

The **stability of the peptide vector** is another important aspect when considering *in vivo* delivery. It is important for the vector to stay intact until the target is reached, because in this way much less compound is required to achieve a sufficient delivery and thereby also minimizing possible side effects. The most common way to increase the peptide stability is the use of the D-form<sup>77</sup> instead of the L-amino acids. D-peptides are much more stable to proteases remaining intact for much longer time when injected *in vivo*. An alternative is the use of non-natural peptide mimics such as beta-peptides,<sup>78</sup> peptoids<sup>79</sup> and oligocarbamates<sup>80</sup> which as the D-peptides offer great stability to proteases (Figure 1.18). Interestingly peptoids have shown a cellular uptake consistently higher than the corresponding peptides. It has been suggested that this increased activity is a result of the increased lipophilicity of the peptoid backbone as determined by the attachment of the side chains to the amide backbone nitrogen which eliminates the polar N-H bond (Figure 1.18).<sup>81</sup>



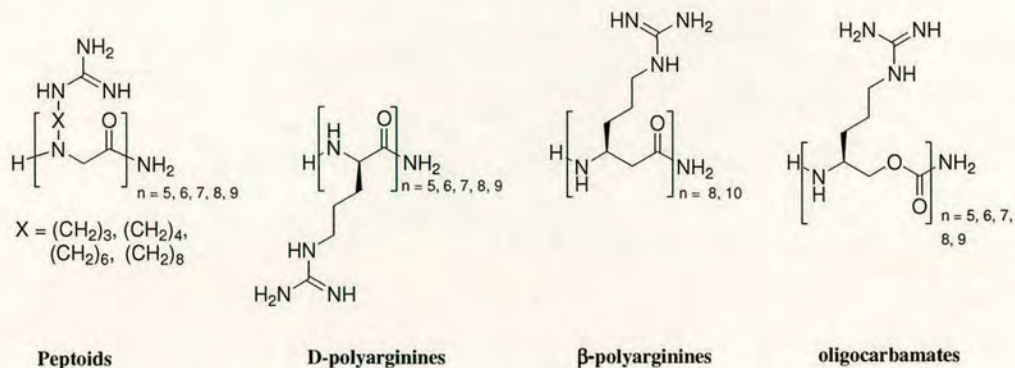


**Figure 1.18.** Cell penetrating peptide mimetics: Peptoids, D-peptides, β-peptides, oligocarbamates.

Another way to improve the delivery yield is the inclusion of specific functional groups in the CPP sequence. It has been reported that the addition of a 20 amino acids sequence from the pH-sensitive fusogenic peptide HA2 (derived from the influenza virus hemagglutinin protein) to a TAT-peptide fusion protein, gave a significant enhancement of protein uptake.<sup>82</sup> Fusogenic peptide HA2 is known to be able to destabilize lipid membranes at low pH and thereby to enhance endosomal escape which leads to improved delivery.<sup>83</sup>

### 1.3.5. Delivery of proteins.

Delivery of proteins using CPPs can offer many advantages compared to the traditional approach consisting in the endogenous expression of the desired protein from a plasmid, approach that presents complications connected with plasmid delivery (particularly *in vivo*) and possible varied protein expression in different cell lines. There are already several example of protein delivery mediated by CPP, including proteins involved in apoptosis,<sup>84</sup> cell cycle regulation and DNA recombination.<sup>82</sup> The protocol most frequently used consists of designing a plasmid encoding for the CPP in the coding frame with the desired protein, producing in this way a cell permeable fusion protein.<sup>85</sup> However, addition of a highly cationic portion to proteins chain may interfere with the protein tertiary structure and cause loss of biological activity. This problem can be overcome using CPP able to form a noncovalent complex with the protein, facilitating its cellular uptake without compromising the native structure and thus biological properties of the protein.<sup>52</sup>



### 1.3.6. Delivery of siRNA and other oligonucleotides.

There are many reports regarding the CPP mediated delivery of oligonucleotides (ON) into several cell lines both in vitro<sup>86</sup> and in vivo<sup>87</sup>. These include CPP delivery of antisense –PNA,<sup>87</sup> DNA decoy-ON,<sup>88</sup> siRNA,<sup>89</sup> and plasmids.<sup>90</sup> Gene silencing (Figure 1.19), especially by siRNA, has emerged as a powerful tool in recent years. As for many other bioactive compounds, one of the major obstacles for the application of siRNA is the delivery across the plasma membrane. Only few peptides have been shown to improve siRNA uptake and down regulation of the desired gene. CPP and oligonucleotides (antisense ON, siRNA, RNAi) have been covalently linked (disulfide bond<sup>39</sup> is widely used) or just incubated together to form a complex through electrostatic interactions.

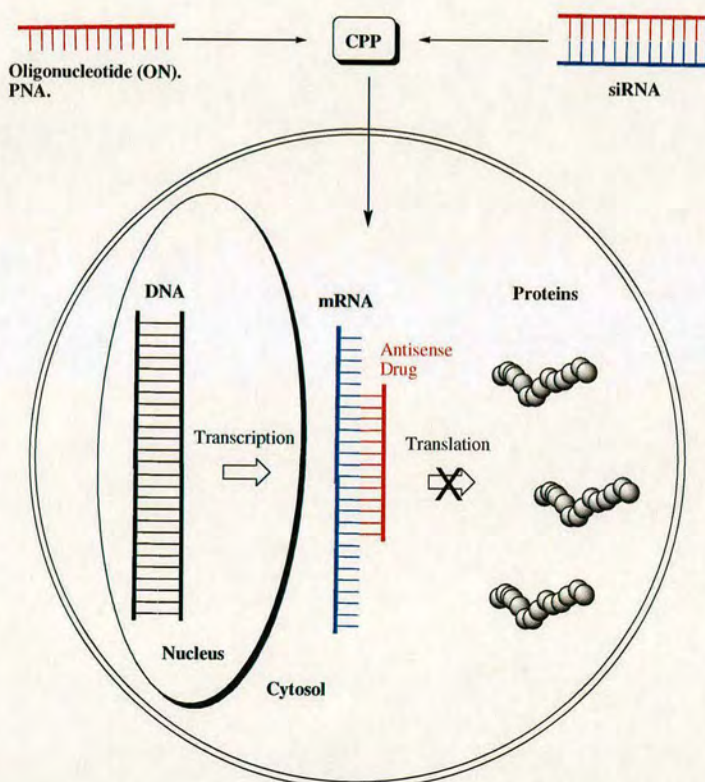


**Figure 1.19.** Gene silencing using CPPs to deliver antisense compounds such as DNA (antisense oligonucleotides), PNA and siRNA.



### ***1.3.7. Commercially available CPPs.***

Over the last few years biotech companies have shown increasing interest in CPPs and today some CPPs are commercially available. One of the most famous is the **Chariot system**, known as Pep-1,<sup>52</sup> (table 1.1, page 16), a carrier with the remarkable characteristic that efficient import of cargo molecules does not require covalent linkage, but instead, it forms noncovalent complexes with its cargoes. Pep-1 is a 21 amino acid peptide, consisting of an 11 amino acid hydrophobic motif containing five tryptophan residues (ETWWETWWTEW) and a second domain corresponding to the NLS (PKKKRKV) of the SV-40 large T antigen, linked through a three amino acids spacer. The first domain interacts with macromolecular cargoes and is required for efficient “targeting” of the complexes to the plasma membrane. The NLS improves the intracellular delivery and solubility of the peptide. Pep-1 has been applied successfully to the delivery of proteins, peptides, and PNAs into mammalian cells. It was shown that membrane crossing of Pep-1 involves formation of a transient transmembrane pore-like structure.

**SynB vectors**<sup>50,51</sup> (from Syntem) are an other example of commercially available CPPs. This family of vectors is derived from the antimicrobial peptide protegrin 1 (PG-1, table 1.1), an 18 amino acid peptide originally isolated from porcine leucocytes. These vectors have been applied to the delivery of two famous anti-cancer drugs: doxorubicin and camptothecin.

**Express-si** (silencing) is a CPP delivery vector for siRNA and oligonucleotides which is based on the MPG peptide<sup>49</sup> (table 1.1). MPG, as described for Pep-1, has the characteristic that efficient import of cargo molecules does not require covalent linkage, forming noncovalent complexes with the cargoes. MPG is composed of 17 amino acid derived from the fusion sequence of HIV-1 gp41, a 3 amino acid spacer, a 7 amino acid nuclear localization sequence (NLS) of SV40 large T antigen, and a C-terminal cysteine amide. It was proposed that translocation proceeds through the transient formation of a transmembrane pore-like structure.



## Chapter II. Peptoid synthesis.

### II.1. Peptidomimetics.

Libraries of oligomeric biomolecules based predominantly on peptides (or proteins) and nucleic acids have been used to investigate and probe a variety of biological processes<sup>91,92</sup>, as for example to map epitopes for antibody binding<sup>93</sup>, to discern ribonucleotide sequences with specific binding<sup>94</sup> or catalytic activity<sup>95</sup> (as aptamers), and to provide initial leads in receptor-based assays<sup>96,97</sup>. Key positive features of these oligomeric systems are the virtually limitless number of compounds that can be generated and the ease with which these oligomers can be made. However such compounds suffer metabolic instability and often poor oral absorption, with the result that any promising material will require extensive modification before any possible application *in vivo*.

These limitations of natural oligomers have suggested that alternative systems which present the same advantages of modularity and ease of the synthesis but which offer metabolic stability could be highly attractive. An important number of systems have been developed for the synthesis and study of peptides analogues which offer markedly different chemical structures and chemical stabilities. A peptide analogue, or peptidomimetic, is generically defined as a substances having a secondary structure as well as other structural features analogous to those of the original peptide (allowing it to displace the original peptide from its receptor) but no longer has classical peptide characteristics, such as enzymatically scissile peptidic bonds.

A large number of peptidomimetic systems have been developed and adapted to solid phase synthesis. This includes,  *$\beta$ -peptides*, *oligomers of N-substituted glycines* (or *peptoids*), *sulfonamidopeptides*, *oligourea peptidomimetics* (Figure 2.1) and many others.<sup>98,99</sup>



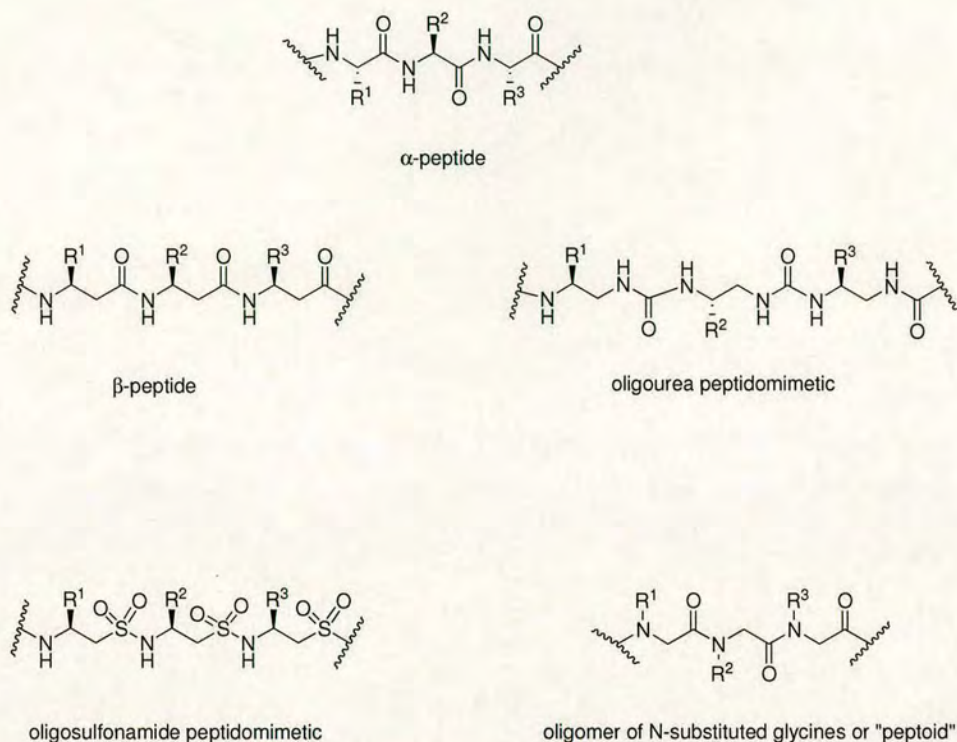


**Figure 2.1.** Structure of:  $\alpha$ -Peptides,  $\beta$ -peptides, Oligomers of N-substituted glycines (or Peptoids), Sulfonamidopeptides, Oligourea peptidomimetics.

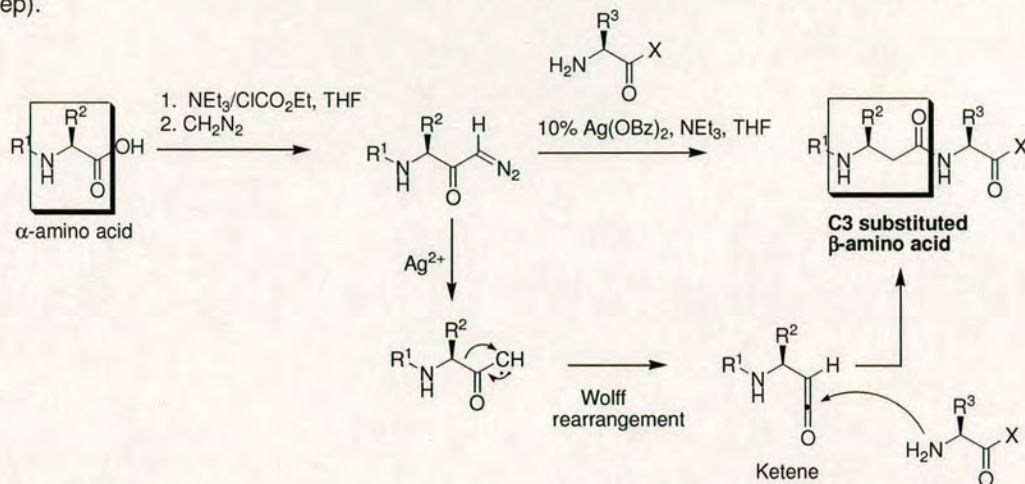
### II.1.1. $\beta$ -Peptides.

$\beta$ -Peptides<sup>100-104</sup> have particular appeal because  $\beta$ -amino acids represent one of the smallest step away from classical amino acids in terms of "backbone space". Like  $\alpha$ -peptides,  $\beta$ -peptides contain amide bonds capable of forming, and stabilizing, intramolecular hydrogen bonds. A large body of structural and synthetic work has laid a solid groundwork of investigations into  $\beta$ -peptides. C3-substituted  $\beta$ -amino acid may be prepared by homologation of  $\alpha$ -amino acids<sup>105</sup> and by a number of other practical routes,<sup>106,107</sup> providing a convenient and highly diverse source of monomers. C2-substituted  $\beta$ -amino acids are not accessible from  $\alpha$ -amino acids and they can be prepared using different enantioselective methods,<sup>106</sup> as for example Evan's enolate chemistry<sup>105,106</sup> (Scheme 2.1). Early investigations onto polymeric  $\beta$ -peptides indicated that they were able to adopt stable helical structures, although the precise helix geometries have been challenging to elucidate.<sup>108,109</sup> Secondary sheet structures

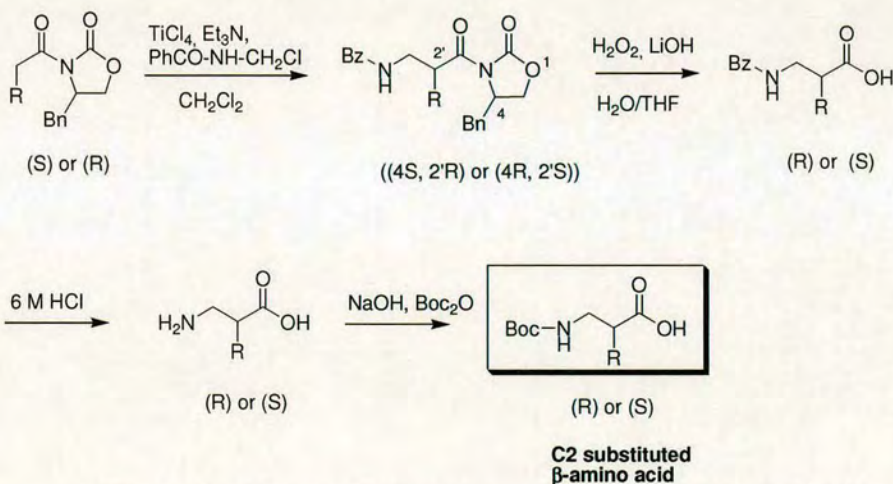


have also been proposed for  $\beta$ -amino acid polymers.<sup>110-112</sup> There have been extensive studies on the structures of cyclic peptides containing  $\beta$ -amino acids.<sup>113-115</sup>

C3 substituted  $\beta$ -amino acids: Arndt-Eistert homologation (combined to peptide coupling step).



C2 substituted  $\beta$ -amino acids: Evan's Enolate.



**Scheme 2.1.** Methods for the preparation of protected  $\beta$ -amino acids.<sup>105,106</sup>

### II.1.2. Sulfonamide peptides.

Among the promising surrogates which can be considered for the replacement of the native amide bond of peptides, a particular place should be reserved for sulfonamido polymers. Sulfonamides are metabolically stable, can effectively interact through hydrogen bond formation (a stronger hydrogen bond donor but a weaker hydrogen



bond acceptor) and adopt secondary structures. Several 'β-sulfonopeptides' inhibitors have been prepared and studied (Figure 2.2).<sup>116-118</sup>

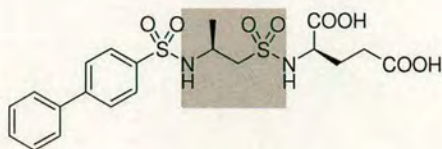
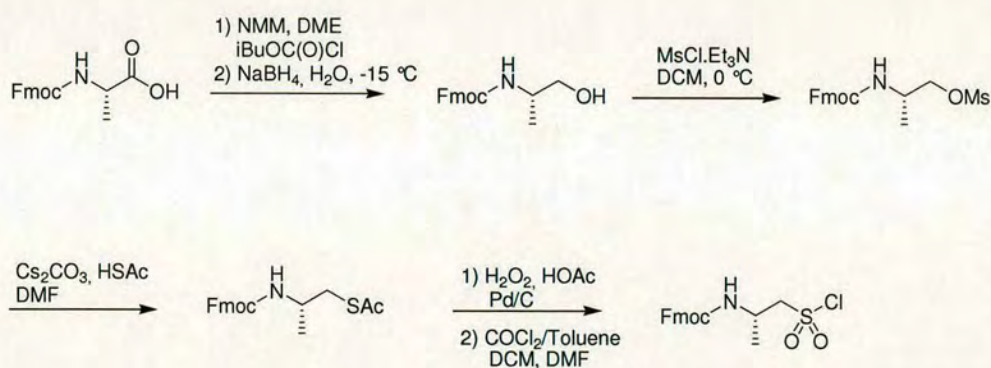


**Figure 2.2.** Inhibitor of bacterial peptidoglycan biosynthesis enzyme MurE.<sup>118</sup>

Originally β-peptidosulfonamides were synthesized by the reaction of a β-amino-ethanesulfinyl chloride with an amine and subsequent oxidation to the sulfonamide.<sup>119,120</sup> The oxidation step did not always result in high yields and was difficult to optimize for use in solid phase synthesis. To circumvent this problem different approaches based on Boc<sup>121,122</sup> or Fmoc<sup>122</sup> protected β-amino-ethanesulfonyl chlorides have been developed (Scheme 2.2).



**Scheme 2.2.** Synthesis of Fmoc protected β-amino-ethanesulfonyl chlorides.<sup>122</sup>

### II.1.3. *Oligourea peptidomimetics.*

In the field of peptide mimetics, the urea moiety as a non-peptide linkage has attracted much attention. The urea fragment is promising for drug discovery and biomedical applications because of its expected resistance to protease degradation and interesting hydrogen bonding properties.<sup>123-125</sup> In the solid state, *N,N*-disubstituted ureas are often involved in self-complementary bidirectional intermolecular hydrogen

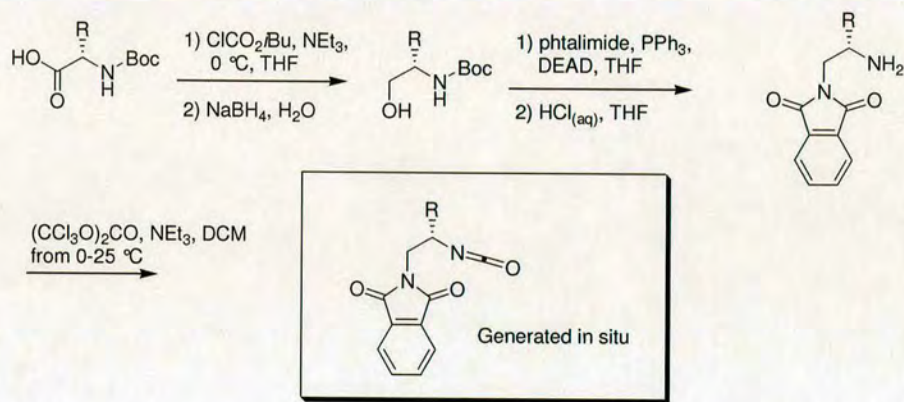


bonds because of the *trans* geometry of the two amide bonds (*Z,Z* conformer).<sup>126-128</sup>

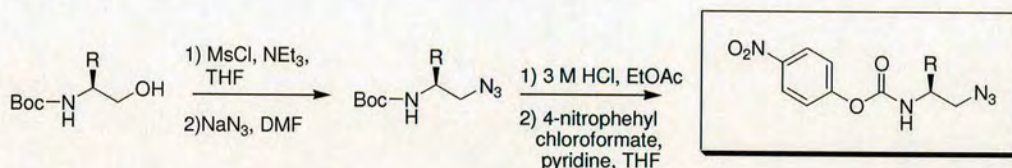
Self-organization at the molecular level has also been documented.<sup>128,129</sup>

Burgess and coworkers<sup>130,131</sup> were the first to describe the solid-phase synthesis of oligourea peptidomimetics, employing phthalimido-protected isocyanates as monomers. Subsequently, Schultz and co-workers<sup>132</sup> developed a procedure using azido 4-nitrophenyl carbamate monomers. More recently Liskamp and others reported protocols for the solid phase synthesis of oligoureas using Boc<sup>133</sup> protected and Fmoc<sup>134</sup> protected monomers (Scheme 2.3).

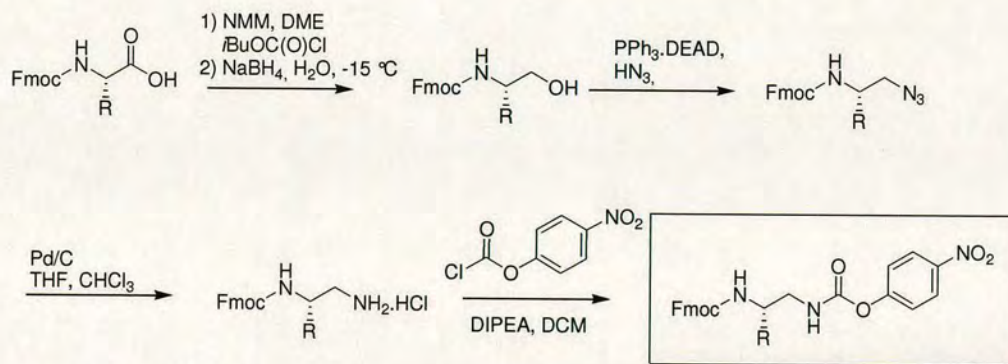
Burgess' phthalimido-protected isocyanates monomers for solid phase synthesis of oligourea peptidomimetics:



Schultz's azido 4-nitrophenyl carbamate monomers for solid phase synthesis of oligourea peptidomimetics:



Liskamp's Fmoc protected monomers for solid phase synthesis of oligourea peptidomimetics:

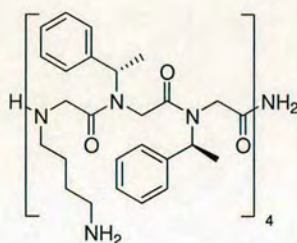


**Scheme 2.3.** Monomers for solid phase synthesis of oligourea peptidomimetics.



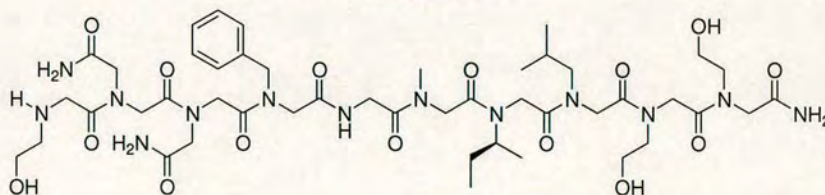
## II.2. Peptoids.

Oligomers of N-substituted glycines or Peptoids<sup>135</sup> are N-alkylated glycine derivatives in which the amino acid side chains are shifted from the  $\alpha$ -carbon to the  $\alpha$ -amino functionality. A variety of applications of this class of compounds in medicinal chemistry<sup>136</sup> has been described in the literature: as protease resistant entities,<sup>137</sup> as antimicrobial agents<sup>138</sup> (**2.1**, Figure 2.3), as inhibitors of protein – protein interactions<sup>139</sup> (**2.2**, Figure 2.3), and artificial protein mimics<sup>140</sup>. Peptoids are non-chiral peptidomimetics, except for the chirality found in any side chain. Moreover, the absence of hydrogen bond donors in the peptoid backbone (except for glycine) and the flexibility of the backbone, due to the presence of tertiary amides which induce cisoid conformations, should abrogate the tendency to form (anti)parallel  $\beta$ -sheets.



**2.1**

Peptoid mimic of Magainin-2 amide.  
Antibacterial.



**2.2**

Peptoid mimic of Amylin (20-29).  
Amyloid inhibitor,  $\beta$ -sheet breaker.

**Figure 2.3.** Bioactive peptoids.

Translation of a peptide sequence may result either in a N-alkylated polyglycine (direct translation) or in a retropeptoid (retrosequence) as is shown in Figure 2.4. In the retropeptoids, the relative orientation of the carbonyl groups to the side chains is maintained and bares better resemblance to the parent peptide, and this may be



responsible for the slightly better biological activities of retropeptoids.<sup>141</sup> In terms of nomenclature peptoid monomers corresponding to natural amino acids are indicated with an N before the name of the natural amino acid, so for example the corresponding monomer for Arg is written NArg.

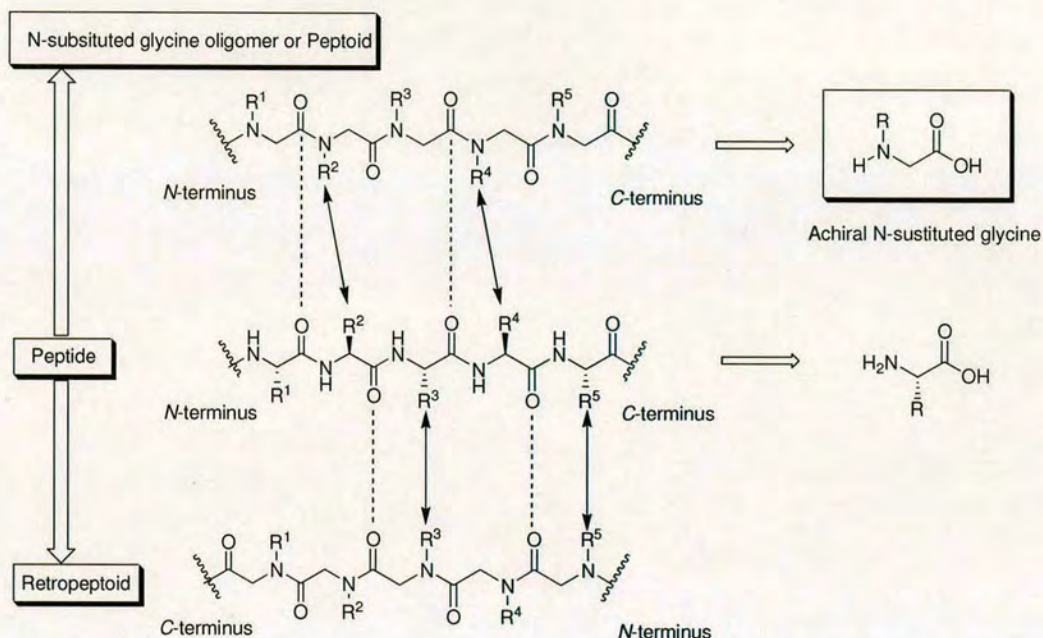


**Figure 2.4.** Translation of a peptide in an N-alkylated polyglycine (direct translation) or in a retropeptoid (retrosequence).

Peptoids are synthesized following two main synthetic routes:

1. Monomer based synthesis (Zuckermann 1992).<sup>135</sup>
2. Sub-Monomer based synthesis (Zuckermann 1992).<sup>142</sup>

### ***II.2.1. Monomer based peptoid synthesis.***

The first synthesis of peptoids<sup>135</sup> was described in 1992 by Zuckermann, who defined five main desirable attributes for any potential substitute to natural oligomers:

1. The monomers should be straightforward to synthesize in large amounts.
2. The monomers should have as broad as possible variety of functional groups as side chains “hanging off” the oligomeric backbone.



3. The linking chemistry should be high yielding and amenable to automation.
4. The linkage should be resistant to hydrolytic enzymes.
5. The monomers should be achiral.

From the analysis of the peptoid structure (Figure 2.4) it is possible to identify the following characteristics:

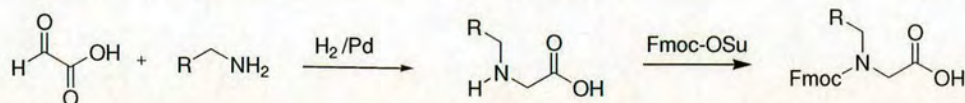
1. Peptoid monomers are achiral (unless R is chiral).
2. A wide range of possible side chain should be easily accessible. (see later)
3. Peptoids are polyamides.
4. Non natural amide bonds are resistant to hydrolytic enzymes.<sup>137</sup>
5. Monomers synthesis readily achievable. (see later)

Thus offering all the 5 desirable properties highlighted by Zuckermann.

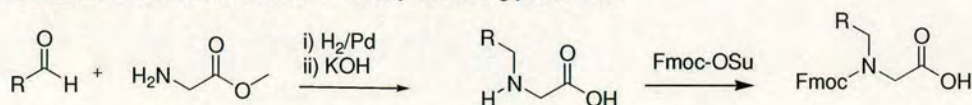
### 2.1.1. Monomers Synthesis.

Fmoc protected N-substituted glycines can be prepared by a number of routes, depending mainly on the needs and desirable properties of the side chain (Scheme 2.4).<sup>135</sup>

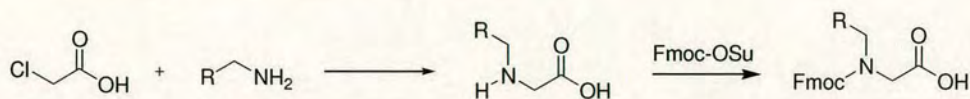
A) Reductive amination of a "side chain" amine with glyoxylic acid.



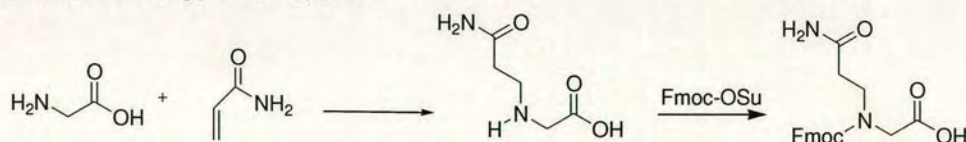
Reductive amination of a "side chain" aldehyde with a glycine ester.



B) Alkylation of a "side chain" amine with chloroacetic acid.



C) Michael addition of glycine to acrylamide.



**Scheme 2.4.** Three synthetic routes towards Fmoc protected N-substituted glycines. All "side chain" R functionalities are protected.

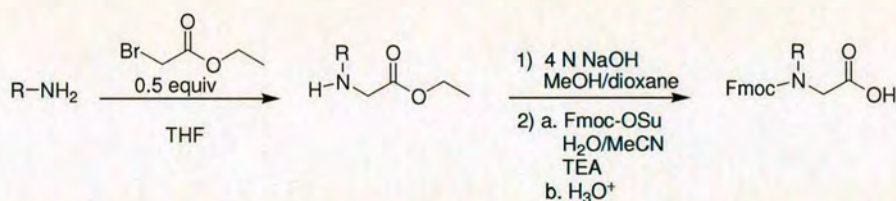


The three main routes being:

- (A) Reductive amination of a side-chain amine with glyoxylic acid, or of a “side-chain” aldehyde with a glycine ester.
- (B) Alkylation of a “side chain” amine with chloroacetic acid.
- (C) Michael addition of glycine to acrylamide.

In all these strategies the “side-chain” functional groups need to be protected. With amino, carboxyl, hydroxyl, indole, guanidine and imidazole moieties protected using the standard protecting groups (t-Butyl, Pmc, Trityl) typically employed in Fmoc based peptide synthesis.

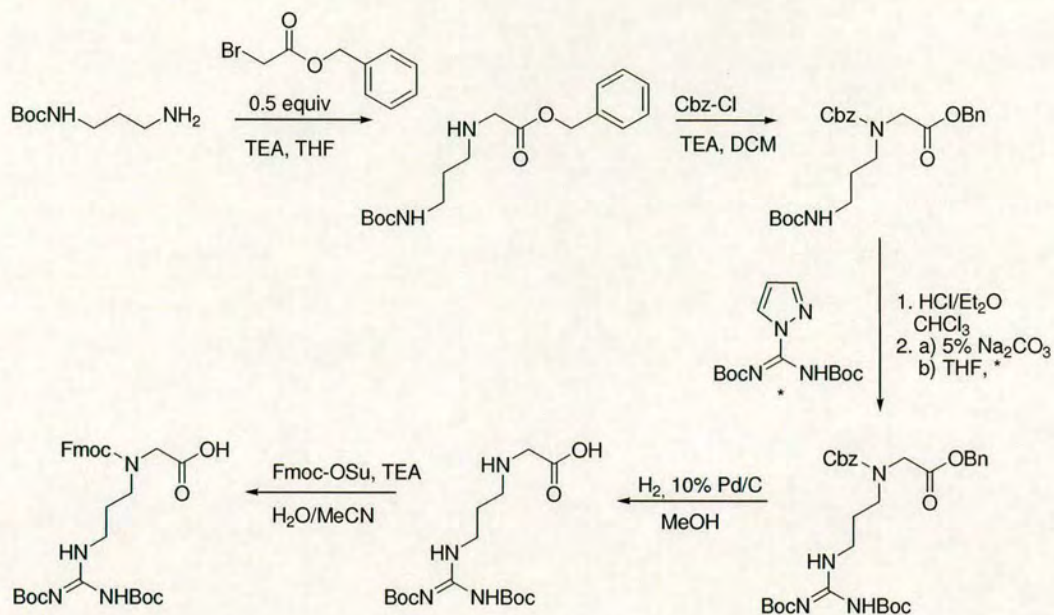
Other routes to these monomers have since been developed. Thus for example Liskamp synthesised the monomers from ethyl bromoacetate *via* alkylation with different amines (Scheme 2.5).<sup>143</sup> The resulting N-substituted glycine ethyl esters were easy to purify by column chromatography (unlike the corresponding free acids). The N-alkylated glycine esters could then be treated with NaOH, to give the corresponding sodium salts prior to Fmoc protection.



**Scheme 2.5.** Liskamp's synthesis of Fmoc protected peptoid monomers.

Liskamp also reported a modification to this protocol for the synthesis of the NArg monomer.<sup>141</sup> Thus ethyl bromoacetate was substituted with benzyl bromoacetate (Scheme 2.6) used to alkylate *N*-Boc-1,3-diaminopropane with the amino group of the resulting *N*-alkyl glycine benzyl ester protected with a Cbz group. The side-chain amine was deprotected selectively under acidic conditions and the free amine subjected to guanylation with *N,N'*-bis(Boc)-1-guanylpurazole to give Cbz-NArg(Boc)<sub>2</sub>-OBn. The benzyl ester and Cbz group were removed by hydrogenolysis (over 10% Pd/C), followed by Fmoc protection of the free amine to give Fmoc-NArg(Boc)<sub>2</sub>-OH.



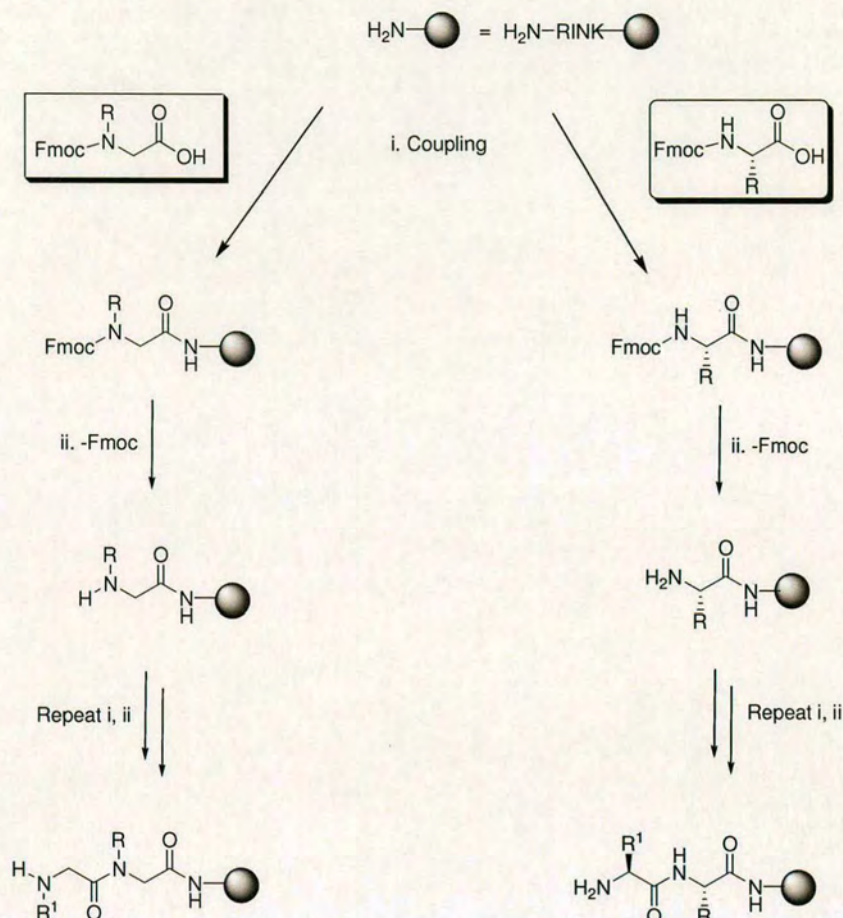


**Scheme 2.6** Synthesis of Fmoc-Narg(Boc)<sub>2</sub>-OH by Liskamp.

### 2.1.2. Peptoid oligomerization.

The oligomerization process is based on the same protocols adopted for peptide chemistry (Scheme 2.7); the only relevant difference is that the couplings involve secondary amines. It is known that N-alkylamino acids often couple poorly under standard conditions,<sup>144</sup> a problem that can affect yield and purity for this particular kind of oligomers, and to minimize this problem standard carbodiimide coupling reagents have often been substituted with PyBOP and PyBrOP, developed for the coupling of hindered or  $\alpha$ -disubstituted amino acids.<sup>145,146</sup> All the other steps, such as Fmoc deprotection and cleavage, were carried out following the usual conditions for peptide synthesis.



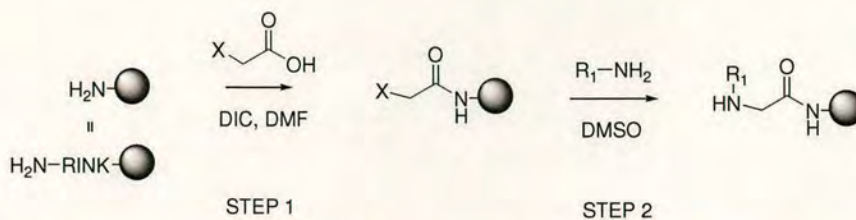


**Scheme 2.7.** Peptoid synthesis vs. Peptide synthesis.

### ***II.2.2. Sub-monomer based peptoid synthesis.***

Immediately after the monomer based synthesis a second synthetic strategy for the preparation of peptoids called “sub-monomer” approach was proposed by Zukerman.<sup>142</sup> Each N-substituted glycine unit was assembled directly on the solid phase using two sub-monomer units: a haloacetic acid and a primary amine. From this perspective the oligomer could be considered as an alternating condensation of the two sub-monomers (Scheme 2.8).





**Scheme 2.8.** Monomer assembly cycle: Acylation (STEP 1), Nucleophilic displacement (STEP 2).

Each monomer was thus added during a two step cycle consisting of an acylation with bromo acetic acid and alkylation of an incoming amine (Scheme 2.8).

The **acylation** (first step) was carried out by activation of the haloacetic acid (Br) with a carbodiimide. Although the acylation of a secondary amine can be difficult, in particular with bulky amino acids, this problem was “minimised” by the use of haloacetic acid which, in the presence of a carbodiimide, are very effective acylating agents.

The **nucleophilic displacement** (second step) introduced the side chain by displacement of the halogen using an excess of a primary amine, with any side-chain groups protected to avoid any secondary reactions. The efficiency of the displacement was also dependent on the halide used in the first step. When reacted with aniline the reported efficiency order of displacement was:  $I \geq Br \gg Cl$ . Zuckerman and colleagues reported that the optimized conditions for displacement of the bromide using *n*-butylamine and cyclopropylamine were 16 equiv (1 M) and 40 equiv (2.5 M) respectively, but due to the solid phase nature of the synthesis the amine in excess was readily washed away. The complete cycle of acylation and nucleophilic displacement, took around 3 h for each “monomer” added.

### 2.2.1. Microwave heating.

In an effort to improve the efficiency of the sub-monomer based peptoid synthesis approach, Kodadek and colleagues investigated the application of microwave irradiation to accelerate the acylation and amination reactions (Scheme 2.9).<sup>147</sup> Acylation was performed with bromoacetic acid (with 1 equiv DIC) at a concentration of 1 M. All the amines were used at a concentration of 1 M. The peptoids were prepared at room temperature, at 37 °C (with conventional heating) and under microwave irradiation (100 W, 2 x 15 s,  $T_{\max}$  around 35 °C). The efficiency of







longer reaction times: 60 min for acylation (2 x 30 min), and 2 h for amine displacement.

The work from Kodadek showed how microwave assisted protocols could be applied successfully to peptoids synthesis using a sub-monomer approach. Unfortunately this was done using a domestic microwave oven, which is potentially dangerous and no longer publishable in most journals due to safety and reproducibility issues. Blackwell and co-workers<sup>148</sup> in 2005 decided to transfer Kodadek's microwave assisted synthesis to a commercial microwave reactor (Milestone Ethos Microsynth multimodal microwave reactor), as the latter systems provide consistently safer and more reproducible microwave methodology. The first attempt to reproduce Kodadek's synthesis<sup>147</sup> (100 W, 30 s per step, 1 M solutions) on identical substrates (homonomers of **2.3-2.5**, Scheme 2.9) gave peptoid products with irreproducible purities and lower yields. More interestingly, their control experiments at room temperature with these unhindered primary amines provided homo 9-mer peptoids with high and reproducible purities with a reaction time of 30 s (1 M solution). The unhindered primary amines did not require neither MW heating nor the standard 3 h room temperature reaction time, allowing the monomer construction to proceed in just 1 min. Continuing their investigation they decided to test the microwave assisted synthesis with electronically deactivated and sterically hindered amines (**2.7-2.11**, Scheme 2.9). The best conditions found were: Acylation, 2 M bromoacetic acid (DIC, 2 M) in DMF, 30 s, 35 °C; Amination, 1 M amine in DMF, 90 s, 95 °C.

The microwave conditions gave some improvement for the amine with some steric hindrance (**2.7**, **2.8**), with a 10% purity enhancement relative to the 25 °C control. However with a reduced steric hindrance of the amine (**2.9**, **2.10**) the microwave conditions gave no significant improvement relative to the 25 °C control. The microwave conditions proved to be much more advantageous for deactivated amines, as for 1-(pentafluorophenyl)ethylamine (**2.11**) with purities doubled from 22% (room temperature) to 56% (microwave conditions).

The results presented by Blackwell indicate that in the absence of sterically or electronically deactivated amines, peptoids can be generated with much reduced reaction times: acylation 30 s, amination 90 s, driven by the use of large excesses of reagent.



### II.2.3. Monomer approach vs sub-monomer approach.

Table 2.1 shows the advantages and drawbacks associated with the two strategies:

Sub- monomer.	Monomer.
<b>Advantages.</b>	<b>Advantages.</b>
No synthesis of protected building block.	Application of standard peptide synthesis .
Large availability of primary amines (not requiring side protection).	Synthesis on solid phase monitored by dibenzofulvene adduct.
Haloacetic acids in presence of carbodiimides are effective acylating agents for secondary amines.	Automation.
<b>Drawbacks</b>	<b>Drawbacks</b>
Large excesses of reagents (amines up to 40 equiv)	Synthesis of protected building blocks in considerable quantities
Completion of acylation and substitution reactions cannot be determined	Need of expensive coupling reagents as PyBrOP or PyBOP

**Table 2.1.** Monomer vs. Sub-monomer strategy.

The *sub-monomer approach* is very attractive. It does not require the synthesis of the building blocks (except the protection of the side chain when required) and the ready availability of primary amines gives it an enormous potential for the creation of libraries of compounds.

It has been shown that with unhindered primary amines the synthesis can be carried out very rapidly at room temperature (1 residue per minute as reported by some authors). In the case of deactivated amines, microwave assisted protocols can be employed to sensibly increase the purities of crude compounds.



However this incredible flexibility has some important limitations. Firstly the synthesis requires a large excess of material up to 40 equiv, with concentrations of primary amine (or haloacetic acid) solutions up to 2 M. Also completion of the acylation and substitution reactions cannot be determined, and this is essential for the preparation of larger peptoids of reasonable purity.

The *monomer approach* has the immediate advantage of the analogy with peptide synthesis. The synthesis requires a limited amount of material (4-5 equiv) per residue, while the use of Fmoc protected monomers allows monitoring of the synthesis on solid phase by quantifying the dibenzofulvene adduct obtained from the cleavage of the Fmoc group. The synthesis can be carried out on a automated peptide synthesizer applying the same protocols used for peptides giving easy access to longer peptoids. But also this approach has important limitations. The most immediate is that the monomers are not commercially available and each of them has to be synthesised. As a consequence the use of large libraries of different monomers is limited, in particular if compared to the direct use of “naked” primary amines. Another relevant aspect is the general lack of reactivity of secondary amines in the amide bond formation, and conventional carbodiimide coupling reagents as DIC may not be efficient.

The “sub-monomer strategy” is potentially the best choice for the synthesis of large libraries of small peptoids (3-5 residues) for two main reasons: easy access to extremely different primary amines and the acceptable purity of the crudes for testing. However “the monomer approach” appears to be a better choice for the synthesis of longer peptoids with defined purity.



## II.3. Cell penetrating peptoid transporter.

### II.3.1. Peptoid monomer synthesis.

The synthesis of the peptoid monomer *N*-Fmoc-*N*-(6-*N*'-Boc-aminohexyl)-glycine (**2.12**) was reported by Peretto.<sup>149</sup> The synthesis (Scheme 2.10) was based on the protocol described by Liskamp (see earlier). Mono-Boc protected 1,6-hexanediamine was reacted with ethyl bromoacetate (1 equiv) to give the corresponding *N*-substituted glycine ethyl ester (55% yield). Saponification of the ester and final Fmoc protection in aqueous conditions (pH 9) gave the peptoid monomer *N*-Fmoc-*N*-(6-*N*'-Boc-aminohexyl)-glycine in 40 % yield over the 2 steps.

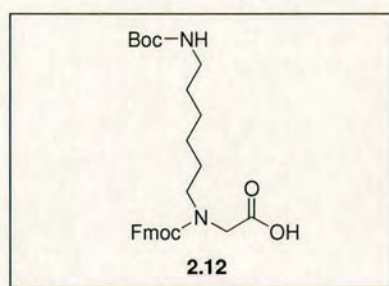
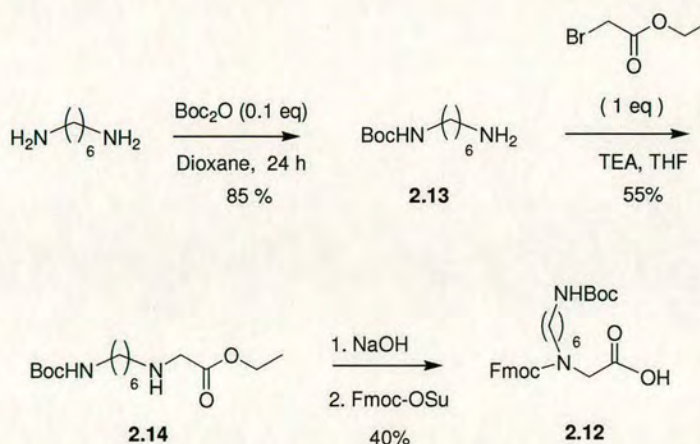


Figure 2.5

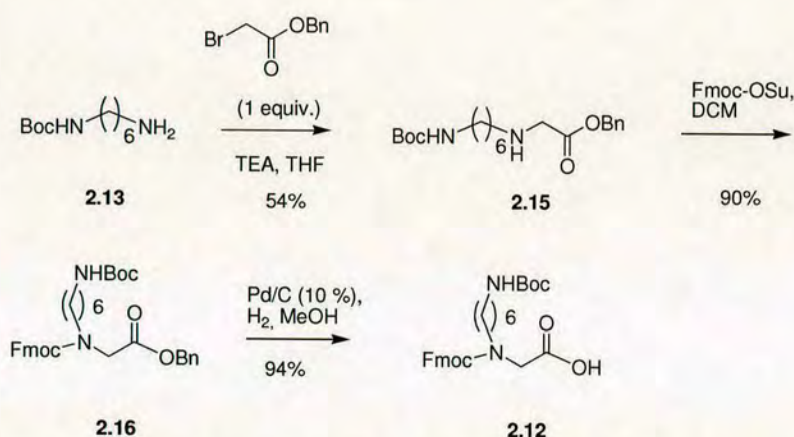
This synthesis was repeated and the yields obtained were consistent with those reported. In contrast the yields reported by Liskamp<sup>141</sup> on a similar substrate (1,4-diaminobutane) were generally much higher (alkylation around 75%, Fmoc protection around 95%).



Scheme 2.10. Synthesis of peptoid monomer **2.12** reported by Peretto.<sup>149</sup>



The lower alkylation yield was not surprising as Liskamp used an excess of primary amine (2 equiv) while in the protocol reported by Peretto the primary amine and the bromoacetate were equimolar, conditions in which dialkylation reduce the desired product. More difficult to explain were the differences in efficiency of the Fmoc protection which was carried out under aqueous condition at controlled pH (pH 8-9). A new approach was thereby developed to allow the monomer to be prepared on a 20-30 g scale.<sup>150</sup> The strategy was based on the Fmoc protection of an N-substituted glycine ester, not the acid, using organic solvents under more controlled conditions, and final conversion of the Fmoc protected ester into the corresponding acid (Scheme 2.11). To do so required an ester functionality that could be removed compatibly with the presence of Boc and Fmoc groups.



**Scheme 2.11.** Synthesis of peptoid monomer **2.12**.

The benzyl ester was chosen because it can be converted into the corresponding acid under mild conditions by simple hydrogenolysis, compatibly with Boc and Fmoc functionalities. Thus ethyl bromoacetate was replaced with benzyl bromoacetate which was alkylated to give the N-substituted glycine benzyl ester **2.15** (54% yield). Fmoc protection was carried out in DCM using Fmoc-OSu (1.1 equiv), with a 90% isolated yield. Conversion of the benzyl ester **2.16** into the corresponding acid **2.12** was carried out by hydrogenolysis (Pd/C 10%, 0.1 equiv) giving after filtration the peptoid monomer in 94% yield (100% purity by ELS analysis). As reported earlier a similar use of the benzyl ester functionality was described by Liskamp (see Scheme 2.6), however in his protocol the benzyl ester was converted into the corresponding



acid before the Fmoc protection step, which was still carried out in aqueous conditions (pH 8-9).

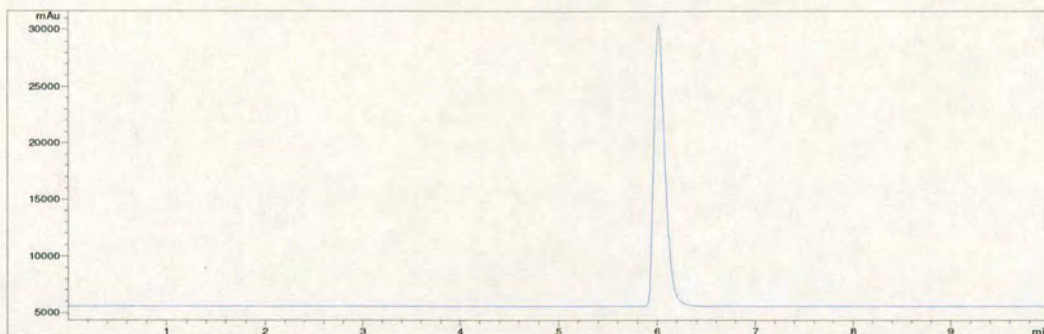
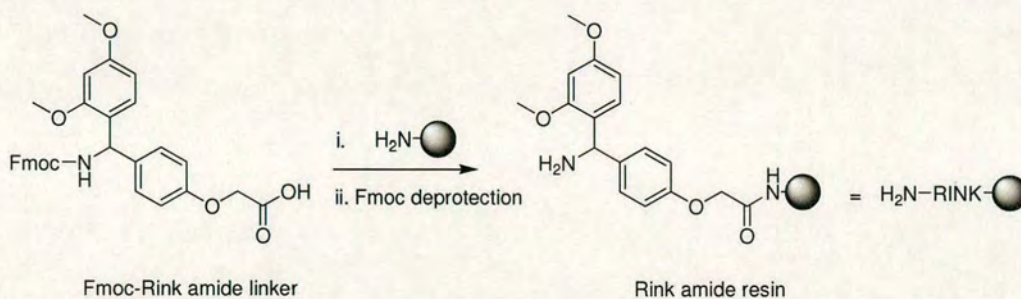


**Figure 2.6** HPLC trace (ELS) of *N*-Fmoc-*N*-(6-*N'*-Boc-aminohexyl)-glycine **2.12**, 100% purity.

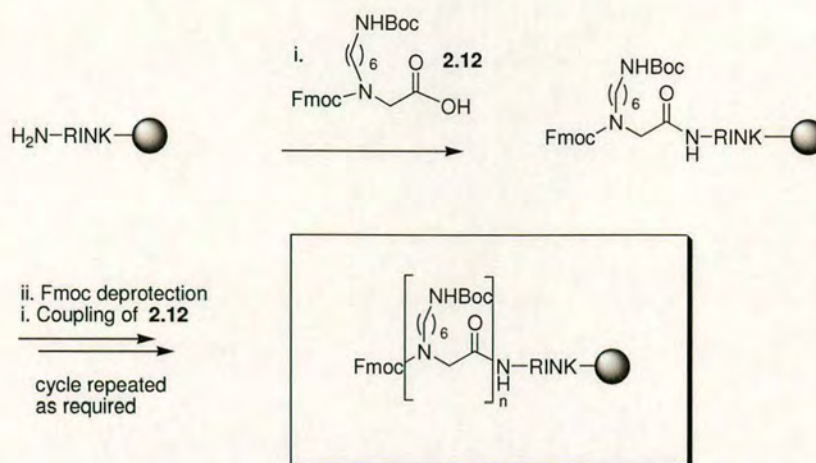
### II.3.2. Solid phase peptoid synthesis.

As reported by Peretto<sup>149</sup> the peptoids were assembled on polystyrene aminomethyl resin functionalised with the Rink<sup>151</sup> amide linker (Scheme 2.12 and Scheme 2.13). In each of the coupling steps monomer **2.12** (2 equiv), PyBrOP (2 equiv) in DCM (0.08 M) and DIPEA (4 equiv) were added to the resin and reacted at room temperature for 4 h. PyBrOP as reported before was necessary to enable efficient coupling of the secondary amine. Deprotection of the Fmoc group (20% piperidine in DMF) and coupling were repeated until oligomers of the required length were obtained.



**Scheme 2.12.** Preparation of Rink amide resin. Reagents and conditions: (i) Fmoc-Rink amide linker (3 equiv, 0.2 M), HOBt (3 equiv, 0.2 M), DIC (3 equiv, 0.2 M) in DMF, 12 h; (ii) 20% piperidine in DMF, 2 x 20 min.





**Scheme 2.13.** Synthesis of peptoid oligomers on solid support. Reagents and conditions: (i) monomer **2.12** (2 equiv, 0.1 M), PyBrOP (2 equiv, 0.1 M), DIPEA (4 equiv, 0.2 M) in DCM, 4 h; (ii) 20% piperidine in DMF, 2 x 20 min.

As outlined previously this general protocol presented two important limitations:

- Use of an expensive coupling reagent (necessary for the coupling of secondary amines).
- Time consuming synthesis (4 h for each residue added).

Cost and time of the synthesis had to be minimised as much as possible. To do so we decided to investigate the use of microwave heating to reduce the coupling reaction time, and the use of the classic and robust DIC/HOBt protocol for acids activation, in order to replace the expensive PyBrOP coupling reagent.

### ***II.3.3. MW assisted solid phase peptide synthesis.***

Microwave heating has been successfully applied to organic synthesis, giving rise to so-called M.A.O.S (Microwave Assisted Organic Synthesis). The field has developed significantly since the first reports of microwave promoted synthesis in 1986.<sup>152,153</sup> Domestic microwave ovens are increasingly being replaced by scientific microwave apparatus for use in synthesis. As well as being safer, these new instruments allow for accurate control of key parameters such as initial microwave power, reaction temperature and, in the case of sealed vessel reactions, internal pressure.



Although the outstanding number of microwave assisted synthetic protocols produced since 1986 it was quite surprising at the time to learn how little precedent was available for microwave-assisted peptide coupling reactions.

The first example of microwave heating applied to peptide synthesis was reported by Wang and co-workers<sup>154</sup> in 1992 (Figure 2.6). Their microwave heating protocol offered a 2–4 fold reduction in amino acid coupling time with two different coupling methods, symmetric anhydride and pre-formed N-hydroxybenzotriazole (HOBt) active ester, especially when using side-chain hindered amino acids. They reported that no significant racemization was observed. The reactions were performed using an un-modified domestic microwave apparatus (10% of the full power, 6 min, with an “estimated” temperature near to 55 °C), thus accurate temperature measurement was not possible and also reproducibility from microwave to microwave proved an issue. While the results appeared promising, lack of proper instrumentation and concerns regarding acceleration of potential side-reactions delayed further exploration.

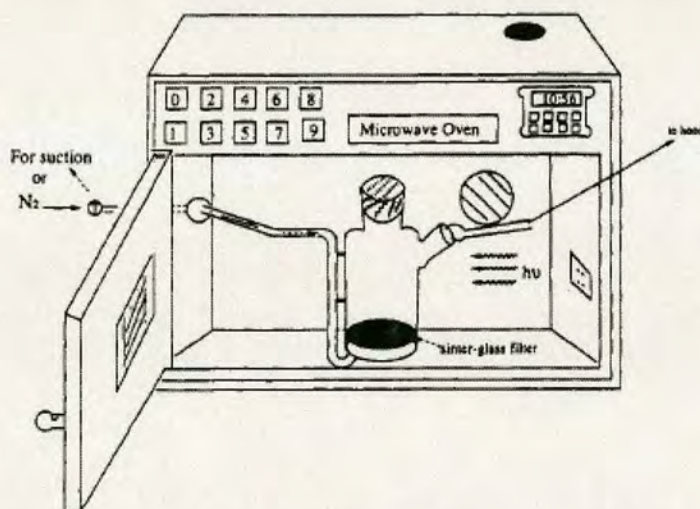


**Figure 2.6.** Wang's MW reactor for peptide synthesis: Microwave oven and the custom-made solid-phase reaction vessel. The vessel was left in the middle of the microwave oven, and a Teflon tube from the side arm of the reaction vessel was connected to a nitrogen source. During microwave irradiation, a stream of nitrogen was blown into the reaction vessel, and the nitrogen gas bubbles served as a stirrer.

After irradiation was stopped, the reaction solution was filtered off via the side arm by suction.<sup>154</sup>

As modern microwave systems that generated a homogeneous microwave field and offered temperature control became available, new interest was generated in peptide



synthesis applications. Almost a decade after Wang's first report,<sup>154</sup> in 2001 Santagada and colleagues<sup>155</sup> reported the difficult coupling of  $\alpha$ -aminoisobutyric acid (Aib) with sterically hindered natural or non coded amino acids, using conventional and microwave heating methods, with either PyBOP/HOBt or HBTU/HOBt as coupling agents. In the microwave heating experiments, the reaction mixture was heated to 55 °C for 15 min followed by a further 15 min at 60 °C. It is interesting to note how conventional heating did not present a really significant improvement, for example the yield for Z-Aib-Val-OMe changed from 74% (HBTU/HOBt, 25 °C, 16 h) to 77% (HBTU/HOBt, 55 °C, 16 h), while under microwave irradiation the yield was increased up to 94% (HBTU/HOBt, 15 min at 55 °C plus further 15 min at 60 °C, in total 30 min). It was also noticed that under microwave irradiation the coupling yields were not influenced by the particular activator employed, the use of PyBOP and HBTU, leading to dipeptides in high yields (range 86-96 %) and with dramatically reduced reaction time, from 16 h to 30 min.

Gogoll and colleagues<sup>156</sup> in 2002 reported the study of common activators TBTU, PyBOP, HATU, Mukaiyama's reagent with microwave heating up to 110 °C and 130 °C, for the coupling of sterically hindered Fmoc-protected amino acids (tripeptide Fmoc-Thr-Val-Ile-NH<sub>2</sub>, dipeptides Fmoc-Ala-Ile-NH<sub>2</sub> and Fmoc-Thr-Ile-NH<sub>2</sub>). The microwave assisted couplings were performed in sealed vessels under temperature control conditions at 110 °C using PyBOP (20 min), TBTU (10 min), and HATU (1.5 min) then at 130 °C using Mukaiyama's reagent (10 min). Surprisingly no particular levels of racemization were observed under any of the conditions described.

Microwave heating has been used for the coupling of sterically hindered glycosylated amino acid building blocks on solid supports.<sup>157,158</sup> These building blocks (Figure 2.7) were used in the synthesis of the 20 amino acid protein MUC1.<sup>159</sup> The solid-phase synthesis was performed on both Tentagel and PEGA supports functionalised with the Rink amide linker. Couplings were performed using HBTU/HOBt, under microwave irradiation (monomode microwave apparatus at 50 °C), under conventional heating (at 50 °C), and at room temperature.







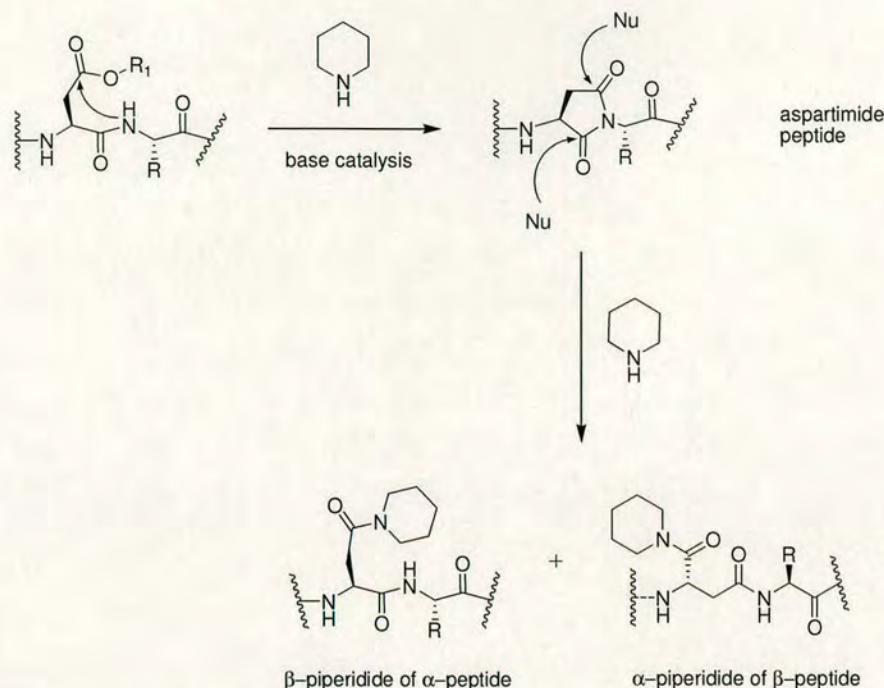
Hexamer  $\beta$ -peptide **2.17** was prepared manually either conventionally at room temperature either under microwave irradiation in a monomode microwave apparatus. When using conventional methodology (room temperature, 1.5 h per coupling, 15 min deprotection) although the penta  $\beta$ -peptide precursor was >95% pure, hexamer **2.17** was only 55% pure with significant quantities (33%) of the unreacted pentamer as well as some of the Fmoc-protected hexamer being present. Under controlled microwave heating (coupling 6 min at 50 °C, deprotection 4 min at 60 °C) hexamer **2.17** was obtained in 80% purity with only 5% of the unreacted pentamer and none of the Fmoc-protected hexamer being observed.

Studies were then extended to deca- $\beta$ -peptide **2.18**. However this was obtained in only 57% purity, indicating the challenge of coupling extra residues to hexamer **2.17**. What proved to be a solution for this problem was the use of a solution of LiCl in DMF in the coupling protocol.<sup>161</sup> Salt additives are known to alleviate, at least in part, the problems of aggregation and/or folding of resin-bound  $\alpha$ -peptides as they increase in length. Thus, in this case, the effects of microwave heating alone may not be enough to disaggregate the  $\beta$ -peptide. With the modified reaction conditions, deca- $\beta$ -peptide **2.18** could be prepared in 88% purity and 81% yield. Using the LiCl modified conditions for the synthesis of hexamer **2.17** the already high purity was increased to 94%. As well as disaggregating the peptide, the salt additive could also enhance the ionic conduction mechanism for conversion of microwave energy into heat in the reaction mixture. Moving to a multimode microwave apparatus, the same group reported the synthesis of a library of 14-helical  $\beta$ -peptides.<sup>162</sup> A recent report describes the use of microwave heating conditions for the solid phase synthesis of pseudopeptides containing an ester bond.<sup>163</sup>

### *3.3.1. Microwave activation and side reactions.*

Peptide synthesis is affected by a series of sequence dependent side reactions that are well-documented.





**Scheme 2.14.** Formation and ring opening reaction of aspartimide.

Aspartimide formation<sup>164,165</sup> (Scheme 2.14) can occur during Fmoc removal with piperidine. Nucleophilic attack by the amide of the neighbouring group to an aspartic acid on the side chain ester (or amide) drives the generation of a 5-membered ring, which can then re-open by nucleophilic attack. This potential side reaction accumulates during each successive deprotection step and can lead to substantially reduced purity. This problem is reduced with bulky protecting groups ( $R_1 = t$ -butyl) but not totally eliminated.

Racemization during the coupling reaction has been extensively documented.<sup>166,167</sup> The two main mechanisms of racemization are direct enolization and oxazolone formation.<sup>168</sup> During the coupling reaction, formation of an activated ester and concomitant increased acidity of the  $\alpha$ -carbon proton can lead to loss of stereochemical integrity. The racemization rate is influenced by the electron-withdrawing effect of the amino acid side chain, the reaction temperature, the solvent, and the activator base. Sterically hindered tertiary amines are used to minimize the base-catalyzed removal of the  $\alpha$ -proton (Figure 2.9).





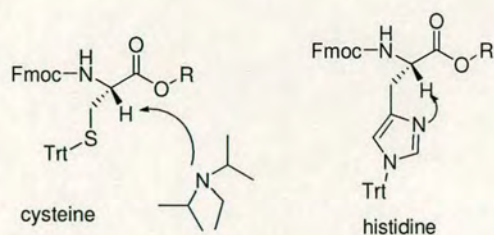
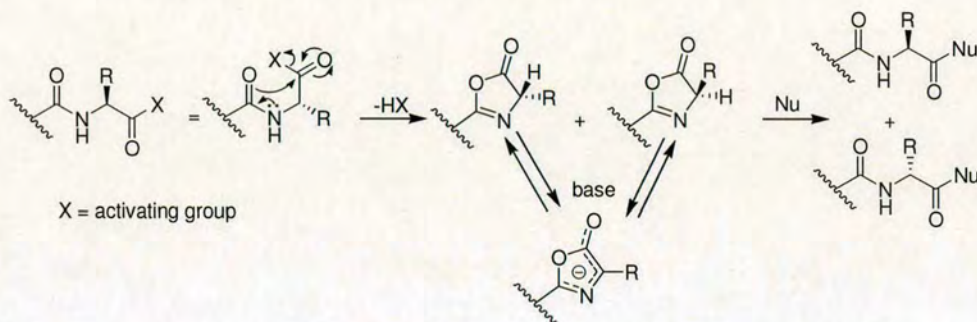


**Figure 2.9** Racemization of activated Fmoc derivatives of cysteine and histidine by direct enolization.

Formation of an oxazolone (Scheme 2.15) can cause the racemization. Enantiomerization by oxazolone formation occurs more frequently during the condensation of peptide fragments, however N-urethane protected amino acids can be susceptible to this reaction.<sup>166</sup>



**Scheme 2.15.** Oxazolone-mediated racemization occurring during peptide coupling.

The first reports regarding microwave peptide synthesis had shown no evidence of increased epimerisation due to microwave heating.<sup>154,156</sup> However, this observations could be attributed to the fact that none of the troublesome residues (Cys or His) were constituent parts of the peptide sequences.

To investigate if the application of microwave conditions could have a negative impact by enhancing side reactions Collins and colleagues<sup>169</sup> prepared a 20-mer model peptide (VYWTSPFMKLIHEQCNRADG-NH<sub>2</sub>) which contained each of the natural 20 amino acids, but with a selectively placed C-terminal Asp-Gly segment to encourage maximum potential aspartimide formation. At room temperature, although the racemization levels were low, the crude product purity was only 68% due to a number of deletions. An initial microwave-promoted synthesis of the 20-mer indicated that the sequence was susceptible to racemization. Deprotection steps of 30



s at 50 W followed by 180 s at 50 W ( $T_{\text{max}} = 80\text{ }^{\circ}\text{C}$ ) and a coupling step of 300 s at 40 W ( $T_{\text{max}} = 80\text{ }^{\circ}\text{C}$ ) led to significant racemization at His, Cys residues and Asp residue. A second coupling protocol of 120 s at 0 W followed by 240 s at 40 W ( $T_{\text{max}} = 50\text{ }^{\circ}\text{C}$ ) in which the reaction mixture did not exceed  $50\text{ }^{\circ}\text{C}$  proved to be effective with high peptide purity (84%) and reduced racemization of His and Cys residues.

Kappe<sup>170</sup> reported a “*cooling before microwave irradiation*” approach for the preparation of peptides with low racemization and high purity. Compared to other microwave protocols the reaction mixture was cooled to  $0\text{ }^{\circ}\text{C}$  before and between microwave irradiations. In Kappe’s synthesis deprotection and coupling reactions were performed in standard glass vials and the washing steps in polypropylene syringes equipped with a frit and valve. Using a power control protocol, the maximum temperature reached in the steps and purity of the final product depended on whether the contents of the reaction mixture were cooled to room temperature ( $T_{\text{max}} 95\text{ }^{\circ}\text{C}$ , 63% purity) or to  $0\text{ }^{\circ}\text{C}$  ( $T_{\text{max}} 64\text{ }^{\circ}\text{C}$ , 86% purity) prior to microwave irradiation. Pre-cooling of reaction mixtures prior to microwave irradiation has shown to lead to peptides in high purity with little racemization, but appears to be inconvenient and not practical either in an automated reactor or when considering performing couplings in parallel or on a large scale.

#### ***II.3.4. Microwave assisted peptoid synthesis.***

Peptoid couplings were carried out in a single-mode microwave reactor (Smith synthesiser) in sealed vials; deprotection and washing steps were performed in a SPE (Solid Phase Extractor), a polypropylene syringe equipped with a frit and a valve (Figure 2.10).



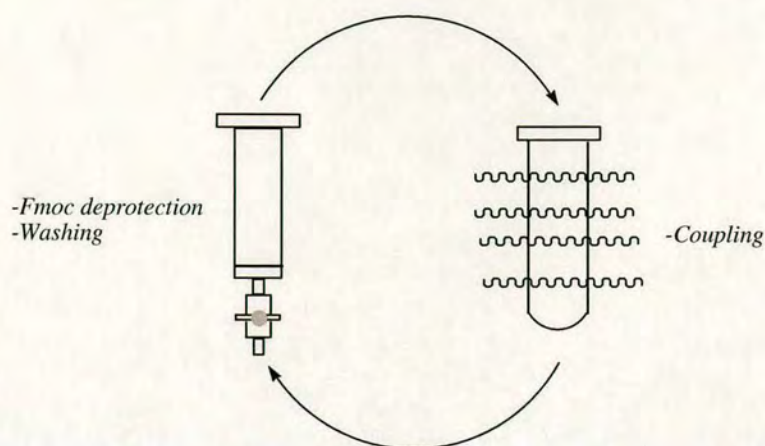


**Figure 2.10.** Schematic representation of the peptoid synthesis. MW assisted coupling in a sealed glass vial and Fmoc deprotection at room temperature in a polypropylene syringes equipped with a frit and a valve (SPE: Solid Phase Extractor).

General conditions for the microwave assisted coupling (Table 2.2) were chosen as follows:

---

**MW Assisted DIC/HOBt Peptoid Coupling**

Equivalents: 3 (0.1-0.2 M)

Temperature: 60 °C

Time: 20 min.

---

**Table 2.2**

**The temperature** was set at 60 °C as:

- The protocol had to be compatible with peptide synthesis. It was reported that higher temperature (over 80 °C) gave high levels of side reactions during peptide synthesis.<sup>160,169</sup>
- A temperature of 60 °C was reported to be sufficient to achieve efficient coupling with very hindered substrate such as Aib, and glycosylated amino acids (Scheme 2.7).<sup>155,157</sup>

Therefore, a temperature of 60 °C looked a good compromise between efficiency and mildness of the reaction conditions.

**The reaction time** was set at 20. As an approximation, the rate of reactions is doubled when the temperature is increased by 10 °C. So, at 60 °C, reactions are approximately

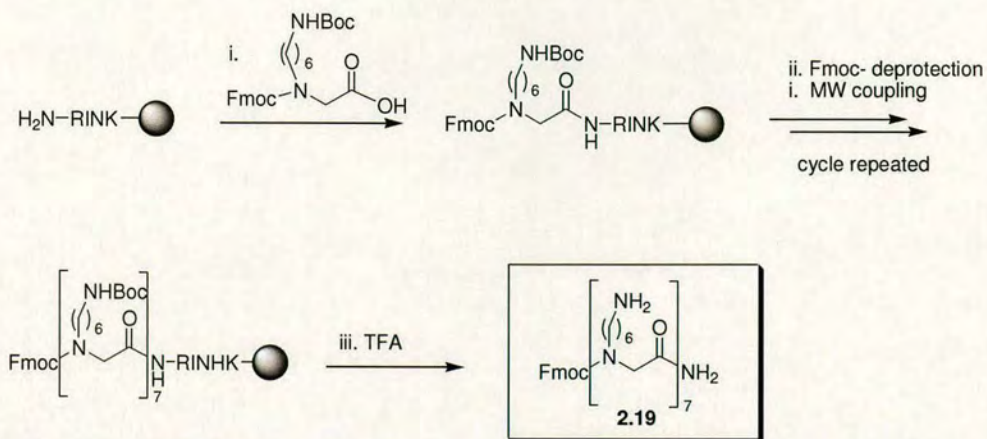


16 times faster than at 20 °C. Couplings with DIC/HOBt are usually carried out at room temperature in 3 h (180 minutes), therefore, at 60 °C it should require only 10-11 minutes. In consideration of the hindered nature of the secondary amine used for the peptoid synthesis, the time was set at 20 minutes. .

**The concentration** of the reagents (3 equivalents) was kept in a range between 0.1 and 0.2 M, and this depending by the loading of the resin used. When using resins with a loading around 1 mmol/g it was possible to keep the concentration of the reagents at 0.2 M. When using resin with lower loading, < 0.5 mmol/g, the concentration of the reagent was reduced to 0.1 M. The number of equivalents used in all the cases was 3; the difference in concentration depended on the need to use identical volumes of solvent to suspend the resin, independently by the loading.

Peptoid monomer **2.12** (3 equiv) was pre-activated with DIC (3 equiv) and HOBt (3 equiv) in DMF (0.1-0.2 M solution, see later) for 2 min before being added to the pre-swollen resin inside a solid phase extractor (SPE). The solution with the resin was transferred (using a plastic pipette) into a microwave glass vial then capped. The couplings were performed at 60 °C, for 20 min with magnetic stirring of the resin. Power and pressure profiles were registered during to ensure maximum reproducibility of the conditions. Coupling completion was monitored by the Chloranil test,<sup>171</sup> a standard colorimetric test used to detect the presence of free secondary amines. The resin was then poured back into a SPE and washed (DMF, DCM) without drying to keep the resin swollen. Fmoc deprotection was performed using a 20% piperidine solution (in DMF) at room temperature (2 x 10 min). Fmoc deprotection reaction time could be reduced with microwave heating but this does not offer a really significant improvement. The synthesis of the 7mer peptoid transporter using microwave conditions was reduced to a single day giving material with a high purity (98% by ELS analysis, Figure 2.11) without the needing for double couplings (Scheme 2.16).<sup>172</sup>





**Scheme 2.16.** Reagents and conditions: (i) **2.12** (3 equiv.), DIC (3 equiv.) and HOBt (3 equiv.) in DMF at 0.1M; microwave irradiation at 60 °C for 20 min. (ii) Fmoc deprotection: 20% piperidine in DMF, 2 x 10 min at room temperature. (iii) TFA/TIS (95/5).

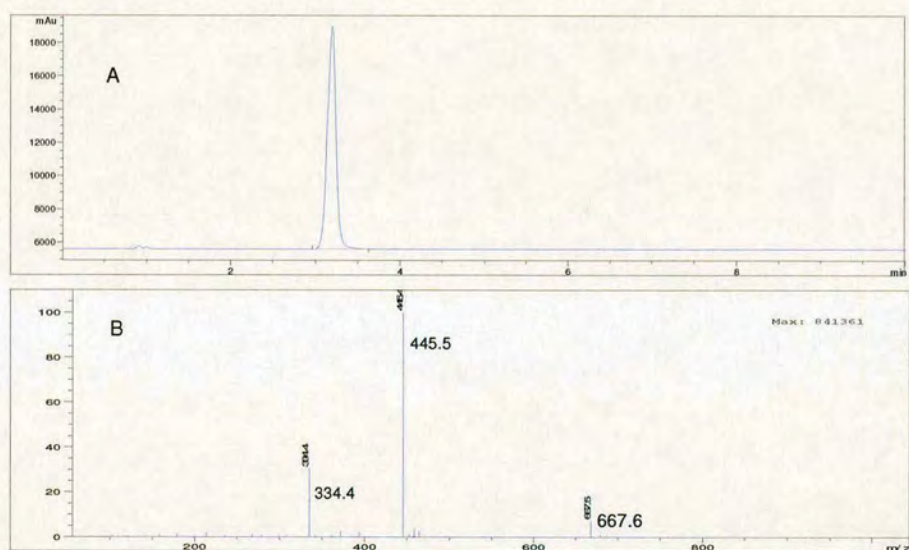


**Figure 2.11.** Crude of Fmoc protected hepta-peptoid **2.19**: A) HPLC trace, 98 % purity according to ELS detection; B) Mass spectrum,  $m/z$  (ES<sup>+</sup>): 667.6 (M+2H)<sup>2+</sup>, 445.5 (M+3H)<sup>3+</sup>, 334.4 (M+4H)<sup>4+</sup>.

In conclusion the combination of standard DIC/HOBt activation and microwave heating proved immediately to be extremely efficient for the preparation of the peptoid. Although further optimisation of the synthetic protocol was possible, such as a further reduction of the coupling time, it was considered not of relevance.



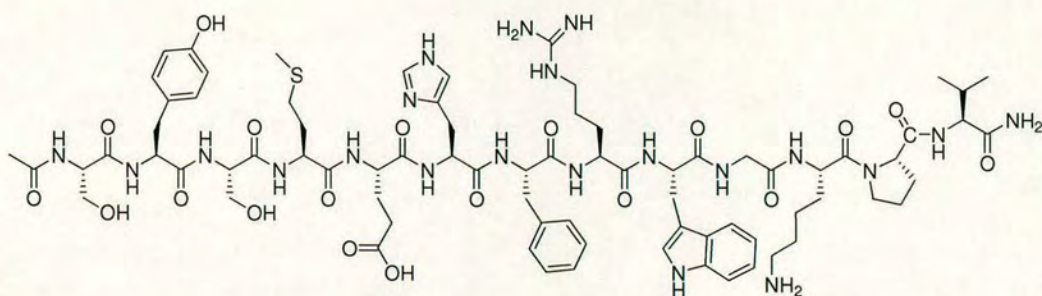
## Chapter III. Peptoid conjugation to cargoes and delivery.

In 2003 Peretto reported the synthesis and cell permeability evaluation of homooligomer peptoids based on monomer **2.12**.<sup>149</sup> Analysis by fluorescence microscopy and FACS indicated that these materials possessed the ability to successfully penetrate the membrane of cells with localisation observed in the cytosol, the nucleus and concentration in the nucleoli. Of the peptoid oligomers tested (tri, penta and hepta-mer) the heptapeptoid exhibited maximum internalisation with > 99% of cells labelled. None of the peptoids assayed were found to be toxic as verified by a MTT<sup>173</sup> toxicity test and trypan blue<sup>174</sup> assay to ascertain cell viability. To study the potentials of these peptoid oligomers as carriers for poor cell permeable molecules, the more effective heptapeptoid was conjugated to different cargoes and tested for delivery into cell and skin. The test cargoes were: a peptide hormone  $\alpha$ -MSH (13mer peptide), peptide nucleic acids (PNA) (9mer, 12mer, 15mer), and a mercapto DNA (19mer). In order to visualize cellular internalisation the heptapeptoid conjugated compounds were typically labelled with fluorescein.

### III.1. $\alpha$ -Melanocyte stimulating hormone ( $\alpha$ -MSH).

The hormone  $\alpha$ -MSH (Ac-SYSMEHFRWGKPV-NH<sub>2</sub>) is a ligand of melanocortin 1 receptor (*MC1R*), a seven pass transmembrane G-protein coupled receptor which is expressed on the surface of melanocytes and melanoma cells.<sup>175,176</sup> Healy and colleagues have shown that  $\alpha$ -MSH ( $10^{-6}$  M) stimulates pigmentation of melanocytes and melanoma cells *in vitro* increasing intracellular cyclic-AMP which starts a complex signalling cascade resulting in an increased production of black or brown eumelanin (Figure 3.2).<sup>177</sup> Melanocortin 1 receptor (*MC1R*) gene variants alter pigment synthesis *in vivo*, and are causally associated with red hair and fair skin in humans due to an increased production of red or yellow pheomelanin.<sup>178,179</sup> *MC1R* variants may represent a predisposition to melanoma as a result of alterations in skin pigmentation, with less eumelanin and more pheomelanin affording less protection against incident ultraviolet radiation.<sup>180,181</sup>





$\alpha$ -MSH: Ac-SYSMEHFRWGKPV-NH<sub>2</sub>

**Figure 3.1.** Hormone  $\alpha$ -MSH.

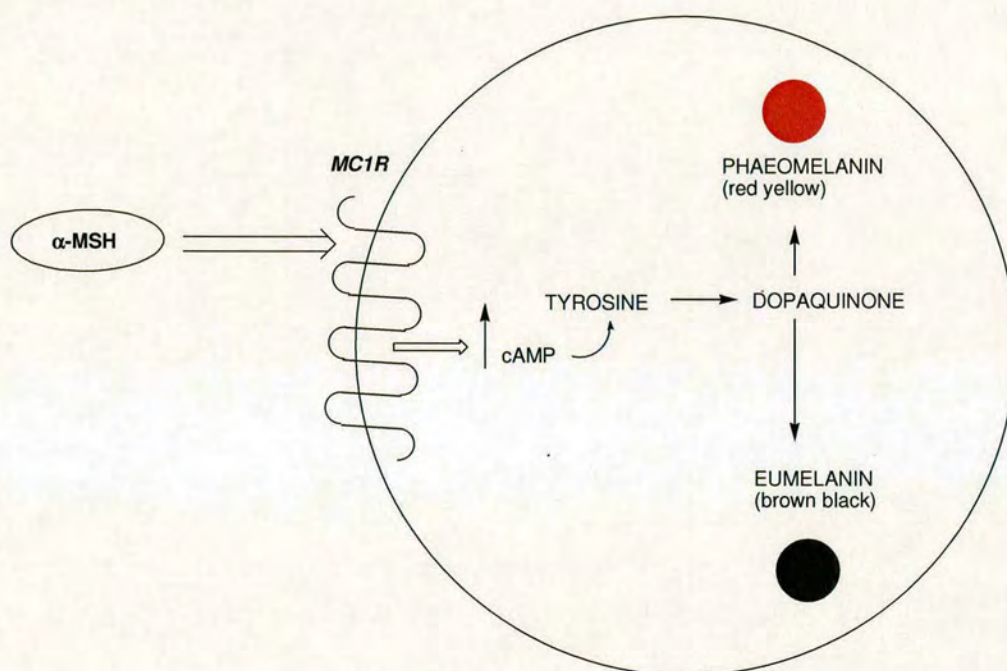


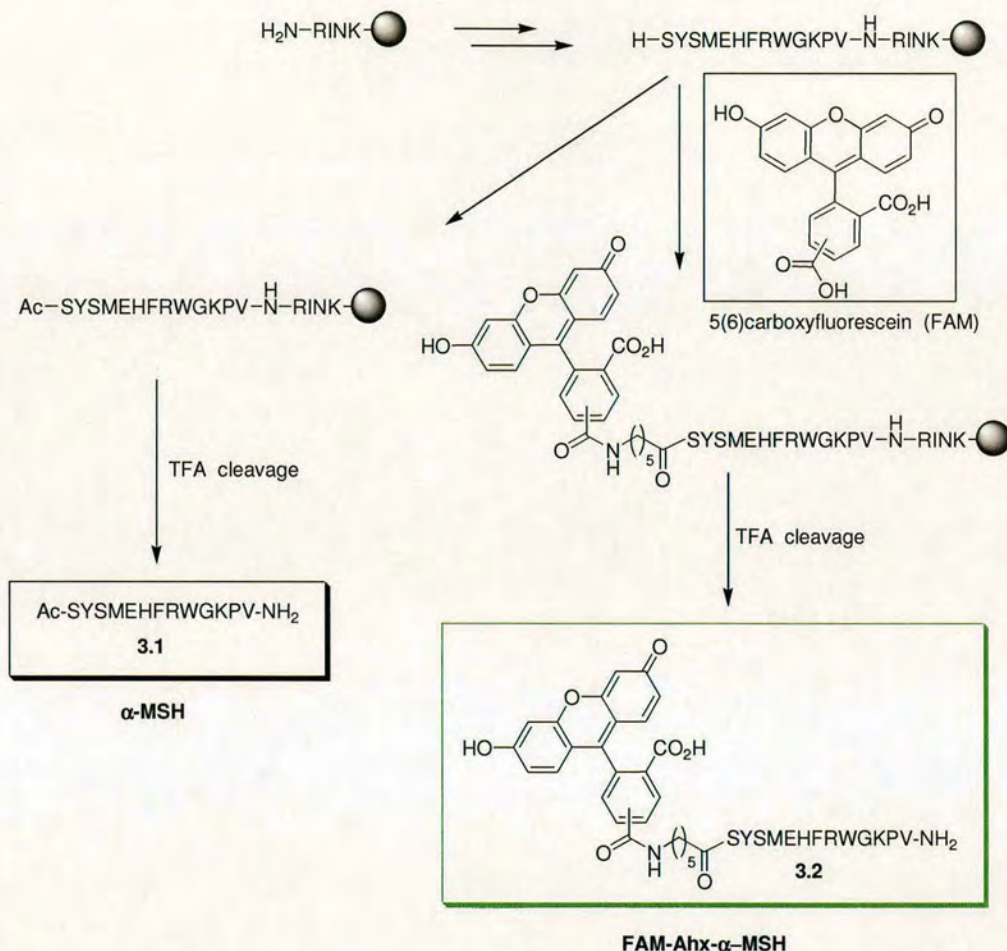
**Figure 3.2.** Schematic of action of  $\alpha$ -MSH at the melanocortin 1 receptor.  $\alpha$ -MSH signaling results in an increased ratio of eumelanin to pheomelanin. In contrast, loss of function of *MC1R* results in increased pheomelanin production.

### ***III.1.1. $\alpha$ -MSH and peptoid conjugation: synthesis and labelling.***

The peptide  $\alpha$ -MSH (3.1) was firstly prepared by standard SPPS using a Rink<sup>151</sup> amide polystyrene resin. Fmoc protected amino acids (3 equiv) were pre-activated with DIC (3 equiv) and HOBt (3 equiv) in DMF (0.2 M) for 5 min, added to the resin and left to react at room temperature for 3 h. The couplings were monitored using a



standard colorimetric test to detect the presence of unreacted amines (Nynidrin<sup>182</sup> test for primary amines, Chloranil<sup>171</sup> test for secondary amines). Fmoc deprotection was carried out using 20% piperidine in DMF (2 x 10 min).



**Scheme 3.1.** Synthesis of α-MSH (3.1) and fluorescein (FAM) labelled α-MSH (3.2). Peptide couplings: amino acids (3 equiv), DIC (3 equiv) and HOBt (3 equiv) in DMF at 0.2 M, room temperature 3 h. Fmoc deprotection: 20% piperidine in DMF, 2 x 10 min at room temperature. Fluorescein labelling: 5(6) carboxyfluorescein (3 equiv), PyBOP (2.8 equiv) and DIPEA (6 equiv) in DMF 0.2 M, room temperature 12 h; Cleavage mixture: 81.5% TFA, 5% thioanisole, 5% phenol, 5% water, 2.5% EDT (1,2 ethanedithiol), 1% TIS (triisopropylsilane). FAM = 5(6) carboxyfluorescein. Side chain protecting groups not indicated.

In order to visualize cellular internalization the peptide α-MSH was labelled with carboxyfluorescein (FAM). Notoriously, 5(6)-carboxyfluorescein<sup>183,184</sup> (Scheme 3.1) is an annoying dye to couple to peptides because of the poor reactivity of the acid and



possible side reactions of the phenolic oxygen to form fluorescein –fluorescein esters.<sup>185</sup> The coupling was carried out at room temperature using PyBOP as coupling reagent (12 h). Before TFA cleavage the resin was treated with 20% piperidine in DMF in order to cleave possible fluorescein-fluorescein esters.<sup>185</sup>

Peptide  $\alpha$ -MSH (**3.1**) prepared via standard SPPS was obtained with a 60% purity (Figure 3.3), with preliminary data indicating that the low purity was determined by difficulties on the coupling of the last 3 aminoacids sequence S-Y-S. Fluorescein labelled  $\alpha$ -MSH **3.2** was obtained with a lower purity, 40% (Figure 3.4).

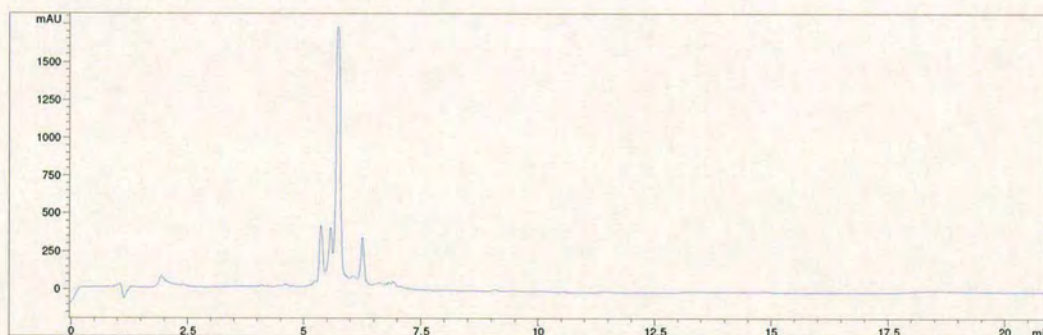


**Figure 3.3.** HPLC trace ( $\lambda = 220$  nm) of crude peptide  $\alpha$ -MSH (**3.1**) prepared at room temperature, purity (63%).

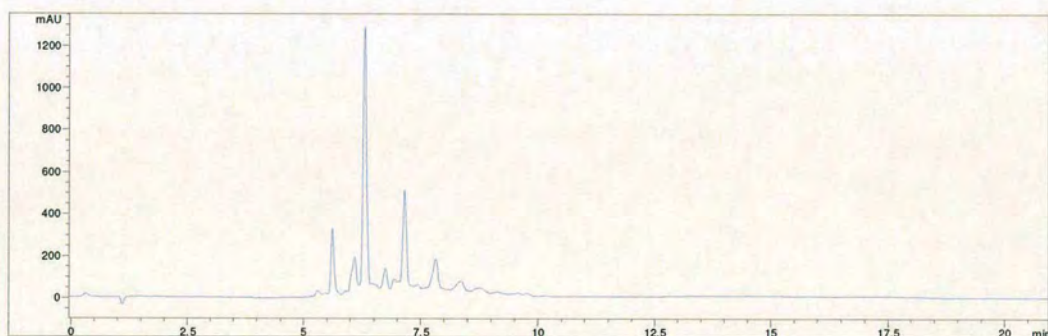


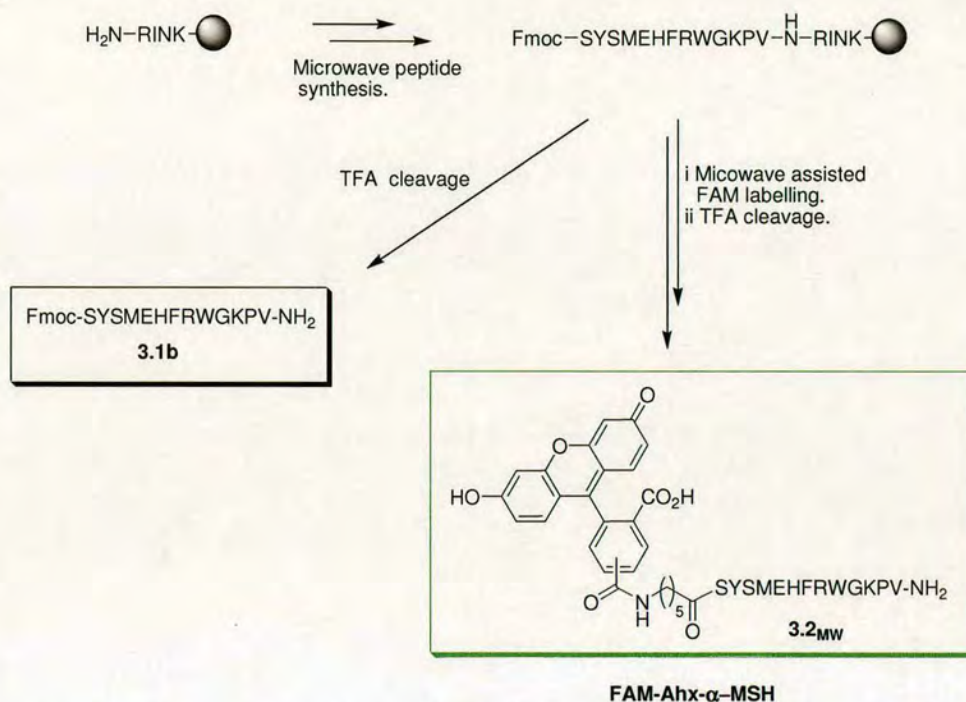
**Figure 3.4.** HPLC trace ( $\lambda = 220$  nm) of crude peptide **3.2** prepared at room temperature, purity (40%).

Compounds **3.1** ( $\alpha$ -MSH) and **3.2** (FAM-Ahx- $\alpha$ -MSH) were purified by RP-HPLC (purity > 95%) before testing on mammalian cells.



### 1.1.1. Microwave assisted synthesis and labelling of $\alpha$ -MSH.

Fluorescein labelled  $\alpha$ -MSH (**3.2**) was re-synthesised under the same microwave heating conditions that proved to be very efficient in the preparation of heptapeptoid **2.19** (Scheme 3.2).



**Scheme 3.2** Microwave assisted synthesis of fluorescein labelled  $\alpha$ -MSH **3.2<sub>MW</sub>**. Reagents and conditions; couplings: acid (3 equiv), DIC (3 equiv) and HOBt (3 equiv) in DMF at 0.2 M; microwave irradiation at 60 °C for 10 min. Fmoc deprotection: 20% piperidine in DMF (2 x 10 min) at room temperature. Cleavage mixture: 81.5% TFA, 5% thioanisole, 5% phenol, 5% water, 2.5% EDT (1,2 ethanedithiol), 1% TIS (triisopropylsilane). FAM = 5(6) carboxyfluorescein.

Couplings were performed at 60 °C for 10 min using 3 equivalents of the required Fmoc protected amino acid, DIC and HOBt, in DMF at a 0.2 M concentration. Fmoc deprotection was performed at room temperature using 20% piperidine in DMF (2 x 10 min). The intermediate sequence Fmoc-SYSMEHFRWGKPV-NH<sub>2</sub> (**3.1b**) was cleaved to check the peptide purity before labelling. The HPLC trace showed purity around 65% (Figure 3.5) comparable with those obtained using longer couplings at room temperature.



The labelling of the peptide with carboxyfluorescein was performed under the same microwave conditions (Scheme 3.2). The coupling proved to be straightforward after the first cycle with no detection of any un-reacted primary amine. Before TFA cleavage the resin was treated with 20% piperidine in DMF in order to cleave possible fluorescein-fluorescein esters.<sup>185</sup> Crude **3.2<sub>MW</sub>** (prepared under microwave heating conditions) was obtained with the same purity (65%) of the intermediate Fmoc-SYSMEHFRWGKPV-NH<sub>2</sub> which indicated a “clean” coupling of the dye. More interestingly the purity of crude **3.2<sub>MW</sub>** appeared to be higher than the purity of crude **3.2**, 65% and 40% respectively. (Figure 3.6)

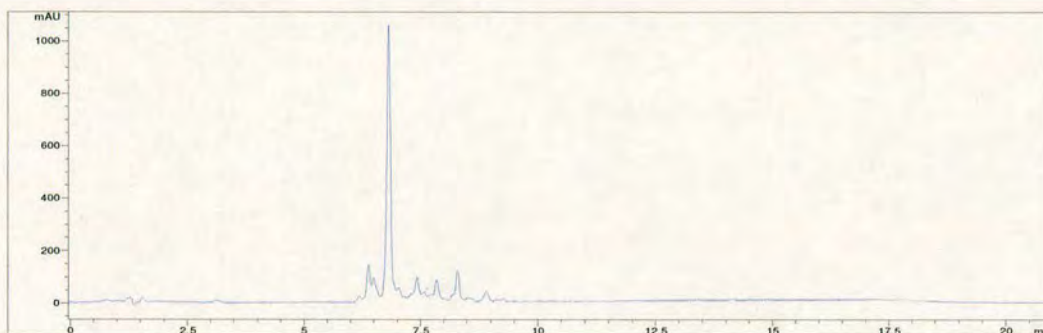


**Figure 3.5.** HPLC trace ( $\lambda = 220$  nm) of crude Fmoc-SYSMEHFRWGKPV-NH<sub>2</sub> prepared under microwave conditions, purity 65%.

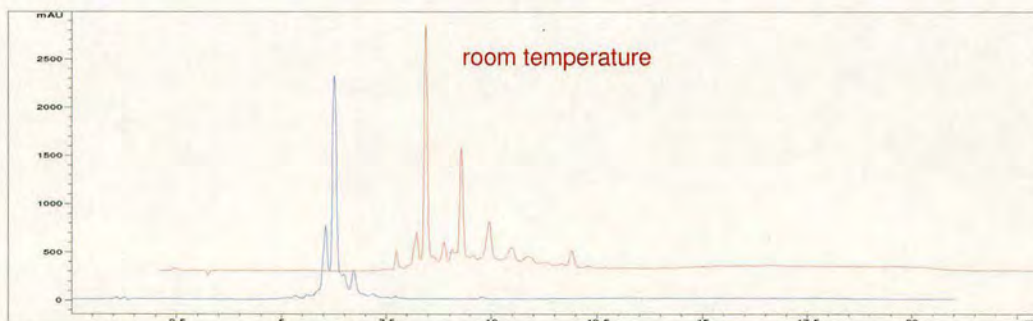


**Figure 3.6.** HPLC trace ( $\lambda = 220$  nm) of crude FAM- $\alpha$ -MSH **3.2** prepared under microwave conditions, purity 65%

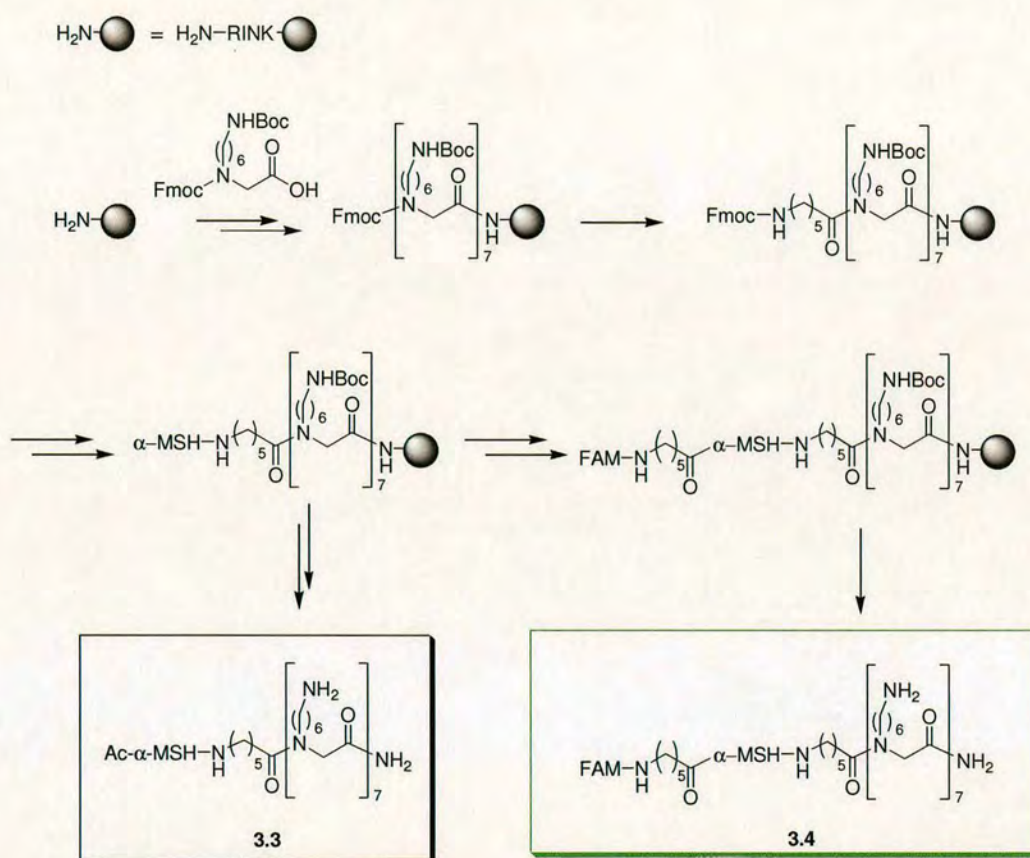
#### *1.1.2. Microwave assisted synthesis and labelling of peptoid conjugated $\alpha$ -MSH.*

Heptapeptoid conjugated  $\alpha$ -MSH were prepared by direct synthesis using two different spacers between the peptide and the peptoid: 6-aminohexanoic acid (Scheme



3.3) and lysine (Scheme 3.4). The synthesis was carried out on Rink amide polystyrene resin under microwave heating conditions.

When the 6-aminohexanoic acid spacer was used, synthesis started with the preparation of the hepta-peptoid followed by the  $\alpha$ -MSH (Scheme 3.3).



**Scheme 3.3.** Synthesis of fluorescently labelled hepta-peptoid conjugate  $\alpha$ -MSH. Couplings: acids (3 equiv), DIC (3 equiv) and HOBt (3 equiv) in DMF at 0.2 M, microwave irradiation at 60 °C for 20 min. Fmoc deprotection: 20% piperidine in DMF (2 x10 min) at room temperature. FAM = 5(6)-carboxyfluorescein.

The microwave conditions used were the same as described above for the peptoid and  $\alpha$ -MSH synthesis. The synthesis was also repeated at room temperature using PyBrOP for the peptoid synthesis (couplings of 4 h), DIC/HOBt for the  $\alpha$ -MSH (couplings of 3 h), and PyBOP to couple the 5(6)-carboxyfluorescein (12 h).

With both protocols (microwave heating and room temperature) **3.4** was obtained with purities around 60%, (Figure 3.7) confirming that the use of microwave heating



offers a faster synthesis compared to standard conditions, but does not improve fundamentally the chemistry.

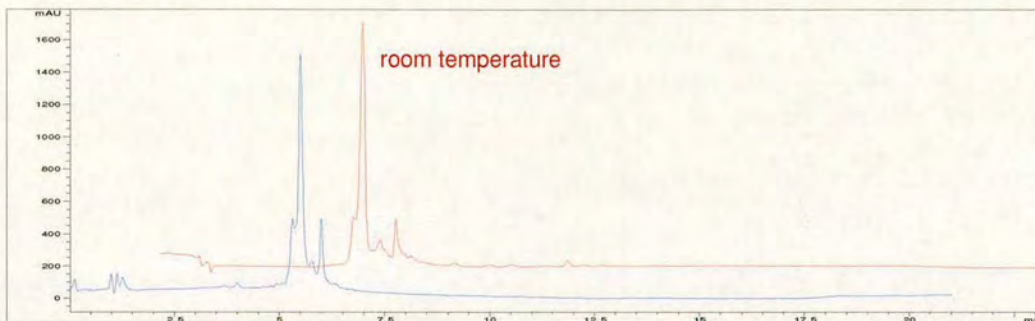


**Figure 3.7.** HPLC trace (220 nm) of crude **3.4** prepared under microwave heating, purity 60%.

When lysine was used as spacer, the synthesis was carried out starting from orthogonally protected Fmoc-Lys(Dde)-OH attached to the Rink amide resin. The  $\alpha$ -MSH sequence was synthesised on the  $\alpha$ -amine group under microwave conditions described for the preparation of the peptide with couplings at 60 °C for 10 min.

After completion of the sequence, the heptapeptoid was built on the  $\epsilon$ -amine group. Again couplings were carried out under microwave heating at 60 °C for 20 min, with Fmoc deprotection performed at room temperature (20% piperidine in DMF). Labelling was done under microwave conditions, with 5(6)-carboxyfluorescein coupled to the N-terminus of the peptoid using a 6-aminohexanoic spacer (Scheme 3.4).

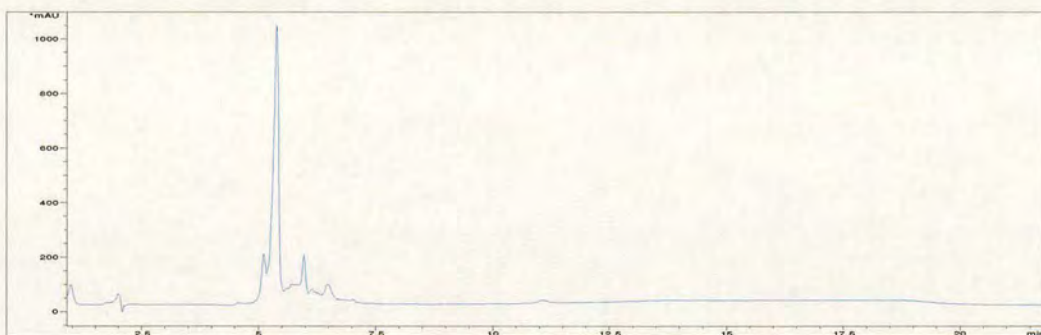
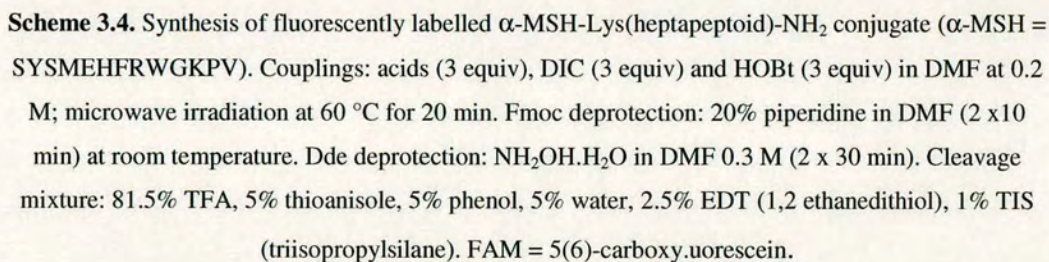


**Figure 3.8.** HPLC trace ( $\lambda = 220$  nm) of crude **3.6**, purity 58 %.







### III.1.2. Cell and skin delivery.\*

#### 1.2.1. Peptoid modified $\alpha$ -MSH peptides retained their activity.

Healy and colleagues reported that  $\alpha$ -MSH ( $10^{-6}$  M) stimulates pigmentation of melanocytes and melanoma cells *in vitro* increasing intracellular cyclic-AMP concentrations.<sup>177</sup>

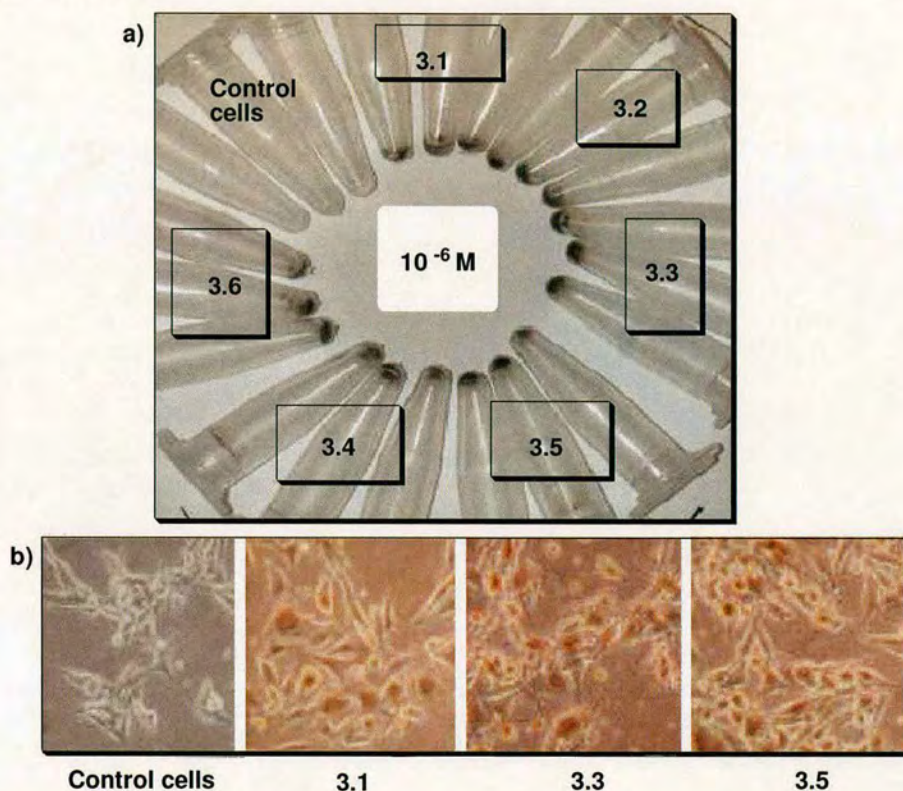


**Figure 3.9** Pigmentation assay of S91 melanoma cells with  $\alpha$ -MSH (**3.1**) and related compounds (**3.2**, **3.3**, **3.4**, **3.5**, **3.6**), 5 days exposure at a  $10^{-6}$  M concentration: (a) cells pelleted in eppendorfs (triplicates); (b) cells in culture.

Pigmentation assays demonstrated that **3.3** ( $\alpha$ -MSH-Ahx-heptapeptoid) and **3.5** ( $\alpha$ -MSH-Lys(heptapeptoid)-NH<sub>2</sub>) as well as **3.2** (FAM-Ahx- $\alpha$ -MSH), **3.4** (FAM-Ahx-

---

\* Modified  $\alpha$ -MSH derivatives were tested by Pawan Kumar, Prof. Eugene Healy group, at Dermatopharmacology, University of Southampton, Southampton.



$\alpha$ -MSH-Ahx-heptapeptoid) and **3.6** ( $\alpha$ -MSH-Lys(FAM-Ahx-heptapeptoid)-NH<sub>2</sub>) stimulated eumelanin synthesis by melanoma cells with similar potency to  $\alpha$ -MSH at 10<sup>-8</sup> M and 10<sup>-6</sup> M (Figure 3.9).

### 1.2.2. Peptoid transports $\alpha$ -MSH into cells.

To examine whether  $\alpha$ -MSH is transported into cells by the peptoid, fluorescently-tagged compounds **3.2** (scheme 3.1), **3.4** (Scheme 3.3) and **3.6** (Scheme 3.4) were employed and intracellular fluorescence documented as a measure of penetration.<sup>186,187</sup> FAM- $\alpha$ -MSH **3.2** did not penetrate into any of the cell types used in these experiments, however, peptoid conjugated **3.4** and **3.6** at a concentration of 10  $\mu$ M entered in large amounts into all cell types tested (B16G4F, B16CWT-3, HEK-293, and B-lymphocytes). Fluorescence microscopy showed bright green fluorescent cells following incubation with 10  $\mu$ M **3.4** and **3.6** for 3 h, suggesting that these compounds had entered into the cell. Confocal microscopy confirmed that the heptapeptoid conjugated compounds had penetrated into the cells, and that uptake had occurred in 95 – 100 % of cells in each culture (Figure 3.10-3.12).

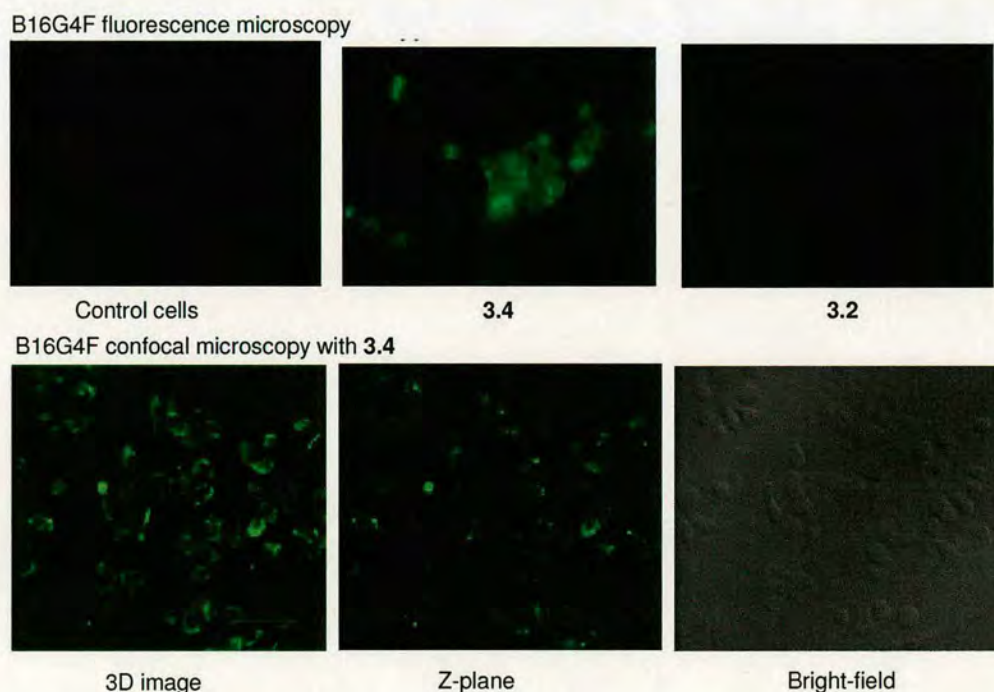
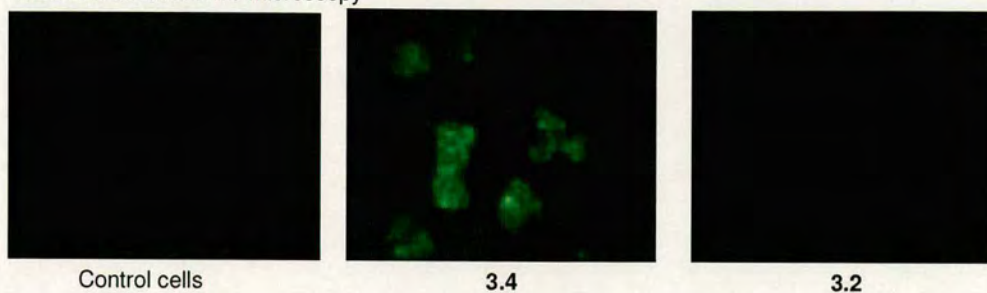


**Figure 3.10.** Fluorescence microscopy and confocal microscopy of B16G4F after incubation with **3.4** and **3.2** (10  $\mu$ M) for 3 h.



HEK 293 fluorescence microscopy



HEK 293 confocal microscopy with 3.4

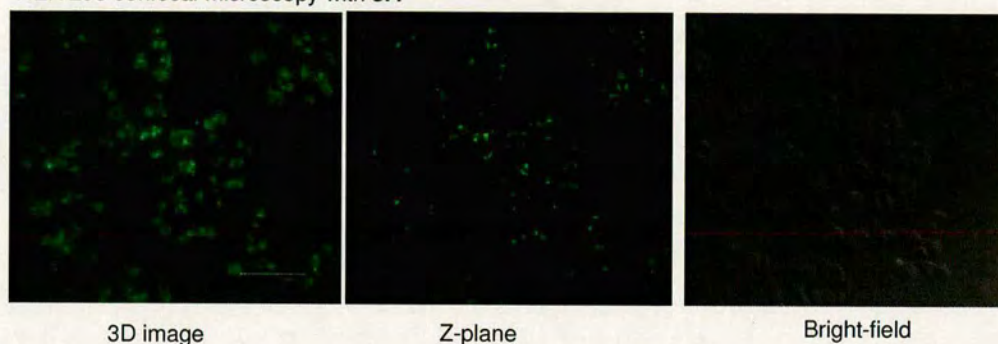


**Figure 3.11.** Fluorescence microscopy and confocal microscopy of HEK 293 after incubation with 3.4 and 3.2 (10  $\mu$ M) for 3 h.

HaCaT confocal microscopy with 3.4

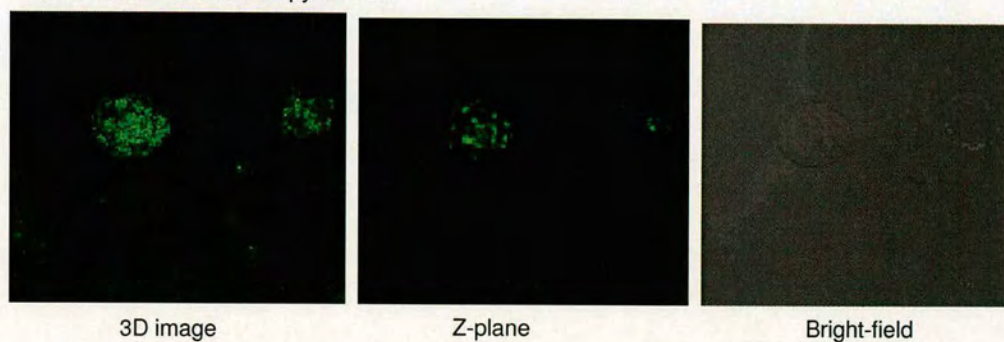


**Figure 3.12.** Confocal microscopy of HaCaT cells after incubation with 3.4 (10  $\mu$ M) for 3 h.



### 1.2.3. Peptoid allows $\alpha$ -MSH to penetrate into skin.

Penetration of heptapeptoid conjugated  $\alpha$ -MSH **3.4** and **3.6** into skin was examined using an ex-vivo mouse, pig and human skin model.<sup>186,187</sup> Briefly, fresh skin was taken separately from the dorsum of euthanized mice, the ear of euthanized pigs, and by excision during surgical procedures on dermatology patients. The skin samples were inserted, with the outer surface upright, into tightly-sealed diffusion chambers (Figure 3.13) and incubated with the compounds under study; these were applied to the outer skin surface for three hours, and then washed carefully prior to fixation of the skin. As can be seen in Figure 3.14, compound **3.6** applied at a concentration of  $10^{-3}$  M penetrated in large amounts into mouse, pig and human skin; by contrast, in multiple experiments **3.2** did not penetrate into skin. Interestingly, **3.4** did not penetrate into skin to the same extent as **3.6**.



**Figure 3.13.** Franz's diffusion chamber. Method of assessing penetration of molecules into skin *ex vivo*.







In conclusion peptoid conjugated  $\alpha$ -MSH derivatives were efficiently prepared on solid phase using a combination of standard DIC/HOBt activation and microwave heating. Peptoid conjugated  $\alpha$ -MSH compounds showed an activity comparable to the unmodified  $\alpha$ -MSH, which indicates that the peptoid oligomer did not inhibit the activity of the hormone.

Cellular uptake of fluorescein labelled  $\alpha$ -MSH and peptoid conjugated  $\alpha$ -MSH derivatives was measured. The fluorescein labelled  $\alpha$ -MSH did not show any cellular uptake when tested on several cell lines. In contrast, fluorescein labelled peptoid conjugated  $\alpha$ -MSH compounds showed a very high cellular uptake when tested on a wide range of cell lines (B16G4F, B16CWT-3, HEK-293, and B-lymphocytes) with an average population of fluorescent cells over 95%. These results clearly show the high potential of the heptapeptoid oligomer for the delivery of peptides of medium size (10-30 residues).

Skin penetration was also evaluated. Fluorescein labelled  $\alpha$ -MSH was not able to penetrate into the skin, in contrast, fluorescein labelled peptoid conjugated  $\alpha$ -MSH **3.6** was able to penetrate into different kinds of skin: human, mouse and pig. These first results indicate that the heptapeptoid oligomer can be a potential tool for topical delivery of compounds.



### III.2. Peptide nucleic acid (PNA).

Peptide nucleic acids (PNAs), first described by Nielsen, in 1991,<sup>188</sup> are a DNA mimic where the deoxyribose phosphate diester backbone of DNA is replaced by a poly(*N*-(2-aminoethyl)glycine)amide backbone carrying the nucleobases via a series of methylenecarbonyl spacers (Figure 3.15).

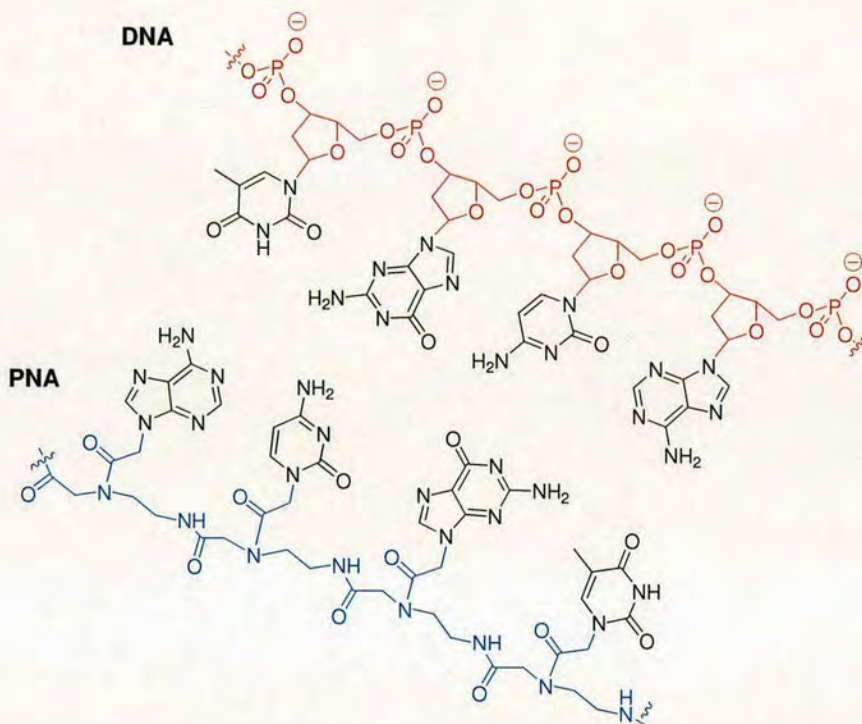


**Figure 3.15.** General structure of PNA and DNA.

Intramolecular distances and configurations of the nucleobases in PNAs are similar to those in DNA, and specific hybridisation occurs between PNA and DNA or RNA sequences. In addition, due to the uncharged nature of the backbone, PNA/DNA duplexes have a higher thermal stability compared to analogous DNA/DNA or RNA/DNA duplexes, where the negative charged backbones display electrostatic repulsion between the two strands. Moreover PNAs are resistant to biological degradation by nucleases and proteases. These properties make PNA an ideal tool in a number of different areas of research such as gene therapy,<sup>189,190</sup> as a tag for microarray screening,<sup>191,192</sup> as well as for SNP (single nucleotide polymorphism) analysis<sup>193,194</sup> and mRNA profiling.<sup>195</sup> Due to its peptidic structure PNA synthesis



can be carried out by straightforward and traditional solid phase peptide synthesis methods (SPPS).<sup>196</sup> However PNAs have a number of limitations such as an inability to be extended enzymatically, and poor cellular uptake. To overcome this second problem several strategies have been reported, involving the use of CPPs,<sup>87,197,198</sup> the delivery of PNA-DNA hybrids using liposomes,<sup>199</sup> and modifications of the backbone structure.<sup>200</sup>

### III.2.1. PNA: Monomer synthesis.

In 2004 Diaz-Mochon reported a strategy for the synthesis of PNA-encoded peptides based on the use of Dde-protected PNA monomers (Figure 3.16).<sup>201</sup> It was shown that the protecting group Dde could be removed without affecting Fmoc functionalities on the molecule, while the Dde group is stable to classic Fmoc deprotection conditions. Using this Dde/Fmoc orthogonality, amino acids can be coupled using a Fmoc strategy, while a PNA synthesis can be carried out using a Dde strategy.<sup>202</sup>

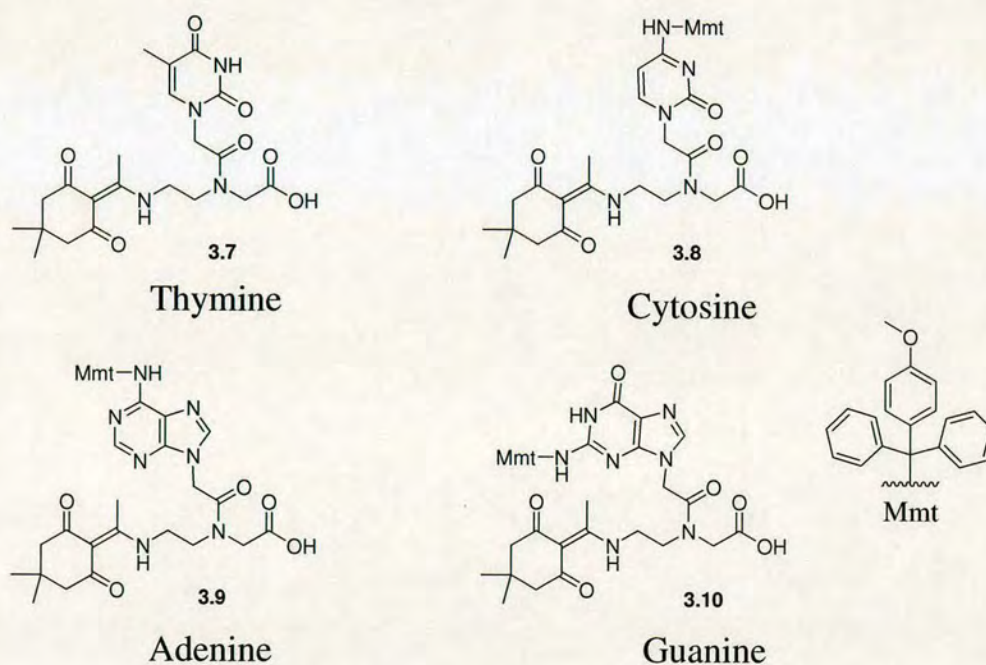
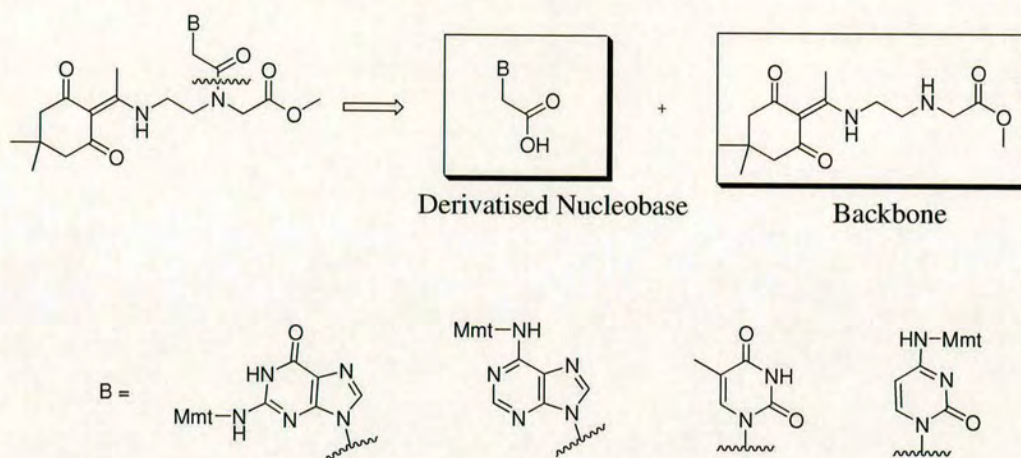


Figure 3.16. Dde/Mmt protected PNA monomers.



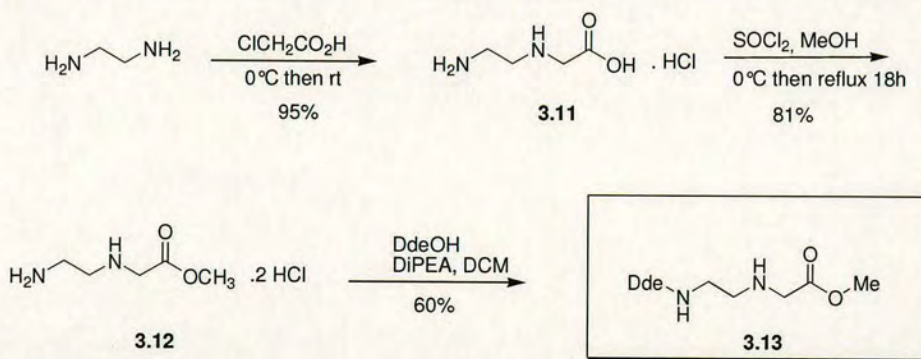
Retro-synthetically, the monomers can be disconnected into two synthons (Scheme 3.5), a backbone and the derivatised nucleobase, and this allows the straightforward synthesis of all four desired PNA monomers



**Scheme 3.5.** PNA monomers, retro-synthesis.

#### 2.1.1. Synthesis of the backbone.

The synthesis of the backbone followed the protocol described by Bialy.<sup>202</sup> The first step consisted of reacting ethylene diamine with chloroacetic acid yielding **3.11** in 95% yield,<sup>203</sup> which was then esterified with thionyl chloride in methanol to form **3.12**.

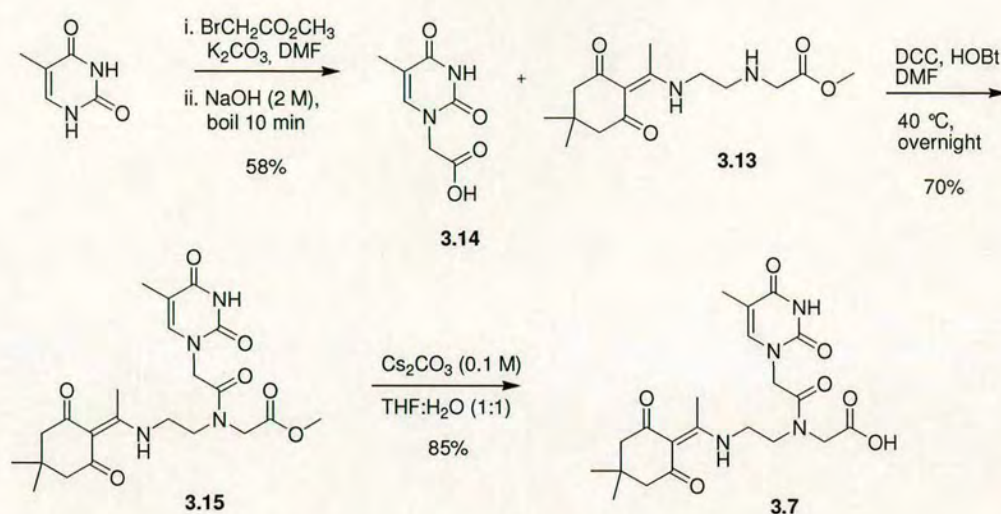


**Scheme 3.6.** Synthesis of the backbone.

The primary amine of **3.12** was then selectively protected with DdeOH in the presence of DIPEA to give **3.13** in 60% yield.



### 2.1.2. Synthesis of the thymine monomer.<sup>202</sup>



**Scheme 3.7.** Synthesis of the thymine monomer.

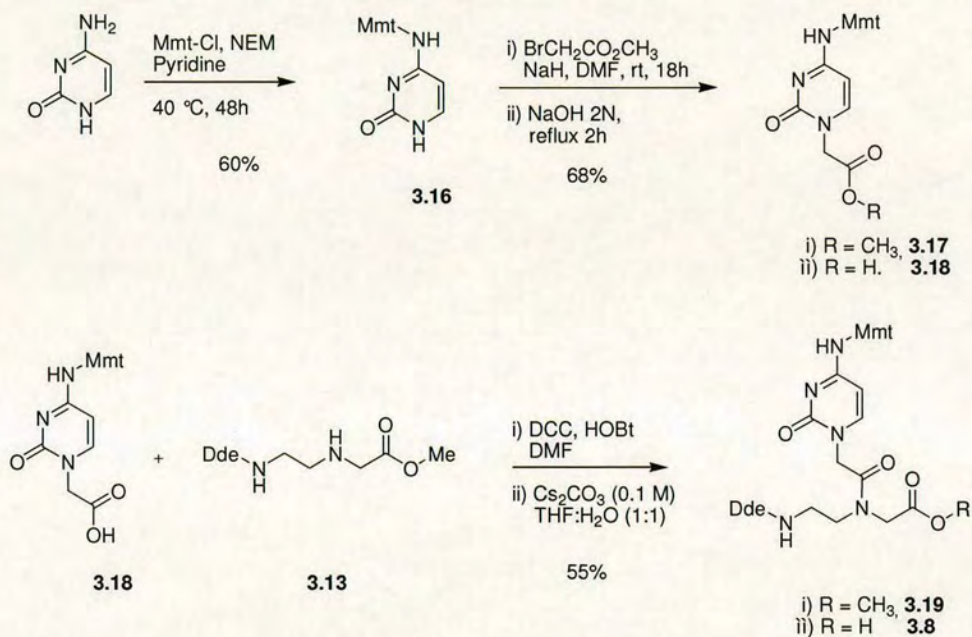
Thymine was alkylated following the procedure described by Buchardt,<sup>196</sup> by treatment with methyl bromoacetate using  $\text{K}_2\text{CO}_3$  as base, followed by saponification of the resulting compound with  $\text{NaOH}$  yielding thymine-1-yl acetic acid **3.14**.

Thymine nucleobase **3.14** and backbone were coupled using DCC as coupling reagent yielding compound **3.15** with a 70% yield. Finally ester **3.15** was treated with 0.1 M  $\text{Cs}_2\text{CO}_3$  (4 equiv in THF:H<sub>2</sub>O 1:1) overnight to yield thymine monomer **3.7** (85% yield). This mild basic condition allowed complete saponification of ester **3.15** without compromising the Dde functionality. Bialy's protocol<sup>202</sup> reported the use of 1 M  $\text{Cs}_2\text{CO}_3$  in MeOH/H<sub>2</sub>O for 1 h. This protocol had the inconvenient result of substantial Dde instability over long periods, thus requiring a careful and continuous monitoring of the reaction in order to avoid the loss of valuable compound at the last step.



### 2.1.3. Synthesis of the cytosine monomer.<sup>202</sup>

Cytosine was suspended in pyridine and reacted with Mmt-Cl in presence of 4-ethylmorpholine at 40 °C for 48 h under N<sub>2</sub> yielding **3.16**<sup>204</sup> with a 60% yield. The low yield was easily explained by the poor solubility of cytosine in pyridine, making the reaction extremely slow due to the heterogeneous conditions. Alkylation of **3.16** with ethylbromoacetate followed by saponification yielded the cytosine nucleobase **3.18** in 68% yield over the two steps.<sup>204</sup> The building block **3.18** was then coupled to the backbone **3.13** using DCC/HOBt (ester **3.19**), followed by saponification with 0.1 M Cs<sub>2</sub>CO<sub>3</sub> to yield cytosine monomer **3.8** in 55% yield.

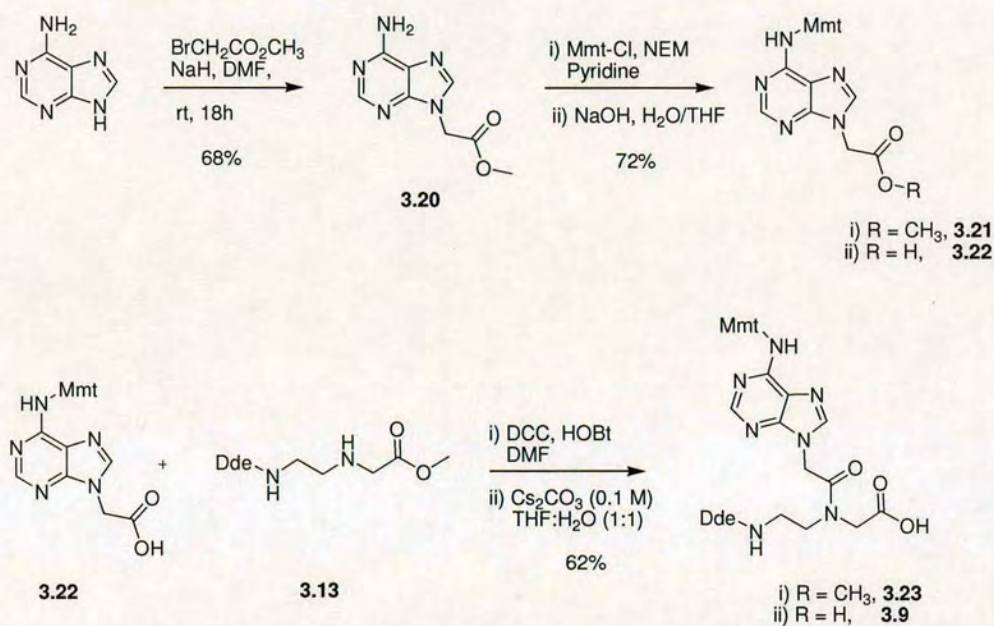


**Scheme 3.8.** Synthesis of the cytosine monomer.



#### 2.1.4. Synthesis of the adenine monomer.<sup>202</sup>

Adenine was deprotonated with NaH in DMF and reacted with methylbromoacetate to give selectively N-9 alkylated adenine **3.20** (68% yield).<sup>196</sup> Exocyclic amino group protection<sup>204</sup> with Mmt-Cl in the presence of 4-ethylmorpholine was followed by saponification with KOH to afford the adenine building block **3.22** in 72% yield over two steps. Adenine nucleobase **3.22** and backbone **3.13** were coupled using DCC/HOBt to yield ester **3.23**, that treated with Cs<sub>2</sub>CO<sub>3</sub> (0.1 M in THF/H<sub>2</sub>O) afforded adenine monomer **3.9** in 62% yield (over two steps).

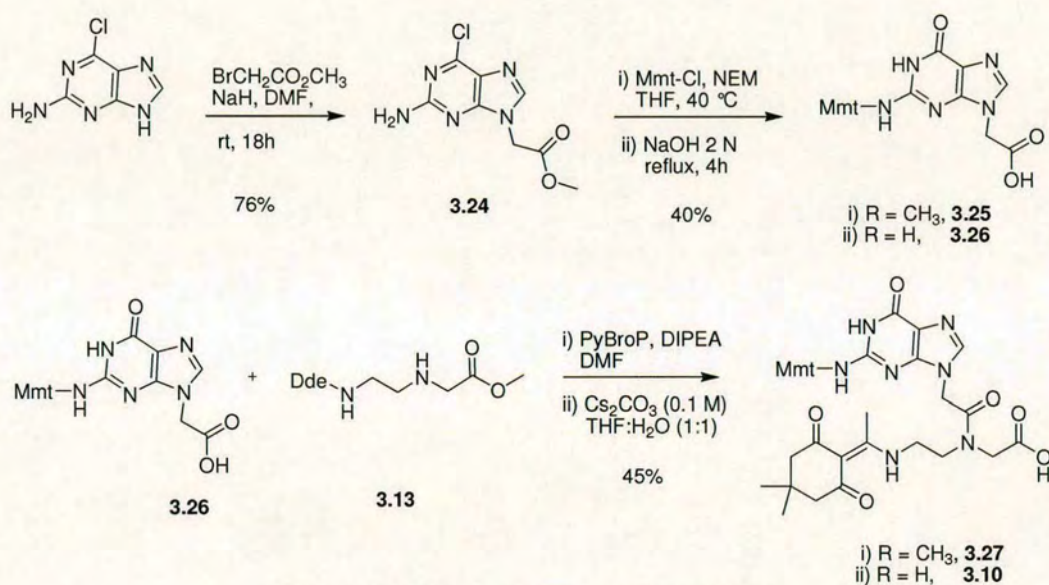


Scheme 3.9. Synthesis of the adenine monomer.



### 2.1.5. Synthesis of the guanine monomer.<sup>202</sup>

2-Amino-6-chloropurine was used as precursor of the guanine nucleobase. This was due to the poor solubility of guanine, the lack of reactivity of its exocyclic amino group and the difficulty in obtaining selectively the N-9 alkyl derivatives. Alkylation<sup>204</sup> and Mmt protection<sup>204</sup> were carried out as for adenine, however dry THF instead of pyridine was used in the Mmt protection step. In the last step, basic hydrolysis of the ester moiety as well as the C-6 chlorine substitution provided the guanine nucleobase **3.26**. Guanine nucleobase **3.26** and backbone were coupled using PyBroP/DIPEA to yield ester **3.27** which was treated with Cs<sub>2</sub>CO<sub>3</sub> (0.1 M in THF/H<sub>2</sub>O) to give the guanine monomer **3.10** in 45% yield (over two steps).



Scheme 3.10. Synthesis of the guanine monomer.

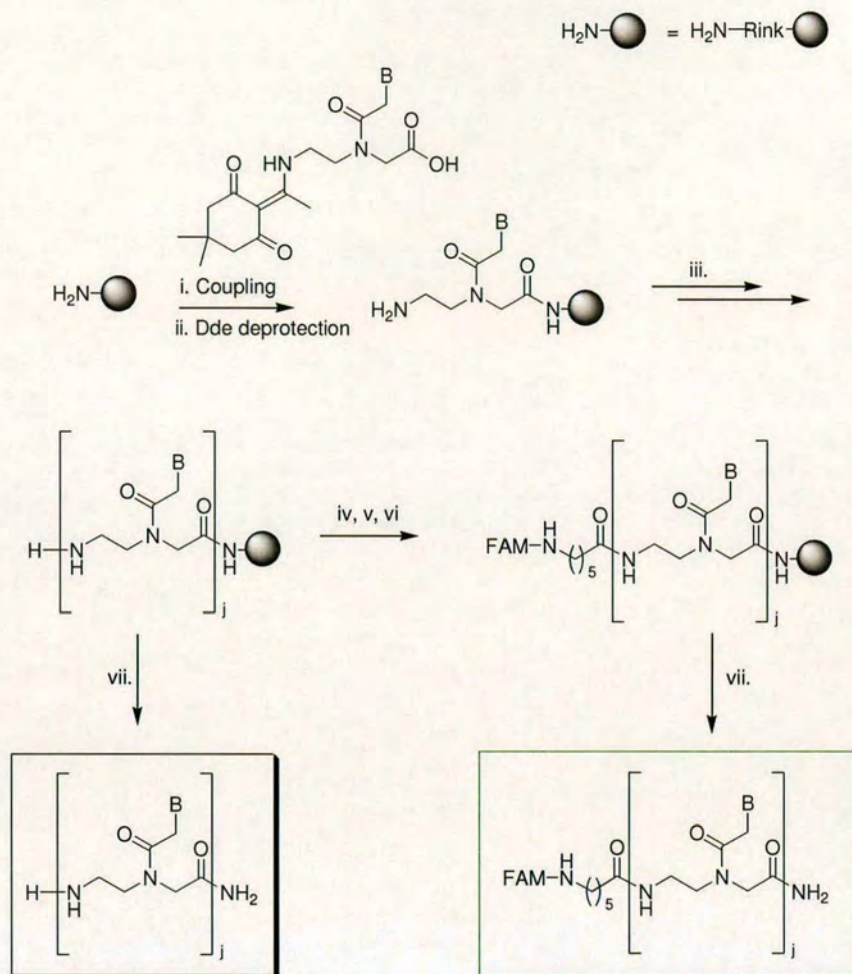


### *III.2.2. Oligomers synthesis.*

To investigate the application of heptapeptoid for the effective delivery of PNA into cell and skin, PNA oligomers with a length of 9, 12, and 15 residues targeting mouse and human tyrosinase were conjugated and labelled with 5(6)-carboxyfluorescein. Human and mouse tyrosinase have different sequences, thus specific sets of PNA targeting the two different mRNA sequences were prepared (Scheme 3.11 and 3.12). PNA oligomers were prepared on Rink<sup>151</sup> amide PEGA resin (Scheme 3.11). Couplings were performed at room temperature following the conditions described by Bialy:<sup>202</sup> PNA monomers (5 equivalents), PyBOP (4.8 equivalents) and NEM (10 equivalents) 0.2 M in DMF, at room temperature for 4 h.

Deprotection of Dde was carried out using a 2% solution of  $\text{NH}_2\text{OH}\cdot\text{H}_2\text{O}$  in DMF (0.3 M) in 1 h (2 x 30 min), instead of the  $\text{NH}_2\text{OH}\cdot\text{HCl}$ /imidazol solution reported by Bialy.<sup>202</sup> After each coupling the resin was treated with a solution of  $\text{Ac}_2\text{O}$  (15%) and HOBt (7.5%) in DMF in order to cap any possible unreacted amine and so to avoid the labelling and conjugation to the heptapeptoid of incomplete (shorter) PNA sequences. Labelling with 5(6)-carboxyfluorescein was carried out under microwave conditions, as described previously, using as a spacer 6-aminohexanoic acid.





#### Mouse tyrosinase

$j = \text{TTT CTC CTT}$  **3.28**  
 $j = \text{CAT TTT CTC CTT}$  **3.29**  
 $j = \text{GAA CAT TTT CTC CTT}$  **3.30**

#### Human tyrosinase

$j = \text{TCT TCC TCT}$  **3.31**  
 $j = \text{CAT TCT TCC TCT}$  **3.32**  
 $j = \text{GAG CAT TCT TCC TCT}$  **3.33**

#### Mouse tyrosinase

$j = \text{TTT CTC CTT}$  **3.34**  
 $j = \text{CAT TTT CTC CTT}$  **3.35**  
 $j = \text{GAA CAT TTT CTC CTT}$  **3.36**

#### Human tyrosinase

$j = \text{TCT TCC TCT}$  **3.37**  
 $j = \text{CAT TCT TCC TCT}$  **3.38**  
 $j = \text{GAG CAT TCT TCC TCT}$  **3.39**

**Scheme 3.11** Synthesis of PNA oligos using Dde protected PNA monomers: i) Dde-PNA-OH (5.5 equiv), PyBOP (5 equiv 0.1 M), NEM (11 equiv) in DMF, 3 h; ii) 2%  $\text{NH}_2\text{OH} \cdot \text{H}_2\text{O}$  in DMF, 2 x 30 min; iii) Repeat (i) and (ii) as necessary; iv) Fmoc-Ahx-OH (3 equiv), DIC (3 equiv) and HOBT (3 equiv) in DMF 0.2 M, 60 °C (MW) 20 min; v) 20% piperidine in DMF, 2 x 10 min; vi) 5(6)-carboxyfluorescein (3 equiv), DIC (3 equiv) and HOBT (3 equiv) in DMF 0.2 M, 60 °C (MW) 20 min; vii) TFA/TIS/ $\text{CH}_2\text{Cl}_2$  (90/5/5), 1 h.



PNA oligomers with 9 residues (**3.28** and **3.34**, Figure 3.17) and 12 residues (**3.29** and **3.35**, Figure 3.18) were obtained with purities > 90% confirming the reliability of the Dde strategy.

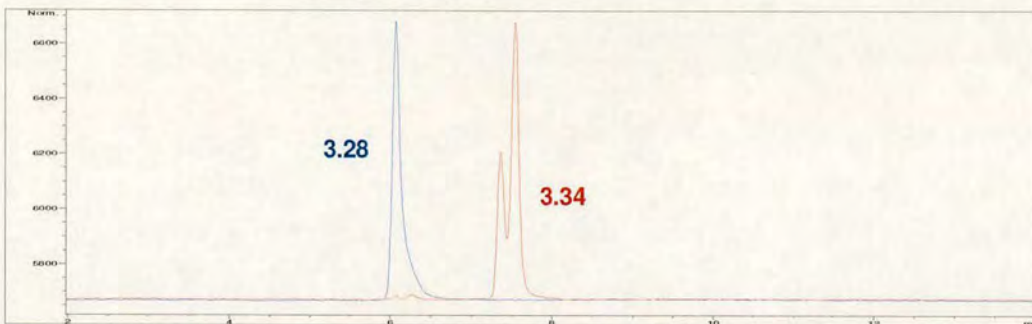


**Figure 3.17.** HPLC trace (ELS) of **3.28** (95% purity) and **3.34** (93% purity). Compound **3.34** showed two peaks corresponding to the two fluorescein isomers.

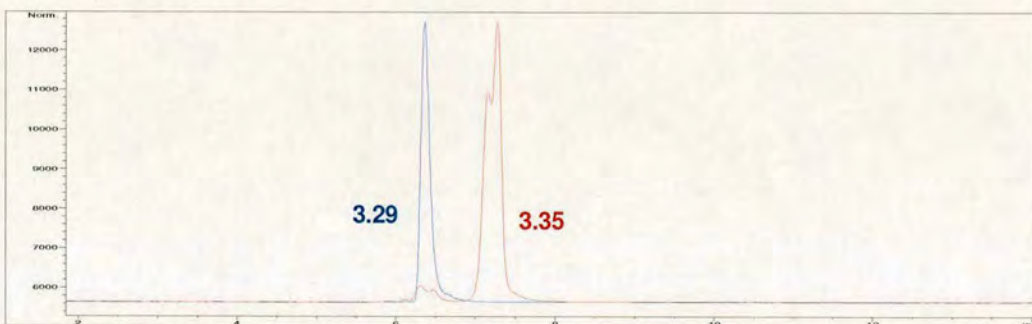
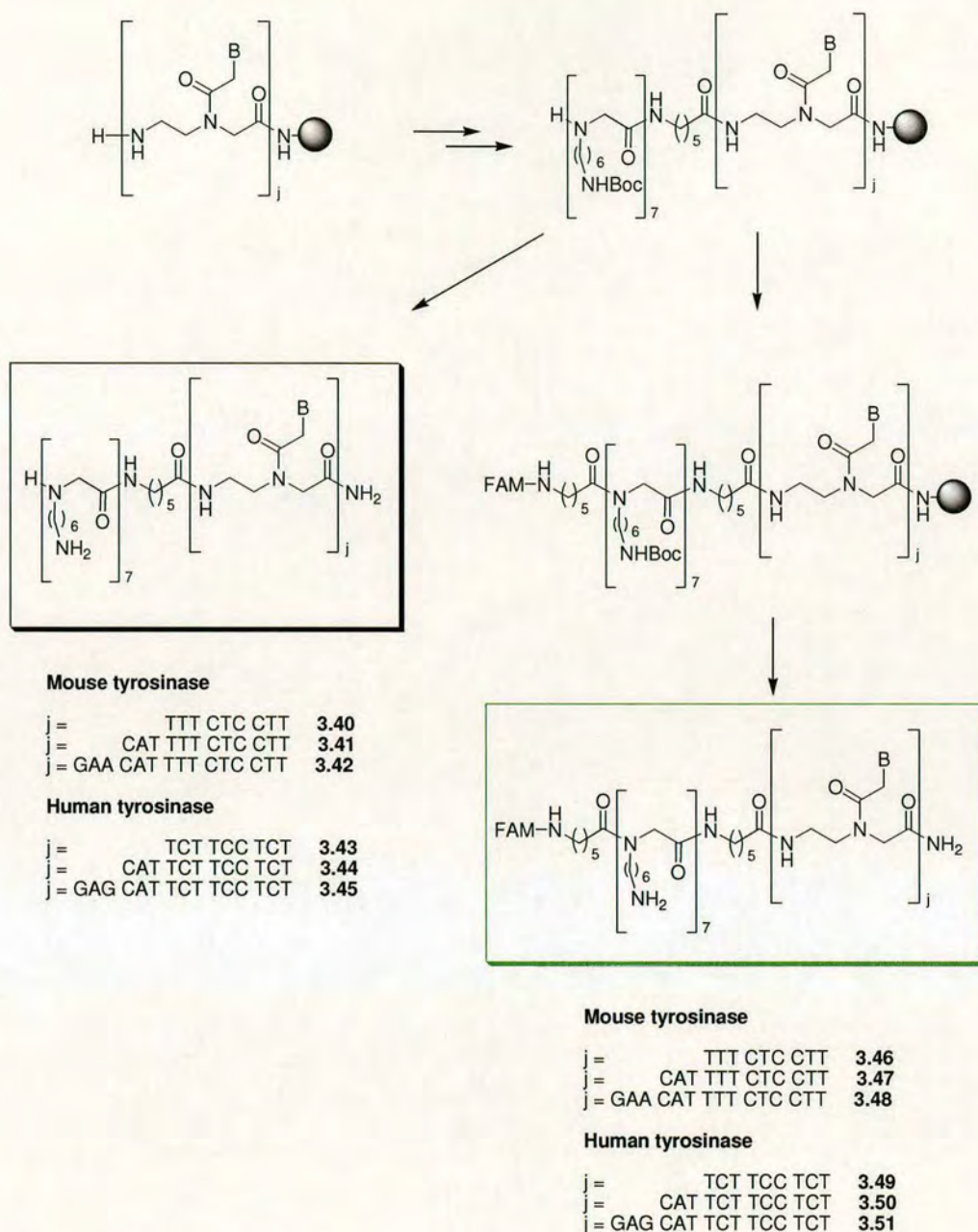


**Figure 3.18.** HPLC trace (ELS) of **3.29** (90%) and **3.35** (90% purity). Compound **3.35** showed two peaks corresponding to the two fluorescein isomers.

The 15mer PNAs were poorly soluble, in particular the fluorescein labelled material, giving HPLC traces of very poor quality with different solvent combinations (acetonitrile/water, methanol/water) and gradients, that did not allow a proper estimation of the crude purity.

The heptapeptoid was synthesised directly following the PNA sequence separated by a spacer (6-aminohexanoic acid). The synthesis was carried out under microwave conditions as described previously.





**Scheme 3.12.** Addition of heptapeptoid and fluorescein labelling to PNA oligomers. Reagents and conditions; couplings: acid (3 equiv), DIC (3 equiv) and HOBt (3 equiv) in DMF at 0.2 M; microwave irradiation at 60 °C for 20 min. Fmoc deprotection: 20% piperidine in DMF (2 x10 min) at room temperature. FAM = 5(6)-carboxyfluorescein.

Crude heptapeptoid conjugated 9mer (**3.40** and **3.46**, Figure 3.19) and 12mer (**3.41** and **3.47**, Figure 3.20) PNAs were obtained with purities > 90%, confirming the reliability of the microwave assisted peptoid synthesis and labelling.



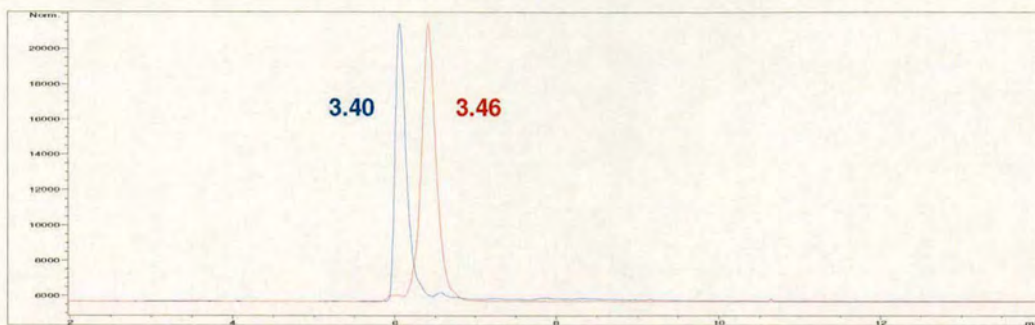


**Figure 3.19.** HPLC trace (ELS) of **3.40** (95% purity) and **3.46** (95% purity).

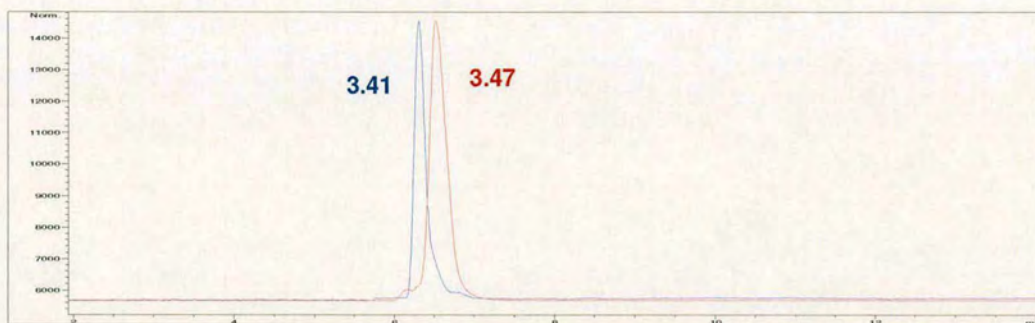


**Figure 3.20.** HPLC trace (ELS) of **3.41** (95% purity) and **3.47** (90% purity).

The heptapeptoid conjugated 15mer PNAs (**3.42** and **3.48**) gave HPLC traces with slightly broader peaks (Figure 3.21), and an estimated purity around 85% for **3.42**, and 75% for **3.48**.

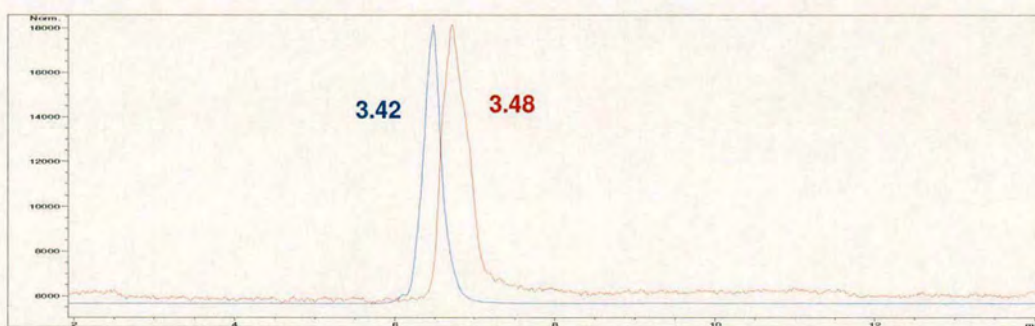


**Figure 3.21.** HPLC trace (ELS) of **3.42** (85% purity) and **3.48** (75% purity) .



### III.2.3. PNA delivery into cell and skin.<sup>†</sup>

Fluorescently labelled PNA and fluorescently labelled heptapeptoid conjugated PNA (only the one targeting mouse tyrosinase) were tested for cellular uptake and skin penetration.<sup>205,206</sup> After incubation with B16F10 cell (3 h) fluorescently labelled PNA (**3.34**, **3.35**, **3.36**) ( $10^{-4}$  M) did not show cellular uptake. However the heptapeptoid proved to be able to deliver efficiently the PNA oligomers independently by the size. The 15mer PNA **3.48** was able to penetrate into B16F10 cells with a cellular uptake > 90% (measured by FACS) after 3 h of incubation (at  $10^{-4}$  M). *Ex vivo* skin penetration studies using Franz's diffusion chamber showed that the heptapeptoid conjugated PNA (**3.46**, **3.47**, **3.48**) (at  $10^{-3}$  M) were able to enter into skin while the PNA (**3.34**, **3.35**, **3.36**) were not (Figure 3.22). Interestingly the heptapeptoid conjugated 12mer PNA **3.47** was able to penetrate deep into the dermis at 3 h, whereas the 15mer PNA **3.48** was situated mainly in the epidermis.

The ability of the heptapeptoid conjugated PNA to inhibit tyrosinase gene function was tested in an *in vitro* B16F10 cell based assay.<sup>205</sup> The results have shown that heptapeptoid conjugate 15mer PNA **3.42** (10  $\mu$ M) (Scheme 3.12) was able to significantly inhibit  $\alpha$ -MSH ( $10^{-10}$  M) induced pigmentation and tyrosinase activity. The corresponding 15mer PNA **3.30** did not show any antisense activity, as it was expected. The PNA oligomer had to bind the mRNA in the cytosol to stop protein translation, but the compound was not able to penetrate inside the cell as indicated by the fluorescein labelled 15mer PNA **3.33**, which did not show any cellular uptake.

---

<sup>†</sup> PNAs were tested by Pawan Kumar, Prof. Eugene Healy, at Dermatopharmacology, University of Southampton, Southampton.



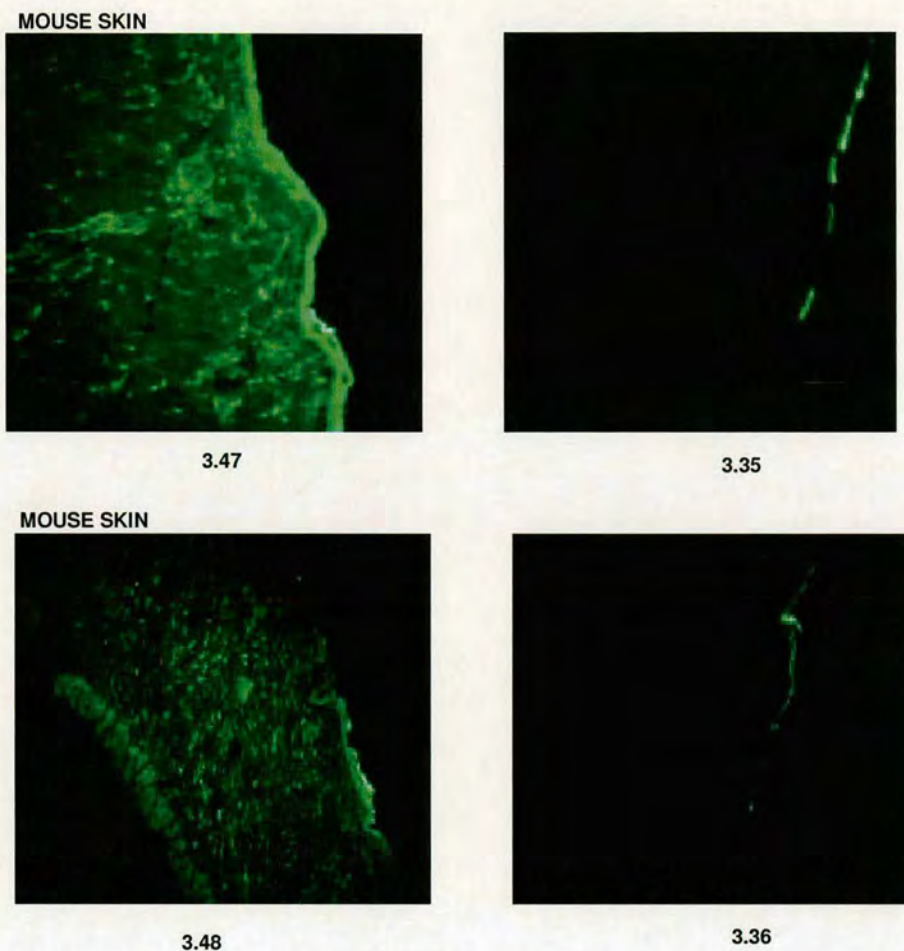


**Figure 3.22.** Fluorescence microscopy. Section of Mouse skin exposed to 1 mM **3.47**(left panel), 1 mM **3.48** (left panel) , 1 mM **3.35** (right panel) and 1 mM **3.36** for 3 h.

In conclusion PNA oligomers and peptoid conjugated PNA oligomers were efficiently prepared on solid phase using Dde protected PNA monomers, obtaining crude materials with high purities, from 75% (**3.48**) up to 95% (**3.40**, **3.41**, **3.46**). Fluorescein labelled compounds were tested for cellular uptake. PNA oligomers alone did not show cellular internalisation. The heptapeptoid oligmer was able to deliver the PNA oligomers (12, 15mer) into B16F10 cells with cellular uptake > 90%. The heptapeptoid conjugated PNAs were also able to penetrate into mouse skin, showing all the potentials of the peptoid carrier for the topical delivery of even very large compounds with molecular weight > 5000.



### III.3. Antisense DNA delivery.

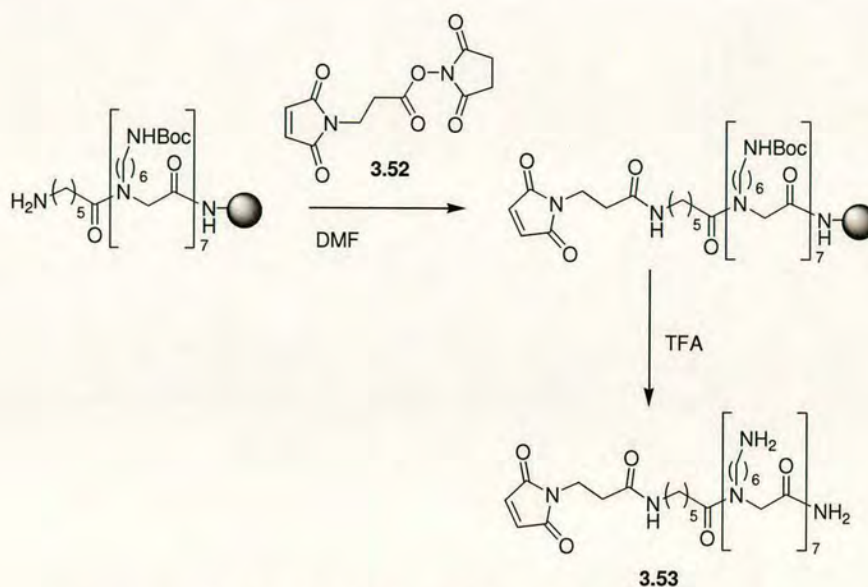
#### III.3.1. Conjugation to the heptapeptoid carrier.

In order to explore further the potential of the heptapeptoid as a “delivery vehicle” we decided to test the possibility of delivering DNA oligos, which can be used for antisense experiments for the inhibition of specific protein expression, as described in Chapter I.

A thiol modified 19mer DNA oligo (5'-HS-CCAAGAACATTTTCTCCTT-3') **3.57** (Scheme 3.15), targeting the translational start site of the tyrosinase gene (mouse), was conjugated to the heptapeptoid using two different ways:

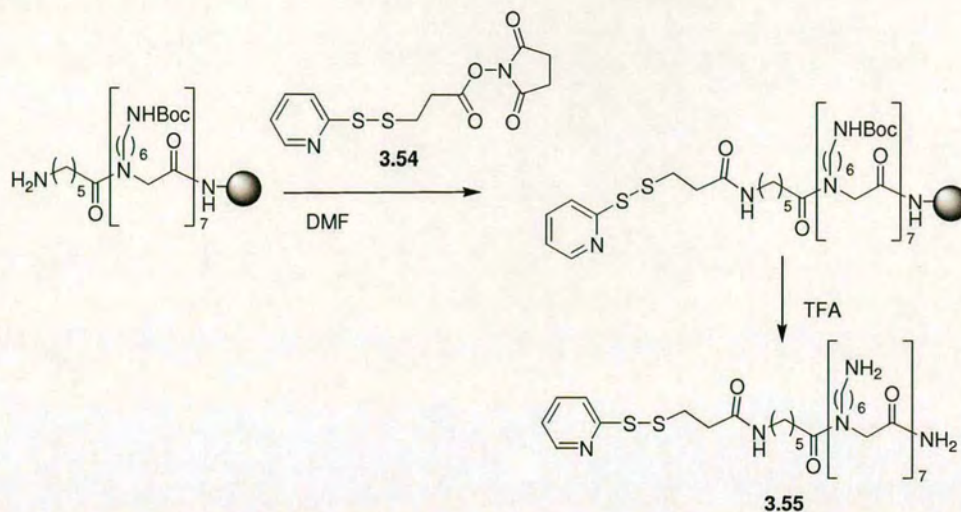
- Disulfide bond, cleavable in cellular environment (**3.59**, Scheme 3.15).
- Sulfide bond, stable in cellular environment (**3.58**, Scheme 3.15).

Heptapeptoid **3.53** with an activated disulfide linker, and heptapeptoid **3.55**, with a maleimido linker, were prepared on solid phase, as described in Scheme 3.13 and Scheme 3.14, with crude purities > 95%. DNA-oligo **3.57** was prepared by reduction of disulfide protected oligo **3.56** (purchased from Sigma) with DTT. It was reacted with heptapeptoid **3.53** (1 equiv) and heptapeptoid **3.55** (1 equiv) in PBS buffer to give the heptapeptoid conjugated oligo **3.58** (sulfide) and the heptapeptoid conjugate oligo **3.59** (disulfide) as described in Scheme 3.15.

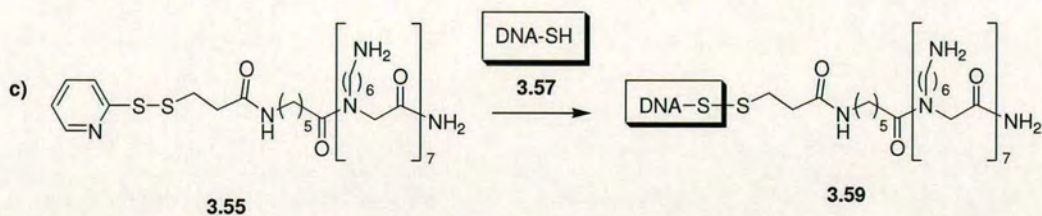
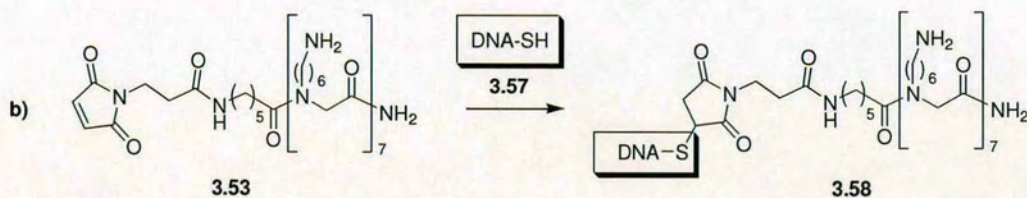
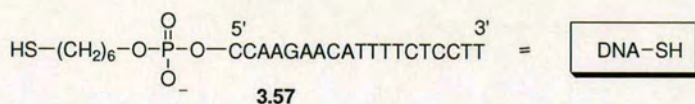
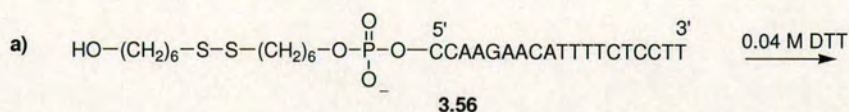


Scheme 3.13. Synthesis of compound **3.53**.





**Scheme 3.14.** Synthesis of compound **3.55**.



**Scheme 3.15.** Synthesis of compounds **3.57**, **3.58**, **3.59**.

DNA-heptapeptoid conjugates were characterised by MALDI-TOF, which gave the expected ions for **3.58** ( $\text{C}_{239}\text{H}_{380}\text{N}_{79}\text{O}_{128}\text{P}_{19}\text{S}$ , calcd 7268, found 7266  $[\text{M-H}]^-$ ) and



**3.59** ( $C_{255}H_{377}N_{78}O_{126}P_{19}S_2$ , calcd 7203, found 7201  $[M-H]^-$ ) as shown in Figure 3.23 (b and c). MALDI-TOF analysis also gave the peaks of residual thiol protected DNA **3.56** (intense peaks compared to **3.58** and **3.59**) and residual un-conjugated free thiol DNA **3.57** (very low intensity peaks compared to **3.58** and **3.59**) as shown in Figure 3.23 (b and c).

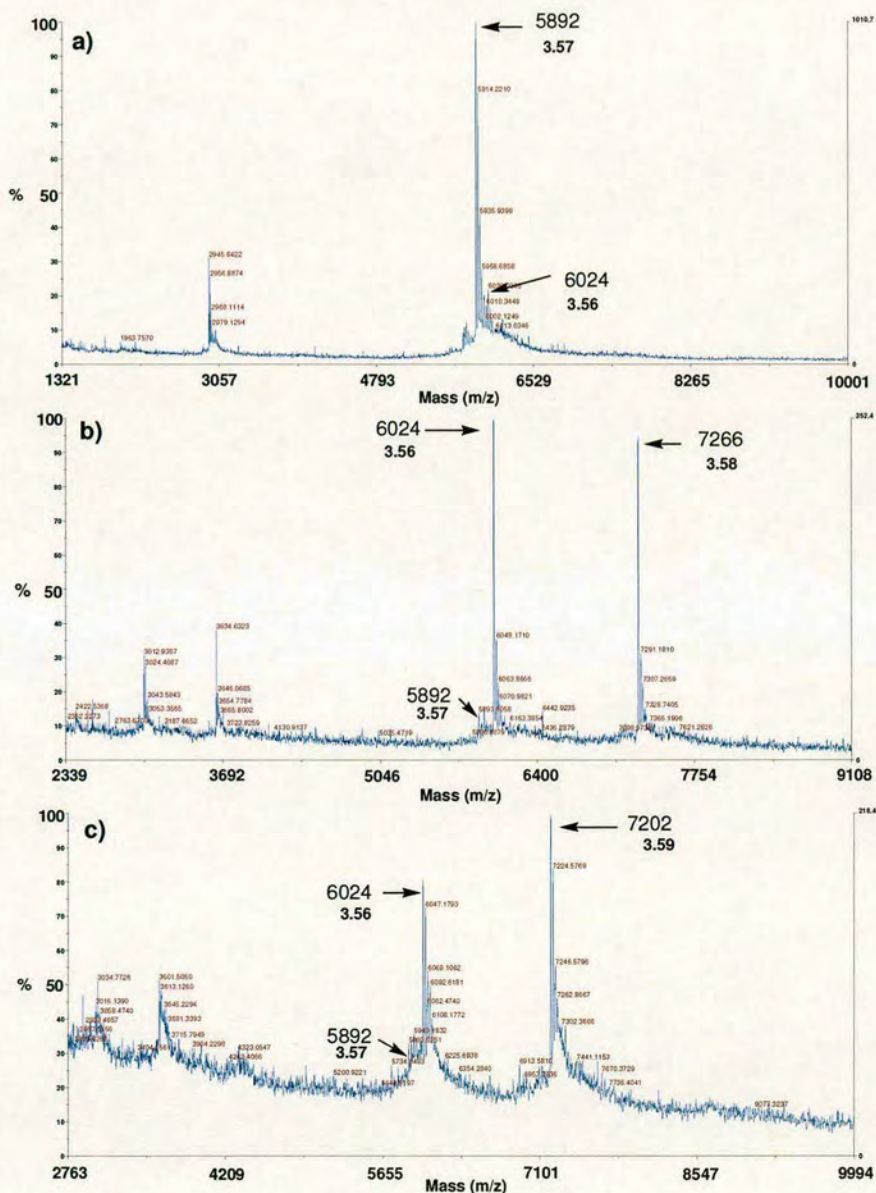


**Figure 3.23.** MALDI- TOF spectra of: (a) compound **3.57**; (b) compound **3.58**; (c) compound **3.59**.



### ***III.3.2 DNA-Peptoid conjugates: antisense activity.<sup>‡</sup>***

As described before hormone  $\alpha$ MSH stimulates pigmentation and tyrosinase activity of melanoma cells by binding the melanocortin 1 receptor (*MC1R*). Oligonucleotide **3.59** (10  $\mu$ M) was able to inhibit tyrosinase activity stimulated by  $\alpha$ -MSH ( $10^{-10}$  M) on B16F10 cells.<sup>205</sup> This result did show the ability of the heptapeptoid carrier to deliver polyanionic cargoes such as a 19mer oligonucleotide and not just neutral or positively charged cargoes.

In contrast, oligonucleotide **3.58** did not inhibit tyrosinase activity, raising questions about the delivery and about possible interferences of the heptapeptoid on the oligonucleotide antisense activity, considering that **3.58**, differently to **3.59**, does not split inside the cell separating the heptapeptoid and the oligonucleotide. These questions unfortunately could not be answered without experiments with fluorescently labelled oligonucleotides that could not be performed.

---

<sup>‡</sup> Antisense test have been carried out by Pawam Kumar, Prof. Eugene Healy group, at Dermatopharmacology, University of Southampton, Southampton.



## **Chapter IV. Macromolecules delivery.**

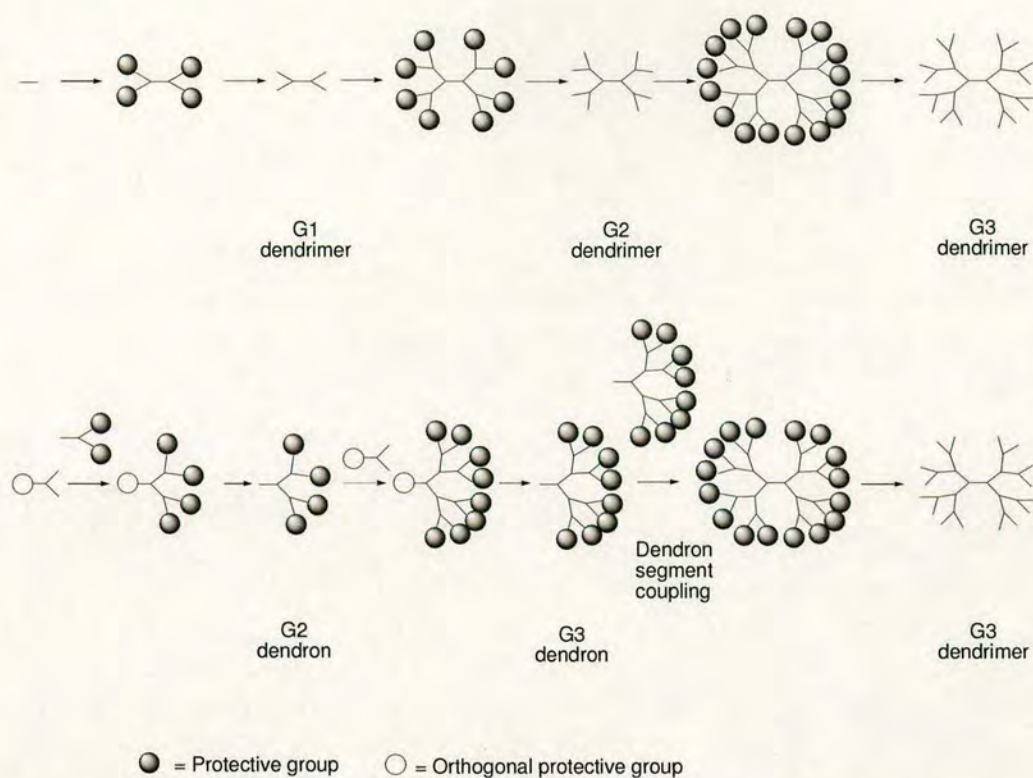
The possibility of using the peptoid for the preparation of carriers able to deliver macromolecules such as proteins and DNA was explored.

- For the delivery of DNA 3 generations of dendrimers based on the peptoid subunit were synthesised.
- For the delivery of proteins, the possibility of exploiting, what is today, a standard approach of tagging proteins for purification, namely the polyhistidine tag, was explored

### **IV.1. Peptoid dendrimers for DNA delivery.**

Dendrimers are fascinating compounds, offering many of the properties of more conventional polymers but with a highly defined shape, molecular mass and with a structure which displays a large number of functional groups on the periphery, while 'hiding' much internal functionality. Two dominant synthetic methodologies have been used to generate dendrimers (Scheme 4.1): (i) a linear approach as initially described by Vögtle,<sup>207</sup> where surface functionalities grow at an exponential rate while the numbers of synthetic steps increases linearly and (ii) a convergent synthesis strategy as introduced by Fréchet,<sup>208</sup> where dendrimeric fragments are synthesised before condensation to give the full dendrimeric structure.





**Scheme 4.1.** Schematic of Dendrimer synthesis. Upper Divergent and lower Convergent strategy.

Polyamidoamines (PAMAMs) (see Figure 4.1 for PAMAM G2, 1,4-diaminobutane core) can be regarded as the classical dendrimeric material and are typically constructed by the reaction of methyl acrylate with an initiation unit such as ammonia, with subsequent treatment with diamines followed by repetitive treatment with methyl acrylate and diamine. Such dendrimers display multiple primary amines on their external surface which can vary from 4 (generation 0) to 4096 (generation 10).

PAMAM dendrimers have found practical application in the area of gene delivery<sup>209-211</sup> and a number of other biomedical applications such as magnetic resonance imaging (MRI).<sup>212-214</sup> Another family of dendrimers, which have seen practical application, are those based on repeating and amplifying amino acid residues, most notably the lysine dendrimers introduced by Tam<sup>215</sup> which offer a chemical route to the development of high-density antigenic peptides. A new step forward would be a hybrid combination of PAMAM and peptide dendrimers in which peptoids (N-alkylglycines) are used both as an initiator and a monomer unit.<sup>216</sup>



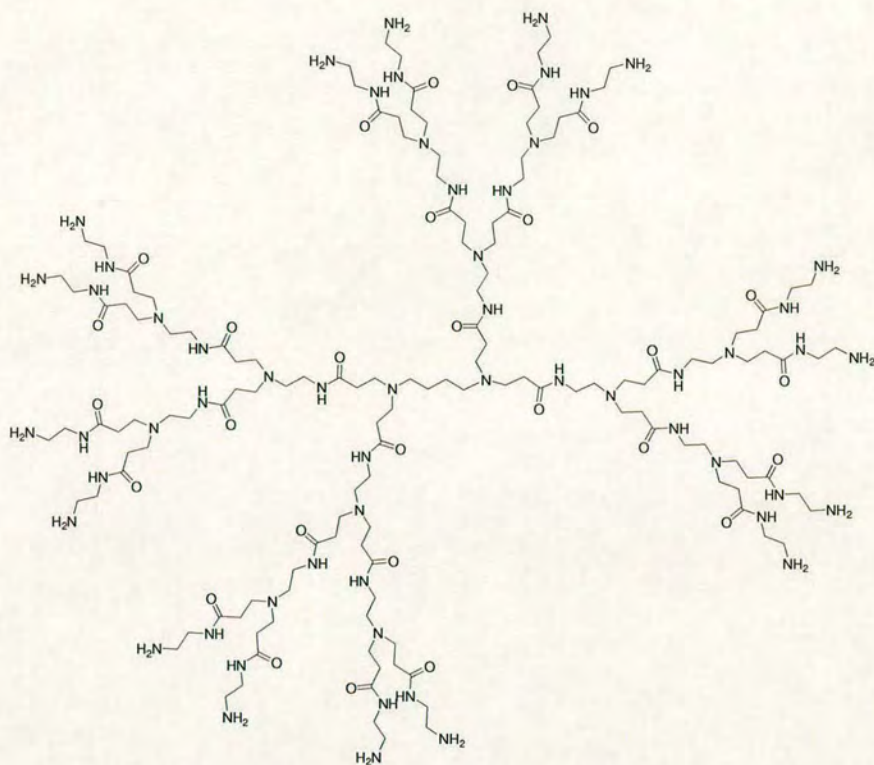
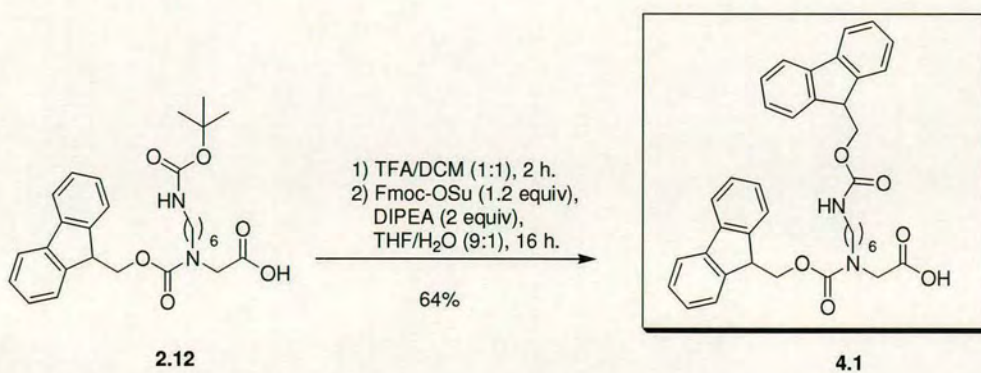


**Figure 4.1.** PAMAM G2, 1,4-diaminobutane core.

#### **IV.1.1. Monomer synthesis.**

In order to prepare the peptoid dendrimer by solid phase synthesis a suitable building block was required. Bis-Fmoc protected peptoid monomer **4.1**<sup>216</sup> was prepared by treating **2.12** with TFA to remove the Boc group followed by Fmoc protection of the side chain amine with Fmoc-OSu (Scheme 4.2, 64% yield). Starting material **2.12** was readily available on large scale (see chapter II).



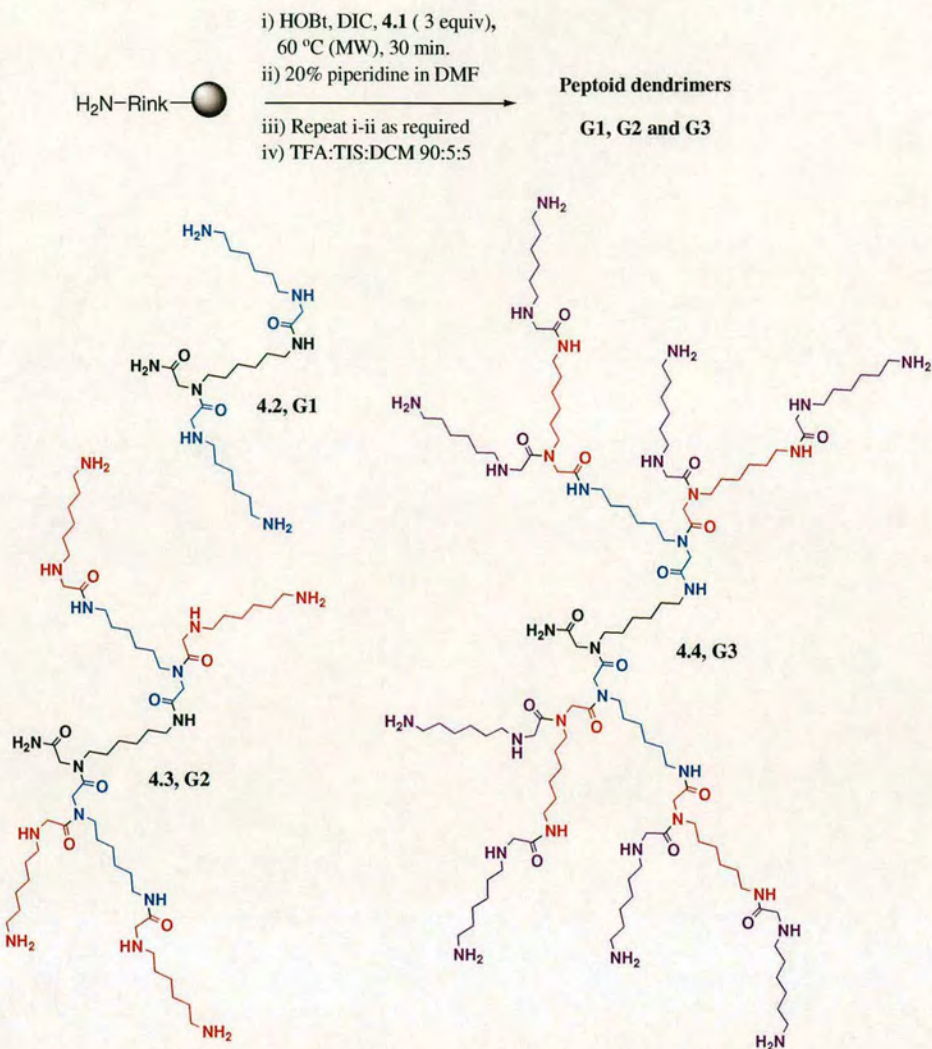
**Scheme 4.2.** Synthesis of monomer **4.1**.



#### ***IV.1.2. Microwave assisted peptoid dendrimer synthesis: G1-G2-G3.***

The dendrimers were assembled with high efficiency using monomer **4.1** on Rink amide polystyrene resin using HOBt/DIC chemistry and microwave irradiation (Scheme 4.3).<sup>216</sup> More generally, microwave irradiation offers huge promise in dendrimer synthesis, allowing reactions to be readily forced. To ensure coupling completion two colorimetric tests were used: (i) The Kaiser<sup>182</sup> test for primary amines and (ii) a chloranil<sup>171</sup> test for detecting secondary amines. The first generation dendrimer gave, not unexpectedly, negative tests after a single coupling, but subsequent generations required a second coupling to ensure 100% reaction. Following final Fmoc removal the polyamidoamines were cleaved from the resin using TFA/TIS/DCM (90:5:5) and precipitated with cold diethyl ether to give the final compounds displaying 4, 8 and 16 amines (half primary and half secondary) on their surface just after 1, 2 and 3 coupling steps (Scheme 4.3) .





**Scheme 4.3.** Solid phase synthesis of peptoid dendrimers **4.2**, **4.3**, **4.4** using monomer **4.1** under microwave conditions.

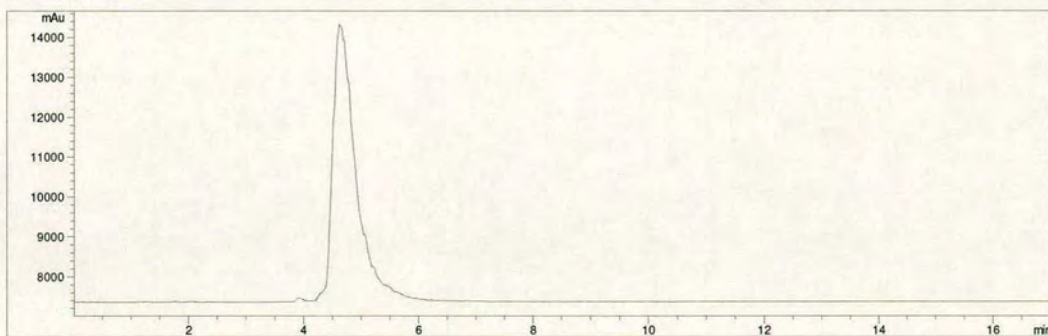


**Figure 4.2.** HPLC trace of peptoid dendrimer **4.4** (G3).



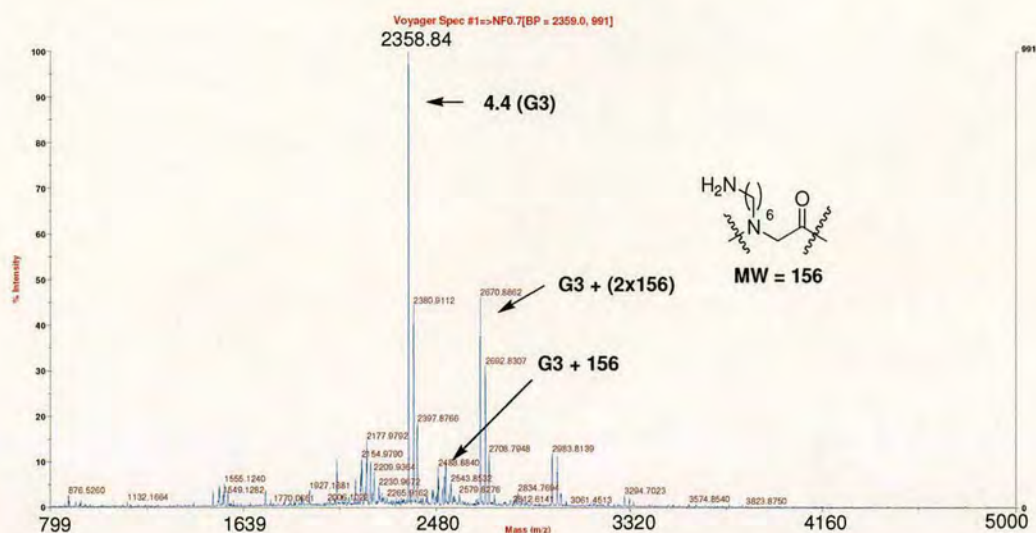


**Figure 4.3.** MALDI-TOF spectra of peptoid dendrimer **4.4** (G3).

MALDI-TOF analysis of **4.4** (G3) (Figure 4.3, HPLC trace in Figure 4.2) showed the desired material as the main ion; however it also showed traces of incomplete dendrimers with some subunits missing. The presence of incomplete dendrimers was expected, since the extension of the branches becomes increasingly difficult with the growth of the molecule. More interestingly the spectra presented peaks that appeared to be the result of over incorporation of monomer **4.1**. This result was unexpected, and could be explained by the loss of Fmoc group during the final couplings. MALDI spectra of dendrimer **4.4** (G3) showed quite a “clean” and “defined” composition, considering that MALDI spectra of dendrimers made in solution which usually show a broad distribution of peaks around the theoretical molecular mass of the desired materials.

#### **IV.1.3. DNA delivery: peptoid dendrimers vs. PAMAM G2.**

To evaluate the properties of these compounds as transfection agents, their complexes with pEGFP-N1 (a plasmid DNA which carries the gene that encodes green fluorescence protein (GFP)) were incubated with human embryonic kidney (HEK293T) cells.<sup>216</sup> PAMAM G2 (Figure 4.1) was used as a control as it also possesses 16 external amino groups. Dendrimer-plasmid complexes were prepared by mixing the dendrimers and plasmid DNA in PBS buffer at different molar ratios



(dendrimer-plasmid 5:1, 10:1, 20:1 and 40:1) defined as moles of dendrimer for 1 mole of nucleotide (g (plasmid DNA) / 330 (nucleotide average molecular weight)) and incubation for 30 minutes before use. Dendrimer-plasmid complexes were added to HEK293T cells in DMEM complete media with 10% FCS (96 well plate, 0.2 µg of plasmid per well), and incubated for 48 h at 37 °C. FACS analysis showed that while **4.2** (G1) and **4.3** (G2) had no noticeable effect, **4.4** (G3) (10:1 molar ratio) was able to transfect HEK293T cells 4 times more efficiently than PAMAM G2 (20:1 molar ratio) (Figure 4.4).

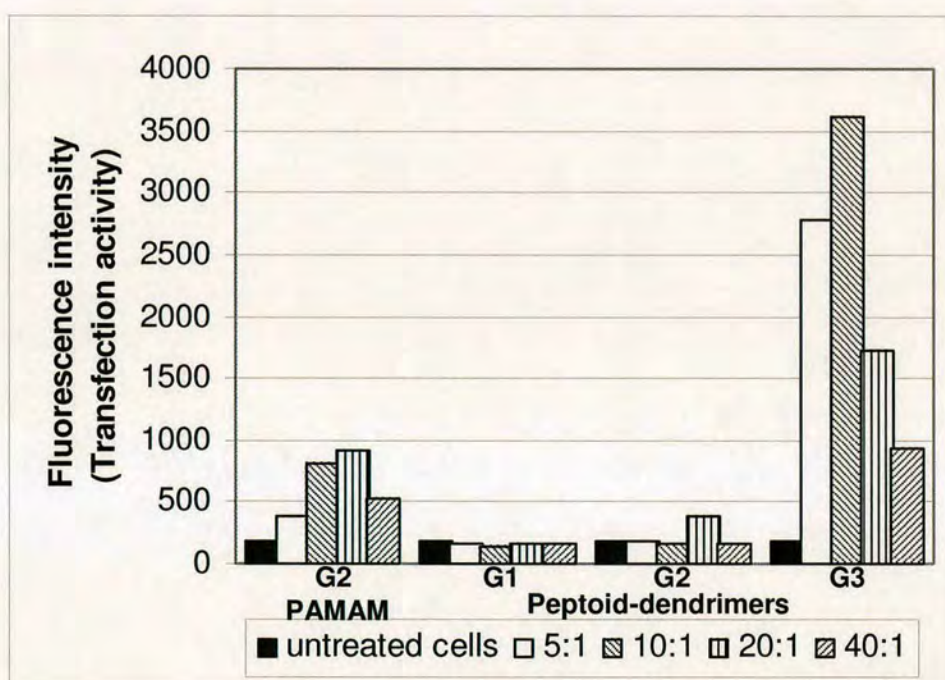


**Figure 4.4.** Transfection activity of peptoid dendrimers **4.2** (G1), **4.3** (G2), **4.4** (G3) and PAMAM G2 with HEK293T cells. Delivery of plasmid DNA (pEGFP-N1) was tested at different dendrimer/plasmid molar ratios (5:1, 10:1, 20:1, 40:1) and determined by FACS analysis of cell fluorescence, as a measure of GFP protein expression.

Transfection activity of **4.4** (G3) had its maximum at a 10:1 molar ratio. The lower generation dendrimers **4.2** (G1) and **4.3** (G2) were probably too small to effectively condensate the plasmid even at high molar ratios. Dendrimer **4.4** (G3) complexes at 20:1 and 40:1 ratio showed a lower activity compared to 5:1 and 10:1 ratios. This lower efficiency might have been due to an increased stability of the complexes and



consequent more difficult “DNA release” even if the dendrimer-plasmid complexes entered in large amounts inside the cell.

Cytotoxicity of **4.4** (G3) and PAMAM 2.0 was evaluated by MTT<sup>173</sup> assay (Figure 4.5). The peptoid dendrimer was found to be non-toxic at all of the ratios tested, reinforcing the idea of employing these molecules as gene delivery agents.

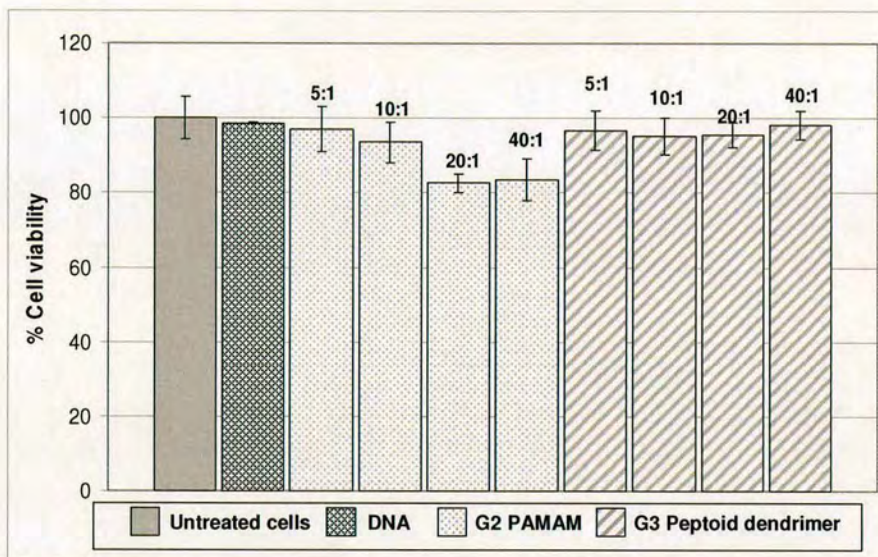


**Figure 4.5.** Cytotoxicity of **4.4** (peptoid dendrimer G3) with HEK293T cells compared to PAMAM G2 as measured by MTT assay.

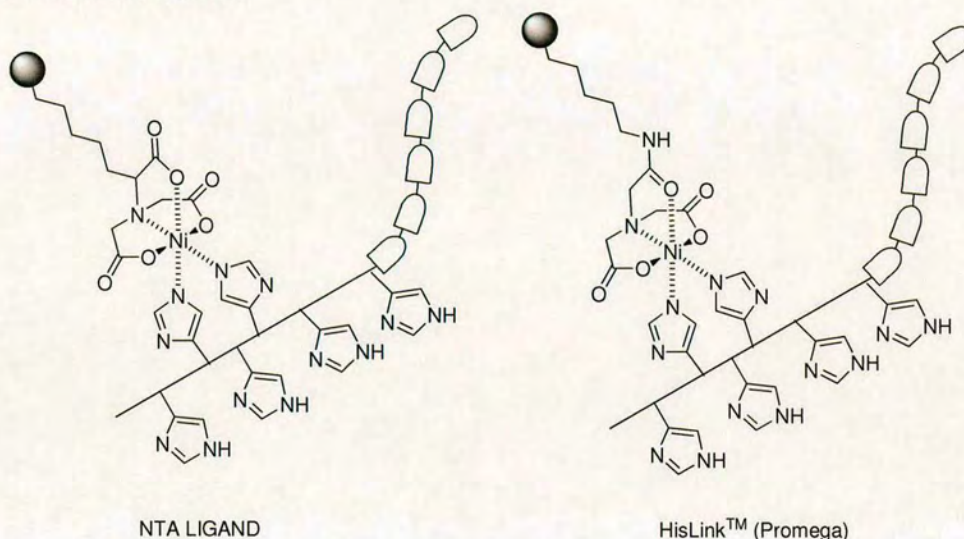
In conclusion, peptoid dendrimers containing primary and secondary amines on their periphery have been successfully synthesised by solid phase synthesis combined with microwave mediated methods using a ‘lysine-type’ peptoid monomer. The higher generation peptoid dendrimer **4.4** (G3, 16 external amines, 8 primary and 8 secondary) was able to transfect cells four times more efficiently than PAMAM G2 (16 external primary amines), and it was found to be non-toxic, making the hypothesis of synthesising and evaluating higher generations of this peptoid dendrimer appealing.



## IV.2. Protein delivery.

The most commonly used tag for purification of recombinant proteins is the polyhistidine (His<sub>6</sub>) tag introduced by Hochuli in 1988.<sup>217</sup> Protein purification using polyhistidine tags relies on the affinity of histidine residues for an immobilized metal such as nickel, which allows selective purification of proteins.<sup>218</sup>

### TETRADENTATE LIGANDS



### TRIDENTATE LIGANDS

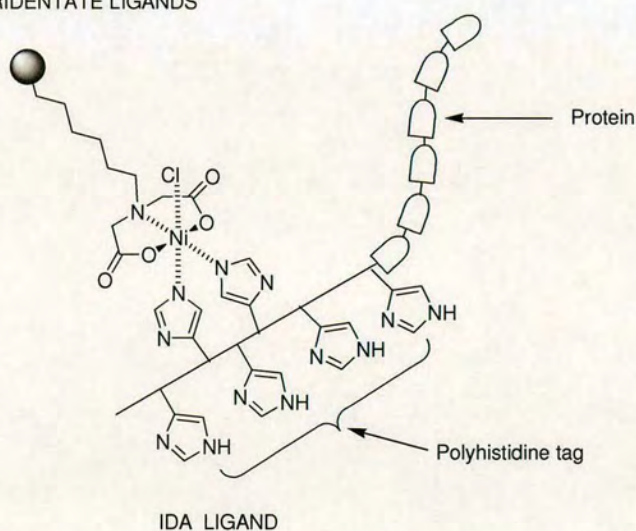


**Figure 4.6.** Schematic representation of immobilised Ni-Polyhistidine tagged protein interaction. NTA,<sup>219</sup> HisLink™ (Promega), and IDA ligands.



This affinity interaction is believed to be a result of the coordination of a nitrogen on the imidazole moieties of polyhistidine with vacant coordination sites on the metal (Figure 4.6).<sup>217</sup> The metal is immobilized through complex formation with a chelate that is covalently attached to a solid support. Two sites are available and are rapidly coordinated with histidine in the presence of a polyhistidine –tagged polypeptide. Polyhistidine tags offer several advantages for protein purification. The small size of the tag renders it less immunogenic than larger tags. Therefore, the tag usually does not need to be removed for downstream applications following purification. A large number of commercial expression vectors that contain polyhistidine are available. The polyhistidine tag may be placed on either the N- or the C- terminus of the protein of interest. Finally the interaction of the polyhistidine tag does not depend on the tertiary structure of the tag, making it possible to purify otherwise insoluble proteins using denaturing conditions. Although protein purification is the main reason for tagging proteins with the polyhistidine residue, there are several reports describing many different applications of the tag such as protein labelling with gold (or silver) nanoparticles<sup>220</sup> used for electron microscopy visualization, protein immobilization on Ni<sup>2+</sup>:NTA coated surfaces<sup>221</sup> and site specific introduction of fluorescent probes using a Ni<sup>2+</sup>:NTA-fluorochrome conjugate.<sup>222</sup> Kapanidis<sup>222</sup> reported the use of Ni<sup>2+</sup>:NTA modified Cy3 and Cy5 fluorescent probes (Figure 4.7) for structural studies of the complex between transcriptional activator protein CAP and DNA by FRET<sup>223</sup> efficiency measurements between the Ni<sup>2+</sup>:NTA modified fluorescent probe (Ni<sup>2+</sup>:NTA -Cy3 or -Cy5) coordinated to the hexahistidine tagged protein and the fluorescein label attached to the DNA. They measured the affinity of the Ni<sup>2+</sup>:NTA modified fluorochromes Cy3 and Cy5 to the hexahistidine tag of the protein CAP (by anisotropic experiments) finding that only **4.7** and **4.8** (Figure 4.7) with 2 Ni<sup>2+</sup>:NTA coordination sites had a sufficiently high affinity for the hexahistidine tag with K<sub>D</sub> values of 1 µM and 0.4 µM respectively. Cy3 **4.5** and Cy5 **4.6** (Figure 4.7) with 1 Ni<sup>2+</sup>:NTA coordination site had poor affinity for the hexahistidine tag with a K<sub>D</sub> of 10 and 40 µM respectively.



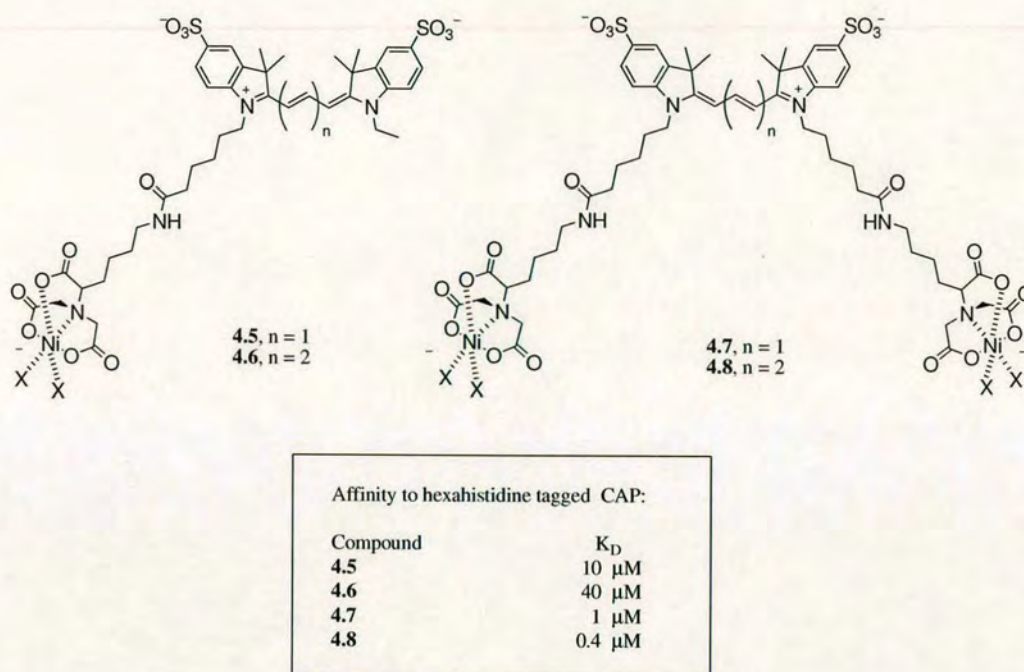


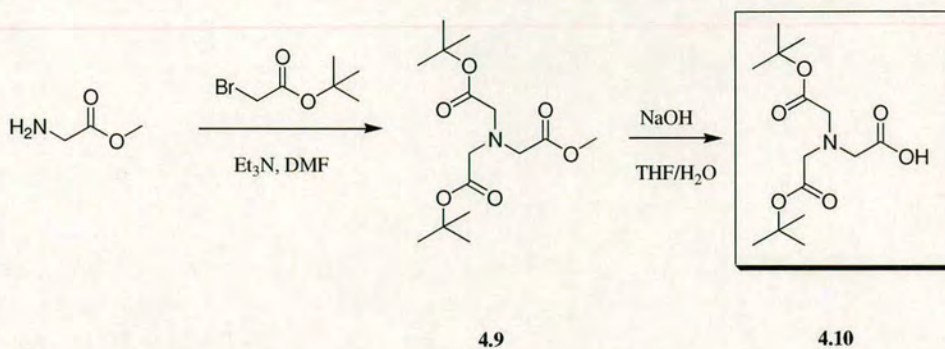
**Figure 4.7.** Ni<sup>2+</sup>:NTA modified Cy3 and Cy5 for site specific fluorescent labelling of hexahistidine tagged proteins.<sup>141,222</sup>

#### IV.2.1. Synthesis of Ni<sup>2+</sup>-ligand functionalised peptoids.

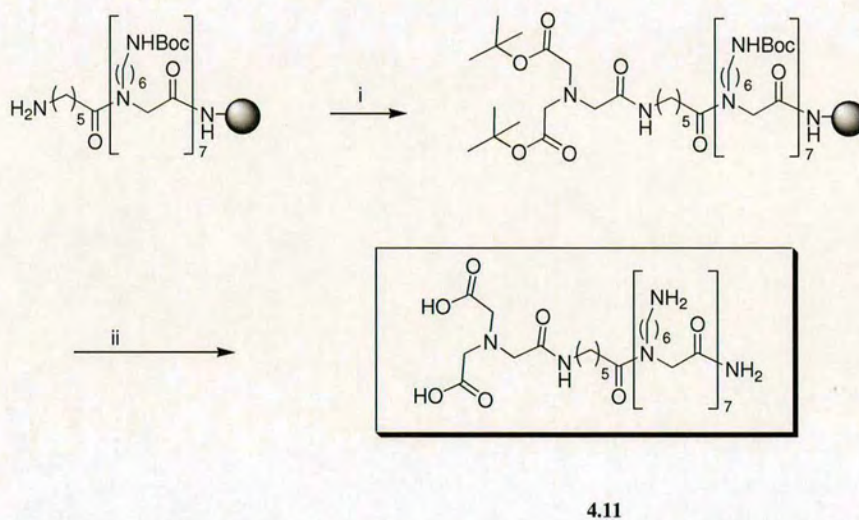
Considering the great availability of vectors expressing hexahistidine tagged proteins the idea of using this tag to conjugate the heptapeptoid carrier to proteins with the intention of allowing their cellular uptake appeared appealing.

For this first attempt a Ni ligand similar to the one employed by Promega (Figure 4.6 and Scheme 4.4) was easily prepared from glycine methyl ester which was dialkylated using 2-bromo 'butylacetate, followed by saponification to yield the 'butyl protected ligand required to be coupled to the heptapeptoid on solid phase. As described in chapter II the heptapeptoid was built using a Rink<sup>151</sup> amide polystyrene resin under microwave conditions. The heptapeptoid was functionalised with one Ni<sup>2+</sup>-ligand (**4.11**, Scheme 4.5) and with two Ni<sup>2+</sup>-ligands (**4.14**, Scheme 4.7) using **4.13**<sup>224</sup> (Scheme 4.6) to introduce two symmetric branches.

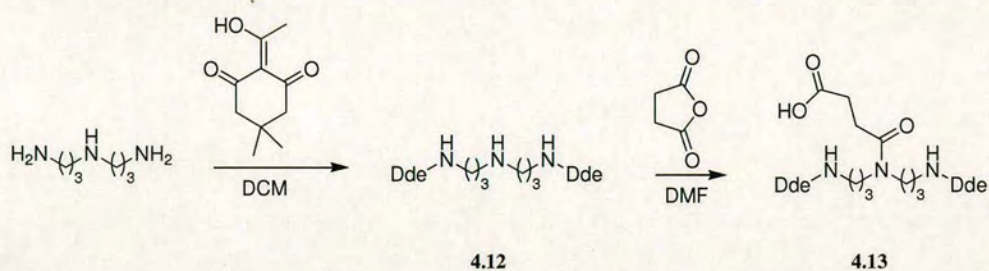




**Scheme 4.4.** Synthesis of compound **4.10**.

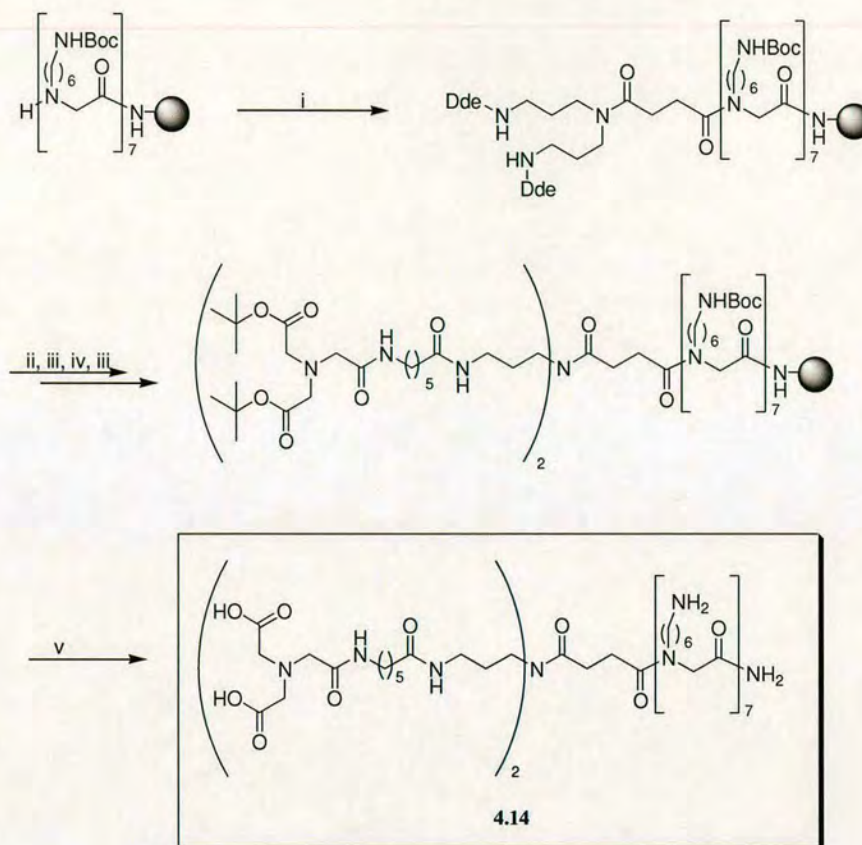


**Scheme 4.5.** Synthesis of **4.11**. Reagents and Conditions: i) **4.10** (3 equiv), DIC (3 equiv) and HOBT (3 equiv) in DMF at 0.2 M; microwave irradiation at 60 °C for 20 min; ii) 95% TFA, 2.5% water, 2.5% TIS (triisopropylsilane), 3 h.



**Scheme 4.6.** Synthesis of compound **4.13**.





**Scheme 4.7.** Synthesis of **4.14**. Reagents and Conditions: i) **4.13** (3 equiv), DIC (3 equiv) and HOBt (3 equiv) in DMF at 0.2 M, microwave irradiation at 60 °C for 20 min; ii)  $\text{NH}_2\text{OH}\cdot\text{H}_2\text{O}$  in DMF 0.3 M (2 x 30 min); iii) Fmoc-Ahx-OH or **4.10** (4 equiv), DIC (4 equiv) and HOBt (4 equiv) in DMF at 0.25 M, microwave irradiation at 60 °C for 20 min; iv) 20% piperidine in DMF, 2 x 10 min; v) 95% TFA, 2.5% water, 2.5% TIS (triisopropylsilane), 3 h.

#### 2.1.1. $\text{Ni}^{2+}$ -ligands do not inhibit the heptapeptoid cellular uptake.

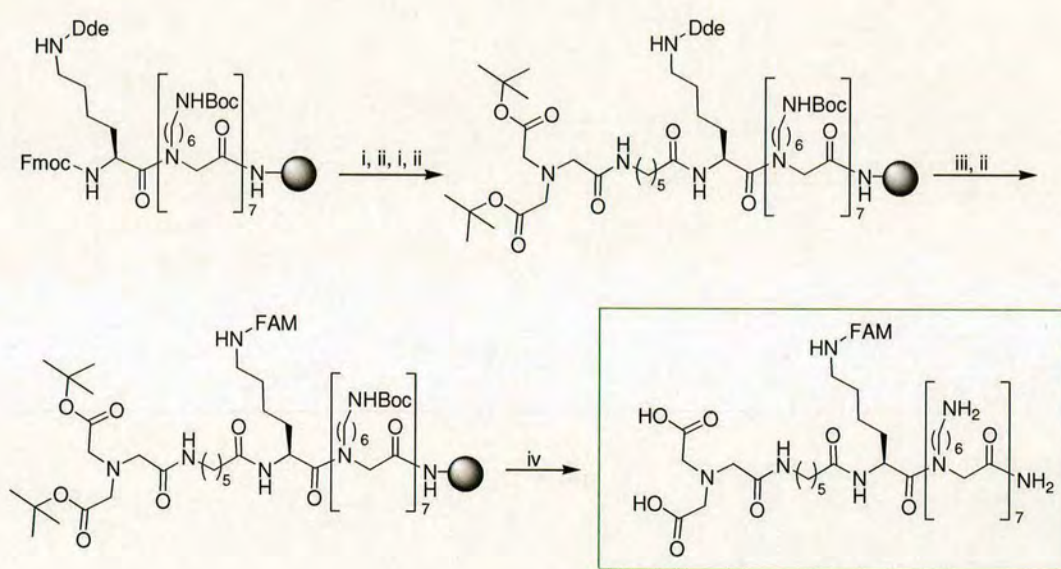
In order to verify if the  $\text{Ni}^{2+}$ -ligand did not inhibit the cellular uptake of the heptapeptoid, fluorescein labelled compounds **4.15** and **4.16** (Scheme 4.8 and Scheme 4.9) were prepared and cellular uptake determined.

The labelling of the compounds was carried out using a Fmoc-Lys(Dde)- residue introduced after the heptapeptoid (Scheme 4.8 and Scheme 4.9). For the synthesis of **4.15** the coupling of 5(6)-carboxyfluorescein was done as last step after Dde deprotection of the  $\epsilon$  amine of the lysine residue. The synthesis of **4.16** required another approach, due to the use of the Dde protected building block **4.13**. Using the labelling approach described by Brock,<sup>185</sup> the dye was coupled to the  $\alpha$  amine of the



lysine followed by tritylation of the phenolic hydroxy groups of the fluorescein moiety, that otherwise could react during the following coupling steps. The rest of the synthesis was carried out on the  $\epsilon$  amine of the lysine as described in Scheme 4.9.

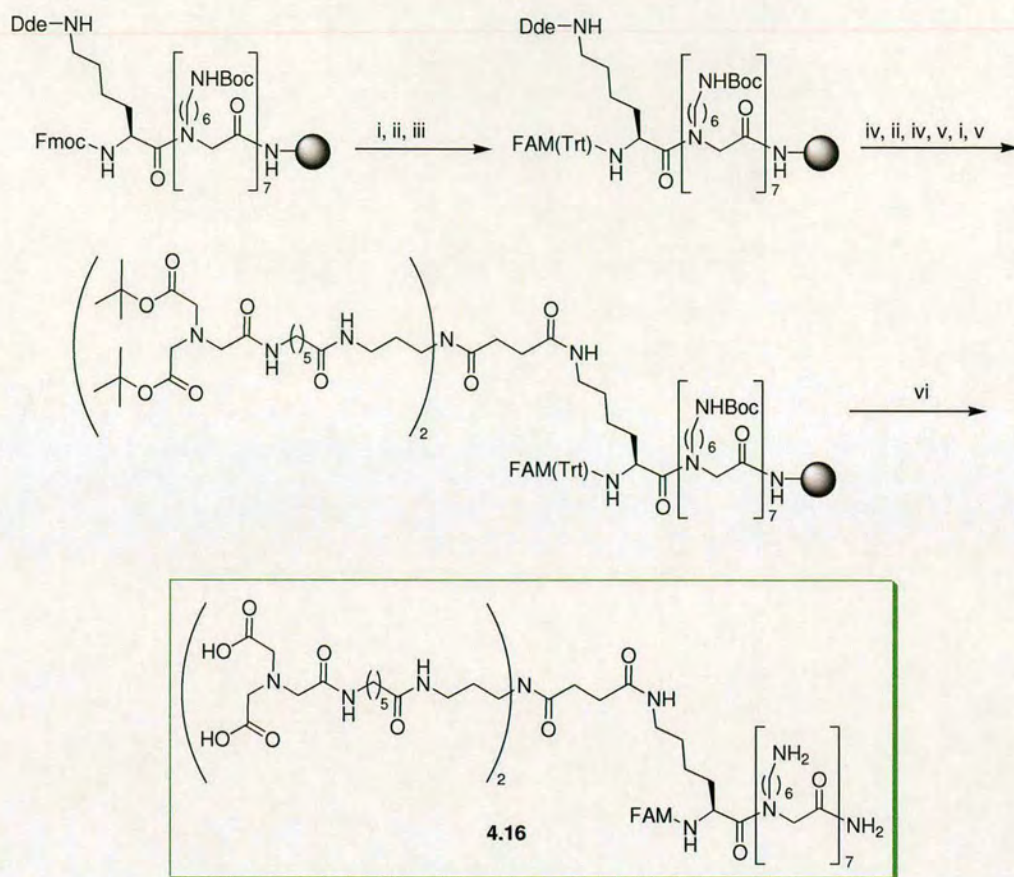
Both the compounds at a 5  $\mu$ M concentration were able to efficiently penetrate B16F10 cells after 4 h of incubation at 37  $^{\circ}$ C, however the percentage of fluorescently labelled cells was reduced to around 80% (Figure 4.8), against the 95% of the heptapeptoid alone, with heptapeptoid **4.16** showing a lower cellular uptake compared to **4.15** (Figure 4.8, panel B) as shown by the lower mean fluorescence intensity of the cells (Figure 4.8, panel C). The result was not completely unexpected since at pH 7.4 the anionic carboxylates (2 in **4.15** and 4 in **4.16**) might reduce the affinity of the heptapeptoid for the cellular membrane.



**4.15**

**Scheme 4.8.** Synthesis of fluorescently labelled **4.15**. Reagents and conditions: i) 20% piperidine in DMF, 2 x 10 min; ii) Fmoc-Ahx-OH (or **4.10**, or 5(6)-carboxyfluorescein) (3 equiv), DIC (3 equiv) and HOBt (3 equiv) in DMF at 0.2 M, microwave irradiation at 60  $^{\circ}$ C for 20 min; iii)  $\text{NH}_2\text{OH}\cdot\text{H}_2\text{O}$  in DMF 0.3 M, 2 x 30 min; iv) 95% TFA, 2.5% water, 2.5% TIS (triisopropylsilane), 3 h.





**Scheme 4.9.** Synthesis of fluorescently labelled **4.16**. Reagents and conditions: i) 20% piperidine in DMF, 2 x 10 min; ii) 5(6)-carboxyfluorescein (or **4.13**) (3 equiv), DIC (3 equiv) and HOBt (3 equiv) in DMF at 0.2 M, microwave irradiation at 60 °C for 20 min; iii) Trityl-Cl (0.1 M) and DIPEA (0.1 M) in DMF, 16 h; iv)  $\text{NH}_2\text{OH}\cdot\text{H}_2\text{O}$  in DMF 0.3 M, 2 x 30 min; v) Fmoc-Ahx-OH (or **4.10**) (4 equiv), DIC (4 equiv) and HOBt (4 equiv) in DMF at 0.25 M, microwave irradiation at 60 °C for 20 min; v) 95% TFA, 2.5% water, 2.5% TIS, 3 h.



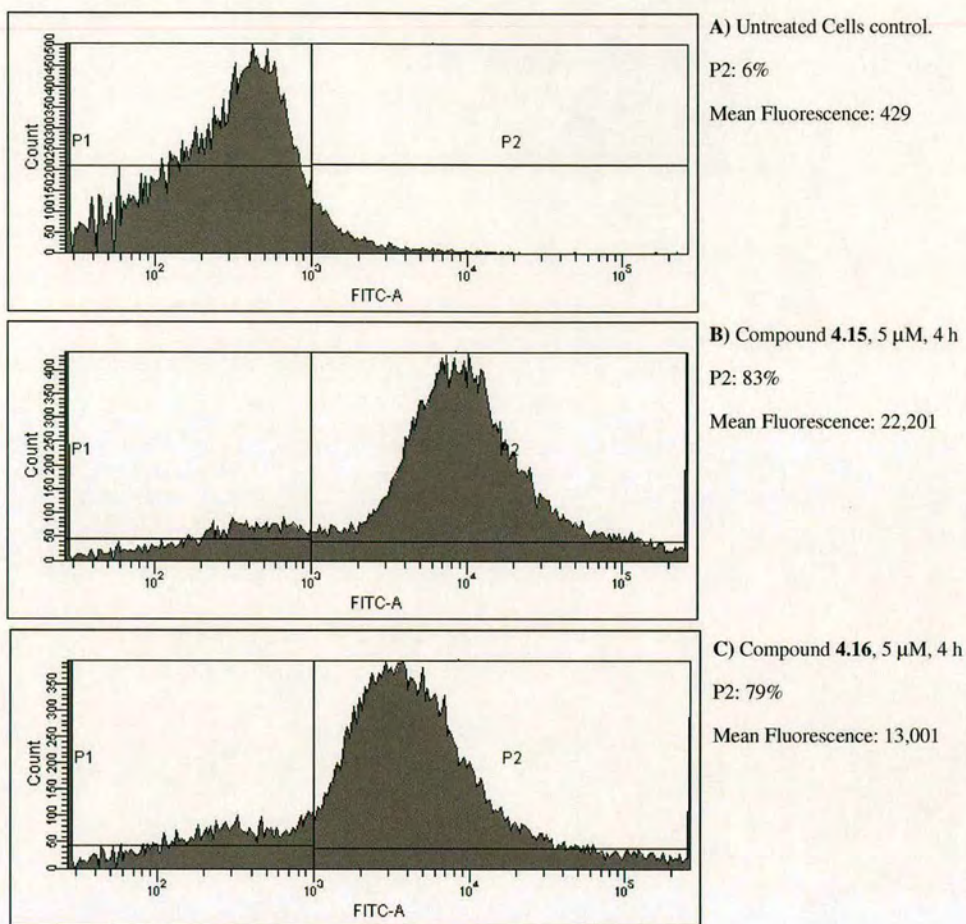


**Figure 4.8.** FACS analysis of: A) B16F10 untreated cells; B) B16F10 cells treated with **4.15** (5  $\mu$ M, 4 h); C) B16F10 cells treated with **4.16** (5  $\mu$ M, 4 h). P2 is the population of cells with a fluorescence intensity > 1000.



#### IV.2.2. Delivery of GFP protein.

The ability of the  $\text{Ni}^{2+}$  modified heptapeptoids **4.11** and **4.14** to induce protein internalisation was tested on hexahistidine tagged green fluorescent protein (His<sub>6</sub>-GFP). The GFP protein was chosen because cellular internalisation can be easily determined by confocal microscopy and quantified by FACS.

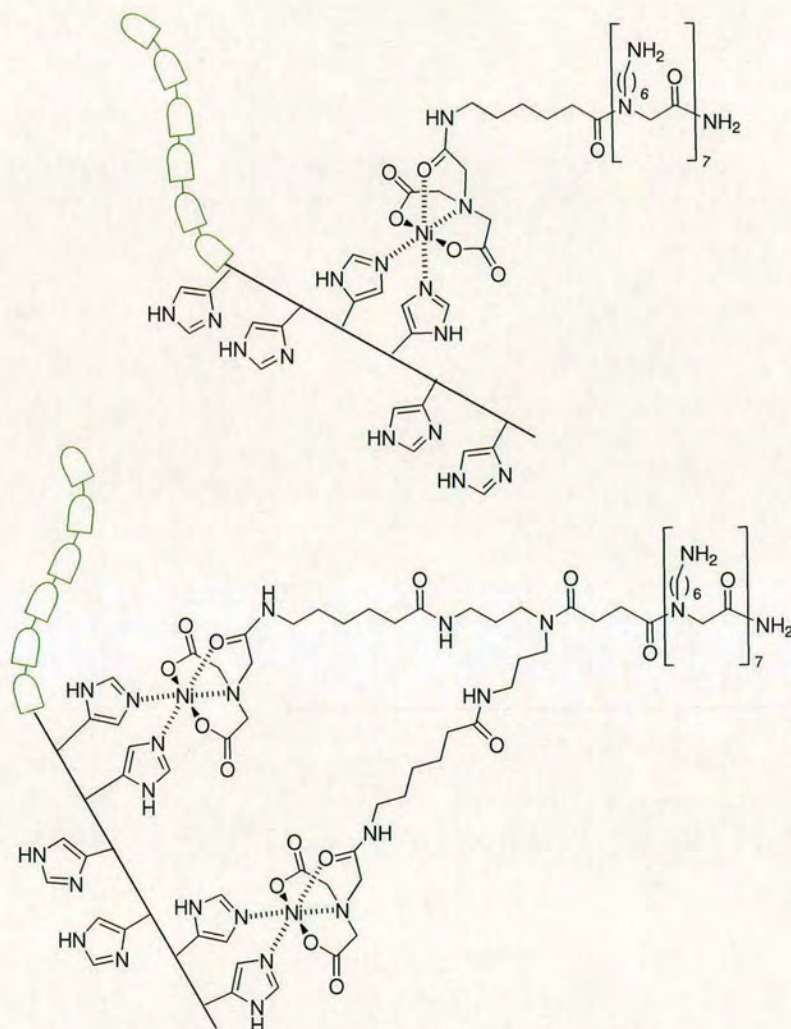


**Figure 4.9.** Hexahistidine tagged GFP- $\text{Ni}^{2+}$ -Heptapeptoid (**4.11** and **4.14**) complexes.

Heptapeptoids **4.11** and **4.14** were dissolved in PBS buffer (pH 7.4) at a concentration of 1 mM, to this solution was added  $\text{NiCl}_2$ . The  $\text{Ni}^{2+}$ -heptapeptoids were mixed with the His<sub>6</sub>-GFP protein (purified His<sub>6</sub>-GFP protein was kindly donated by Dr. David Nagel, Aston University, Birmingham) at a 1:1 molar ratio and incubated for 1 h at



room temperature. The heptapeptoids-Ni<sup>2+</sup>-GFP complexes were tested on B16F10 cells at different concentrations (1, 2, 5, and 10  $\mu$ M) under serum and serum free conditions. Both the heptapeptoids **4.11** and **4.14** did not give any significant positive result at any of the conditions tested. However, heptapeptoid **4.14**-Ni<sup>2+</sup>-(His<sub>6</sub>-GFP) complex (10  $\mu$ M) did show a slight increment in fluorescent labelling compared to the controls (Figure 4.10), although it was not very significant. Confocal microscopy showed that the protein was mostly on the cellular membrane and very little was visible inside the cell, mainly localised in endosomal vesicles (Figure 4.11).

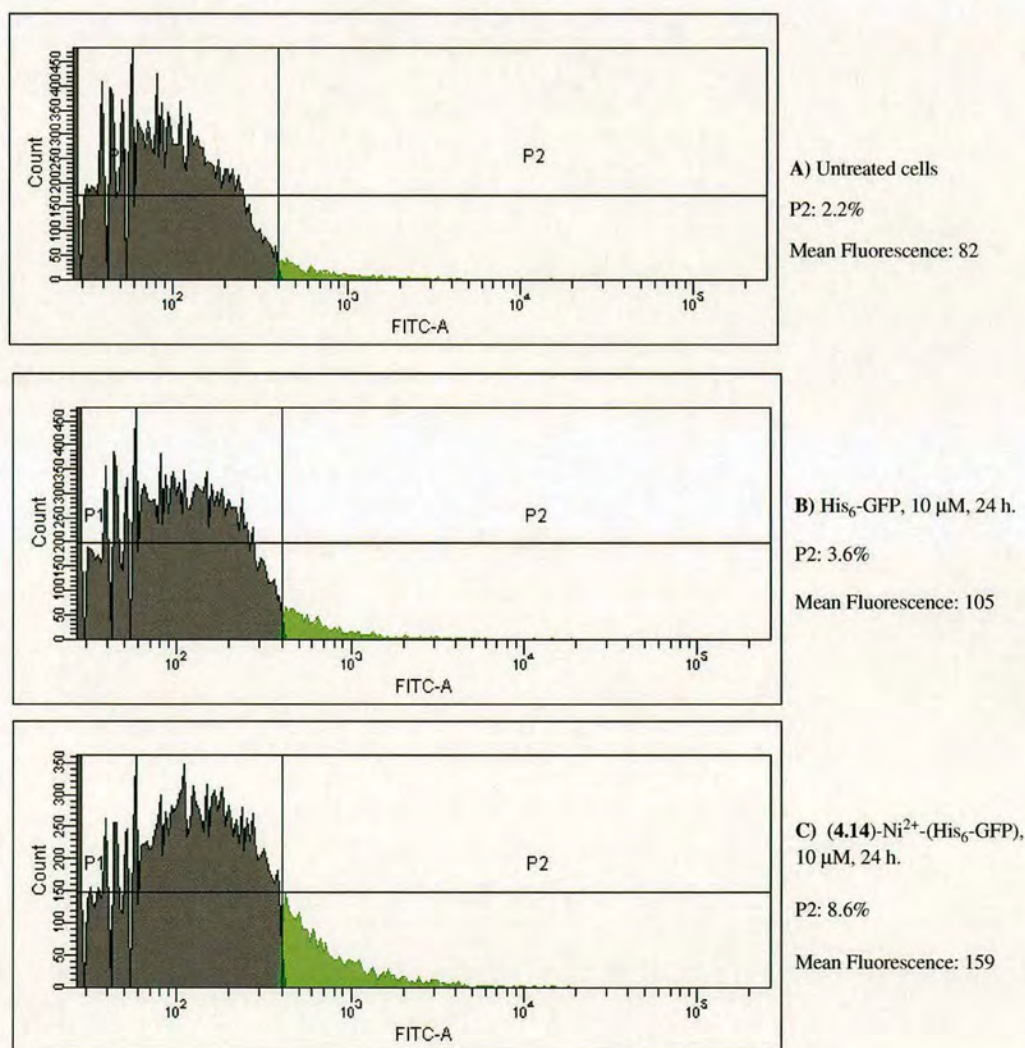


**Figure 4.10.** FACS analysis of: A) B16F10 untreated cells; B) B16F10 treated with His<sub>6</sub>-GFP (10  $\mu$ M, 24 h); C) B16F10 treated with (**4.14**)-Ni<sup>2+</sup>-(His<sub>6</sub>-GFP) complex (10  $\mu$ M, 24 h). P2 is the population of cells with a fluorescence intensity > 400.



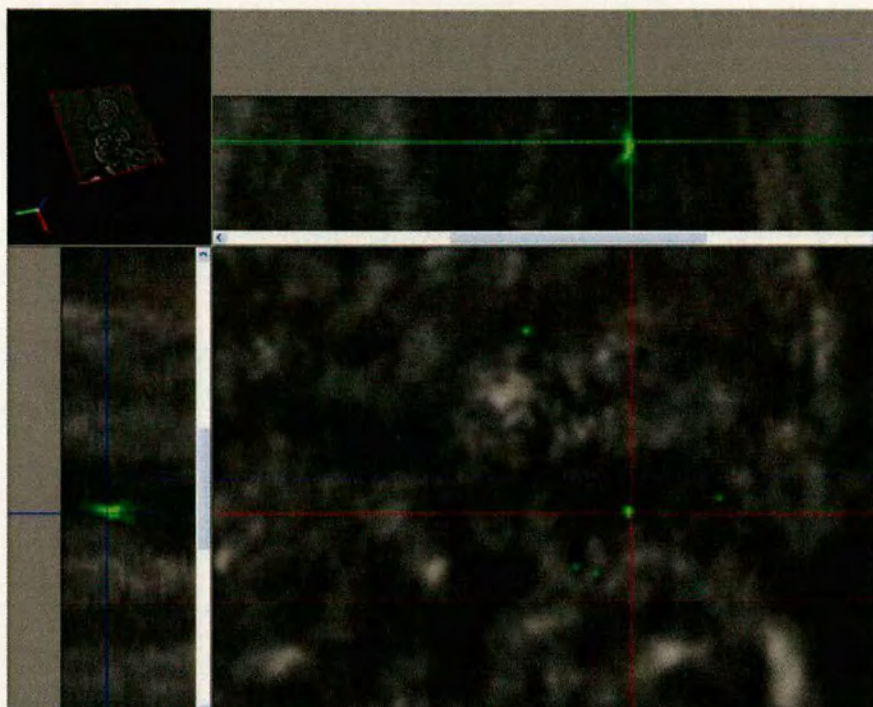


**Figure 4.11.** Confocal microscopy image of B16F10 treated with (4.14)-Ni<sup>2+</sup>- (His<sub>6</sub>-GFP) complex (10 μM, 24 h).

In conclusion heptapeptoids functionalised with Ni<sup>2+</sup> ligands for conjugation to hexahistidine tagged proteins were prepared by solid phase synthesis. The presence of 1 or 2 Ni<sup>2+</sup>-ligands did not inhibit significantly the cellular uptake of the heptapeptoid. The first attempts to deliver His<sub>6</sub>-GFP unfortunately gave negative results, however the work is still at an embryonic stage and many modifications can be attempted in order to achieve the delivery of hexahistidine tagged proteins, as for example the use of different metal ions such as Co<sup>2+</sup> or Cu<sup>2+</sup>, and experimentation of other ligands such as the NTA and IDA.



### IV.3. Peptoid carriers Summary: peptide, protein and plasmid delivery.

This thesis describes the preparation of peptoid oligomers and their application as carriers for cellular delivery of compounds such as peptides, PNAs, DNAs and proteins. The synthesis of the oligomer unit (**2.12**, page 43) has been optimised to allow a straightforward preparation on large scale (up to 30 g). The application of microwave heating to the synthesis of the peptoid oligomer led to a significant reduction in preparation time (DIC/HOBt, 60 °C, 20 min for each coupling) and to obtain the compound with high purity (crude purity > 95%, see page 53-56). The heptapeptoid carrier has proved to be extremely efficient in delivering peptides (13mer peptide  $\alpha$ -MSH) and PNAs (12 and 15mer) into different cell lines (B16G4F, B16CWT-3, HEK293, B-lymphocytes) and even more into skin (pig, mouse and human), one of the most challenging targets for the delivery of molecules with high molecular weight. Also the delivery of a polyanionic cargo such as an antisense DNA oligo (19mer oligonucleotide) gave positive preliminary results, providing a platform for further investigation. To achieve the delivery of macromolecules such as proteins the heptapeptoid carrier was modified with a  $\text{Ni}^{2+}$  ligand (see pages 100-104), in order to allow the conjugation of His<sub>6</sub> tagged proteins that can coordinate the  $\text{Ni}^{2+}$  using two histidine residues of the hexa-histidine tag (see page 98). Preliminary results are not positive, but several modifications are still possible, such as the use of different metals ( $\text{Co}^{2+}$ ,  $\text{Cu}^{2+}$ ) and ligands (NTA, IDA). To achieve the delivery of macromolecules such as plasmids, the peptoid unit was used to prepare 3 generations of a peptoid dendrimer (see page 94). The peptoid dendrimer G3 (**4.4**, page 94) was able to deliver a GFP plasmid into HEK293T cells 4 times more efficiently than PAMAM G2. The work described in this thesis shows how the peptoid carrier strategy can be effectively applied to a wide range of cargoes with different sizes and charges. Regarding the efficiency of the delivery (usually > 90% of cell population), it was observed that it is not dependent on the particular cell line used. High cellular uptake is obviously a strongly positive aspect of the peptoid carrier, however, the actual absence of selectivity is a serious limitation for its application in vivo. At this stage I would consider a clear step forward for this research to develop the aspect of the carrier selectivity towards different cell lines and tissues.



## Chapter V. Experimental.

### V.1. General information.

Reagents commercially available were used without further purification. Solvents were not dried or distilled except where specified.

All solution-phase reactions were stirred magnetically, unless otherwise stated, and followed by HPLC or thin-layer chromatography (TLC) where appropriate, using aluminium-coated Silica Gel 60 (Macheray Nagel: 0.20 mm layer). TLC visualisation was performed using short wavelength UV light (254 nm) and/or potassium permanganate oxidation.

**NMR spectra** were recorded on Bruker DPX 300 or ARX 250 spectrometers in the solvents indicated at 298 K. Chemical shifts are reported on the  $\delta$  scale in ppm and are referenced to residual non-deuterated solvent resonances. All  $^{13}\text{C}$  NMR experiments were supported with DEPT assignment.

**IR spectra** were obtained on a Thermo Mattson Satellite FTIR spectrometer or a Bruker Tensor 27 Spectrometer, with 16 scans, at a resolution of  $\pm 4\text{ cm}^{-1}$ . The FTIR spectrometers were fitted with a Specac single reflection diamond ATR Golden Gate, and neat compounds were used for analysis. Frequencies are reported in  $\text{cm}^{-1}$  and only frequencies corresponding to significant functional groups are reported.

**Mass spectra** were recorded either on a water ZMD single quadrupole MS, with a 2700 Autosampler and a 600 Pump, or an Agilent Technologies LC/MSD Series 1100 Quadrupole Mass Spectrometer (QMS), both with an electrospray ion source.

**MALDI-TOF** spectra were recorded on a Applied Biosystems Voyager DESTRO MALDI-TOF mass spectrometer.

**HPLC** were recorded using an Agilent 1100 with a U.V. absorption detector coupled to a Polymer Lab 100 ES Evaporative Light Scattering Detector (ELSD).

The following HPLC conditions were used:

Column 1: Sulpelco Discovery 50 mm x 2.1 mm, 5  $\mu\text{m}$  C18 column.

Column 2: Phenomenex Prodigy 150 x 4.6 mm, 5  $\mu\text{m}$  (ODS3) C18 column.

Column 3: Phenomenex Gemini C18, 5  $\mu\text{m}$ , 10 cm column

HPLC grade solvents: water (0.1% TFA), MeOH (0.1% TFA), MeCN (0.042% TFA). The following methods were used:



Method 1 (column 1, H<sub>2</sub>O/MeCN, 1 mL/min): 0 min (90/10), 3 min (10/90), 4 min (10/90).

Method 2 (column 2, H<sub>2</sub>O/MeCN, 1 mL/min): 0 min (90/10), 10 min (10/90), 15 min (10/90).

Method 3 (column 2, H<sub>2</sub>O/MeOH, 1 mL/min): 0 min (95/5), 4 min (5/95), 12 min (5/95).

Method 4 (column 2, H<sub>2</sub>O/MeOH, 1 mL/min): 0 min (95/5), 3 min (95/5), 8 min (5/95), 12 (5/95).

Method 5 (column 3, H<sub>2</sub>O/MeCN, 1 mL/min): 0 min (95/5), 6 min (5/95), 9 min (5/95).

Method 6 (column 2, H<sub>2</sub>O/MeOH, 1 mL/min): 0 min (95/5), 12 (5/95), 13 min (5/95).

**Semi-preparative HPLC** separations were performed on an Agilent Technologies 1100 HPLC equipped with automated fraction collection triggered by absorbance at 220 nm, using water (0.1% TFA), MeCN (0.042% TFA) and a Phenomenex Prodigy C18 250 × 10.0 mm, 5 µm (ODS3) C18 column. Method (H<sub>2</sub>O/MeCN, 2.5 mL/min): 0 min (100/0), 40 min (0/100), 45 min (0/100).

**Melting points** (Pyrex capillaries) are uncorrected.

**HRMS analyses** were performed by the Mass Spectrometry Service of Edinburgh University, UK.

**Flow cytometry analyses** and sorting were carried out on a Becton Dickinson FACS Aria™ using FACSDiva™.

For **cell viability**, 96-well plates were read on a Benchmark® Bio-Rad microplate reader at 570 nm using Microplate manager® 4.0.

**Confocal images** were taken on a Delta Vision RT Microscope fitted with a water contact lens 63x.

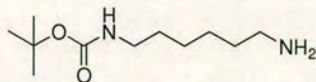
**Microwave reactions** were carried using a Smith Synthesizer, monomodal microwave reactor (Biotage).



## V.2. Experimental: Chapters II and III.

### V.2.1. Peptoid monomer synthesis.

#### 2.1.1. 1,6-Diamino-N-tert-Butyloxycarbonylhexane **2.13**.<sup>225</sup>



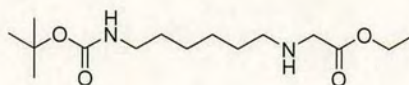
A solution of (Boc)<sub>2</sub>O (10.0 g, 45.8 mmol) in DCM (100 mL) was added dropwise over a period of 2 h to a solution of 1,6-hexanediamine (42.5 g, 366 mmol) in DCM (150 mL). The reaction mixture was stirred for 24 h. The solution was filtered and the filtrate was concentrated *in vacuo*. The oily residue was suspended in water (200 mL) and extracted with DCM (3 x 150 mL). The organic phase was washed with brine (2 x 100 mL) and dried over MgSO<sub>4</sub>. The solvent was removed *in vacuo* to give compound **2.13** (7.5 g, 34 mmol) as a yellowish oil, in 78% yield.

**m/z** (ES<sup>+</sup>): 217.0 [M+H]<sup>+</sup> (100%).

**<sup>1</sup>H NMR** (CDCl<sub>3</sub>, 300 MHz)  $\delta$  = 4.58 (br s, 1H, BocNHCH<sub>2</sub>), 3.12 (m, 2H, BocNHCH<sub>2</sub>), 2.65 (m, 2H, CH<sub>2</sub>NH<sub>2</sub>), 1.60-1.33 (m, 19H, CH<sub>2</sub>NH<sub>2</sub>, BocNHCH<sub>2</sub>(CH<sub>2</sub>)<sub>4</sub>CH<sub>2</sub> and C(CH<sub>3</sub>)<sub>3</sub>).



2.1.2. Ethyl ({6-[(*tert*-butoxycarbonyl)amino]hexyl}amino)acetate **2.14**.<sup>149</sup>



A solution of ethyl bromoacetate (3.8 mL, 34 mmol) in THF (20 mL) was added dropwise to a solution of 1,6-Diamino-*N*-*tert*-Butyloxycarbonylhexane (**2.13**, 7.34 g, 34 mmol) and TEA (14 mL, 102 mmol) in THF (50 mL). The reaction mixture was stirred for 24 h. The solvent was evaporated *in vacuo* and the residue was re-suspended in diethyl ether. The reaction mixture was filtered to remove triethylamine hydrobromide, the residue was washed with ether and the filtrate was concentrated *in vacuo*. Column chromatography (silica, eluent: DCM/MeOH, 9/1) gave **2.14** (5.64 g, 18.7 mmol), as an oil in 50 % yield.

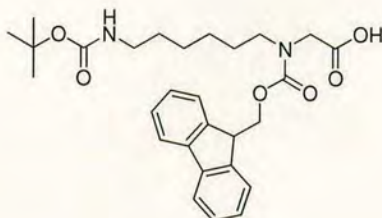
$R_f$  (DCM/ MeOH, 9/1) = 0.45.

$m/z$  (ES<sup>+</sup>): 303.2 [M + H]<sup>+</sup> (100 %); 325.1 [M + Na]<sup>+</sup> (48 %).

<sup>1</sup>H NMR (CDCl<sub>3</sub>, 300 MHz)  $\delta$  = 4.62 (br s, 1H, BocNHCH<sub>2</sub>), 4.13 (q,  $J$  = 7.0 Hz, 2H, OCH<sub>2</sub>CH<sub>3</sub>), 3.33 (s, 2H, NHCH<sub>2</sub>CO), 3.05 (m, 2H, BocNHCH<sub>2</sub>), 2.55 (m, 2H, CH<sub>2</sub>CH<sub>2</sub>NHCH<sub>2</sub>), 1.70 (br s, 1H, CH<sub>2</sub>NHCH<sub>2</sub>), 1.59-1.28 (m, 17H, BocNHCH<sub>2</sub>(CH<sub>2</sub>)<sub>4</sub>CH<sub>2</sub> and C(CH<sub>3</sub>)<sub>3</sub>), 1.22 (t,  $J$  = 7.0 Hz, 3H, OCH<sub>2</sub>CH<sub>3</sub>).



2.1.3. {{6-[(*tert*-butoxycarbonyl)amino]hexyl}[(9*H*-fluoren-9-ylmethoxy)carbonyl]amino}acetic acid **2.12**.<sup>149</sup>



NaOH (0.4 g, 10 mmol) was added to a solution of **2.14** (3 g, 10 mmol) in MeOH (15 mL), H<sub>2</sub>O (4 mL) and dioxane (35 mL). After stirring for 60 min at room temperature the reaction mixture was concentrated *in vacuo* to give sodium ({6-[(*tert*-butoxycarbonyl)amino]hexyl}amino)acetate, which was used without purification. The sodium salt was dissolved in water (25 mL) and the pH was adjusted to 9.0-9.5 with concentrated hydrochloric acid. To this mixture a solution of Fmoc-OSu (3.37 g, 10 mmol) in acetonitrile (25 mL) was added in one portion. Stirring was continued for 45 minutes, and the pH was maintained at 8.5-9.0 by the addition of TEA. The reaction mixture was concentrated *in vacuo* to remove the acetonitrile, and the residual solution was poured into 20% citric acid (30 mL). The aqueous layer was extracted with DCM (3 x 40 mL), the combined organic layers were washed with brine, dried (MgSO<sub>4</sub>) and concentrated *in vacuo*. Column chromatography (silica, eluent: gradient EtOAc to EtOAc/MeOH = 90/10), gave **2.12** (1.8 g, 4 mmol) as a white solid in 40 % yield.

**R<sub>f</sub>** ( EtOAc/MeOH, 1/1) = 0.32.

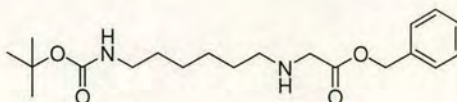
**HPLC** (method 1): purity 100% (220 nm), RT 4.22 min.

**m/z** ( ES<sup>+</sup> ): 519.4 [M + Na]<sup>+</sup> (100 %), 1015.8 [2M + Na]<sup>+</sup> (35 %).

**<sup>1</sup>H NMR** (CDCl<sub>3</sub>, 300 MHz) two rotamers δ = 7.72 (d, *J* = 7.2 Hz, 2H, Ar*H*-Fmoc), 7.53 (d, *J* = 6.8 Hz, 2H, Ar*H*-Fmoc), 7.35 (m, 2H, Ar*H*-Fmoc), 7.26 (m, 2H, Ar*H*-Fmoc), 4.58 (br s, 1H, BocNHCH<sub>2</sub>), 4.51 and 4.45 (two m, 2H, CH<sub>2</sub>-Fmoc), 4.10 (m, 1H, CH-Fmoc), 3.81 and 3.89 (two s, 2H, NCH<sub>2</sub>CO), 3.23 and 3.07 (two m, 4H, BocNCH<sub>2</sub> and FmocNCH<sub>2</sub>CH<sub>2</sub>), 1.61-1.32 (m, 17H, BocNHCH<sub>2</sub>(CH<sub>2</sub>)<sub>4</sub>CH<sub>2</sub> and C(CH<sub>3</sub>)<sub>3</sub>).



2.1.4. Benzyl ({6-[(*tert*-butoxycarbonyl)amino]hexyl}amino)acetate **2.15**.



A solution of benzyl 2-bromacetate (5.8 g, 25 mmol) in THF (20 mL) was added drop-wise to a stirred solution of 1,6-Diamino-*N*-*tert*-Butyloxycarbonylhexane (**2.13**) (5.5 g, 25 mmol) and triethylamine (5.4 g, 0.075 mol) in THF (50 ml) over 2h, and stirred for a further 24 h. After filtration of the white solid, the solution was concentrated *in vacuo*. Column chromatography (silica, eluent: ethyl acetate) gave compound **2.15** (5.0 g, 13 mmol) as a pale yellow oil in 54 % yield.

$R_f$  (EtOAc) = 0.42.

HPLC (method 1): purity 100% (220 nm), RT 3.20 min.

IR (neat oil): 3339 (N-H, w), 1737 (C=O<sub>ester</sub>, s), 1697 (C=O<sub>urethane</sub> s) cm<sup>-1</sup>.

m/z (ES<sup>+</sup>): 365.0 [M+H]<sup>+</sup> (100%).

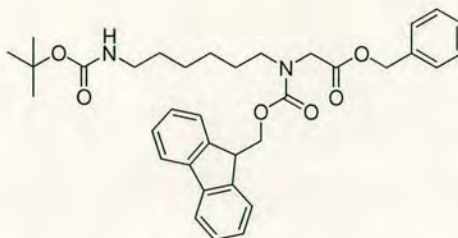
<sup>1</sup>H NMR (300 MHz, CDCl<sub>3</sub>)  $\delta$  = 7.35 (m, 5H, ArH), 5.14 (s, 2H, COOCH<sub>2</sub>), 4.61 (br s, 1H, BocNHCH<sub>2</sub>), 3.42 (s, 2H, NCH<sub>2</sub>CO), 3.10 (m, 2H, BocNHCH<sub>2</sub>), 2.56 (t, *J* = 7.3 Hz, 2H, CH<sub>2</sub>CH<sub>2</sub>NHCH<sub>2</sub>), 1.58 (br s, 1H, CH<sub>2</sub>NHCH<sub>2</sub>), 1.50-1.23 (m, 17H, BocNHCH<sub>2</sub>(CH<sub>2</sub>)<sub>4</sub>CH<sub>2</sub> and C(CH<sub>3</sub>)<sub>3</sub>).

<sup>13</sup>C NMR (62.9 MHz, CDCl<sub>3</sub>)  $\delta$  = 172.5 (NCH<sub>2</sub>CO), 156.0 (Boc C=O), 135.7 (Ar-C), 128.6, 128.4, 128.3 (Ar-CH), 79.0 (C(CH<sub>3</sub>)<sub>3</sub>), 66.5 (NCH<sub>2</sub>COOCH<sub>2</sub>), 51.0 (NCH<sub>2</sub>CO), 49.5 (CH<sub>2</sub>CH<sub>2</sub>NHCH<sub>2</sub>), 40.5 (BocNHCH<sub>2</sub>), 30.0, 29.9 (BocNHCH<sub>2</sub>CH<sub>2</sub>(CH<sub>2</sub>)<sub>2</sub>CH<sub>2</sub>), 28.5 (C(CH<sub>3</sub>)<sub>3</sub>), 26.8, 26.6 (BocNH(CH<sub>2</sub>)<sub>2</sub>CH<sub>2</sub>CH<sub>2</sub>CH<sub>2</sub>).

HRMS (FAB) for C<sub>20</sub>H<sub>33</sub>N<sub>2</sub>O<sub>4</sub> [M+H]<sup>+</sup> calcd 365.2440, found 365.2439.



2.1.5. Benzyl {[6-[(*tert*-butoxycarbonyl)amino]hexyl][(9*H*-fluoren-9-ylmethoxy)carbonyl]amino}acetate **2.16**.



Fmoc-OSu (4.6 g, 13.7 mmol) was added to a solution of **2.15** (5.0 g, 13.7 mmol) in DCM (50 ml). The reaction was monitored by TLC until completion (4h). The solvent was removed *in vacuo* and the crude product was purified by column chromatography (silica, eluent: EtOAc/Hexane, 1:1) to give **2.16** (7.2 g, 12.3 mmol) as a light yellow oil in 90 % yield.

**R<sub>f</sub>** ( EtOAc/Hexane 1:1) = 0.35.

**HPLC** (method 1): purity 100% (220 nm), RT 4.82 min.

**IR** (neat oil): 1753 (C=O<sub>ester</sub>, s), 1701 (C=O<sub>urethane</sub>, s) cm<sup>-1</sup>.

**m/z** (ES<sup>+</sup>): 587.3 [M+H]<sup>+</sup> (60%), 609.2 [M+Na]<sup>+</sup> (100%).

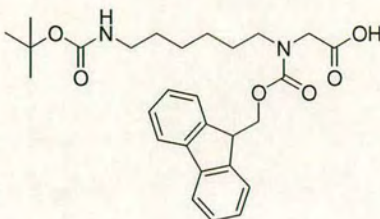
**<sup>1</sup>H NMR** (300 MHz, CDCl<sub>3</sub>) two rotamers δ = 7.79 (m, 2H, Ar*H*-Fmoc), 7.57 (m, 2H, Ar*H*-Fmoc), 7.44-7.27 (m, 9H, Ar*H*-Fmoc and Ph), 5.13 and 5.18 (two s, 2H, COOCH<sub>2</sub>), 4.55 (br s, 1H, BocNHCH<sub>2</sub>), 4.53 and 4.40 (two d, *J* = 6.2 Hz, 2H, CH<sub>2</sub>-Fmoc), 4.13 and 4.26 (two t, *J* = 6.2 Hz, 1H, CH-Fmoc), 3.96 and 4.03 (two s, 2H, NCH<sub>2</sub>CO), 3.13 and 3.49 (two m, 4H, BocNHCH<sub>2</sub> and FmocNCH<sub>2</sub>CH<sub>2</sub>), 1.47-1.13 (m, 17H, BocNHCH<sub>2</sub>(CH<sub>2</sub>)<sub>4</sub>CH<sub>2</sub> and C(CH<sub>3</sub>)<sub>3</sub>).

**<sup>13</sup>C NMR** (75 MHz, CDCl<sub>3</sub>) two rotamers δ = 169.7 and 169.6 (NCH<sub>2</sub>CO), 156.5, 156.0 and 155.9 (Boc C=O and Fmoc C=O), 144.1 (ArC-Fmoc), 141.5 and 141.4 (ArC-Fmoc), 135.5 and 135.4 (ArC-Ph), 128.6 and 128.5, 128.3, 127.7, 127.1, 124.9 and 124.8, 120.0 (ArCH-Fmoc and ArCH-Ph), 79.1 (C(CH<sub>3</sub>)<sub>3</sub>), 67.6 and 67.4 (CH<sub>2</sub>-Fmoc), 67.0 (NCH<sub>2</sub>COOCH<sub>2</sub>), 49.2 (NCH<sub>2</sub>CO), 48.8 and 48.7 (CH<sub>2</sub>CH<sub>2</sub>NCH<sub>2</sub>), 47.4 (CH-Fmoc), 40.5 (BocNHCH<sub>2</sub>), 30.0 and 29.9 (BocNHCH<sub>2</sub>CH<sub>2</sub>), 28.4 (C(CH<sub>3</sub>)<sub>3</sub>), 28.2 and 27.9 (CH<sub>2</sub>CH<sub>2</sub>NCH<sub>2</sub>), 26.4, 26.3 (BocNH(CH<sub>2</sub>)<sub>2</sub>CH<sub>2</sub>CH<sub>2</sub>CH<sub>2</sub>).

**HRMS** (FAB) for C<sub>35</sub>H<sub>43</sub>N<sub>2</sub>O<sub>6</sub> [M+H]<sup>+</sup> calc. 587.3121, found: 587.3113.



2.1.6. {{6-[(*tert*-butoxycarbonyl)amino]hexyl}}[(9*H*-fluoren-9-ylmethoxy)carbonyl]amino}acetic acid **2.12**<sup>149</sup> (by hydrogenolysis of benzyl ester **2.16**).



Compound **2.16** (4.0 g, 6.8 mmol) and Pd/C 10% (0.24 g) were dispersed in MeOH (100 ml). The reaction mixture was stirred under hydrogen atmosphere (1 atm) for 4h at room temperature. The reaction mixture was filtered through celite to remove Pd/C and the filtrate was concentrated *in vacuo*. The product was filtrated on silica gel (DCM/MeOH, 10/1) to give **2.12** (2.7 g, 5.4 mmol) as a white solid in 80 %. (m/z and <sup>1</sup>H identical to the one reported for **2.12** in section V.2.1.3).



## ***V.2.2. Detection of primary and secondary amines on solid supports.***

### ***2.2.1. Qualitative Ninhydrin test for primary amines.***<sup>182</sup>

To a small sample of washed resin in a test tube were added 1 drop of reagent A and 3 drops of reagent B. The mixture was heated at 100°C for 5 minutes and the resulting blue or yellow color of the solution indicated a positive or negative test respectively.

Reagent A: Solution 1) Reagent grade phenol (40 g) was dissolved in absolute ethanol (10 mL) with warming and then stirred over Amberlite mixed-bed resin MB-3 (4 g) for 45 min. The mixture was then filtered. Solution 2) Potassium cyanide (65 mg) was dissolved in water (100 mL). A 2 mL aliquot of this solution was diluted with pyridine (freshly distilled from ninhydrin) and stirred over Amberlite mixed-bed resin MB-3 (4 g). The solution was filtered and mixed with solution 1 to form reagent A.

Reagent B: Ninhydrin (2.5 g) was dissolved in absolute ethanol (50 mL).

### ***2.2.2. Chloranil test for secondary amines.***<sup>171</sup>

To a small sample of washed resin in a test tube were added few drops of acetaldehyde (2% in DMF) followed by one drop of a saturated solution of chloranil in toluene. A resulting dark-blue resin or a colourless resin indicated a positive or negative test respectively.



### ***V.2.3. General protocols for peptide and PNA synthesis, labelling and cleavage.***

General rule for the ratio of solvent- resin used for couplings: 10 mL of solvent for 1 g of resin.

All the conditions described are for 200 mg of resin. All peptides were prepared on polystyrene resin (1% DVB, loading = 1 mmol/g) using a Rink<sup>151</sup> amide linker. All PNAs were prepared on PEGA resin (loading = 0.4 mmol/g) using a Rink<sup>151</sup> amide linker. For Rink amide resin preparation see section V.2.3.10.

#### ***2.3.1. Amino acids coupling at room temperature.***

The Fmoc-protected amino acids (3 equiv, 0.2 M) and HOBt (3 equiv, 0.2 M) were dissolved in DMF, DIC (3 equiv, 0.2 M) was then added and the solution stirred for 10 minutes. The solution was added to the resin (pre-swollen in DMF for 20 min) and the mixture stirred for 3 h at room temperature. The resin was then washed with DMF (3 x 5 mL) and DCM (3 x 5 mL). Couplings were monitored using qualitative colorimetric tests and repeated if unsatisfactory.

#### ***2.3.2. Amino acids coupling under microwave irradiation.***

The Fmoc-protected amino acids (3 equiv. 0.2 M) and HOBt (3 equiv, 0.2 M) were dissolved in DMF, DIC (3 equiv, 0.2 M) was then added and the solution stirred for 5 minutes. The solution was added to the resin (pre-swollen in DMF for 20 min) and the mixture transferred into a 5 mL microwave vessel. The vessel was capped and subjected to microwave irradiation to keep the temperature at 60 °C for 10 min (peptide synthesis) or 20 min (peptoid synthesis) under magnetic stirring using a single-mode microwave. The resin was then transferred to a solid phase extractor (SPE), a polypropylene syringe equipped with a frit and a valve, and washed with DMF (3 x 5 mL) and DCM (3 x 5 mL). Couplings were monitored using qualitative colorimetric test and repeated if unsatisfactory.

#### ***2.3.3. PNA monomers coupling.***

Dde PNA monomers (5 equiv, 0.2 M) and PyBOP (4.8 equiv) were dissolved in DMF followed by the addition of NEM (10 equiv). The resulting solution was mixed for 10 sec. before adding to the resin (pre-swollen in DMF) and the mixture was then shaken



for 4 h. Resins were washed with DMF (3 x 5 mL) and DCM (3 x 5 mL). Couplings were monitored using qualitative colorimetric tests and repeated if unsatisfactory.

#### 2.3.4. Capping protocol.

The peptide resin was treated for 20 minutes with a capping solution of 15% acetic anhydride, 7.5% HOBt in DMF.

#### 2.3.5. Fmoc deprotection.

Fmoc deprotection was carried out by suspending the resin in 20% piperidine in DMF (5 mL) and shaking for 10 min. The resin was then filtered, washed with DMF (3 x 5 mL), DCM (3 x 5 mL) and re-suspended in 20% piperidine in DMF (5 mL) and shaken for a further 10 min after which time the resin was washed with DMF ((3 x 5 mL), DCM (3 x 5 mL).

#### 2.3.6. Dde deprotection.

Dde deprotection was carried out by suspending the resin in 2%  $\text{NH}_2\text{OH}\cdot\text{H}_2\text{O}$  in DMF (3 x 5 mL) and shaking for 30 min. The resin was then filtered, washed with DMF (3 x 5 mL), DCM (3 x 5 mL) and re-suspended in 2%  $\text{NH}_2\text{OH}\cdot\text{H}_2\text{O}$  in DMF (3 x 5 mL) and shaken for a further 30 min after which time the resin was washed with DMF (3 x 5 mL) and DCM (3 x 5 mL).

#### 2.3.7. Fluorescein labelling at room temperature.<sup>185</sup>

5(6)-Carboxyfluorescein (3 equiv, 0.2 M) and PyBop (2.8 equiv, 0.2 M) were dissolved in DMF. Then DIPEA (6 equiv) was added and the solution added to the pre-swollen resin. The mixture was stirred for 12 h. The resin was then washed with DMF (until obtaining a colourless solution) and treated with 20% piperidine in DMF for 1 h (under stirring).<sup>185</sup> The resin was then washed with DMF and treated again with 20% piperidine in DMF for 10 minutes, if a fluorescent solution was generated, the resin was left to stir for 1 h. The treatment was repeated until a colourless solution was obtained. The resin was then washed with DMF and DCM.



#### 2.3.8. Fluorescein labelling under microwave irradiation.

5(6)-Carboxyfluorescein (3 equiv, 0.2 M) and HOBt (3 equiv, 0.2 M) were dissolved in DMF. DIC (3 equiv, 0.2 M) was then added and the solution stirred for 5 minutes. The solution was added to the resin (pre-swollen in DMF for 20 min) and the mixture transferred into a microwave vessel (5 or 2.5 mL). The vessel was capped and subjected to microwave irradiation to keep the temperature constant at 60 °C for 10 min under magnetic stirring using a single-mode microwave. The resin was then transferred to a solid phase extractor (SPE), washed with DMF and treated with 20% piperidine in DMF (see above). The resin was then washed again with DMF and DCM.

#### 2.3.9. TFA cleavage and cold ether precipitation.

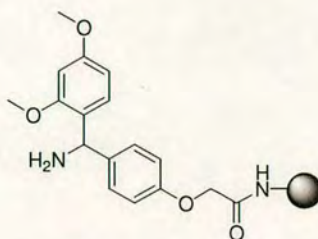
The resin was washed with DMF (3 x 5 mL), DCM (3 x 5 mL), MeOH (3 x 5 mL), Et<sub>2</sub>O (3 x 5 mL) and dried *in vacuo*. Washed dry resin was suspended in TFA (5 mL of solution 1 or 2,) and stirred for 4 h. The solution was then separated by filtration from the resin which was washed with 5 mL of TFA solution. The TFA solutions were collected and concentrated *in vacuo* (1 mL ca.) and transferred in a centrifuge tube containing cold diethyl ether (12 ml). The precipitated peptide was separated by centrifugation, washed with ether (3 x 12 mL) and then dried *in vacuo*.

Solution 1: 95% TFA, 2.5% TIS, 2.5% H<sub>2</sub>O.

Solution 2: 81.5% TFA, 5% thioanisole, 5% phenol, 5 % water, 2.5% EDT (1,2 ethanedithiol) , 1% TIS ( triisopropylsilane).



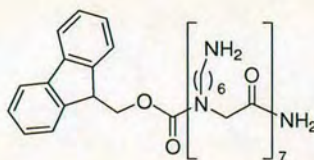
### 2.3.10. Preparation of Rink<sup>151</sup> amide resin.



Fmoc-Rink amide linker was coupled to the polystyrene resin as described in section V.2.3.1. The linker was coupled to the PEGA resin as described in section V.2.3.1, but the number of reagent equivalents was increased to 5. Fmoc deprotection was carried out using 20% piperidine in DMF (V.2.3.5).

#### V.2.4. $\alpha$ -MSH Peptides and Peptide-Peptoid conjugates.

#### 2.4.1. Fmoc-heptapeptoid 2.19.



Fmoc-heptapeptoid **2.19** was prepared on Rink amide polystyrene resin (1% DVB, 1 mmol/g) under microwave conditions (section V.2.3.2). Compound **2.19** was cleaved with TFA (solution 1) and precipitated in cold ether.

**HPLC** (method 2) purity 100% (220 nm), RT 3.41 minutes.

**m/z** (ES+) 667.6 [M+2H]<sup>2+</sup> (15%), 445.4 [M+3H]<sup>3+</sup> (32%), 334.4 [M+4H]<sup>4+</sup> (25%).

#### 2.4.2 $\alpha$ -MSH (Ac-SYSMEHFRWGKPV-NH<sub>2</sub>) 3.1.

Peptide  $\alpha$ -MSH **3.1** was prepared using Rink amide polystyrene resin (100 mg, 1 mmol/g, 0.1 mmol). Peptide couplings (Side chain protected amino acids: Fmoc-Lys(Boc)-OH, Fmoc-Trp(Boc)-OH, Fmoc-Arg(Pbf)-OH, Fmoc-His(1-Trt)-OH, Fmoc-Glu(O<sup>t</sup>Bu)-OH, Fmoc-Ser(<sup>t</sup>Bu)-OH, Fmoc-Tyr(<sup>t</sup>Bu)-OH) were performed at

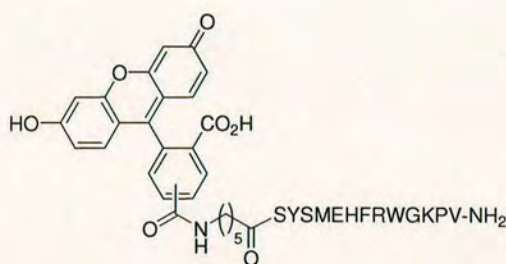


room temperature (see V.2.3.1). After Fmoc deprotection of the last residue the resin was capped (see section V.2.3.4, two cycles). TFA cleavage (see section V.2.3.9, solution 2), cold ether precipitation and semipreparative HPLC (RT 31.3 min) gave peptide **3.1** (40 mg, 0.025 mmol) in 25% overall isolated yield.

**HPLC** (method 2) purity 95% (crude 63 %) (220 nm), RT 5.73 minutes.

**m/z** (ES+) 833.2  $[M+2H]^{2+}$  (32%), 556.0  $[M+3H]^{3+}$  (100%).

#### 2.4.3. FAM- $\alpha$ -MSH (FAM-Ahx-SYSMEHFRWGKPV-NH<sub>2</sub>) **3.2**.



Peptide FAM- $\alpha$ -MSH **3.2** was prepared using Rink amide polystyrene resin (100 mg, 1 mmol/g, 0.1 mmol). Peptide couplings and fluorescein labelling were performed at room temperature (see V.2.3.1 and V.2.3.7). TFA cleavage (see V.2.3.9, solution 2), cold ether precipitation and semipreparative HPLC (RT 36.8 min) gave peptide **3.2** (41 mg, 0.02 mmol) in 20% overall isolated yield.

**HPLC** (method 2) purity > 95% (crude 40 %) (220 nm), RT 6.21 minutes.

**m/z** (MALDI-TOF) for C<sub>102</sub>H<sub>128</sub>N<sub>22</sub>O<sub>25</sub>S calcd 2094.3, found 2095.8  $[M+H]^+$ .

#### 2.4.4. Fmoc-SYSMEHFRWGKPV-NH<sub>2</sub> **3.1b**.

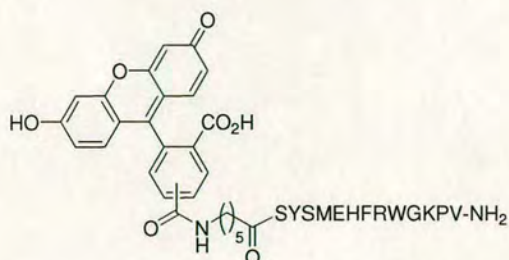
Peptide **3.1b** was prepared using Rink amide polystyrene resin (1 mmol/g). Peptide couplings were performed under microwave conditions (see V.2.3.2). The Fmoc group on the last residue (Ser) was not removed. Peptide **3.1b** was cleaved using TFA (see V.2.3.9, solution 2) and precipitated in cold ether.

**HPLC** (method 1) purity 65% (220 nm), RT 6.81 minutes.

**m/z** (ES+) 924.1  $[M+2H]^{2+}$  (35%), 616.3  $[M+3H]^{3+}$  (100%).



#### 2.4.5. FAM- $\alpha$ -MSH (FAM-Ahx-SYSMEHFRWGKPV-NH<sub>2</sub>) 3.2 <sub>$\mu$ W</sub>.

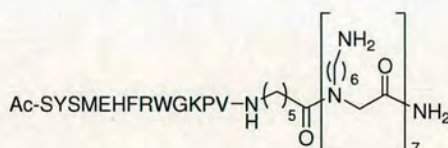


Peptide FAM-  $\alpha$ -MSH **3.2** was prepared using Rink amide polystyrene resin (200 mg, 1 mmol/g, 0.2 mmol). Peptide couplings and fluorescein labelling were performed under microwave conditions (see V.2.3.2 and V.2.3.8). TFA cleavage (see V.2.3.9, solution 2), cold ether precipitation and semipreparative HPLC (RT 36.8 min) gave peptide **3.2** (120 mg, 0.058 mmol) in 30% overall isolated yield.

**HPLC** (method 2) purity > 95% (crude 65 %) (220 nm), RT 6.21 minutes.

**m/z** (MALDI-TOF) for C<sub>102</sub>H<sub>128</sub>N<sub>22</sub>O<sub>25</sub>S calcd 2094.3, found 2095.9 [M+H]<sup>+</sup>.

#### 2.4.6. $\alpha$ -MSH-Ahx-heptapeptoid **3.3**.

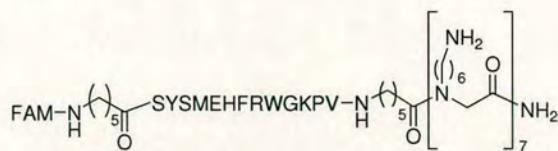


$\alpha$ -MSH-Ahx-heptapeptoid **3.3** was prepared using Rink amide polystyrene resin (100 mg, 1 mmol/g, 0.2 mmol). Peptide couplings and peptoid couplings were performed under microwave conditions (see V.2.3.2). After Fmoc deprotection of the last residue (Ser) the resin was capped (see V.2.3.4, two cycles). TFA cleavage (solution 2), cold ether precipitation and semipreparative HPLC (RT 15.7 min) gave peptide **3.3** (80 mg, 0.028 mmol) in 28% overall isolated yield.

**HPLC** (method 2) purity > 95% (crude 63 %) (220 nm), RT 5.12 minutes.

**m/z** (MALDI-TOF) for C<sub>139</sub>H<sub>232</sub>N<sub>36</sub>O<sub>27</sub>S calcd 2871.6, found 2872.8 [M+H]<sup>+</sup>.

#### 2.4.7. FAM-Ahx- $\alpha$ -MSH-Ahx-heptapeptoid **3.4**.



FAM-Ahx- $\alpha$ -MSH-Ahx-heptapeptoid **3.4** was prepared using Rink amide polystyrene resin (100 mg, 1 mmol/g) at room temperature and under microwave conditions.

Peptide couplings, peptoid couplings and fluorescein labelling were performed under microwave conditions (see V.2.3.2 and V.2.3.8). TFA cleavage (see V.2.3.9, solution 2), cold ether precipitation and semipreparative HPLC (RT 15.7 min) gave peptide **3.4** (105 mg, 0.032 mmol) in 32% overall isolated yield.

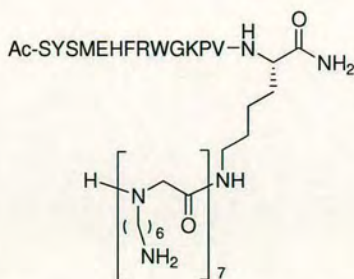
**HPLC** (method 2) purity > 95% (crude 58 %) (220 nm), RT 5.46 minutes.

**m/z** (MALDI-TOF) C<sub>164</sub>H<sub>251</sub>N<sub>37</sub>O<sub>33</sub>S: calcd 3301.04, found 3302.2 [M+H]<sup>+</sup>.

Peptide couplings, peptoid couplings and fluorescein labelling were performed at room temperature (see V.2.3.1 and V.2.3.7). Compound **3.4** was cleaved using TFA (solution 2) and precipitated in cold ether.

**HPLC** (method 2): crude purity 60 % (220 nm),

#### 2.4.8. $\alpha$ -MSH-Lys(heptapeptoid)-NH<sub>2</sub> **3.5**.



$\alpha$ -MSH-Lys(heptapeptoid)-NH<sub>2</sub> **3.5** was prepared using Rink amide polystyrene resin (100 mg, 1 mmol/g, 0.1 mmol). Peptide couplings and peptoid couplings were

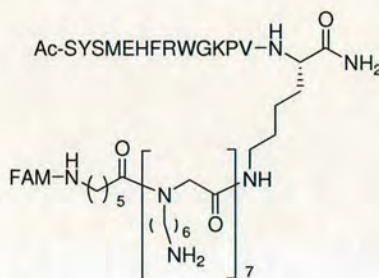


performed under microwave conditions (see V.2.3.2). Fmoc-Lys(Dde)-OH was coupled to the Rink amide resin and used as core for the synthesis of **3.5**.  $\alpha$ -MSH was prepared on the  $\alpha$ -amine group after selective Fmoc deprotection of the Fmoc-Lys(Dde)-Rink-resin.  $\alpha$ -MSH-Lys(Dde)-Rink-resin was Dde deprotected (see V.2.3.6) and the peptoid was built on the  $\epsilon$ -amine group of the lysine core. TFA cleavage (solution 2), cold ether precipitation and semipreparative HPLC (RT 16.54 min) gave peptide **3.5** (100 mg, 0.035 mmol) in 35% overall isolated yield.

**HPLC** (method 2) purity > 95% (crude 65 %) (220 nm), RT 4.94 minutes.

**m/z** (MALDI-TOF) for  $C_{102}H_{128}N_{22}O_{25}S$  calcd 2885.65, found 2886.9  $[M+H]^+$ .

#### 2.4.9. $\alpha$ -MSH-Lys(FAM-Ahx-heptapeptoid)-NH<sub>2</sub> **3.6**.



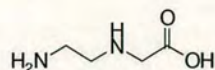
$\alpha$ -MSH-Lys(FAM-Ahx-heptapeptoid)-NH<sub>2</sub> **3.6** was prepared using Rink amide polystyrene resin (250 mg, 1 mmol/g). Peptide couplings, peptoid couplings and fluorescein labelling were performed under microwave conditions (see V.2.3.2 and V.2.3.8). Fmoc-Lys(Dde)-OH was coupled to the resin and used as core for the synthesis of **3.6**.  $\alpha$ -MSH was prepared on the  $\alpha$ -amine group after selective Fmoc deprotection of the Fmoc-Lys(Dde)-Rink-resin.  $\alpha$ -MSH-Lys(Dde)-Rink-resin was Dde deprotected (see V.2.3.6) and the FAM-Ahx-heptapeptoid was built on the  $\epsilon$ -amine group of the lysine core. TFA cleavage (see V.2.3.9, solution 2), cold ether precipitation and semipreparative HPLC (RT 18.8 min) gave peptide **3.6** (104 mg, 0.031 mmol) in 31% overall isolated yield.

**HPLC** (method 2) purity > 95% (crude 58 %) (220 nm), RT 5.31 minutes.

**m/z** (MALDI-TOF) for  $C_{166}H_{254}N_{38}O_{34}S$  calcd 3358.09, found 3359.5  $[M+H]^+$ .

### V.2.5. Dde-Mmt protected PNA monomers.

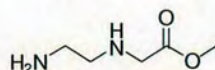
#### 2.5.1. N-(2-amino ethyl) glycine . HCl **3.11**.<sup>203</sup>



Ethylendiamine (140 mL, 213 mmol) was stirred at 4° C while 2-chloroacetic acid (20 g, 213 mmol) was added portion-wise. The reaction was stirred at room temperature overnight. The excess diamine was evaporated *in vacuo* at 50 °C to give an oil that was triturated with DMSO (500 mL). The resulting solid was collected by filtration, washed with DMSO (3 x 100 mL) and diethyl ether (3 x 100 mL) and dried in a vacuum oven at 50 °C for 24 h to give the title compound as a white solid (24.5 g, 95%).

<sup>1</sup>H NMR (250 MHz, D<sub>2</sub>O) δ = 3.18 (s, 2H, NHCH<sub>2</sub>COOH), 2.96-2.87 (m, 4H, CH<sub>2</sub>CH<sub>2</sub>)

#### 2.5.2. Methyl N-(2-amino ethyl)glycinate . 2HCl **3.12**.<sup>203</sup>



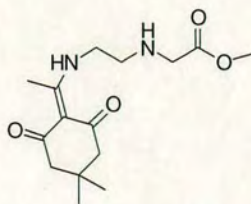
To a stirred solution of acid **3.11** (5 g, 42.3 mmol) in MeOH (60 mL) at 0 °C was added SOCl<sub>2</sub> (30 mL, 423 mmol). Then the reaction was refluxed for 12 h before cooling to 0 °C to give compound **3.12** (7 g, 81 %) as a white solid which was collected by filtration, washed with MeOH:DCM (1:1), diethyl ether and dried in a vacuum oven at 50 °C for 24 h.

**m/z** (ES<sup>+</sup>): 133 [M+H]<sup>+</sup> (100%)

<sup>1</sup>H NMR (250 MHz, D<sub>2</sub>O) δ = 4.12 (s, 3H, COOCH<sub>3</sub>), 3.83 (s, 2H, CH<sub>2</sub>NHCH<sub>2</sub>COOH), 3.30-3.20 (m, 4H, CH<sub>2</sub>CH<sub>2</sub>).



2.5.3. Methyl N-{2-[1-(4,4-Dimethyl-2,6-dioxo-cyclohexyliden)-ethylamino]-ethyl}-glycinate **3.13**.<sup>202</sup>



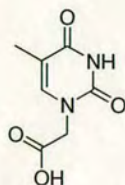
To a stirred solution of diamine salt **3.12** (25 g, 122 mmol) and DIPEA (42 mL, 244) in DCM/MeOH (1:1, 250 mL) was added Dde-OH (22.2 g, 122 mmol). The solution was stirred at room temperature for 16 h before evaporating the solvent *in vacuo*. The crude was taken up in EtOAc (200 mL) and the insoluble DIPEA salt removed by filtration. The compound was extracted into 1 M KHSO<sub>4</sub> (4 x 50 mL). The pH was then brought to 9 with NaHCO<sub>3</sub> and the compound re-extracted with EtOAc (3 x 100 mL). The organic phase was washed with brine (1 x 100 mL), dried over MgSO<sub>4</sub> and concentrated *in vacuo* to give the title compound as a brown solid (21.6 g, 60%).

**HPLC** (method 1) purity 98% (254nm), RT 2.36 min

**m/z** (ES<sup>+</sup>): 297 [M+H]<sup>+</sup> (100%).

**<sup>1</sup>H NMR** (250 MHz, CDCl<sub>3</sub>)  $\delta$  = 13.48 (br s, 1H, NH-Dde), 3.71 (s, 3H, OCH<sub>3</sub>), 3.43-3.47 (m, 4H, NH(CH<sub>2</sub>)<sub>2</sub>), 2.92 (t, *J* = 6.0 Hz, 2 H, NHCH<sub>2</sub>CO), 2.54 (s, 3H, CCH<sub>3</sub>), 2.33 (s, 4H, CH<sub>2</sub>-Dde), 1.87 (br s, 1H, NH), 0.99 (s, 6H, C(CH<sub>3</sub>)<sub>2</sub>).

#### 2.5.4. Thymine-1-ylacetic Acid **3.14**.<sup>196</sup>



To a suspension of Thymine (25 g, 198.5 mmol) and  $K_2CO_3$  (27.4 g, 198.5) in dry DMF (600 mL) was added methyl bromoacetate (18.75 mL, 198.5 mmol), and the mixture was stirred vigorously overnight under  $N_2$ . The mixture was filtered and evaporated to dryness, *in vacuo*. The solid residue was cooled to 0 °C, treated with water (188 mL) and 4 M HCl (aqueous, 8 mL), and stirred for 30 min. The precipitate was collected by filtration and washed with water (3 x 100 mL). The precipitate was treated with water (200 mL) and 2 M NaOH (aqueous, 100 mL) and boiled for 10 min. The mixture was cooled to 0 °C, treated with 4 M HCl (aqueous, 67.5 mL), and stirred for 30 min. The title compound was collected by filtration, washed with water (3 x 100 mL) and dried over  $P_2O_5$  (21 g, 58%).

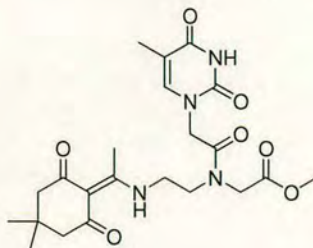
**HPLC** (method 3) purity 100% (ELSD), RT 3.44 min

**m/z** (ES<sup>+</sup>): 185 [M+H]<sup>+</sup> (100%), 207 [M+Na]<sup>+</sup> (90%),

**<sup>1</sup>H NMR** (250 MHz,  $CD_3SOCD_3$ )  $\delta$  = 11.32 (s, 1H, NH), 7.46 (s, 1H, CH), 4.36 (s, 2H,  $CH_2$ ), 1.74 (s, 3H,  $CH_3$ ).



2.5.5. Methyl N-[2-(Thymin-1-yl)-acetyl]-N-{2-[1-(4,4-dimethyl-2,6-dioxo-cyclohexyliden) ethylamino]-ethyl}-glycinate **3.15**<sup>202</sup>



Acid **3.14** (5 g, 27.5 mmol) was dissolved in DMF (55 mL), DCC (5.7 g, 27.5 mmol) and HOBt (4.2 g, 27.5 mmol) were added to the solution which was left to stir at 40 °C for 20 min. Compound **3.13** (8.2 g, 27.5 mmol) was then added and the solution stirred at 40 °C overnight. DCU was removed by filtration and washed with DMF, the combined solutions were concentrated *in vacuo*. The oil residue was taken up in DCM (250 mL) and washed with 1 M KHSO<sub>4</sub> (3 x 75 mL), 1 M NaHCO<sub>3</sub> (3 x 75 mL), and brine (3 x 75 mL). After drying over MgSO<sub>4</sub> the solvent was removed *in vacuo*. Column chromatography (silica, eluent: DCM/MeOH, 95:5) gave **3.15** (8.8 g, 19.25 mmol) as a white solid in 70% yield.

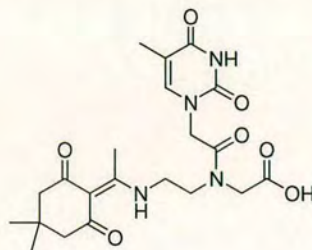
**R<sub>f</sub>** (DCM/MeOH, 95:5) = 0.35.

**HPLC** (method 3) purity 100% (ELSD), RT 4.99 min

**m/z** (ES<sup>+</sup>): 463 [M+H]<sup>+</sup> (100%), 485 [M+Na]<sup>+</sup> (60%), 947 [2M+Na]<sup>+</sup> (60%).

**<sup>1</sup>H NMR** (250 MHz, CDCl<sub>3</sub>) (two rotamers) δ = 13.54 and 13.34 (two s, 1H, Dde-NH), 10.20 (br s, 1H, NH<sub>Thy</sub>), 7.17 and 7.04 (two s, 1H, CH<sub>Thy</sub>), 4.62 and 4.44 (two s, 2H, CH<sub>2</sub>CO<sub>2</sub>CH<sub>3</sub>), 4.24 and 4.06 (two s, 2H, CH<sub>2</sub>CON), 3.72 and 3.64 (two s, 3H, CH<sub>2</sub>CO<sub>2</sub>CH<sub>3</sub>), 3.68-3.58 (m, 4H, CH<sub>2</sub>CH<sub>2</sub>), 2.53 and 2.48 (two s, 3H, CCH<sub>3</sub>), 2.31 and 2.28 (two s, 4H, CH<sub>2</sub>-Dde), 1.81 and 1.82 (two s, 3H, CH<sub>3</sub>Thy), 0.94 (s, 6H, C(CH<sub>3</sub>)<sub>2</sub>).

2.5.6. *N*-[2-(Thymin-1-yl)-acetyl]-*N*-{2-[1-(4,4-dimethyl-2,6-dioxo-cyclohexyliden)-ethylamino]-ethyl}-glycine **3.7**.<sup>202</sup>



Compound **3.15** ( 5 g , 10.8 mmol) was suspended in a 1:1 (v/v) mixture of THF and 0.2 M Cs<sub>2</sub>CO<sub>3</sub> (400 mL) and stirred at room temperature overnight. The THF was removed *in vacuo* and the aqueous phase was acidified with 4 N HCl (pH = 1), the water was then removed *in vacuo* and the residue was treated with hot 2-propanol. The hot suspension was filtered to remove the salt and the 2-propanol solution collected. After removing the solvent *in vacuo* the residue was sonicated in water (20 mL), filtrated and dried over P<sub>2</sub>O<sub>5</sub> *in vacuo* to give **3.7** (4.2 g, 9.18 mmol) as a white solid in 85 % yield.

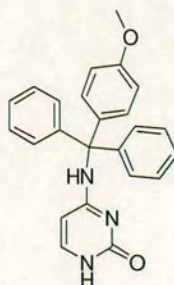
**HPLC** (method 3) purity 100% (ELSD), RT 5.73 min.

**m/z** (ES<sup>+</sup>): 449 [M+H]<sup>+</sup> (100%), 471 [M+Na]<sup>+</sup> (60%).

**<sup>1</sup>H NMR** (250 MHz, CDCl<sub>3</sub>) two rotamers δ = 13.19 and 13.13 (two s, 1H, Dde-NH), 11.29 and 11.27 (two s, 1H, NH<sub>Thy</sub>), 7.32 and 7.31 (two s, 1H, CH<sub>Thy</sub>), 4.66 and 4.51 (two s, 2H, CH<sub>2</sub>CO<sub>2</sub>CH<sub>3</sub>), 4.27 and 4.02 (two s, 2H, CH<sub>2</sub>CON), 3.68-3.58 (m, 4H, CH<sub>2</sub>CH<sub>2</sub>), 2.53 and 2.47 (two s, 3H, CCH<sub>3</sub>), 2.29 and 2.26 (two s, 4H, CH<sub>2</sub>-Dde), 1.75 (s, 3H, CH<sub>3</sub>Thy), 0.94 and 0.93 (two s, 6H, C(CH<sub>3</sub>)<sub>2</sub>).



2.5.7. *N*<sup>4</sup>-(4-methoxytrityl)-cytosine **3.16**.



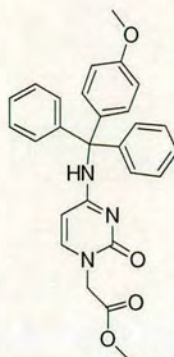
Cytosine (4.5 g, 40 mmol) was dissolved in dry pyridine (200 mL). Mmt-Cl (18.6 g, 60 mmol) and NEM (6.45 mL, 40 mmol) were added and the solution stirred at 40 °C for 48 h under N<sub>2</sub>. The solvent was removed *in vacuo*, water (150 mL) and DCM (150 mL) were added. Diethyl ether was added until formation of a precipitate which was collected by filtration and dried over P<sub>2</sub>O<sub>5</sub> affording **3.16** as a white solid (9.2 g, 60 %).

**HPLC** (method 3) purity 100% (ELSD), RT 5.12 min

**m/z** (ES<sup>+</sup>): 273 [Mmt]<sup>+</sup> (100%), 767 [2M+H]<sup>+</sup> (20%)

(The title compound was insoluble in common deuterated solvents and therefore could not be analysed by NMR as reported in the literature for a Z-protected cytosine<sup>196</sup>).

2.5.8. Methyl [*N*<sup>4</sup>-(4-methoxytrityl)-cytosin-1-yl]-acetate **3.17**.<sup>204</sup>



Compound **3.16** (10.0 g, 26 mmol) was dissolved in dry DMF (100 mL). NaH (1.04 g, 60% in mineral oil, 26 mmol) was added portion-wise to the stirred solution. After stirring for 1 h at room temperature methyl 2-bromoacetate (3.4 mL, 31 mmol) was added dropwise and the solution was left to stir for other 16 h at room temperature. The reaction was then quenched by adding MeOH (1 mL) and the solvent evaporated *in vacuo*. To the resulting oil was added water (50 mL), the white precipitate was collected by filtration and washed with water (2 x 25 mL) to give a white solid which was dried over P<sub>2</sub>O<sub>5</sub> *in vacuo* (10 g, 85 %).

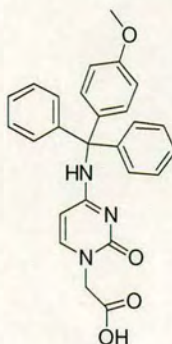
**HPLC** (method 1) purity 98% (254 nm), RT 3.51 min.

**m/z** (ES<sup>+</sup>): 273 [Mmt]<sup>+</sup> (90%), 912 [2M+H]<sup>+</sup> (100%).

**<sup>1</sup>H NMR** (250 MHz, CD<sub>3</sub>SOCD<sub>3</sub>) δ = 8.44 (br s, 1H, NH), 7.47 (d, *J* = 7.0 Hz, 1H, CH<sub>Cyt</sub>), 7.28 - 7.16 (m, 12H, CH<sub>Mmt</sub>), 6.84 (d, *J* = 8.2 Hz, 2H, CH<sub>Mmt</sub>), 6.21 (d, *J* = 7.0 Hz, 1H, CH<sub>Cyt</sub>), 4.32 (s, 2H, CH<sub>2</sub>), 3.72 (s, 3H, CH<sub>3</sub>OAr), 3.61 (s, 3H, COOCH<sub>3</sub>).



2.5.9. [*N*<sup>4</sup>-(4-methoxytrityl)-cytosin-1-yl]-acetic acid **3.18**.<sup>202,204</sup>



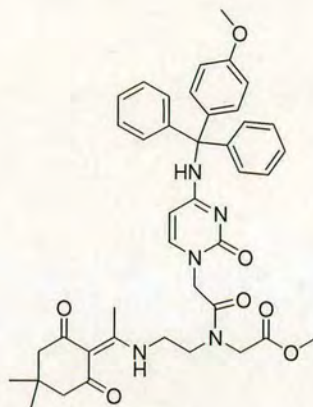
Compound **3.17** (10 g, 22 mmol) was suspended in 2N aqueous NaOH (100 mL) and the mixture was stirred for 2 h at reflux. The reaction was cooled to room temperature and washed with DCM (3 x 20 mL). The solution was then acidified with 2 N aqueous HCl until pH 2. The precipitate was collected by filtration and washed with small portion of water until the filtrate was neutral (pH = 7), and dried *in vacuo* over P<sub>2</sub>O<sub>5</sub> overnight to give **3.18** (8 g, 17.6 mmol) as a white solid in 80 % yield.

**HPLC** (method 1) purity 95% (254 nm), RT 3.51 min.

**m/z** (ES<sup>+</sup>): 273 [Mmt]<sup>+</sup> (100%), 884 [2M+H]<sup>+</sup> (30%).

**<sup>1</sup>H NMR** (250 MHz, CD<sub>3</sub>SOCD<sub>3</sub>) δ = 8.37 (br s, 1H, NH), 7.44 (d, *J* = 7.2 Hz, 1H, CH<sub>Cyt</sub>), 7.26-7.16 (m, 12H, CH<sub>Mmt</sub>), 6.83 (d, *J* = 6.9 Hz, 2H, CH<sub>Mmt</sub>), 6.19 (d, *J* = 7.2 Hz, 1H, CH<sub>Cyt</sub>), 4.24 (s, 2H, CH<sub>2</sub>), 3.72 (s, 3H, CH<sub>3</sub>).

2.5.10. Methyl *N*-{2-[*N*<sup>4</sup>-(4-methoxytrityl)-cytosin-1-yl]-acetyl}-*N*-{2-[1-(4,4-dimethyl-2,6-dioxo-cyclohexyliden) ethylamino]ethyl}-glycinate **3.19**.<sup>202</sup>



Acid **3.18** (10 g, 22 mmol) was dissolved in DMF (44 mL). DCC (4.56 g, 22 mmol) and HOBt (3.36 g, 22 mmol) were added to the solution and left to stir at 40 °C for 20 min. Compound **3.13** (6.6 g, 27.5 mmol) was then added and the solution stirred at 40 °C overnight. DCU was removed by filtration and washed with DMF (2 x 10 mL). The solvent was removed *in vacuo* and the residue was taken up in DCM (250 mL) and washed with 1 M KHSO<sub>4</sub> (3 x 75 mL), 1 M NaHCO<sub>3</sub> (3 x 75 mL), and brine (3 x 75 mL). After drying over MgSO<sub>4</sub> the solvent was removed *in vacuo*. Column chromatography (silica, eluent: EtOAc/MeOH, 4:1) gave **3.19** (10.4 g, 14.52 mmol) as a white solid in 66% yield.

**R<sub>f</sub>** (EtOAc/MeOH, 4:1) = 0.4.

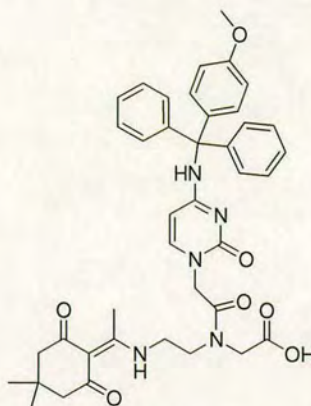
**HPLC** (method 3) purity 97% (ELSD), RT 6.25 min.

**m/z** (ES<sup>+</sup>): 273 [Mmt]<sup>+</sup> (92%), 720 [M+H]<sup>+</sup> (100%)

**<sup>1</sup>H NMR** (250 MHz, CD<sub>3</sub>OD) two rotamers δ = 7.30-7.16 (m, 12H, CH<sub>Mmt</sub>, 1H, CH<sub>Cyt</sub>), 6.83 (d, *J* = 8.5 Hz, 2H, CH<sub>Mmt</sub>), 5.19 (d, *J* = 6.9 Hz, 1 H, CH<sub>Cyt</sub>), 4.67 and 4.51 (two s, 2H, CH<sub>2</sub>CO<sub>2</sub>Me), 4.38 and 4.13 (two s, 2H, CH<sub>2</sub>CON), 3.74-3.63 (m, 3H, OCH<sub>3Mmt</sub>, 4H, CH<sub>2</sub>CH<sub>2</sub>, 3H, COOCH<sub>3</sub>), 2.57 and 2.52 (two s, 3H, CCH<sub>3</sub>), 2.31 and 2.28 (two s, 4H, CH<sub>2</sub>-Dde), 0.96 and 0.95 (two s, 6H, C(CH<sub>3</sub>)<sub>2</sub>).



2.5.11. *N*-{2-[*N*<sup>4</sup>-(4-methoxytrityl)-cytosin-1-yl]-acetyl}-*N*-{2-[1-(4,4-dimethyl-2,6-dioxo-cyclohexyliden) ethylamino]ethyl}-glycine **3.8**.<sup>202</sup>



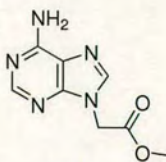
Compound **3.19** (7.76 g , 10.8 mmol) was suspended in a 1:1 (v/v) mixture of THF and 0.2 M Cs<sub>2</sub>CO<sub>3</sub> (400 mL) and stirred at room temperature overnight. The THF was removed *in vacuo*, the aqueous phase was acidified with 1M KHSO<sub>4</sub> (pH = 2), and extracted with DCM (3 x 200 mL). The organic phase was washed with brine (2 x 100 mL), dried over MgSO<sub>4</sub>. The solvent was removed *in vacuo* to give **3.8** (6.24 g, 8.8 mmol) as a white solid in 82% yield.

**HPLC** (method 3) purity 100% (ELSD), RT 9.51 min.

**m/z** (ES<sup>+</sup>): 273 [Mmt]<sup>+</sup> (100%), 706 [M+H]<sup>+</sup> (20%).

**<sup>1</sup>H NMR** (250 MHz, CD<sub>3</sub>OD) two rotamers δ = 7.28-7.16 (m, 12H, CH<sub>Mmt</sub>, 1H, CH<sub>Cyt</sub>), 6.84 (d, *J* = 8.7 Hz, 2H, CH<sub>Mmt</sub>), 5.25 and 5.21 (two d, *J* = 7.5 Hz, 1H, CH<sub>Cyt</sub>), 4.68 and 4.50 (two s, 2H, CH<sub>2</sub>CO<sub>2</sub>H), 4.22 and 4.09 (two s, 2H, CH<sub>2</sub>CON), 3.73-3.61 (m, 3H, OCH<sub>3</sub><sub>Mmt</sub>, 4H, CH<sub>2</sub>CH<sub>2</sub>), 2.53 and 2.50 (two s, 3H, CCH<sub>3</sub>), 2.30 and 2.26 (two s, 4H, CH<sub>2</sub>-Dde), 0.92 and 0.96 (two s, 6H, C(CH<sub>3</sub>)<sub>2</sub>).

2.5.12. Methyl adenine-9-ylacetate **3.20**.<sup>196</sup>



Adenine (32.8 g, 230 mmol) was suspended in dry DMF (500 mL). NaH (10.58 g, 60% in mineral oil, 260 mmol) was added portion-wise with mechanical stirring. The reaction mixture was stirred at room temperature for 2 h. Methyl 2-bromoacetate (33 mL, 345 mmol) was added dropwise during 3 h, and stirred for a further 2 h. The solvent was removed by evaporation *in vacuo*, the remaining oil was stirred with water (450 mL) resulting in the precipitation of a white solid. The solid was collected by filtration and washed with water (2 x 50 mL), followed by recrystallization from EtOH (34.2 g, 68 %).

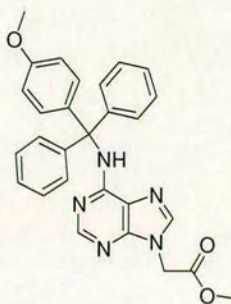
**HPLC** (method 1) purity 100% (254 nm), RT 1.35 min

**m/z** (ES+) 208 [M+H]<sup>+</sup> (100%).

**<sup>1</sup>H NMR** (250 MHz, CD<sub>3</sub>SOCD<sub>3</sub>)  $\delta$  = 8.14 (s, 1H, CH), 8.12 (s, 1H, CH), 7.32 (s, 2H, NH<sub>2</sub>), 5.09 (s, 2H, CH<sub>2</sub>), 3.69 (s, 3H, OCH<sub>3</sub>).



2.5.13. Methyl [*N*<sup>6</sup>-(4-methoxytrityl)-adenin-9-yl]acetate **3.21**.<sup>204</sup>



Compound **3.20** (25 g, 120 mmol), NEM (15 mL, 120 mmol) and Mmt-Cl (55 g, 1180 mmol) in dry pyridine (350 mL) were stirred at 45 °C for 48 h under N<sub>2</sub>. The solvent was removed *in vacuo* and the remaining oil was dissolved in DCM (250 mL), washed with 1 N aqueous KHSO<sub>4</sub> (3 x 50 mL), 10% aqueous NaHCO<sub>3</sub> (3 x 50 mL), brine (3 x 50 mL) and dried over MgSO<sub>4</sub>. Column chromatography (silica, eluent: AcOEt) gave **3.21** (39 g, 92.4 mmol) as a white solid in 77% yield.

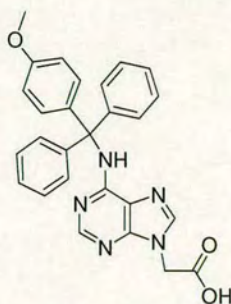
**R<sub>f</sub>** (AcOEt)= 0.45.

**HPLC** (method 1) purity 100% (254 nm), RT 3.88 min.

**m/z** (ES<sup>+</sup>): 273 [Mmt]<sup>+</sup> (100%), 480 [M+H]<sup>+</sup> (35%)

**<sup>1</sup>H NMR** (250 MHz, CD<sub>3</sub>SOCD<sub>3</sub>) δ = 8.22 (s, 1H, CH<sub>pur</sub>), 7.94 (s, 1H, CH<sub>pur</sub>), 7.30-7.20 (m, 12H, CH<sub>Mmt</sub>), 6.85 (d, *J* = 8.9 Hz, 2H, CH<sub>Mmt</sub>), 5.11 (s, 2H, CH<sub>2</sub>), 3.70 (s, 3H, COCH<sub>3</sub>), 3.69 (s, 3H, COOCH<sub>3</sub>).

2.5.14. [*N*<sup>6</sup>-(4-methoxytrityl)-adenin-9-yl]acetic acid **3.22**.<sup>204</sup>



Compound **3.21** (38 g, 79 mmol) was suspended in a 1:1 (v/v) mixture of THF and 2 N NaOH (150 mL) and stirred at room temperature overnight. The THF was removed *in vacuo*, the aqueous phase was acidified with 1M KHSO<sub>4</sub> (200 mL) and extracted with EtOAc (3 x 100 mL). The organic phase was washed with brine (3 x 50 mL) and dried over MgSO<sub>4</sub>. The solvent was removed *in vacuo* to give **3.22** (32.7 g, 62.41mmol) as a white solid in 89 % yield.

**HPLC** (method 1) purity 100% (254 nm), RT 3.61 min.

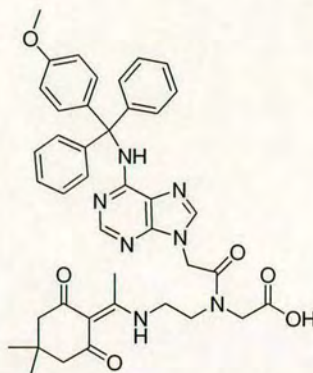
**m/z** (ES<sup>+</sup>): 273 [Mmt]<sup>+</sup> (100%), 466 [M+H]<sup>+</sup> (35%).

**<sup>1</sup>H NMR** (250 MHz, CD<sub>3</sub>SOCD<sub>3</sub>) δ = 8.20 (s, 1H, CH<sub>pur</sub>), 7.91 (s, 1H, CH<sub>pur</sub>), 7.30-7.20 (m, 12H, CH<sub>Mmt</sub>), 6.85 (d, *J* = 8.7 Hz, 2H, CH<sub>Mmt</sub>), 4.96 (s, 2H, CH<sub>2</sub>), 3.71 (s, 3H, COCH<sub>3</sub>).





2.5.16. *N*-{2-[*N*<sup>6</sup>-(4-methoxytrityl)-adenin-9-yl]-acetyl}-*N*-{2-[1-(4,4-dimethyl-2,6-dioxo-cyclohexyliden) ethylamino]ethyl}glycine **3.9**.<sup>202</sup>



Compound **3.23** (8 g, 10.8 mmol) was suspended in a 1:1 (v/v) mixture of THF and 0.2 M Cs<sub>2</sub>CO<sub>3</sub> (400 mL) and stirred at room temperature overnight. The THF was removed *in vacuo*, the aqueous phase was acidified with 1M KHSO<sub>4</sub> (pH = 2), and extracted with DCM (3 x 200 mL). The organic phase was washed with brine (2 X 100 mL), dried over MgSO<sub>4</sub>. The solvent was removed *in vacuo* to give **3.9** (7.1 g, 9.72) as a white solid in 90% yield.

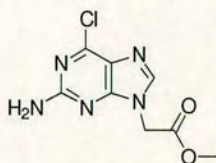
**HPLC** (method 1) purity 100% (254 nm), RT 3.69 min.

**m/z** (ES<sup>+</sup>): 273 [Mmt]<sup>+</sup> (100%), 730 [M+H]<sup>+</sup> (55%).

**<sup>1</sup>H NMR** (250 MHz, CD<sub>3</sub>SOCD<sub>3</sub>) two rotamers δ = 13.16 (s, 1H, Dde-NH), 8.13 (s, 1H, CH<sub>pur</sub>), 7.92 (s, 1H, CH<sub>pur</sub>), 7.34-7.21 (m, 12H, CH<sub>Mmt</sub>), 6.90 (d, *J* = 8.5 Hz, 2H, CH<sub>Mmt</sub>), 5.22 and 5.12 (s, 2H, CH<sub>2</sub>CO<sub>2</sub>H), 3.95 (s, 2H, CH<sub>2</sub>CON), 3.77-3.53 (m, 3H, OCH<sub>3</sub>Mmt, 4H, CH<sub>2</sub>CH<sub>2</sub>), 2.56 and 2.50 (s, 3H, CCH<sub>3</sub>), 2.30 (s, 4H, CH<sub>2</sub>-Dde), 0.96 (s, 6H, C(CH<sub>3</sub>)<sub>2</sub>).



2.5.17. Methyl (2-amino-6-chloropurin-9-yl)acetate **3.24**.<sup>204</sup>



2-Amino-6-chloropurine (15 g, 88 mmol) was suspended in dry DMF (250 mL). NaH (3.6 g, 60% in mineral oil, 88 mmol) was added portionwise to the stirred suspension. The reaction mixture was stirred at room temperature for 2 h, and methyl 2-bromoacetate (12.6 mL, 132 mmol) was added dropwise over 1 h. The mixture was then stirred for a further 2 h. The solvent was removed *in vacuo*, the remaining oil was stirred with water (200 mL) resulting in the precipitation of a white solid. The solid was collected by filtration, washed with water (2 x 50 mL) and dried *in vacuo* over P<sub>2</sub>O<sub>5</sub>. Column chromatography (silica, eluent: DCM/MeOH, 9:1) gave **3.24** (16.1 g, 68 mmol) as a white solid in 76 % yield.

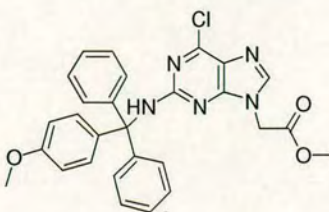
**R<sub>f</sub>** (DCM/MeOH, 9:1) = 0.44.

**HPLC** (method 5) purity 100% (ELSD), RT 4.69 min.

**m/z** (ES<sup>+</sup>): 242 (<sup>35</sup>Cl) and 244 (<sup>37</sup>Cl) [M+H]<sup>+</sup> (100%), 264 (<sup>35</sup>Cl) and 266 (<sup>37</sup>Cl) [M+Na]<sup>+</sup> (75%).

**<sup>1</sup>H NMR** (250 MHz, CD<sub>3</sub>SOCD<sub>3</sub>)  $\delta$  = 8.12 (s, 1H, CH), 7.01 (s, 2H, NH<sub>2</sub>), 5.01 (s, 2H, CH<sub>2</sub>), 3.68 (s, 3H, CH<sub>3</sub>).

2.5.18. Methyl *N*<sup>2</sup>-(4-methoxytrityl)-amino-6-chloropurin-9-yl acetate **3.25**.<sup>202</sup>



Compound **3.24** (5 g, 20 mmol), 4-methoxytrityl chloride (9.58 g, 30 mmol) and DIPEA (3.6 mL, 20 mmol) in dry THF (135 mL) were stirred at 40 °C under N<sub>2</sub> atmosphere for 12 h. The solvent was removed by evaporation *in vacuo* and the remaining oil was taken up in Et<sub>2</sub>O (150 mL). The solution was washed with 1 M KHSO<sub>4</sub> (3 x 25 mL), 10% aqueous NaHCO<sub>3</sub> (3 x 25 mL), brine (1 x 25 mL) and dried over MgSO<sub>4</sub>. The solvent was removed *in vacuo* and the remaining oil was triturated with petroleum ether 40-60 °C to give **3.25** (5.3 g, 10.2 mmol) as a yellowish solid in 51% yield.

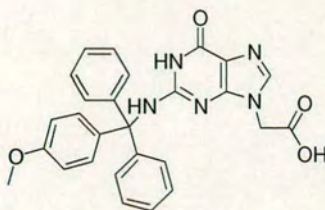
**HPLC** (method 5) purity 100% (ELSD), RT 10.03 min.

**m/z** (ES+) 514.2 (<sup>35</sup>Cl) and 516.2 (<sup>37</sup>Cl) [M+H]<sup>+</sup> (100%).

**<sup>1</sup>H NMR** (250 MHz, CDCl<sub>3</sub>) δ = 7.67 (s, 1H, CH<sub>pur</sub>), 7.35–7.24 (m, 12H, CH<sub>Mmt</sub>), 6.81 (d, *J* = 8.6 Hz, 2H, CH<sub>Mmt</sub>), 6.65 (s, 1H, NH-Mmt), 4.37 (s, 2H, CH<sub>2</sub>), 3.81 (s, 3H, OCH<sub>3Mmt</sub>), 3.67 (s, 3H, COOCH<sub>3</sub>).



2.5.19. [*N*<sup>2</sup>-(4-methoxytrityl)-guanin-9-yl]acetic acid **3.26**.<sup>202</sup>



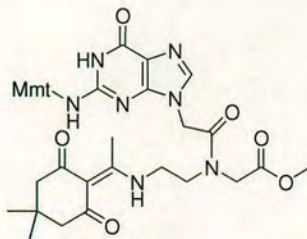
Ester **3.25** (5.0 g, 9.6 mmol), was suspended in 2 N aqueous NaOH (150 mL) and the mixture was stirred for 4 h at reflux. The reaction was cooled to room temperature and acidified with 2 N aqueous HCl (pH=2). The precipitate was collected by filtration, washed with water and dried *in vacuo* overnight giving a solid which was washed with diisopropyl ether to give **3.26** (3.5 g, 7.2 mmol) as a yellowish solid in 75% yield.

**HPLC** (method 5) purity 100% (ELSD), RT 7.50 min.

**m/z** (ES+) 482.2 [M+H]<sup>+</sup> (100%).

**<sup>1</sup>H NMR** (250 MHz, CD<sub>3</sub>SOCD<sub>3</sub>) δ = 11.15 (s, 1H, NH<sub>pur</sub>), 8.12 (s, 1H, NH-Mmt), 8.06 (s, 1H, CH<sub>pur</sub>), 7.29–7.16 (m, 12H, CH<sub>Mmt</sub>), 6.81 (d, *J* = 8.4 Hz, 2H, CH<sub>Mmt</sub>), 4.28 (s, 2H, CH<sub>2</sub>), 3.72 (s, 3H, OCH<sub>3Mmt</sub>)

2.5.20. Methyl *N*-{2-[*N*<sup>2</sup>-(4-methoxytrityl)-guanine-9-yl]-acetyl}-*N*-{2-[1-(4,4-dimethyl-2,6-dioxo-cyclohexyliden) ethylamino]ethyl}glycinate **3.27**.<sup>202</sup>



PyBrOP (5.07 g, 10.9 mmol) and DIPEA (3.7 mL, 21.8 mmol) were added to a solution of acid **3.26** (5.24 g, 10.9 mmol) and amine **3.13** (3.38 g, 10.9 mmol) in DMF (25 mL) at 0 °C. The reaction solution was removed from the ice bath and stirred under N<sub>2</sub> at 25 °C for 2 h. The solvent was removed *in vacuo* and the residue was taken up in DCM (300 mL). The solution was washed with 1 M KHSO<sub>4</sub> (100 mL), 10% aqueous NaHCO<sub>3</sub> (100 mL) and brine (100 mL). The organic phase was dried over MgSO<sub>4</sub> and concentrated *in vacuo* to afford **3.27** as a brown solid (3.9 g, 50%) which was used for the next step without any further purification.

Analytical sample purified by chromatography (DCM/MeOH, 5:1).

**R<sub>f</sub>** (DCM/MeOH, 5:1): 0.31.

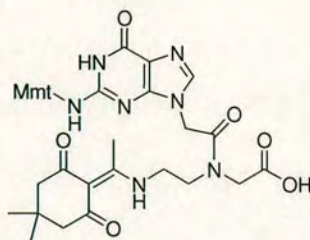
**HPLC** (method 5) purity 96% (ELSD), RT 8.42 min.

**m/z** (ES<sup>+</sup>) 760.4 [M+H]<sup>+</sup> (100%).

**<sup>1</sup>H NMR** (250 MHz, CD<sub>3</sub>SOCD<sub>3</sub>) two rotamers δ = 13.23 and 13.17 (s, 1H, Dde-NH), 10.58 and 10.55 (two br s, 1H, NH<sub>pur</sub>), 7.44 and 7.42 (two s, 1H, CH<sub>pur</sub>), 7.30–7.13 (m, 12H, CH<sub>Mmt</sub>), 6.81 (d, *J* = 8.7 Hz, 2H, CH<sub>Mmt</sub>), 4.41 and 4.22 (two s, 2H, CH<sub>2</sub>COOMe), 4.10 and 4.05 (two s, 2H, CH<sub>2</sub>CO), 3.72–3.43 (m, 3H, OCH<sub>3Mmt</sub>, 4H, CH<sub>2</sub>CH<sub>2</sub>, 3H, COOCH<sub>3</sub>), 2.51 and 2.48 (two s, 3H, CH<sub>3</sub>C), 2.30 and 2.26 (two s, 4H, CH<sub>2</sub>-Dde), 0.95 and 0.94 (two s, 6H, C(CH<sub>3</sub>)<sub>2</sub>)



2.5.21. *N*-{2-[*N*<sup>2</sup>-(4-methoxytrityl)-guanine-9-yl]-acetyl}-*N*-{2-[1-(4,4-dimethyl-2,6-dioxo-cyclohexyliden) ethylamino]ethyl}glycine **3.10**.<sup>202</sup>



Compound **3.27** (3 g, 4 mmol) was suspended in a 1:1 (v/v) mixture of THF and 0.2 M Cs<sub>2</sub>CO<sub>3</sub> (160 mL) and stirred at room temperature overnight. The THF was removed *in vacuo*, and the aqueous phase was washed with DCM (3 x 20 mL). The basic water solution was acidified with 1M KHSO<sub>4</sub> (pH = 2). The precipitate was collected by filtration and washed with water. The solid was dissolved in a minimum volume of MeOH and re-precipitated with the addition of water. The solid was collected by filtration and dried *in vacuo* to give **3.10** (5 g, 3.2 mmol) as a brown solid in 80% yield.

**HPLC** (method 5) purity 94% (ELSD), RT 7.07 min.

**m/z** (ES+) 746.3[M+H]<sup>+</sup> (100%).

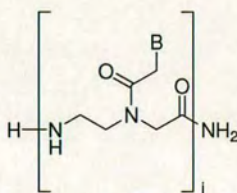
**<sup>1</sup>H NMR** (250 MHz, CD<sub>3</sub>SOCD<sub>3</sub>) two rotamers δ = 13.16 and 13.15 (two br s, 1H, Dde-NH), 10.51 (br s, 1H, NH<sub>pur</sub>), 7.45 and 7.43 (two s, 1H, CH<sub>pur</sub>), 7.27–7.15 (m, 12H, CH<sub>Mmt</sub>), 6.81 (d, *J* = 8.7 Hz, 2H, CH<sub>Mmt</sub>), 4.45 and 4.23 (two s, 2H, CH<sub>2</sub>COO), 3.98 and 3.93 (two s, 2H, CH<sub>2</sub>CO), 3.73–3.41 (m, 3H, OCH<sub>3Mmt</sub>, 4H, CH<sub>2</sub>CH<sub>2</sub>), 2.50 and 2.47 (two s, 3H, CH<sub>3</sub>C), 2.31 and 2.28 (two s, 4H, CH<sub>2</sub>-Dde), 0.95 and 0.94 (two s, 6H, C(CH<sub>3</sub>)<sub>2</sub>).

### V.2.6. PNAs and PNA-peptoid conjugates.

PNAs and PNA-peptoid hybrids were prepared using Rink<sup>151</sup> amide PEGA resin (25 mg, loading 0.4 mmol/g, 10  $\mu$ mol).

- Peptoid couplings and fluorescein labelling were carried out under microwave conditions (see V.2.3.2 and V.2.3.8).
- PNA couplings were followed by a capping step (see V.2.3.4).
- Dde deprotection and Fmoc deprotection were carried out as described in sections V.2.3.5 and V.2.3.6.
- TFA cleavage (solution 1) and ether precipitation were accomplished as described in V.2.3.9.

#### 2.6.1. PNA oligomers 3.28-3.33.



TTT CTC CTT (3.28).

**Yield:** 7.2 mg, 2.6  $\mu$ mol.

**HPLC** (method 4) crude purity 95% (ELSD), RT 6.06 minutes.

**m/z** (MALDI-TOF) for C<sub>96</sub>H<sub>126</sub>N<sub>40</sub>O<sub>33</sub> calcd 2368.27, found 2368.56 [M+H]<sup>+</sup>.

CAT TTT CTC CTT (3.29).

**Yield:** 9.3 mg, 2.5  $\mu$ mol.

**HPLC** (method 4) crude purity > 95% (ELSD), RT 6.35 minutes.

**m/z** (MALDI-TOF) for C<sub>128</sub>H<sub>166</sub>N<sub>56</sub>O<sub>42</sub> calcd 3161.03, found 3158.38 [M+H]<sup>+</sup>.

GAA CAT TTT CTC CTT (3.30).

**Yield:** 15.4 mg, 3.1  $\mu$ mol.

**HPLC** (method 4) poor solubility, broad peak RT 6.68 minutes.

**m/z** (MALDI-TOF) for C<sub>161</sub>H<sub>205</sub>N<sub>77</sub>O<sub>49</sub> calcd 4002.83, found 3998.34 [M+H]<sup>+</sup>.





**m/z** (MALDI-TOF) for  $C_{155}H_{187}N_{57}O_{49}$  calcd 3632.49, found 3633.10  $[M+H]^+$ .

FAM-Ahx-GAA CAT TTT CTC CTT (**3.36**).

**Yield:** 16.2 mg, 3  $\mu$ mol.

**HPLC** (method 4) very poor solubility, broad peak.

**m/z** (MALDI-TOF) for  $C_{188}H_{226}N_{78}O_{56}$  calcd 4474.29, found 4477.06  $[M+H]^+$ .

FAM-Ahx-TCT TCC TCT (**3.37**).

**Yield:** 8.7 mg, 2.6  $\mu$ mol.

**HPLC** (method 4) crude purity > 95% (ELSD), two isomers RT 7.05-7.24 minutes.

**m/z** (MALDI-TOF) for  $C_{122}H_{146}N_{42}O_{39}$  calcd 2824.72, found 2825.84  $[M+H]^+$ .

FAM-Ahx-CAT TCT TCC TCT (**3.38**).

**Yield:** 13.5 mg, 3.1  $\mu$ mol.

**HPLC** (method 4) crude purity 85% (ELSD), two isomers RT 7.03 and 7.16 minutes.

**m/z** (MALDI-TOF) for  $C_{154}H_{186}N_{58}O_{48}$  calcd 3617.48, found 3618.84  $[M+H]^+$ .

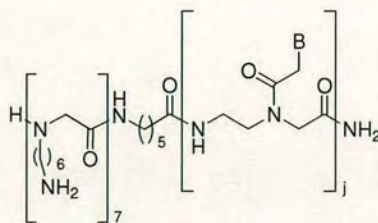
FAM-Ahx-GAG CAT TCT TCC TCT (**3.39**).

**Yield:** 13 mg, 2.4  $\mu$ mol.

**HPLC** (method 4) very poor solubility, broad peak.

**m/z** (MALDI-TOF) for  $C_{187}H_{225}N_{79}O_{56}$  calcd 4475.28, found 4477.37  $[M+H]^+$ .

#### 2.6.3. Heptapeptoid-Ahx-PNA oligomers **3.40-3.45**.



Heptapeptoid-Ahx-TTT CTC CTT (**3.40**).

**Yield:** 12.5 mg, 2.6  $\mu$ mol.

**HPLC** (method 4) crude purity 95% (ELSD), RT 6.06 minutes.



**m/z** (MALDI-TOF) for  $C_{158}H_{249}N_{55}O_{41}$  calcd 3575.01, found 3578.30  $[M+H]^+$ .

Heptapeptoid -Ahx-CAT TTT CTC CTT (**3.41**).

**Yield:** 13.7 mg, 3.1  $\mu$ mol.

**HPLC** (method 4) crude purity 95% (ELSD), RT 6.30 minutes.

**m/z** (MALDI-TOF) for  $C_{190}H_{289}N_{71}O_{50}$  calcd 4367.77, found 4367.26  $[M+H]^+$ .

Heptapeptoid -Ahx-GAA CAT TTT CTC CTT (**3.42**).

**Yield:** 15.5 mg, 2.2  $\mu$ mol.

**HPLC** (method 4) crude purity 85% (ELSD), RT 6.62 minutes.

**m/z** (MALDI-TOF) for  $C_{223}H_{328}N_{92}O_{57}$  calcd 5209.57, found 5209.06  $[M+H]^+$ .

Heptapeptoid -Ahx-TCT TCC TCT (**3.43**).

**Yield:** 13.5 mg, 2.8  $\mu$ mol.

**HPLC** (method 4) crude purity 93% (ELSD), RT 5.92 minutes.

**m/z** (MALDI-TOF) for  $C_{157}H_{248}N_{56}O_{40}$  calcd 3560.00, found 3560.34  $[M+H]^+$ .

Heptapeptoid -Ahx-CAT TCT TCC TCT (**3.44**).

**Yield:** 12.8 mg, 2.2  $\mu$ mol.

**HPLC** (method 4) crude purity 86 % (ELSD), RT 6.27 minutes.

**m/z** (MALDI-TOF) FOR  $C_{189}H_{288}N_{72}O_{49}$  calcd 4352.76, found 4353.55  $[M+H]^+$ .

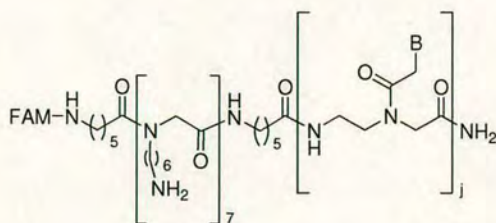
Heptapeptoid -Ahx-GAG CAT TCT TCC TCT (**3.45**).

**Yield:** 18.4 mg, 2.6  $\mu$ mol.

**HPLC** (method 4) crude purity 55% (ELSD), RT 6.60 minutes.

**m/z** (MALDI-TOF) for  $C_{222}H_{327}N_{93}O_{57}$  calcd 5210.56, found 5212.81  $[M+H]^+$ .

2.6.4. FAM-Ahx-heptapeptoid-Ahx-PNA oligomers **3.46-3.51**.



FAM-Ahx-heptapeptoid-Ahx-TTT CTC CTT (**3.46**).

**Yield:** 14.4 mg, 2.7  $\mu\text{mol}$ .

**HPLC** (method 4) crude purity > 95% (ELSD), RT 6.33 minutes.

**m/z** (MALDI-TOF) for  $\text{C}_{185}\text{H}_{270}\text{N}_{56}\text{O}_{48}$  calcd 4046.46, found 4047.83  $[\text{M}+\text{H}]^+$ .

FAM-Ahx-heptapeptoid -Ahx-CAT TTT CTC CTT (**3.47**).

**Yield:** 14.3 mg, 2.3  $\mu\text{mol}$ .

**HPLC** (method 4) crude purity 90% (ELSD), RT 6.34 minutes.

**m/z** (MALDI-TOF) for  $\text{C}_{217}\text{H}_{310}\text{N}_{72}\text{O}_{57}$  calcd 4839.23, found 4839.79  $[\text{M}+\text{H}]^+$ .

FAM-Ahx-heptapeptoid -Ahx-GAA CAT TTT CTC CTT (**3.48**).

**Yield:** 15.5 mg, 2.0  $\mu\text{mol}$ .

**HPLC** (method 4) crude purity 75% (ELSD), RT 6.48 minutes.

**m/z** (MALDI-TOF) for  $\text{C}_{250}\text{H}_{349}\text{N}_{93}\text{O}_{64}$  calcd 5681.03, found 5683.37  $[\text{M}+\text{H}]^+$ .

FAM-Ahx-heptapeptoid -Ahx-TCT TCC TCT (**3.49**).

**Yield:** 15.6 mg, 2.9  $\mu\text{mol}$ .

**HPLC** (method 4) crude purity > 95% (ELSD), RT 6.29 minutes.

**m/z** (MALDI-TOF) for  $\text{C}_{184}\text{H}_{269}\text{N}_{57}\text{O}_{43}$  calcd 4031.45, found 4032.40  $[\text{M}+\text{H}]^+$ .

FAM-Ahx-heptapeptoid -Ahx-CAT TCT TCC TCT (**3.50**).

**Yield:** 15 mg, 2.4  $\mu\text{mol}$ .

**HPLC** (method 4) crude purity 84% (ELSD), RT 6.28 minutes.

**m/z** (MALDI-TOF) for  $\text{C}_{216}\text{H}_{309}\text{N}_{73}\text{O}_{56}$  calcd 4824.22, found 4826.12  $[\text{M}+\text{H}]^+$ .



FAM-Ahx-heptapeptoid -Ahx-GAG CAT TCT TCC TCT (**3.51**).

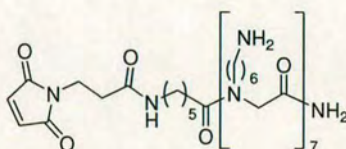
**Yield:** 18 mg, 2.4  $\mu\text{mol}$ .

**HPLC** (method 4) crude purity 65% (ELSD), RT 6.33 minutes.

**m/z** (MALDI-TOF) for  $\text{C}_{249}\text{H}_{348}\text{N}_{94}\text{O}_{64}$  calcd 5682.01, found 5686.36  $[\text{M}+\text{H}]^+$ .

### V.2.7. DNA oligo-peptoid conjugates.

#### 2.7.1. Maleimido-heptapeptoid **3.53**.



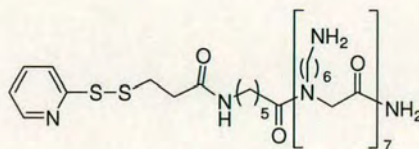
Maleimido-heptapeptoid **3.53** was prepared on Rink<sup>151</sup> amide polystyrene resin (25 mg, 1 mmol/g, 25  $\mu\text{mol}$ ).  $\text{H}_2\text{N}$ -Ahx-heptapeptoid-Rink-resin (polystyrene) was prepared under microwave conditions (see V.2.3.2). 3-(Maleimido)propionic acid N-hydroxysuccinimide ester **3.52** (3 equiv, 0.2 M) in DMF was added to the resin and the mixture stirred overnight. Compound **3.53** was cleaved using TFA (see V.2.3.9, solution 1) and precipitated in cold ether.

**Yield:** 21 mg, 16  $\mu\text{mol}$ .

**HPLC** (method 5) crude purity > 95% (ELSD), RT 3.68 minutes.

**m/z** (ES+)  $\text{C}_{69}\text{H}_{132}\text{N}_{17}\text{O}_{11}$   $[\text{M}+\text{H}]^+$  calcd 1375.9, found: 688.4  $[\text{M}+2\text{H}]^{2+}$  (35%), 459.3  $[\text{M}+3\text{H}]^{3+}$  (100%), 344.8  $[\text{M}+4\text{H}]^{4+}$  (55%).

#### 2.7.2. Pyridyldithio-heptapeptoid **3.55**.



3-(2-Pyridyldithio)propionic acid N-hydroxysuccinimide ester **3.54** (3 equiv, 0.2 M) in DMF was added to the  $\text{H}_2\text{N}$ -Ahx-heptapeptoid-Rink-resin (see above) and the

mixture stirred overnight. Compound **3.55** was cleaved using TFA (see V.2.3.9, solution 1) and precipitated in cold ether.

**Yield:** 24 mg, 15  $\mu\text{mol}$ .

**HPLC** (method 5) crude purity > 95% (ELSD), RT 4.36 minutes.

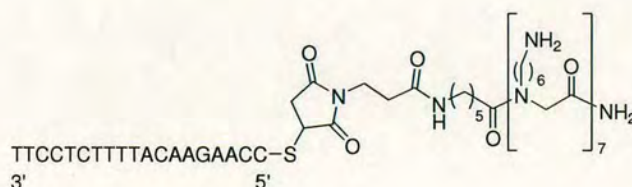
**m/z** (ES+)  $\text{C}_{70}\text{H}_{134}\text{N}_{17}\text{O}_9\text{S}_2$   $[\text{M}+\text{H}]^+$  calcd 1422.0, found: 711.4  $[\text{M}+2\text{H}]^{2+}$  (30%), 474.6  $[\text{M}+3\text{H}]^{3+}$  (100%), 356.3  $[\text{M}+4\text{H}]^{4+}$  (70%).

### 2.7.3. Preparation of HS-CCAAGAACATTTCTCCTT **3.57**.

Disulfide protected 5'-thiol modified DNA oligonucleotide **3.56** (52.5 nmol, from Sigma) was dissolved in 1 mL of DTT solution (0.004 M in 0.17 M phosphate buffer, pH = 8) and incubated for 16 h to cleave the disulfide linkage. Thiol oligonucleotide **3.57** was purified using a size exclusion NAP-10 column following the manufacturer instructions (eluent DNase free water, low molecular weight compounds such as DTT and thiol by-products eluted after the oligo). The fractions containing oligonucleotide **3.57** (verified by absorbance reading at 260 nm) were dried and the DNA oligo re-suspended in DNase free water, 0.525 mL.

**m/z** (MALDI-TOF)  $\text{C}_{190}\text{H}_{249}\text{N}_{62}\text{O}_{117}\text{P}_{19}\text{S}$  calcd 5893.93, found 5892.16  $[\text{M}-\text{H}]^-$ .

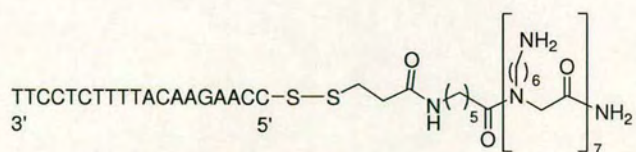
### 2.7.4. Oligonucleotide-S-heptapeptoid **3.58**.



Thiol oligonucleotide **3.57** (0.2 mL, 100  $\mu\text{M}$ ) and Maleimido-heptapeptoid **3.53** (0.2 mL, 100  $\mu\text{M}$  in PBS) were mixed and incubated overnight. **m/z** (MALDI-TOF) for  $\text{C}_{259}\text{H}_{380}\text{N}_{79}\text{O}_{128}\text{P}_{19}\text{S}$  calcd 7268.71, found 7266.09  $[\text{M}-\text{H}]^-$ .



2.7.5. *Oligonucleotide-S-S-heptapeptoid 3.59.*

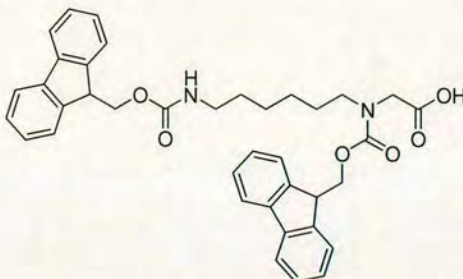


Thiol oligonucleotide **3.57** (0.2 mL, 100  $\mu$ M) and Pyridildithio-heptapeptoid **3.54** (0.2 mL, 100  $\mu$ M in PBS) were mixed and incubated overnight. **m/z** (MALDI-TOF) for  $C_{255}H_{377}N_{78}O_{126}P_{19}S_2$  calcd 7203.81, found 7201.62  $[M-H]^-$ .

### V.3. Experimental to chapter IV.

#### V.3.1. Peptoid dendrimer: synthesis and gene delivery.

##### 3.1.1. *N*-Fmoc-*N*-(6-*N'*-Fmoc-aminohexyl)-glycine **4.1**.<sup>216</sup>



Compound **2.12** (1 g, 2 mmol) was dissolved in TFA/DCM (1:1, 20 mL), and stirred for 2 h to remove the Boc protecting group. The solution was concentrated *in vacuo* and the crude compound precipitated with diethyl ether to give a sticky oil. The compound was dissolved in THF/H<sub>2</sub>O (9:1, 20 mL) before adding Fmoc-OSu (0.8 g, 2.4 mmol) and DIPEA (0.64 mL, 4 mmol). The reaction mixture was stirred at room temperature for 16 h. 1 N HCl (20 mL) was added to the solution before removing the THF *in vacuo*. The compound was extracted with DCM (3 x 30 mL), the organic phase was washed with brine (3 x 20 mL), dried over magnesium sulfate and concentrated *in vacuo*. Column chromatography (silica, eluent: from DCM to DCM/MeOH 9:1) to give acid **4.1** (800 mg, 1.3 mmol) as a white powder in 64% yield.

**R<sub>f</sub>** (DCM/MeOH 9:1) = 0.34.

**mp** = 95–100 °C.

**HPLC** (method 2) purity 100% (ELSD), RT 9.39 min.

**IR** (solid): 3100-2600 (COO-H), 1703 (C=O, s) cm<sup>-1</sup>.

**m/z** (ES+) 619 [M+H]<sup>+</sup> (100%), 641 [M+Na]<sup>+</sup> (25%).

**<sup>1</sup>H NMR** (CDCl<sub>3</sub>, 250 MHz) two rotamers δ = 7.76–7.70 (m, 4H, ArH-Fmoc), 7.60–7.52 (m, 4H, ArH-Fmoc), 7.34–7.23 (m, 8H, ArH-Fmoc), 4.89 and 4.78 (two br s, 1H, FmocNH), 4.50 and 4.39 (two m, 4H, 2 x CH<sub>2</sub>-Fmoc), 4.17 (m, 2H, 2 x CH-Fmoc), 3.95 and 3.86 (two br s, 2H, NCH<sub>2</sub>CO), 3.35 and 3.12 (two br m, 4H, 2 x FmocNCH<sub>2</sub>CH<sub>2</sub>), 1.46–1.09 (m, 8H, CH<sub>2</sub>(CH<sub>2</sub>)<sub>4</sub>CH<sub>2</sub>).



**<sup>13</sup>C NMR** (CDCl<sub>3</sub>, 62.9 MHz):  $\delta$  = 174.2 (COOH), 156.8, 156.1 (NCOO), 143.9 (ArC-Fmoc), 141.4 (ArC-Fmoc), 127.7, 127.1, 125.0 and 124.8, 120.0 (ArCH-Fmoc), 68.1 and 67.8 (CH<sub>2</sub>-Fmoc), 48.5 (CH<sub>2</sub>CH<sub>2</sub>NCH<sub>2</sub>), 47.3 (CH-Fmoc), 40.9 (FmocNHCH<sub>2</sub>), 29.7 (FmocNHCH<sub>2</sub>CH<sub>2</sub>), 28.1 (CH<sub>2</sub>CH<sub>2</sub>NCH<sub>2</sub>), 27.7 (CH<sub>2</sub>CH<sub>2</sub>CH<sub>2</sub>NCH<sub>2</sub>), 26.1 and 26.2 (FmocNHCH<sub>2</sub>CH<sub>2</sub>CH<sub>2</sub>).

**HRMS** (ES<sup>+</sup>): for C<sub>38</sub>H<sub>42</sub>N<sub>3</sub>O<sub>6</sub> [M+NH<sub>4</sub>]<sup>+</sup> calcd 636.3068, found, 636.3067.

### 3.1.2. Synthesis of peptoid dendrimers **4.3**, **4.4**, **4.5**.

*Core (G0).* To a solution of compound **4.1** (0.1 M, 3 equiv) in DMF were added HOBt (3 equiv) and DIC (3 equiv) and the solution was stirred for 2 min and then added to pre-swollen PS-Rink<sup>151</sup> amide resin in a SPE (Solid Phase Extractor) syringe. The mixture was transferred into a 5 mL microwave vessel (Biotage). The vessel was capped and subjected to microwave irradiation (60 °C for 20 min with magnetic stirring). Resin was transferred into a SPE and washed with DMF and DCM. Chloranil<sup>171</sup> and Kaiser<sup>182</sup> test were carried out before Fmoc deprotection (20% piperidine in DMF (2 x 10 min)). In case of a positive colorimetric test the couplings were repeated.

*Growing peptoid dendrimer generations.* The number (mmols) of amines (primary and secondary) on the solid support was theoretically doubled after each generation, and so as consequence quantity of reagents and solvent had to be doubled to keep consistent coupling conditions: 3 equivalents and a 0.1 M solution. However in order to save reagents and solvent, coupling solutions were prepared following the relation:

Equivalents of monomer **4.1** =  $2^n + 2$  with  $n = 1$  (G1), 2 (G2), 3 (G3)

The equivalents were calculated on the initial loading of the resin, and the amount of solvent used was the volume required to give 0.1 M solutions with 3 equivalents of reagent.

In this way for each coupling there were 2 extra equivalents of reagents to push to completion the coupling of the residual amines on the resin. The relatively low generation of the dendrimers prepared allowed the use of this strategy without having any problem of reagent solubility or coupling failure.



Following final Fmoc removal the polyamidoamines were cleaved from the resin using TFA/TIS/DCM (90:5:5) and precipitated with cold diethyl ether.

Peptoid dendrimer **4.3** (G1).

**m/z** (ES<sup>+</sup>): 486.3 [M+H]<sup>+</sup> (70%), 243.7 [M+2H]<sup>2+</sup> (100%).

**HPLC** (method 2) purity 94% (ELSD), RT 6.42 min.

Peptoid dendrimer **4.4** (G2).

**m/z** (MALDI-TOF) for C<sub>56</sub>H<sub>115</sub>N<sub>15</sub>O<sub>7</sub> calcd 1109.91 (average mass), found m/z: 1110.64 [M+H]<sup>+</sup>.

**HPLC** (method 2) purity 85% (ELSD), RT 4.51 min.

Peptoid dendrimer **4.5** (G3).

**m/z** (MALDI-TOF) for C<sub>120</sub>H<sub>243</sub>N<sub>31</sub>O<sub>15</sub> calcd 2358.92 (average mass), found 2359.94 [M+H]<sup>+</sup>.

**HPLC** (method 6) broad peak, RT 4.63 min.

### *3.1.3. General protocols for cell based assay.*

PAMAM dendrimer, 1,4-diaminobutane core, generation 2.0 was purchased from Sigma –Aldrich.

#### *Cell culture.*

B16F10 murine melanoma cells and HEK293T (human embryonic kidney) cells were grown in Dulbecco's Modified Eagles Medium (DMEM) supplemented with 10% foetal calf serum (FCS), 4 mM L-glutamine and 100 units/mL penicillin / streptavidin (complete Dulbecco's medium) in T75 cell culture flask until 80% confluence. Cells were suspended using trypsin / EDTA and counted on a hemacytometer (an etched glass chamber that holds a quartz coverslip in a total surface area of 9 mm<sup>2</sup>) after resuspension in trypan blue (10 µL cell suspension, 40 µL trypan blue, repeated 3 times). Cells were seeded in 96-well plates (2 x 10<sup>4</sup> cells/well) or 24-well plates (4 x 10<sup>4</sup> cells/well). Cell cultures were then incubated at 37°C in a 5% CO<sub>2</sub> atmosphere for the required periods.



#### *Flow cytometry analysis (FACS).*

Cells were washed twice with PBS, harvested with trypsin/EDTA, washed again with PBS and re-suspended in 2% FCS in PBS buffer. Cell fluorescence (determined by GFP synthesis) was analyzed by flow cytometry analysis using a FACSAria flow cytometer (Becton Dickinson). A total of 10,000 events per sample were analyzed. Cell samples were excited with a 488-nm (Coherent® Sapphire<sup>TM</sup> solid state) laser and a 530/30 nm (Fluorescein) band pass filters was used for fluorescence analysis.

#### *3.1.4. Preparation of dendrimer-DNA complexes.*

Dendrimer-DNA complexes were prepared at different molar ratios (5:1, 10:1, 20:1, 40:1). The molar ratio is equal to: (moles of transfection agent) / (number of plasmid equivalents). Plasmid equivalents are equal to: (mass of plasmid used) / 330, where 330 is the average mass of a single nucleotide, and is approximately equal to the number of moles of phosphate within the plasmid. Appropriate volumes of dendrimer solution (5 mM in PBS) were added to 2.5  $\mu$ L of DNA solution (4.7 Kb plasmid pEGFP-N1) containing 0.20  $\mu$ g of DNA ( $0.5 \times 10^{-9}$  equiv in TE buffer). PBS buffer was then added to correct the volume to 10  $\mu$ L. The solutions were incubated at room temperature for 30 minutes.

#### *3.1.5. Transfection protocol.*

HEK-293T (human embryonic kidney) cells were seeded in a 96 well plate and incubated overnight (37 °C, 5% CO<sub>2</sub>) until 50-70% confluence (see above). The growth medium was replaced with 100  $\mu$ L of fresh medium (10% FCS). DNA-Dendrimer complex solution, 10  $\mu$ L containing 0.2  $\mu$ g of plasmid, was then added to the cells. Transfection activities were measured by FACS analysis (see above) following 48 h of incubation.

	PAMAM G2	4.3 (G1)	4.4 (G2)	4.5 G3
Untreated Cells	176	-	-	-
5:1	382	156	182	2778
10:1	821	150	165	3605



20:1	904	161	382	1728
40:1	537	154	165	943

**Table 5.1** Fluorescence intensity of HEK cells transfected with plasmid pEGFP-N1 using PAMAM G2, **4.3** (G1), **4.4** (G2), **4.5** (G3) at different dendrimer/plasmid molar ratios.

### 3.1.6. Cytotoxicity: Cell viability assay (MTT assay).<sup>173</sup>

Cells were seeded in a 96-well plate and allowed to attach for 15 hours. The growth medium was replaced with 100  $\mu$ L of fresh Dulbecco's complete medium. To each well were added 10  $\mu$ L of dendrimer-plasmid complex solution (0.2  $\mu$ g of DNA). After 48 h of incubation cells were washed with PBS buffer pH 7.4 and the medium replaced with a phenol red-free medium (90  $\mu$ L). 10  $\mu$ L of MTT solution (1 mg/mL, in PBS buffer) were added and cells were incubated at 37°C for 3 hours. Formazan formed during this period was dissolved by adding 100  $\mu$ L of a 10% TRITON X-100 in acidic isopropanol (0.1 N HCl) solution and thoroughly mixed. The 96-well plate was read on a microplate reader at 570 nm and cellular viability was calculated according to the following equation:

$$\text{Cellular viability} = A_{570} \text{ sample} / A_{570} \text{ ref}$$

Where:

$A_{570} \text{ sample}$  = absorbance at 570 nm of the sample (treated cells),

$A_{570} \text{ ref}$  = absorbance at 570 nm of the reference sample (untreated cells).

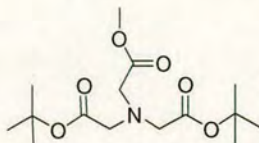
	PAMAM G2	<b>4.3</b> (G1)	<b>4.4</b> (G2)	<b>4.5</b> (G3)
Untreated Cells	100	-	-	-
Only DNA	98.7	-	-	-
5:1	97	102	100	96
10:1	93	97	99	95
20:1	82	101	92	95
40:1	83	97	90	98

**Table 5.2** Percentage of cell viability (HEK293) after 48 h of incubation with the DNA-dendrimer complexes different dendrimer/plasmid molar ratios.



### V.3.2. $\text{Ni}^{2+}$ complex mediated delivery of His<sub>6</sub>-GFP.

#### 3.2.1. Methyl 2-(bis((tert-butoxycarbonyl)methyl)amino)-acetate **4.9**.



Gly-OMe.HCl (1.25 g, 10 mmol), TEA (3.78 mL, 30 mmol), and bromotertbutylacetate (3 mL, 20 mmol) in DMF (50 mL) were stirred at room temperature for 3 days. The solution was filtrated and the filtrate was concentrated *in vacuo*. The resulting oil was then dissolved in DCM (100 mL) and washed with a saturated  $\text{NaHCO}_3$  solution (2 x 30 mL). The organic phase was dried over  $\text{MgSO}_4$  and then concentrated *in vacuo*. Column chromatography (silica, eluent: Hexane/AcOEt, 2:1) gave compound **4.9** (2.38 g, 7.5 mmol) as a colorless oil in 75% yield.

$R_f$  (Hexane/AcOEt, 2:1) = 0.45

IR (neat oil): 1741 (C=O, s), 1142 (C-O, s)  $\text{cm}^{-1}$ .

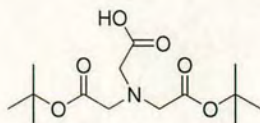
$m/z$  (ES+) 318  $[\text{M}+\text{H}]^+$  (55%), 340  $[\text{M}+\text{Na}]^+$  (100%).

$^1\text{H}$  NMR (250 MHz,  $\text{CDCl}_3$ )  $\delta$  3.63 (s, 3H,  $\text{OCH}_3$ ), 3.56 (s, 2H,  $\text{NCH}_2\text{CO}_2\text{Me}$ ), 3.45 (s, 4H, 2 x  $\text{NCH}_2\text{CO}_2^t\text{But}$ ), 1.37 (s, 18H, 2 x  $\text{C}(\text{CH}_3)_3$ ).

$^{13}\text{C}$  NMR (62.9 MHz,  $\text{CDCl}_3$ )  $\delta$  171.2 ( $\text{CH}_2\text{CO}_2\text{Me}$ ), 170.3 ( $\text{CH}_2\text{CO}_2^t\text{But}$ ), 81.4 ( $\text{C}(\text{CH}_3)_3$ ), 56.2 ( $\text{NCH}_2\text{CO}_2^t\text{But}$ ), 55.1 ( $\text{NCH}_2\text{CO}_2\text{Me}$ ), 51.9 ( $\text{OCH}_3$ ), 28.4  $\text{C}(\text{CH}_3)_3$ .

HRMS (FAB) for  $\text{C}_{15}\text{H}_{28}\text{NO}_6$   $[\text{M}+\text{H}]^+$  calcd 318.1916, found 318.1906.

3.2.2. 2-(bis((tert-butoxycarbonyl)methyl)amino)-acetic acid **4.10**.



Compound **4.9** (2.10 g, 6 mmol) was dissolved in THF (10 mL) and NaOH 1 N (12 mL) was added. The solution was stirred at room temperature until complete loss of starting material (1 h) (reaction was followed by TLC). The THF was removed *in vacuo*, and HCl 1 N was added until pH 3. The compound was extracted with DCM (3 x 20 mL), the organic phase was then washed with brine (1 x 20 mL) and dried over MgSO<sub>4</sub>. The solution was concentrated *in vacuo* to give compound **4.10** (1.55 g, 5.1 mmol) as a white solid in 85% yield.

**Mp:** 82-85 °C (DCM).

**IR** (solid): 3100-2600 (COO-H), 1731 (C=O, s) cm<sup>-1</sup>.

**m/z** (ES+) 304 (80%), 326 (100%)

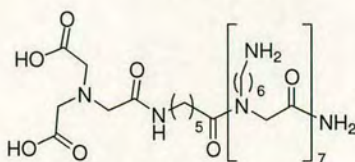
**<sup>1</sup>H NMR** (250 MHz, CD<sub>3</sub>OD) δ 3.55 (s, 2H, NCH<sub>2</sub>CO<sub>2</sub>H), 3.52 (s, 4H, NCH<sub>2</sub>CO<sub>2</sub><sup>t</sup>But), 1.47 (s, 18H, C(CH<sub>3</sub>)<sub>3</sub>).

**<sup>13</sup>C NMR** (62.9 MHz, CD<sub>3</sub>OD) δ 174.5 (CH<sub>2</sub>CO<sub>2</sub>H), 171.8 (CH<sub>2</sub>CO<sub>2</sub><sup>t</sup>But), 82.6 (C(CH<sub>3</sub>)<sub>3</sub>), 57.0 (NCH<sub>2</sub>CO<sub>2</sub><sup>t</sup>But), 56.5 (NCH<sub>2</sub>CO<sub>2</sub>H), 28.3 (C(CH<sub>3</sub>)<sub>3</sub>).

**HRMS** (FAB) for C<sub>14</sub>H<sub>26</sub>NO<sub>6</sub> [M+H]<sup>+</sup> calcd 304.1760, found 304.1766.



### 3.2.3. ( $\text{Ni}^{2+}$ )Ligand-heptapeptoid **4.11**.

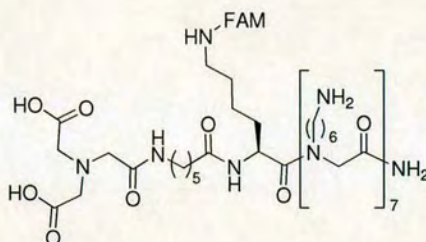


Compound **4.11** was prepared on a Rink<sup>151</sup> amide resin (polystyrene) (100 mg, 1 mmol/g, 0.1 mmol). The synthesis followed the peptide synthesis protocols described in section V.2.3 (2.3.2, 2.3.5, 2.3.9). TFA cleavage (solution 1), and ether precipitation gave **4.11** (133 mg, 62  $\mu\text{mol}$ ).

**HPLC** (method 5) crude purity 95% (ELSD), RT 3.45 min.

**m/z** (ES+) 699.4  $[\text{M}+2\text{H}]^{2+}$  (30%), 466.7  $[\text{M}+3\text{H}]^{3+}$  (70%), 350.3  $[\text{M}+4\text{H}]^{4+}$  (100%).

### 3.2.4. ( $\text{Ni}^{2+}$ )Ligand-Lys(FAM)-heptapeptoid **4.15**.

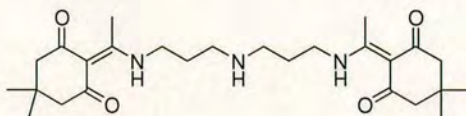


Compound **4.15** was prepared on Rink<sup>151</sup> amide resin (PEGA) (25 mg, 0.4 mmol/g, 10  $\mu\text{mol}$ ). Synthesis followed those described in section (V.2.3). Dde protected side chain of the lysine was deprotected using  $\text{NH}_2\text{OH}$  and 5(6) carboxyfluorescein was coupled to the  $\epsilon$  lysine amine (carried out as last step). TFA cleavage (solution 1) and ether precipitation gave **4.15** (15 mg, 5.9  $\mu\text{mol}$ ).

**HPLC** (method 5) purity 93% (ELSD), RT 4.38 min.

**m/z** (MALDI-TOF) for  $(\text{C}_{95}\text{H}_{155}\text{N}_{19}\text{O}_{20})$  calcd. 1883.36 (average mass), found 1884.37  $[\text{M}+\text{H}]^+$ .

3.2.5. *N*<sup>1</sup>,*N*<sup>9</sup>-bis-1-(4,4-dimethyl-2,6-dioxocyclohexylidene)ethyl-norspermidine  
**4.12.**<sup>224</sup>



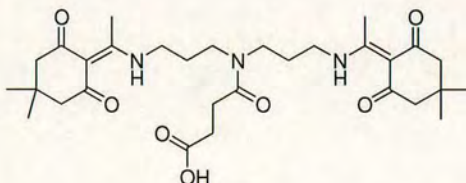
Norspermidine (2.5 g, 19 mmol) and 2-acetyldimedone (10.4 g, 57 mmol) in DCM (50 mL) were stirred overnight. The solvent was removed *in vacuo*. Column chromatography (DCM/MeOH, 9/1) gave compound **4.12** (6 g, 13 mmol) as a brown solid in 68% yield.

*R*<sub>f</sub> (CH<sub>2</sub>Cl<sub>2</sub>/MeOH, 9:1) = 0.30.

<sup>1</sup>H NMR (250 MHz, CDCl<sub>3</sub>) δ = 13.44 (br s, 2H, NH-Dde), 3.43 (m, 4H, 2 x CH<sub>2</sub>NHDde), 2.67 (t, *J* = 7.0 Hz, 4H, CH<sub>2</sub>NHCH<sub>2</sub>), 2.48 (s, 6H; 2 x C=CCH<sub>3</sub>), 2.27 (s, 8H, COCH<sub>2</sub>), 1.76 (tt, *J* = 7.1, 7.0 Hz, 4H, 2 x CH<sub>2</sub>CH<sub>2</sub>CH<sub>2</sub>), 0.94 (s, 12H, 2 x C(CH<sub>3</sub>)<sub>2</sub>).

*m/z* (ES+) 460.1 [M+H]<sup>+</sup> (100%).

3.2.6. *N*<sup>1</sup>,*N*<sup>9</sup>-bis-1,1-(4,4-dimethyl-2,6-dioxocyclohexylidene)ethyl-*N*<sup>5</sup>-(3-carboxypropanoyl)-norspermidine **4.13.**<sup>224</sup>



Succinic anhydride (0.5 g, 4.74 mmol) was added to a solution of **4.12** (2.0 g, 4.31 mmol) in DCM (5 mL) and the mixture was stirred for 1 h. The reaction mixture was poured into water (200 mL) and extracted with EtOAc (2 x 100 mL). The combined organic layers were dried over anhydrous Na<sub>2</sub>SO<sub>4</sub> and evaporated under reduced pressure to afford the title compound as a brown amorphous solid (2.22 g, 95%).

*R*<sub>f</sub> (CH<sub>2</sub>Cl<sub>2</sub>/MeOH, 9:1) = 0.45.

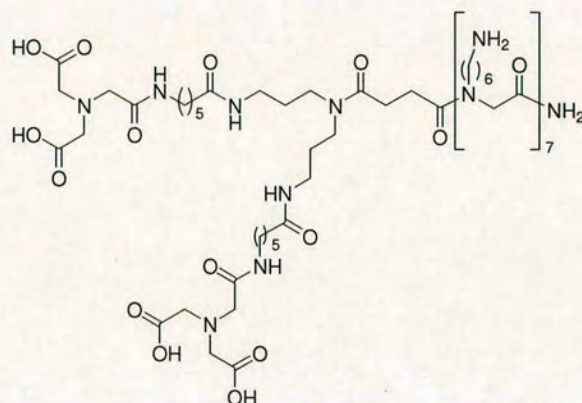
HPLC (method 5): 7.67 min.



**<sup>1</sup>H NMR** (250 MHz, CDCl<sub>3</sub>) δ = 13.51 and 13.34 (two br s, 2H, NH-Dde), 3.31-3.49 (m, 8H, 2 x NHCH<sub>2</sub>CH<sub>2</sub>CH<sub>2</sub>N), 2.60 (m, 2H, CH<sub>2</sub>CO<sub>2</sub>H), 2.52 (m, 2H, CH<sub>2</sub>CH<sub>2</sub>CO<sub>2</sub>H), 2.50 and 2.46 (two s, 6H, 2 x C=C-CH<sub>3</sub>-Dde), 2.29 and 2.28 (two s, 8H, CH<sub>2</sub>CO-Dde), 1.97 and 1.85 (two m, 4H, 2 x NCH<sub>2</sub>CH<sub>2</sub>CH<sub>2</sub>NH), 0.95 and 0.94 (two s, 12H, 2 x C(CH<sub>3</sub>)<sub>2</sub>).

**m/z** (ES+) 560.5 [M+H]<sup>+</sup> (100%), 582.5 [M+Na]<sup>+</sup> (90%).

### 3.2.7. [(Ni<sup>2+</sup>)Ligand]<sub>2</sub>-heptapeptoid **4.14**.

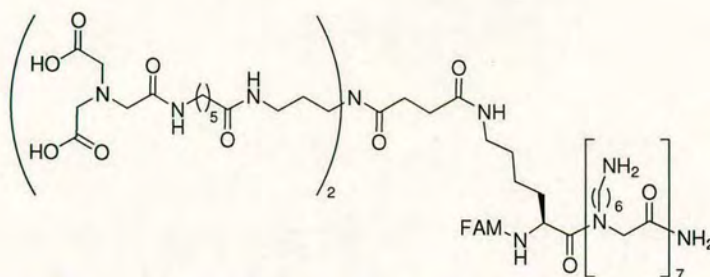


Compound **4.14** was prepared on Rink amide resin (PEGA) (100 mg, 0.4 mmol/g, 40 μmol). The synthesis followed the protocols described in section (V.2.3) (couplings under microwave conditions, Fmoc deprotection, Dde deprotection). TFA cleavage (solution 1), and ether precipitation gave **4.14** (61 mg, 23 μmol).

**HPLC** (method 5) purity 95% (ELSD), RT 3.81 min.

**m/z** (ES+) 949.3 [M+2H]<sup>2+</sup> (30%), 633.2 [M+3H]<sup>3+</sup> (90%), 475.2 [M+4H]<sup>4+</sup> (100%).

### 3.2.8. $[(Ni^{2+})Ligand]_2$ -Lys(FAM)-heptapeptoid **4.16**.



Compound **4.16** was prepared on Rink<sup>151</sup> amide resin (PEGA) 25 mg, 0.4 mmol/g, 10  $\mu$ mol). Synthesis followed the peptide synthesis protocols described in section V.2.3 (couplings under microwave conditions, Fmoc deprotection, Dde deprotection, TFA cleavage and ether precipitation). Fmoc-Lys(Dde)-Heptapeptoid resin was Fmoc deprotected and 5(6) carboxyfluorescein was coupled to the  $\alpha$  lysine amine. FAM-Lys(Dde)-Heptapeptoid resin was treated with a solution of trityl chloride (0.1 M) and DIPEA (0.1 M) in DMF for 16 h (protection of the phenolic groups of carboxyfluorescein).<sup>185</sup> FAM(Tr)-Lys(Dde)-Heptapeptoid resin was Dde deprotected and the remaining building blocks (**4.13**, Fmoc-Ahx-OH and **4.11**) were coupled to the  $\epsilon$  lysine amine. TFA cleavage (solution 1), and ether precipitation gave **4.16** (13 mg, 5  $\mu$ mol).

**HPLC**(method 5) purity 95% (ELSD), RT 4.62 min.

**m/z** (MALDI-TOF) for  $C_{117}H_{192}N_{24}O_{28}$  calcd. 2382.92, found 2383.91  $[M+H]^+$ .



### 3.2.9. Cellular uptake of Ni ligand functionalised peptoids.

Compounds **4.15** and **4.16** were dissolved in PBS buffer at a 100  $\mu\text{M}$  concentration. Peptoid solution (17.5  $\mu\text{L}$ ) was added to B16F10 cells in a 24 well plate (350  $\mu\text{L}$  DEMEM complete medium with 10% FCS) to give a final concentration of 5  $\mu\text{M}$ . Cellular uptake of fluorescently labelled heptapeptoid **4.15** and **4.16** was measured by FACS analysis (see V.3.1.3) following 4 h incubation.

	Mean fluorescence	% of cell with fluorescence Intensity > 1000
Untreated cells	429	6
4.15 5 $\mu\text{M}$	22,201	83
4.16 5 $\mu\text{M}$	13,011	79

**Table 5.3** Uptake of **4.15** and **4.16** with B16F10 cells after 4h incubation

### 3.2.10. $\text{Ni}^{2+}$ mediated delivery of His<sub>6</sub>-GFP.

Heptapeptoids **4.11** and **4.14** were dissolved in PBS buffer (pH 7.4) at a concentration of 1mM. To this solution was added 1 equivalent of  $\text{NiCl}_2$  (1mM solution in PBS), and the solution (0.5 mM) gently stirred for 1 h. To this solution was then added 1 equivalent of His<sub>6</sub>-GFP (0.5 mM in PBS). The solution (0.25 mM) was incubated for 1 h with occasional gentle mixing. After the incubation the solution was diluted to 100  $\mu\text{M}$  with PBS. The 100  $\mu\text{M}$  solution (3.5, 7, 17.5, 35  $\mu\text{L}$ ) containing the GFP-(His<sub>6</sub>)- $\text{Ni}^{2+}$ -heptapeptoid (**4.11** and **4.14**) complex was added to B16F10 cells in a 24 well plate (350  $\mu\text{L}$  of DEMEM complete medium, with FCS (10%) and without FCS). GFP cellular uptake was measured by FACS analysis (see V.3.1.3) following 24 h of incubation.

	Mean fluorescence	% of cell with fluorescence Intensity > 400
Untreated cells	82	2.2
GFP 10 $\mu$ M	105	3.6
<b>4.11</b> 10 $\mu$ M	95	2.9
<b>4.14</b> 10 $\mu$ M	159	8.6

**Table 5.4** Fluorescence of B16F10 cells incubated with His<sub>6</sub>-GFP and GFP-His<sub>6</sub>-Ni<sup>2+</sup>-(**4.11** or **4.14**) for 24 h with 10% FCS.

### 3.2.11. Confocal microscopy analysis.

For the confocal assay  $4 \times 10^5$  cells were seeded onto a glass coverslip within a 6-well plate (1.6 mL) and incubated over night. The day after the medium was replaced and 160  $\mu$ L of the GFP-(His<sub>6</sub>)-Ni<sup>2+</sup>-(**4.14**) solution (100  $\mu$ M) were added to the cell which were incubated for 24 h. Before analysis cells were washed twice with warm PBS. Confocal experiments were carried out on living cells using a Delta Vision RT Microscope with excitation at 488 nm.



## References.

- (1) Forster, S.; Lloyd, J. B. *Biochim. Biophys. Acta* **1988**, *947*, 465-91.
- (2) de Duve, C.; de Barsy, T.; Poole, B.; Trouet, A.; Tulkens, P.; Van Hoof, F. *Biochem. Pharmacol.* **1974**, *23*, 2495-531.
- (3) Celis, J. E. *Biochem. J.* **1984**, *223*, 281-91.
- (4) Hapala, I. *Crit. Rev. Biotechnol.* **1997**, *17*, 105-22.
- (5) McNeil, P. L. *Methods Cell. Biol.* **1989**, *29*, 153-73.
- (6) Clark, H. A.; Hoyer, M.; Philbert, M. A.; Kopelman, R. *Anal. Chem.* **1999**, *71*, 4831-6.
- (7) Heiser, W. C. *Anal. Biochem.* **1994**, *217*, 185-96.
- (8) Williams, R. S.; Johnston, S. A.; Riedy, M.; DeVit, M. J.; McElligott, S. G.; Sanford, J. C. *Proc. Natl. Acad. Sci. U. S. A.* **1991**, *88*, 2726-30.
- (9) Gregoriadis, G. *Trends Biotechnol.* **1995**, *13*, 527-37.
- (10) Gregoriadis, G. *N. Engl. J. Med.* **1976**, *295*, 704-10.
- (11) Poste, G.; Papahadjopoulos, D. *Nature* **1976**, *261*, 699-701.
- (12) Torchilin, V. P.; Zhou, F.; Huang, L. *J. Liposome Res.* **1993**, *3*, 201-55.
- (13) Simoes, S.; Moreira, J. N.; Fonseca, C.; Duzgunes, N.; Pedroso de Lima, M. C. *Adv. Drug Delivery Rev.* **2004**, *56*, 947-965.
- (14) Sakurai, F.; Nishioka, T.; Yamashita, F.; Takakura, Y.; Hashida, M. *Eur. J. Pharm. Biopharm.* **2001**, *52*, 165-72.
- (15) Yessine, M.-A.; Leroux, J.-C. *Adv. Drug Delivery Rev.* **2004**, *56*, 999-1021.
- (16) Chang, J. S.; Choi, M. J.; Cheong, H. S.; Kim, K. *Vaccine* **2001**, *19*, 3608-3614.
- (17) Meyer, O.; Kirpotin, D.; Hong, K.; Sternberg, B.; Park, J. W.; Woodle, M. C.; Papahadjopoulos, D. *J. Biol. Chem.* **1998**, *273*, 15621-7.
- (18) Zelphati, O.; Szoka, F. C., Jr. *J. Controlled Release* **1996**, *41*, 99-119.
- (19) Aulenta, F.; Hayes, W.; Rannard, S. *Eur. Polym. J.* **2003**, *39*, 1741-1771.
- (20) Capitosti, G. J.; Guerrero, C. D.; Binkley, D. E., Jr.; Rajesh, C. S.; Modarelli, D. A. *J. Org. Chem.* **2003**, *68*, 247-261.
- (21) Milhem, O. M.; Myles, C.; McKeown, N. B.; Attwood, D.; D'Emanuele, A. *Int. J. Pharm.* **2000**, *197*, 239-241.
- (22) How, S. E.; Yingyongnarongkul, B.; Fara, M. A.; Diaz-Mochon, J. J.; Mittoo, S.; Bradley, M. *Comb. Chem. High. Throughput Screen* **2004**, *7*, 423-30.
- (23) Shah, D. S.; Sakthivel, T.; Toth, I.; Florence, A. T.; Wilderspin, A. F. *Int. J. Pharm.* **2000**, *208*, 41-8.
- (24) Lebedeva, I.; Benimetskaya, L.; Stein, C. A.; Vilenchik, M. *Eur. J. Pharm. Biopharm.* **2000**, *50*, 101-119.
- (25) Kono, K.; Liu, M.; Frechet, J. M. *Bioconjug. Chem.* **1999**, *10*, 1115-21.
- (26) Boussif, O.; Lezoualc'h, F.; Zanta, M. A.; Mergny, M. D.; Scherman, D.; Demeneix, B.; Behr, J.-P. *Proc. Natl. Acad. Sci. U. S. A.* **1995**, *92*, 7297-301.
- (27) Behr, J. P. *Chimia* **1997**, *51*, 34-36.
- (28) Haensler, J.; Szoka, F. C., Jr. *Bioconjug. Chem.* **1993**, *4*, 372-9.



- (29) Sonawane, N. D.; Szoka, F. C., Jr.; Verkman, A. S. *J. Biol. Chem.* **2003**, *278*, 44826-44831.
- (30) De Rosa, G.; Quaglia, F.; La Rotonda, M. I.; Besnard, M.; Fattal, E. *Int. J. Pharm.* **2002**, *242*, 225-228.
- (31) Sinha, V. R.; Trehan, A. *J. Control. Release* **2003**, *90*, 261-280.
- (32) Cheung, R. Y.; Ying, Y.; Rauth, A. M.; Marcon, N.; Wu, X. Y. *Biomaterials* **2005**, *26*, 5375-5385.
- (33) Li, C. *Adv. Drug Deliv. Rev.* **2002**, *54*, 695-713.
- (34) Athanasiou, K. A.; Niederauer, G. G.; Agrawal, C. M. *Biomaterials* **1996**, *17*, 93-102.
- (35) Waeckerle-Men, Y.; Groettrup, M. *Adv. Drug Deliv. Rev.* **2005**, *57*, 475-482.
- (36) Rojas, M.; Donahue, J. P.; Tan, Z.; Lin, Y.-Z. *Nat. Biotechnol.* **1998**, *16*, 370-375.
- (37) Schwarze, S. R.; Ho, A.; Vocero-Akbani, A.; Dowdy, S. F. *Science* **1999**, *285*, 1569-1572.
- (38) Hawiger, J. *Curr. Opin. Immunol.* **1997**, *9*, 189-194.
- (39) Muratovska, A.; Eccles, M. R. *FEBS Lett.* **2004**, *558*, 63-68.
- (40) Simeoni, F.; Morris, M. C.; Heitz, F.; Divita, G. *Nucleic Acids Res.* **2003**, *31*, 2717-2724.
- (41) Lewin, M.; Carlesso, N.; Tung, C.-H.; Tang, X.-W.; Cory, D.; Scadden, D. T.; Weissleder, R. *Nat. Biotechnol.* **2000**, *18*, 410-414.
- (42) Derossi, D.; Joliot, A. H.; Chassaing, G.; Prochiantz, A. *J. Biol. Chem.* **1994**, *269*, 10444-50.
- (43) Vives, E.; Brodin, P.; Lebleu, B. *J. Biol. Chem.* **1997**, *272*, 16010-16017.
- (44) Cashman, S. M.; Sadowski, S. L.; Morris, D. J.; Frederick, J.; Kumar-Singh, R. *Mol. Ther.* **2002**, *6*, 813-823.
- (45) Oehlke, J.; Scheller, A.; Wiesner, B.; Krause, E.; Beyermann, M.; Klauschenz, E.; Melzig, M.; Bienert, M. *Biochim. Biophys. Acta, Biomembr.* **1998**, *1414*, 127-139.
- (46) Pooga, M.; Hallbrink, M.; Zorko, M.; Langel, U. *FASEB J.* **1998**, *12*, 67-77.
- (47) Mitchell, D. J.; Kim, D. T.; Steinman, L.; Fathman, C. G.; Rothbard, J. B. *J. Pept. Res.* **2000**, *56*, 318-325.
- (48) Futaki, S.; Suzuki, T.; Ohashi, W.; Yagami, T.; Tanaka, S.; Ueda, K.; Sugiura, Y. *J. Biol. Chem.* **2001**, *276*, 5836-40.
- (49) Morris, M. C.; Vidal, P.; Chaloin, L.; Heitz, F.; Divita, G. *Nucleic Acids Res.* **1997**, *25*, 2730-2736.
- (50) Drin, G.; Cottin, S.; Blanc, E.; Rees, A. R.; Temsamani, J. *J. Biol. Chem.* **2003**, *278*, 31192-31201.
- (51) Rousselle, C.; Clair, P.; Lefauconnier, J.-M.; Kaczorek, M.; Scherrmann, J.-M.; Temsamani, J. *Mol. Pharmacol.* **2000**, *57*, 679-686.
- (52) Morris, M. C.; Depollier, J.; Mery, J.; Heitz, F.; Divita, G. *Nat. Biotechnol.* **2001**, *19*, 1173-1176.
- (53) Lindgren, M.; Hallbrink, M.; Prochiantz, A.; Langel, U. *Trends Pharmacol. Sci.* **2000**, *21*, 99-103.
- (54) Green, M.; Loewenstein, P. M. *Cell* **1988**, *55*, 1179-88.



- (55) Thoren, P. E. G.; Persson, D.; Isakson, P.; Goksor, M.; Onfelt, A.; Norden, B. *Biochem. Biophys. Res. Commun.* **2003**, 307, 100-107.
- (56) Derossi, D.; Calvet, S.; Trembleau, A.; Brunissen, A.; Chassaing, G.; Prochiantz, A. *J. Biol. Chem.* **1996**, 271, 18188-18193.
- (57) Pouny, Y.; Rapaport, D.; Mor, A.; Nicolas, P.; Shai, Y. *Biochemistry* **1992**, 31, 12416-23.
- (58) Suzuki, T.; Futaki, S.; Niwa, M.; Tanaka, S.; Ueda, K.; Sugiura, Y. *J. Biol. Chem.* **2002**, 277, 2437-2443.
- (59) Rothbard, J. B.; Jessop, T. C.; Lewis, R. S.; Murray, B. A.; Wender, P. A. *J. Am. Chem. Soc.* **2004**, 126, 9506-9507.
- (60) Vives, E.; Richard, J. P.; Rispal, C.; Lebleu, B. *Curr. Protein Pept. Sci.* **2003**, 4, 125-132.
- (61) Console, S.; Marty, C.; Garcia-Echeverria, C.; Schwendener, R.; Ballmer-Hofer, K. *J. Biol. Chem.* **2003**, 278, 35109-35114.
- (62) Richard, J. P.; Melikov, K.; Vives, E.; Ramos, C.; Verbeure, B.; Gait, M. J.; Chernomordik, L. V.; Lebleu, B. *J. Biol. Chem.* **2003**, 278, 585-590.
- (63) Fittipaldi, A.; Ferrari, A.; Zoppe, M.; Arcangeli, C.; Pellegrini, V.; Beltram, F.; Giacca, M. *J. Biol. Chem.* **2003**, 278, 34141-34149.
- (64) Fischer, R.; Waizenegger, T.; Kohler, K.; Brock, R. *Biochim. Biophys. Acta, Biomembr.* **2002**, 1564, 365-374.
- (65) Deshayes, S.; Heitz, A.; Morris, M. C.; Charnet, P.; Divita, G.; Heitz, F. *Biochemistry* **2004**, 43, 1449-1457.
- (66) Silhol, M.; Tyagi, M.; Giacca, M.; Lebleu, B.; Vives, E. *Eur. J. Biochem.* **2002**, 269, 494-501.
- (67) Tuinnemann, G.; Martin, R. M.; Haupt, S.; Patsch, C.; Edenhofer, F.; Cardoso, M. C. *FASEB J.* **2006**, 20, 1775-1784.
- (68) Maiolo, J. R.; Ferrer, M.; Ottinger, E. A. *Biochim. Biophys. Acta, Biomembr.* **2005**, 1712, 161-172.
- (69) Fretz Marjan, M.; Penning Neal, A.; Al-Taei, S.; Futaki, S.; Takeuchi, T.; Nakase, I.; Storm, G.; Jones Arwyn, T. *Biochem. J.* **2007**, 403, 335-42.
- (70) Jiang, T.; Olson, E. S.; Nguyen, Q. T.; Roy, M.; Jennings, P. A.; Tsien, R. Y. *Proc. Natl. Acad. Sci. U. S. A.* **2004**, 101, 17867-17872.
- (71) Christian, S.; Pilch, J.; Akerman, M. E.; Porkka, K.; Laakkonen, P.; Ruoslahti, E. *J. Cell Biol.* **2003**, 163, 871-878.
- (72) Bullok, K. E.; Dyszlewski, M.; Prior, J. L.; Pica, C. M.; Sharma, V.; Piwnica-Worms, D. *Bioconjug. Chem.* **2002**, 13, 1226-1237.
- (73) Kameyama, S.; Horie, M.; Kikuchi, T.; Omura, T.; Takeuchi, T.; Nakase, I.; Sugiura, Y.; Futaki, S. *Bioconjug. Chem.* **2006**, 17, 597-602.
- (74) Wright, L. R.; Rothbard, J. B.; Wender, P. A. *Curr. Protein Pept. Sci.* **2003**, 4, 105-124.
- (75) Rothbard, J. B.; Garlington, S.; Lin, Q.; Kirschberg, T.; Kreider, E.; McGrane, L. P.; Wender, P. A.; Khavari, P. A. *Nat. Med.* **2000**, 6, 1253-1257.
- (76) Chen, L.; Wright, L. R.; Chen, C. H.; Oliver, S. F.; Wender, P. A.; Mochly-Rosen, D. *Chem. Biol.* **2001**, 8, 1123-9.
- (77) Brugidou, J.; Legrand, C.; Mery, J.; Rabie, A. *Biochem. Biophys. Res. Commun.* **1995**, 214, 685-93.
- (78) Rueping, M.; Mahajan, Y.; Sauer, M.; Seebach, D. *ChemBioChem* **2002**, 3, 257-259.



- (79) Wender, P. A.; Mitchell, D. J.; Pattabiraman, K.; Pelkey, E. T.; Steinman, L.; Rothbard, J. B. *Proc. Natl. Acad. Sci. U. S. A.* **2000**, *97*, 13003-13008.
- (80) Wender, P. A.; Rothbard, J. B.; Jessop, T. C.; Kreider, E. L.; Wylie, B. L. *J. Am. Chem. Soc.* **2002**, *124*, 13382-13383.
- (81) Kwon, Y.-U.; Kodadek, T. *J. Am. Chem. Soc.* **2007**, *129*, 1508-1509.
- (82) Wadia, J. S.; Stan, R. V.; Dowdy, S. F. *Nat. Med.* **2004**, *10*, 310-315.
- (83) Han, X.; Bushweller, J. H.; Cafiso, D. S.; Tamm, L. K. *Nat. Struct. Biol.* **2001**, *8*, 715-720.
- (84) Cao, G.; Pei, W.; Ge, H.; Liang, Q.; Luo, Y.; Sharp, F. R.; Lu, A.; Ran, R.; Graham, S. H.; Chen, J. *J. Neurosci.* **2002**, *22*, 5423-5431.
- (85) Zender, L.; Kuhnle, F.; Kock, R.; Manns, M.; Kubicka, S. *Cancer Gene Ther.* **2002**, *9*, 489-496.
- (86) Gait, M. J. *Cell. Mol. Life Sci.* **2003**, *60*, 844-853.
- (87) Pooga, M.; Soomets, U.; Hallbrink, M.; Valkna, A.; Saar, K.; Rezaei, K.; Kahl, U.; Hao, J.-X.; Xu, X.-J.; Wisenfeld-Hallin, Z.; Hokfelt, T.; Bartfai, T.; Langel, U. *Nat. Biotechnol.* **1998**, *16*, 857-861.
- (88) El-Andaloussi, S.; Johansson, H.; Magnusdottir, A.; Jaerver, P.; Lundberg, P.; Langel, U. *J. Control. Release* **2005**, *110*, 189-201.
- (89) Simeoni, F.; Morris, M. C.; Heitz, F.; Divita, G. *Methods Mol. Biol.* **2005**, *309*, 251-260.
- (90) Rittner, K.; Benavente, A.; Bompard-Sorlet, A.; Heitz, F.; Divita, G.; Brasseur, R.; Jacobs, E. *Mol. Ther.* **2002**, *5*, 104-114.
- (91) Borghouts, C.; Kunz, C.; Groner, B. *Comb. Chem. High Throughput Screening* **2008**, *11*, 135-145.
- (92) Drude, I.; Dombos, V.; Vauleon, S.; Mueller, S. *Mini-Rev. Med. Chem.* **2007**, *7*, 912-931.
- (93) Geysen, H. M.; Meloen, R. H.; Barteling, S. J. *Proc. Natl. Acad. Sci. U. S. A.* **1984**, *81*, 3998-4002.
- (94) Ellington, A. D.; Szostak, J. W. *Nature* **1990**, *346*, 818-22.
- (95) Joyce, G. F. *Gene* **1989**, *82*, 83-7.
- (96) Lam, K. S.; Salmon, S. E.; Hersh, E. M.; Hruby, V. J.; Kazmierski, W. M.; Knapp, R. J. *Nature* **1991**, *354*, 82-4.
- (97) Devlin, J. J.; Panganiban, L. C.; Devlin, P. E. *Science* **1990**, *249*, 404-6.
- (98) Giannis, A.; Kolter, T. *Angew. Chem., Int. Ed.* **1993**, *105*, 1303-26.
- (99) Gante, J. *Angew. Chem., Int. Ed.* **1994**, *106*, 1780-802.
- (100) Gellman, S. H. *Acc. Chem. Res.* **1998**, *31*, 173-180.
- (101) Iverson, B. L. *Nature* **1997**, *385*, 113, 115.
- (102) Seebach, D.; Matthews, J. L. *Chem. Commun.* **1997**, 2015-2022.
- (103) DeGrado, W. F.; Schneider, J. P.; Hamuro, Y. *J. Pept. Res.* **1999**, *54*, 206-217.
- (104) Cheng, R. P.; Gellman, S. H.; DeGrado, W. F. *Chem. Rev.* **2001**, *101*, 3219-3232.
- (105) Seebach, D.; Abele, S.; Gademann, K.; Guichard, G.; Hintermann, T.; Jaun, B.; Matthews, J. L.; Schreiber, J. V.; Oberer, L.; Hommel, U.; Widmer, H. *Helv. Chim. Acta* **1998**, *81*, 932-982.
- (106) Juaristi, E.; Quintana, D.; Escalante, J. *Aldrichim. Acta* **1994**, *27*, 3-11.



- (107) Podlech, J.; Seebach, D. *Angew. Chem., Int. Ed. Engl.* **1995**, *34*, 471-2.
- (108) Lopez-Carrasquero, F.; Aleman, C.; Munoz-Guerra, S. *Biopolymers* **1995**, *36*, 263-71.
- (109) Fernandez-Santin, J. M.; Aymami, J.; Rodriguez-Galan, A.; Munoz-Guerra, S.; Subirana, J. A. *Nature* **1984**, *311*, 53-4.
- (110) Bestian, H. *Angew. Chem., Int. Ed. Engl.* **1968**, *7*, 278-85.
- (111) Chen, F.; Lepore, G.; Goodman, M. *Macromolecules* **1974**, *7*, 779-83.
- (112) Yuki, H.; Okamoto, Y.; Taketani, Y.; Tsubota, T.; Marubayashi, Y. *J. Polym. Sci., Polym. Chem.* **1978**, *16*, 2237-51.
- (113) Clark, T. D.; Buehler, L. K.; Ghadiri, M. R. *J. Am. Chem. Soc.* **1998**, *120*, 651-656.
- (114) Pavone, V.; Lombardi, A.; Saviano, M.; Di Blasio, B.; Natri, F.; Fattorusso, R.; Maglio, O.; Isernia, C. *Biopolymers* **1994**, *34*, 1505-15.
- (115) Schumann, F.; Mueller, A.; Koks, M.; Mueller, G.; Sewald, N. *J. Am. Chem. Soc.* **2000**, *122*, 12009-12010.
- (116) Obreza, A.; Gobec, S. *Curr. Med. Chem.* **2004**, *11*, 3263-3278.
- (117) Paik, S.; White, E. H. *Tetrahedron* **1996**, *52*, 5303-18.
- (118) Humljan, J.; Kotnik, M.; Boniface, A.; Solmajer, T.; Urleb, U.; Blanot, D.; Gobec, S. *Tetrahedron* **2006**, *62*, 10980-10988.
- (119) Moree, W. J.; Van der Marel, G. A.; Liskamp, R. M. J. *Tetrahedron Lett.* **1992**, *33*, 6389-92.
- (120) de Bont, D. B. A.; Moree, W. J.; Liskamp, R. M. J. *Bioorg. Med. Chem.* **1996**, *4*, 667-672.
- (121) Gude, M.; Piarulli, U.; Potenza, D.; Salom, B.; Gennari, C. *Tetrahedron Lett.* **1996**, *37*, 8589-8592.
- (122) de Bont, D. B. A.; Dijkstra, G. D. H.; den Hartog, J. A. J.; Liskamp, R. M. J. *Bioorg. Med. Chem. Lett.* **1996**, *6*, 3035-3040.
- (123) Lam, P. Y. S.; Jadhav, P. K.; Eyermann, C. J.; Hodge, C. N.; Ru, Y.; Bacheler, L. T.; Meek, O. M. J.; Rayner, M. M. *Science* **1994**, *263*, 380-4.
- (124) Du, X.; Hansell, E.; Engel, J. C.; Caffrey, C. R.; Cohen, F. E.; McKerrow, J. H. *Chem. Biol.* **2000**, *7*, 733-742.
- (125) Kozikowski, A. P.; Zhang, J.; Nan, F.; Petukhov, P. A.; Grajkowska, E.; Wroblewski, J. T.; Yamamoto, T.; Bzdega, T.; Wroblewska, B.; Neale, J. H. *J. Med. Chem.* **2004**, *47*, 1729-1738.
- (126) Corbin, P. S.; Zimmerman, S. C.; Thiessen, P. A.; Hawryluk, N. A.; Murray, T. J. *J. Am. Chem. Soc.* **2001**, *123*, 10475-10488.
- (127) Moriuchi, T.; Tamura, T.; Hirao, T. *J. Am. Chem. Soc.* **2002**, *124*, 9356-9357.
- (128) Semetey, V.; Didierjean, C.; Briand, J.-P.; Aubry, A.; Guichard, G. *Angew. Chem., Int. Ed.* **2002**, *41*, 1895-1898.
- (129) Schaffner, A.-P.; Lena, G.; Roussel, S.; Wawrezinieck, A.; Aubry, A.; Briand, J.-P.; Didierjean, C.; Guichard, G. *Chem. Commun.* **2006**, 4069-4071.
- (130) Burgess, K.; Linthicum, D. S.; Shin, H. *Angew. Chem., Int. Ed.* **1995**, *34*, 907-9.
- (131) Burgess, K.; Ibarzo, J.; Linthicum, D. S.; Shin, H.; Shitangkoon, A.; Totani, R.; Zhang, A. J. *J. Am. Chem. Soc.* **1997**, *119*, 1556-1564.



- (132) Kim, J.-M.; Bi, Y.; Paikoff, S. J.; Schultz, P. G. *Tetrahedron Lett.* **1996**, 37, 5305-5308.
- (133) Boeijen, A.; Liskamp, R. M. J. *Eur. J. Org. Chem.* **1999**, 2127-2135.
- (134) Boeijen, A.; van Ameijde, J.; Liskamp, R. M. J. *J. Org. Chem.* **2001**, 66, 8454-8462.
- (135) Simon, R. J.; Kania, R. S.; Zuckermann, R. N.; Huebner, V. D.; Jewell, D. A.; Banville, S.; Ng, S.; Wang, L.; Rosenberg, S.; Marlowe, C. K. *Proc. Natl. Acad. Sci. U. S. A.* **1992**, 89, 9367-71.
- (136) Kruijtzter, J. A. W.; Nijenhuis, W. A. J.; Wanders, N.; Gispen, W. H.; Liskamp, R. M. J.; Adan, R. A. H. *J. Med. Chem.* **2005**, 48, 4224-4230.
- (137) Miller, S. M.; Simon, R. J.; Ng, S.; Zuckermann, R. N.; Kerr, J. M.; Moos, W. H. *Bioorg. Med. Chem. Lett.* **1994**, 4, 2657-62.
- (138) Patch, J. A.; Barron, A. E. *J. Am. Chem. Soc.* **2003**, 125, 12092-12093.
- (139) Ruijtenbeek, R.; Kruijtzter, J. A. W.; Van de Wiel, W.; Fischer, M. J. E.; Fluck, M.; Redegeld, F. A. M.; Liskamp, R. M. J.; Nijkamp, F. P. *ChemBioChem* **2001**, 2, 171-179.
- (140) Burkoth, T. S.; Beausoleil, E.; Kaur, S.; Tang, D.; Cohen, F. E.; Zuckermann, R. N. *Chem. Biol.* **2002**, 9, 647-654.
- (141) Kruijtzter, J. A. W.; Hofmeyer, L. J. F.; Heerma, W.; Versluis, C.; Liskamp, R. M. J. *Chem. Eur. J.* **1998**, 4, 1570-1580.
- (142) Zuckermann, R. N.; Kerr, J. M.; Kent, S. B. H.; Moos, W. H. *J. Am. Chem. Soc.* **1992**, 114, 10646-7.
- (143) Kruijtzter, J. A. W.; Liskamp, R. M. J. *Tetrahedron Lett.* **1995**, 36, 6969-72.
- (144) Van der Auwera, C.; Anteunis, M. J. O. *Int. J. Pept. Protein Res.* **1987**, 29, 574-88.
- (145) Frerot, E.; Coste, J.; Pantaloni, A.; Dufour, M. N.; Jouin, P. *Tetrahedron* **1991**, 47, 259-70.
- (146) Coste, J.; Dufour, M. N.; Pantaloni, A.; Castro, B. *Tetrahedron Lett.* **1990**, 31, 669-72.
- (147) Olivos Hernando, J.; Alluri Prasanna, G.; Reddy, M. M.; Salony, D.; Kodadek, T. *Org. Lett.* **2002**, 4, 4057-9.
- (148) Gorske, B. C.; Jewell, S. A.; Guerard, E. J.; Blackwell, H. E. *Org. Lett.* **2005**, 7, 1521-1524.
- (149) Peretto, I.; Sanchez-Martin, R. M.; Wang, X.-h.; Ellard, J.; Mittoo, S.; Bradley, M. *Chem. Commun.* **2003**, 2312-2313.
- (150) Unciti-Broceta, A.; Diezmann, F.; Ou-Yang, C. Y.; Fara, M. A.; Bradley, M. *Bioorg. Med. Chem.* **2008**, in press.
- (151) Rink, H. *Tetrahedron Lett.* **1987**, 28, 3787-90.
- (152) Giguere, R. J.; Bray, T. L.; Duncan, S. M.; Majetich, G. *Tetrahedron Lett.* **1986**, 27, 4945-8.
- (153) Gedye, R.; Smith, F.; Westaway, K.; Ali, H.; Baldisera, L.; Laberge, L.; Rousell, J. *Tetrahedron Lett.* **1986**, 27, 279-82.
- (154) Yu, H. M.; Chen, S. T.; Wang, K. T. *J. Org. Chem.* **1992**, 57, 4781-4.
- (155) Santagada, V.; Fiorino, F.; Perissutti, E.; Severino, B.; De Filippis, V.; Vivenzio, B.; Caliendo, G. *Tetrahedron Lett.* **2001**, 42, 5171-5173.
- (156) Erdelyi, M.; Gogoll, A. *Synthesis* **2002**, 1592-1596.



- (157) Matsushita, T.; Hinou, H.; Kurogochi, M.; Shimizu, H.; Nishimura, S. *Org. Lett.* **2005**, 7, 877-880.
- (158) Matsushita, T.; Hinou, H.; Fumoto, M.; Kurogochi, M.; Fujitani, N.; Shimizu, H.; Nishimura, S.-I. *J. Org. Chem.* **2006**, 71, 3051-3063.
- (159) Hanisch, F.-G.; Muller, S. *Glycobiology* **2000**, 10, 439-449.
- (160) Murray, J. K.; Gellman, S. H. *Org. Lett.* **2005**, 7, 1517-1520.
- (161) Hendrix, J. C.; Halverson, K. J.; Jarrett, J. T.; Lansbury, P. T., Jr. *J. Org. Chem.* **1990**, 55, 4517-18.
- (162) Murray, J. K.; Gellman, S. H. *J. Comb. Chem.* **2006**, 8, 58-65.
- (163) Joshi, B. P.; Park, J.-w.; Kim, J.-m.; Lohani, C. R.; Cho, H.; Lee, K.-H. *Tetrahedron Lett.* **2007**, 49, 98-101.
- (164) Nicolas, E.; Pedroso, E.; Giralt, E. *Tetrahedron Lett.* **1989**, 30, 497-500.
- (165) Martinez, J.; Bodanszky, M. *Int. J. Pept. Protein Res.* **1978**, 12, 277-83.
- (166) Han, Y.; Albericio, F.; Barany, G. *J. Org. Chem.* **1997**, 62, 4307-4312.
- (167) Angell, Y. M.; Alsina, J.; Albericio, F.; Barany, G. *J. Pept. Res.* **2002**, 60, 292-9.
- (168) Kaiser, T.; Nicholson, G. J.; Kohlbau, H. J.; Voelter, W. *Tetrahedron Lett.* **1996**, 37, 1187-90.
- (169) Palasek, S. A.; Cox, Z. J.; Collins, J. M. *J. Pept. Sci.* **2007**, 13, 143-148.
- (170) Bacsá, B.; Desai, B.; Dibo, G.; Kappe, C. O. *J. Pept. Sci.* **2006**, 12, 633-638.
- (171) Vojkovsky, T. *Pept. Res.* **1995**, 8, 236-7.
- (172) Fara, M. A.; Diaz-Mochon, J. J.; Bradley, M. *Tetrahedron Lett.* **2006**, 47, 1011-1014.
- (173) Mosmann, T. *J. Immunol. Methods* **1983**, 65, 55-63.
- (174) Phillips, H. J.; Terryberry, J. E. *Exp. Cell. Res.* **1957**, 13, 341-7.
- (175) Abdel-Malek, Z. A. *Cell. Mol. Life Sci.* **2001**, 58, 434-41.
- (176) Mountjoy, K. G.; Robbins, L. S.; Mortrud, M. T.; Cone, R. D. *Science* **1992**, 257, 1248-51.
- (177) Robinson, S. J.; Healy, E. *Oncogene* **2002**, 21, 8037-8046.
- (178) Valverde, P.; Healy, E.; Jackson, I.; Rees, J. L.; Thody, A. J. *Nat. Genet.* **1995**, 11, 328-30.
- (179) Flanagan, N.; Healy, E.; Ray, A.; Philips, S.; Todd, C.; Jackson, I. J.; Birch-Machin, M. A.; Rees, J. L. *Hum. Mol. Genet.* **2000**, 9, 2531-2537.
- (180) Valverde, P.; Healy, E.; Sikkink, S.; Haldane, F.; Thody, A. J.; Carothers, A.; Jackson, I. J.; Rees, J. L. *Hum. Mol. Genet.* **1996**, 5, 1663-6.
- (181) Kennedy, C.; ter Huurne, J.; Berkhout, M.; Gruis, N.; Bastiaens, M.; Bergman, W.; Willemze, R.; Bavinck, J. N. *J. Invest. Dermatol.* **2001**, 117, 294-300.
- (182) Kaiser, E.; Colescott, R. L.; Bossinger, C. D.; Cook, P. I. *Anal. Biochem.* **1970**, 34, 595-8.
- (183) Weber, P. J. A.; Bader, J. E.; Folkers, G.; Beck-Sickinger, A. G. *Bioorg. Med. Chem.* **1998**, 8, 597-600.
- (184) Fulop, L.; Penke, B.; Zarandi, M. *J. Pept. Sci.* **2001**, 7, 397-401.



- (185) Fischer, R.; Mader, O.; Jung, G.; Brock, R. *Bioconjugate Chem.* **2003**, *14*, 653-660.
- (186) Kumar, P.; Fara, M. A.; Bradley, M.; Friedmann, P. S.; Healy, E. J. *Invest. Dermatol.* **2006**, *126*, 19-19.
- (187) Kumar, P.; Fara, M. A.; Bradley, M.; Friedmann, P. S.; Healy, E. *Br. J. Dermatol.* **2006**, *155*, 237-237.
- (188) Nielsen, P. E.; Egholm, M.; Berg, R. H.; Buchardt, O. *Science* **1991**, *254*, 1497-500.
- (189) Marin, V. L.; Roy, S.; Armitage, B. A. *Expert Opin. Biol. Ther.* **2004**, *4*, 337-348.
- (190) Xodo, L. E.; Cogoi, S.; Rapozzi, V. *Curr. Pharm. Des.* **2004**, *10*, 805-819.
- (191) Diaz-Mochon, J. J.; Bialy, L.; Bradley, M. *Chem. Commun.* **2006**, 3984-3986.
- (192) Pouchain, D.; Diaz-Mochon, J. J.; Bialy, L.; Bradley, M. *ACS Chem. Biol.* **2007**, *2*, 810-818.
- (193) Al Attar, H. A.; Norden, J.; O'Brien, S.; Monkman, A. P. *Biosens. Bioelectron.* **2008**, *23*, 1466-1472.
- (194) Gaylord, B. S.; Massie, M. R.; Feinstein, S. C.; Bazan, G. C. *Proc. Natl. Acad. Sci. U. S. A.* **2005**, *102*, 34-39.
- (195) Stender, H.; Fiandaca, M.; Hyldig-Nielsen, J. J.; Coull, J. J. *Microbiol. Methods* **2002**, *48*, 1-17.
- (196) Dueholm, K. L.; Egholm, M.; Behrens, C.; Christensen, L.; Hansen, H. F.; Vulpius, T.; Petersen, K. H.; Berg, R. H.; Nielsen, P. E.; Buchardt, O. *J. Org. Chem.* **1994**, *59*, 5767-73.
- (197) Koppelhus, U.; Nielsen, P. E. *Adv. Drug Deliv. Rev.* **2003**, *55*, 267-280.
- (198) Diaz-Mochon, J. J.; Bialy, L.; Watson, J.; Sanchez-Martin, R. M.; Bradley, M. *Chem. Commun.* **2005**, 3316-3318.
- (199) Nastruzzi, C.; Cortesi, R.; Esposito, E.; Gambari, R.; Borgatti, M.; Bianchi, N.; Feriotto, G.; Mischiatì, C. *J. Controlled Release* **2000**, *68*, 237-249.
- (200) Zhou, P.; Wang, M.; Du, L.; Fisher, G. W.; Waggoner, A.; Ly, D. H. *J. Am. Chem. Soc.* **2003**, *125*, 6878-6879.
- (201) Diaz-Mochon Juan, J.; Bialy, L.; Bradley, M. *Org. Lett.* **2004**, *6*, 1127-9.
- (202) Bialy, L.; Diaz-Mochon, J. J.; Specker, E.; Keinicke, L.; Bradley, M. *Tetrahedron* **2005**, *61*, 8295-8305.
- (203) Heimer, E. P.; Gallo-Torres, H. E.; Felix, A. M.; Ahmad, M.; Lambros, T. J.; Scheidl, F.; Meienhofer, J. *Int. J. Pept. Prot. Res.* **1984**, *23*, 203-11.
- (204) Breipohl, G.; Knolle, J.; Langner, D.; O'Malley, G.; Uhlmann, E. *Bioorg. Med. Chem. Lett.* **1996**, *6*, 665-670.
- (205) Kumar, P.; Pickard, C.; Fara, M. A.; Bradley, M.; Friedmann, P. S.; Healy, E. *Br. J. Dermatol.* **2007**, *156*, 1105-1105.
- (206) Kumar, P.; Fara, M.; Bradley, M.; Friedmann, P.; Healy, E. *J. Invest. Dermatol.* **2007**, *127*, S48-S48.
- (207) Buhleier, E.; Wehner, W.; Voegtle, F. *Synthesis* **1978**, 155-8.
- (208) Hawker, C. J.; Frechet, J. M. J. *J. Am. Chem. Soc.* **1990**, *112*, 7638-47.



- (209) Sanclimens, G.; Shen, H.; Giralt, E.; Albericio, F.; Saltzman, M. W.; Royo, M. *Biopolymers* **2005**, *80*, 800-814.
- (210) Zhou, J.; Wu, J.; Hafdi, N.; Behr, J.-P.; Erbacher, P.; Peng, L. *Chem. Commun.* **2006**, 2362-2364.
- (211) Lesniak, W. G.; Kariapper, M. S. T.; Nair, B. M.; Tan, W.; Hutson, A.; Balogh, L. P.; Khan, M. K. *Bioconjugate Chem.* **2007**, *18*, 1148-1154.
- (212) Kobayashi, H.; Brechbiel, M. W. *Adv. Drug Deliv. Rev.* **2005**, *57*, 2271-2286.
- (213) Venditto, V. J.; Regino, C. A. S.; Brechbiel, M. W. *Mol. Pharm.* **2005**, *2*, 302-311.
- (214) Stiriba, S.-E.; Frey, H.; Haag, R. *Angew. Chem., Int. Ed.* **2002**, *41*, 1329-1334.
- (215) Sadler, K.; Tam, J. P. *Rev. Mol. Biotechnol.* **2002**, *90*, 195-229.
- (216) Diaz-Mochon, J. J.; Fara, M. A.; Sanchez-Martin, R. M.; Bradley, M. *Tetrahedron Lett.* **2008**, *49*, 923-926.
- (217) Hochuli, E.; Bannwarth, W.; Doebeli, H.; Gentz, R.; Stueber, D. *BioTechnol.* **1988**, *6*, 1321-5.
- (218) Crowe, J.; Dobeli, H.; Gentz, R.; Hochuli, E.; Stuber, D.; Henco, K. *Methods Mol. Biol.* **1994**, *31*, 371-87.
- (219) Hochuli, E.; Dobeli, H.; Schacher, A. *J. Chromatogr.* **1987**, *411*, 177-84.
- (220) Hainfeld, J. F.; Liu, W.; Halsey, C. M. R.; Freimuth, P.; Powell, R. D. *J. Struct. Biol.* **1999**, *127*, 185-198.
- (221) Haddour, N.; Cosnier, S.; Gondran, C. *J. Am. Chem. Soc.* **2005**, *127*, 5752-5753.
- (222) Kapanidis, A. N.; Ebright, Y. W.; Ebright, R. H. *J. Am. Chem. Soc.* **2001**, *123*, 12123-12125.
- (223) Clegg, R. M. *Curr. Opin. Biotechnol.* **1995**, *6*, 103-10.
- (224) Yingyongnarongkul, B.-e.; Howarth, M.; Elliott, T.; Bradley, M. *Chem. Eur. J.* **2004**, *10*, 463-473.
- (225) Pons, J.-F.; Fauchere, J.-L.; Lamaty, F.; Molla, A.; Lazaro, R. *Eur. J. Org. Chem.* **1998**, 853-859.